

FROM MOLECULAR TO MACROMOLECULAR AND BACK:
INVESTIGATION OF HEXACOORDINATED PHOSPHORUS(V) ANIONS AND
POLY(METHYLENEPHOSPHINE)S

by

Paul Wai-Man Siu

B.Sc., University of Victoria, 2006

A THESIS SUBMITTED IN PARTIAL FULFILLMENT OF
THE REQUIREMENTS FOR THE DEGREE OF

DOCTOR OF PHILOSOPHY

in

THE FACULTY OF GRADUATE STUDIES

(Chemistry)

THE UNIVERSITY OF BRITISH COLUMBIA

(Vancouver)

August 2012

© Paul Wai-Man Siu, 2012

Abstract

Alkali metal salts of tris(benzenediolato)phosphate $[1]^-$, $K[1]$ and $Na[1]$, were prepared and examined as halide abstraction reagents. Compound $K[1]$ reacts with $(dppp)PdCl_2$ [$dppp = 1,3$ -bis(diphenylphosphino)propane] (1:1 ratio) or $[(cod)RhCl]_2$ (2:1 ratio) to afford $[(dppp)Pd(\mu-Cl)]_2[1]_2$ and $(cod)Rh[1]$, respectively. Brønsted acids $H(DMSO)_2[1]$ and $H(DMF)_2[1]$ were isolated as crystalline solids. The basicity of $[1]^-$ was examined using IR spectroscopy and determined to be comparable to $[BF_4]^-$. Brønsted acid $H(DMF)_2[1]$ is effective in the protonolysis of late transition metal-alkyl bonds. Its stoichiometric reaction with $(dppe)PdMe_2$ [$dppe = 1,2$ -bis(diphenylphosphino)ethane] affords either $[(dppe)Pd(NCMe)Me][1]$ (1:1 ratio) or $[(dppe)Pd(NCMe)_2][1]_2$ (1:2 ratio). Brønsted acid $H(DMF)_2[1]$ initiates the cationic polymerization of *n*-butyl vinyl ether at 17 °C to afford moderate molecular weight poly(*n*-butyl vinyl ether) ($M_n = 10,000 \text{ g mol}^{-1}$, PDI = 2.80).

Brønsted acids of tris(tetrachlorobenzenediolato)phosphate $[2]^-$, $H(OEt_2)_2[2]$ and $H(OEt_2)(NCMe)[2]$, were isolated as crystalline solids. Brønsted acid $H(OEt_2)_2[2]$ was shown to be an effective initiator for the cationic polymerizations of *n*-butyl vinyl ether, styrene and isoprene. High molecular weight poly(*n*-butyl vinyl ether) was isolated from polymerization at -78 °C ($M_n = 122,000 \text{ g mol}^{-1}$, PDI = 1.19). Atactic polystyrene of moderate molecular weight was isolated from polymerization at -50 °C ($M_n = 55,400 \text{ g mol}^{-1}$, PDI = 1.62). Moderate molecular weight *trans*-polyisoprene was isolated from polymerization at -38 °C ($M_n = 77,000 \text{ g mol}^{-1}$, PDI = 1.34).

Poly(methylenephosphine) and poly(methylenephosphine) oxide were coated onto paper sheets made from thermomechanical pulp. TAPPI (Technical Association of Pulp and Paper Industry) Standard Method T461 cm-00 was used to evaluate the flame retardant properties of

the polymers. Paper samples coated with the phosphorus-based polymers exhibited a higher degree of charring when compared to untreated paper and were comparable to paper treated with the monobasic ammonium phosphate standard.

The microstructure of the 1-(2,2,6,6-tetramethylpiperidinyloxy)-1-phenylethane initiated poly(methylenephosphine) was examined by NMR spectroscopy. Evidence suggests the occurrence of 1,5-hydrogen abstraction rearrangement during the propagation step of polymerization. The unexpected microstructure was modeled using $\text{PhCH}_2\text{P}(\text{Mes})\text{CHPh}_2$.

Preface

A version of Chapter 2 has been accepted for publication. Paul W. Siu and Derek P. Gates. “M[P(1,2-O₂C₆H₄)₃] (M = K or Na): Synthesis, Characterization and Use in Halide Abstraction.” *Can. J. Chem.*, **2012**, *Accepted*. I performed all the syntheses, characterizations, X-ray crystallographic data collections and refinements. Prof. Derek Gates and I prepared the manuscript jointly.

A version of Chapter 3 has been published. Paul W. Siu and Derek P. Gates. “HL₂[P(1,2-O₂C₆H₄)₃] (L = DMSO or DMF): A Convenient Proton Source with a Weakly Basic Phosphorus(V) Anion” *Organometallics* **2009**, 28, 4491. I performed all the syntheses and characterizations. Joshua I. Bates collected the X-ray crystallographic data for compound H(DMSO)₂[**3.1**] and solved its structure. All other X-ray crystallographic data collections and refinements were conducted by me. Prof. Derek Gates and I prepared the manuscript jointly.

A version of Chapter 4 will be submitted for publication. Paul W. Siu and Derek P. Gates. *To be submitted*. I performed all the syntheses, characterizations, X-ray crystallographic data collections and refinements.

A version of Chapter 5 will be submitted for publication. Paul W. Siu, Thomas Q. Hu and Derek P. Gates. *To be submitted*. I performed all the syntheses, characterizations and flame tests. Dr. Thomas Hu is our collaborator at FPInnovations.

A version of Chapter 6 will be submitted for publication. Paul W. Siu, Ivo Krummenacher and Derek P. Gates. *To be submitted*. Poly(methylenephosphine) was synthesized by Dr. Ivo Krummenacher. Dr. Ivo Krummenacher also carried out the characterization by triple detection gel permeation chromatography (GPC-LLS) and ³¹P{¹H}

NMR spectroscopy. I carried out all other characterizations of the polymer. I also synthesized and characterized model compound **6.8**.

Table of Contents

| | |
|----------------------------------------------------------------------|------------|
| Abstract | ii |
| Preface | iv |
| Table of Contents..... | vi |
| List of Tables..... | xi |
| List of Figures | xii |
| List of Schemes..... | xiv |
| List of Symbols and Abbreviations | xvi |
| Acknowledgements | xx |
| Dedication..... | xxi |
| Chapter 1: Introduction..... | 1 |
| 1.1 Prevalence of p-Block Elements..... | 1 |
| 1.2 Polymeric Materials..... | 1 |
| 1.3 Catalysis..... | 3 |
| 1.4 Weakly Coordinating Anions | 5 |
| 1.4.1 Boron-Based Weakly Coordinating Anions | 6 |
| 1.4.1.1 Fluoroarylborates | 6 |
| 1.4.1.2 Carborane Anions | 10 |
| 1.4.2 Aluminum- and Gallium-Based Weakly Coordinating Anions..... | 12 |
| 1.4.3 Weakly Coordinating Anions of Other p-Block Elements..... | 15 |
| 1.4.3.1 Phosphorus-Based Weakly Coordinating Anions | 16 |
| 1.5 Outline of Thesis..... | 17 |

| | |
|-------------------------------------------------------------------------------------------------------------------------------|-----------|
| Chapter 2: Synthesis, Characterization and Use of a Halide Abstraction Reagent with a Phosphorus(V)-Based Anion* | 20 |
| 2.1 Introduction | 20 |
| 2.2 Results and Discussion | 21 |
| 2.2.1 Synthesis and Characterization of Alkali Metals Salts of [2.1] ⁻ | 21 |
| 2.2.2 Application of K[2.1] in Metal-Halide Abstraction | 28 |
| 2.3 Summary | 33 |
| 2.4 Experimental Section | 34 |
| 2.4.1 General Procedures | 34 |
| 2.4.2 Synthesis of K[2.1] | 34 |
| 2.4.3 Synthesis of Na[2.1] | 35 |
| 2.4.4 Synthesis of [(dppp)Pd(μ-Cl)] ₂ [2.1] ₂ | 36 |
| 2.4.5 Synthesis of (cod)Rh[2.1] | 36 |
| 2.4.6 X-ray Crystallography | 37 |
| Chapter 3: Solid Brønsted Acids with a Weakly Basic Phosphorus(V) Anion* | 39 |
| 3.1 Introduction | 39 |
| 3.2 Results and Discussion | 40 |
| 3.2.1 Synthesis and Characterization of Brønsted Acids of [3.1] ⁻ | 40 |
| 3.2.2 Placement of [3.1] ⁻ on Infrared Scale for Weakly Basic Anions | 46 |
| 3.2.3 Application of H(DMF) ₂ [3.1] in Metal-Carbon Bond Protonolysis | 46 |
| 3.3 Summary | 52 |
| 3.4 Experimental Section | 52 |
| 3.4.1 General Procedures | 52 |
| 3.4.2 Synthesis of H(DMSO) ₂ [3.1] | 53 |

| | | |
|--------------------------------------------------------------------------------|-----------------------------------------------------------------------------------------------------------------------|-----------|
| 3.4.3 | Synthesis of H(DMF) ₂ [3.1] | 54 |
| 3.4.4 | Synthesis of (C ₈ H ₁₇) ₃ NH[3.1] | 54 |
| 3.4.5 | Synthesis of [(dppe)Pd(NCMe)Me][3.1] | 55 |
| 3.4.6 | Synthesis of [(dppe)Pd(NCMe) ₂][3.1] ₂ | 56 |
| 3.4.7 | Reaction of (dppe)PdMe ₂ with HCl | 56 |
| 3.4.8 | X-ray Crystallography | 57 |
| Chapter 4: Novel Cationic Polymerization Initiators for Vinyl Monomers* | | 59 |
| 4.1 | Introduction | 59 |
| 4.2 | Results and Discussion | 61 |
| 4.2.1 | H(DMF) ₂ [4.1] Initiated Cationic Polymerizations | 61 |
| 4.2.2 | Synthesis and Characterization of Brønsted Acids of [4.2] ⁻ | 63 |
| 4.2.3 | Molecular Structures of H(OEt ₂) ₂ [4.2] and H(OEt ₂)(NCMe)[4.2] | 69 |
| 4.2.4 | H(OEt ₂) ₂ [4.2] Initiated Cationic Polymerizations | 71 |
| 4.2.4.1 | Cationic Polymerizations at 17 °C | 71 |
| 4.2.4.2 | Cationic Polymerizations at Low Temperatures | 74 |
| 4.2.4.3 | Cationic Polymerizations at Varying Monomer to Initiator Ratio | 78 |
| 4.3 | Summary | 80 |
| 4.4 | Experimental | 81 |
| 4.4.1 | General Procedures | 81 |
| 4.4.2 | Synthesis of H(OEt ₂) ₂ [4.2] | 82 |
| 4.4.3 | Synthesis of H(OEt ₂)(NCMe)[4.2] | 83 |
| 4.4.4 | H(DMF) ₂ [4.1] Initiated Cationic Polymerizations of <i>n</i> -Butyl Vinyl Ether | 83 |
| 4.4.5 | H(OEt ₂) ₂ [4.2] Initiated Cationic Polymerizations of <i>n</i> -Butyl Vinyl Ether | 84 |
| 4.4.6 | H(OEt ₂) ₂ [4.2] Initiated Cationic Polymerizations of Styrene | 84 |

| | | |
|----------------------------------------------------------------------------------------------------------|-----------------------------------------------------------------------------------|-----------|
| 4.4.7 | H(OEt) ₂ [4.2] Initiated Cationic Polymerizations of Isoprene | 85 |
| 4.4.8 | X-ray Crystallography | 85 |
| Chapter 5: Poly(methylenephosphine)s as Macromolecular Flame Retardant Additives for Paper* | | 88 |
| 5.1 | Introduction | 88 |
| 5.2 | Results and Discussion | 90 |
| 5.2.1 | Synthesis of Poly(methylenephosphine)s 5.7 and 5.8 | 90 |
| 5.2.2 | Flame Retardancy Tests..... | 91 |
| 5.2.3 | pH Measurements of Burnt Paper Samples | 94 |
| 5.3 | Summary..... | 94 |
| 5.4 | Experimental Section..... | 95 |
| 5.4.1 | General Procedures..... | 95 |
| 5.4.2 | Synthesis of Poly(methylenephosphine) 5.7 | 96 |
| 5.4.3 | Synthesis of Poly(methylenephosphine) Oxide 5.8 | 96 |
| 5.4.4 | Preparation of NH ₄ H ₂ PO ₄ Treated Paper | 97 |
| 5.4.5 | Preparation of 5.7 Treated Paper | 97 |
| 5.4.6 | Preparation of 5.8 Treated Paper | 97 |
| 5.4.7 | Flame Retardancy Test of Paper Samples | 98 |
| Chapter 6: The Unexpected Microstructure of Poly(methylenephosphine)* | | 99 |
| 6.1 | Introduction | 99 |
| 6.2 | Results and Discussion | 101 |
| 6.2.1 | The Microstructure of Alkoxyamine Initiated Poly(methylenephosphine)..... | 101 |
| 6.2.2 | Synthesis and Characterization of Model Compound 6.8 | 105 |
| 6.2.3 | Rationalization for the Proposed Microstructure 6.7 | 107 |

| | | |
|-----------------------------------|--------------------------------------------------------|------------|
| 6.3 | Summary..... | 108 |
| 6.4 | Experimental Section..... | 108 |
| 6.4.1 | General Procedures..... | 108 |
| 6.4.2 | Synthesis of Poly(methylenephosphine) 6.6 | 109 |
| 6.4.3 | Synthesis of PhCH ₂ Li..... | 110 |
| 6.4.4 | Synthesis of Model Compound 6.7 | 110 |
| Chapter 7: Conclusion..... | | 112 |
| 7.1 | Summary of Thesis Work..... | 112 |
| 7.1.1 | Hexacoordinated Phosphorus(V) Anions | 112 |
| 7.1.2 | Poly(methylenephosphine)s..... | 114 |
| References..... | | 116 |

List of Tables

| | |
|------------------------------------------------------------------------------------------------------------------------------------------------------------------------------------------------------------------------------------------------------------------------------------------------------------------------------------------------------------------|----|
| Table 2.1 X-ray crystallographic data for $K_2(\text{DMSO})_6[\mathbf{2.1}]_2$, $\{[\text{K}(\text{MeCN})_2][\mathbf{2.1}]\}_6$, $[(\text{dppp})\text{Pd}(\mu_2\text{-Cl})]_2[\mathbf{2.1}]_2$ and $(\text{cod})\text{Rh}[\mathbf{2.1}]$ | 38 |
| Table 3.1 X-ray crystallographic data of $\text{H}(\text{DMSO})_2[\mathbf{3.1}]$, $\text{H}(\text{DMF})_2[\mathbf{3.1}]$, $[(\text{dppe})\text{Pd}(\text{NCMe})\text{Me}][\Lambda\text{-}\mathbf{3.1}]$, $[(\text{dppe})\text{Pd}(\text{NCMe})\text{Me}][\Delta\text{-}\mathbf{3.1}]$ and $[(\text{dppe})\text{Pd}(\text{NCMe})_2][\mathbf{3.1}]_2$.. | 58 |
| Table 4.1 $\text{H}(\text{DMF})_2[\mathbf{4.1}]$ initiated cationic polymerizations of <i>n</i> -butyl vinyl ether, styrene and isoprene in CH_2Cl_2 at 17 °C. | 62 |
| Table 4.2 $\text{H}(\text{OEt}_2)_2[\mathbf{4.2}]$ initiated cationic polymerizations of <i>n</i> -butyl vinyl ether, styrene and isoprene in CH_2Cl_2 at 17 °C. | 72 |
| Table 4.3 Temperature dependencies of $\text{H}(\text{OEt}_2)_2[\mathbf{4.2}]$ initiated cationic polymerizations of <i>n</i> -butyl vinyl ether, styrene and isoprene in CH_2Cl_2 | 75 |
| Table 4.4 $\text{H}(\text{OEt}_2)_2[\mathbf{4.2}]$ initiated cationic polymerization of <i>n</i> -butyl vinyl ether, styrene and isoprene in CH_2Cl_2 with varying monomer to initiator ratio..... | 78 |
| Table 4.5 Polymerization time dependence for $\text{H}(\text{OEt}_2)_2[\mathbf{4.2}]$ initiated cationic polymerization of styrene in CH_2Cl_2 | 80 |
| Table 4.6 X-ray crystallographic data of $\text{H}(\text{OEt}_2)_2[\mathbf{4.2}]$ and $\text{H}(\text{OEt}_2)(\text{NCMe})[\mathbf{4.2}]$ | 87 |
| Table 5.1 Flame retardancy test results..... | 93 |

List of Figures

| | |
|----------------------------------------------------------------------------------------------------------------------------------------------------------------------------------------------------------------------------------------------------------------------------------------------------------------------------------------------------------------------------------------------------------------------------------------------------|----|
| Figure 2.1 Molecular structure of Δ,Δ - $K_2(\text{DMSO})_6[\mathbf{2.1}]_2$ | 25 |
| Figure 2.2 Molecular structure of $\{K(\text{MeCN})_2[\mathbf{2.1}]\}_6$ | 27 |
| Figure 2.3 Three dimensional stacking of the $\{K(\text{MeCN})_2[\mathbf{2.1}]\}_6$ | 28 |
| Figure 2.4 Molecular structure of $[(\text{dppp})\text{Pd}(\mu_2\text{-Cl})_2[\mathbf{2.1}]_2$ | 30 |
| Figure 2.5 ^{31}P NMR (162 MHz, CD_3CN) spectrum of $[(\text{dppp})\text{PdCl}(\text{NCCD}_3)][\mathbf{2.1}]$ at 25 °C..... | 30 |
| Figure 2.6 Molecular structure of $(\text{cod})\text{Rh}[\mathbf{2.1}]$ | 32 |
| Figure 2.7 (a) ^1H NMR (300 MHz, CD_2Cl_2) spectrum of $K[\mathbf{2.1}]$ at 25 °C. (b) ^1H NMR (400 MHz, CD_2Cl_2) spectrum of $(\text{cod})\text{Rh}[\mathbf{2.1}]$ at 25 °C. | 33 |
| Figure 3.1 ^1H NMR (300 MHz, CD_3CN) spectrum of $\text{H}(\text{DMSO})_2[\mathbf{3.1}]$ at 25 °C..... | 42 |
| Figure 3.2 ^1H NMR (300 MHz, CD_3CN) spectrum of $\text{H}(\text{DMF})_2[\mathbf{3.1}]$ at 25 °C..... | 42 |
| Figure 3.3 Molecular structure of $\text{H}(\text{DMSO})_2[\mathbf{3.1}]$ | 44 |
| Figure 3.4 Molecular structure of $\text{H}(\text{DMF})_2[\mathbf{3.1}]$ | 44 |
| Figure 3.5 (a) ^{31}P NMR (162 MHz, CD_3CN) spectrum of $(\text{dppe})\text{PdMe}_2$ at 25 °C. (b) $^{31}\text{P}\{^1\text{H}\}$ NMR (121 MHz, CD_3CN) spectrum of $[(\text{dppe})\text{Pd}(\text{NCMe})\text{Me}][\mathbf{3.1}]$ at 25 °C. (c) ^{31}P NMR (162 MHz, CD_3CN) spectrum of $[(\text{dppe})\text{Pd}(\text{NCMe})_2][\mathbf{3.1}]_2$ at 25 °C..... | 48 |
| Figure 3.6 Molecular structures of Λ - and Δ -isomers of $[(\text{dppe})\text{Pd}(\text{NCMe})\text{Me}][\mathbf{3.1}]$ | 50 |
| Figure 3.7 Molecular structure of $[(\text{dppe})\text{Pd}(\text{NCMe})_2][\mathbf{3.1}]_2$ | 51 |
| Figure 4.1 Molecular structure of $\text{H}(\text{OEt}_2)_2[\mathbf{4.2}]$ | 65 |
| Figure 4.2 Molecular structure of $\text{H}(\text{OEt}_2)(\text{NCMe})[\mathbf{4.2}]$ | 66 |
| Figure 4.3 ^1H NMR (400 MHz, CD_3CN) spectrum of $\text{H}(\text{OEt}_2)_2[\mathbf{4.2}]$ at 25 °C..... | 67 |
| Figure 4.4 ^1H NMR (400 MHz, CD_2Cl_2) spectrum of $\text{H}(\text{OEt}_2)_2[\mathbf{4.2}]$ at -80 °C. | 68 |

| | |
|-----------------------------------------------------------------------------------------------------------------------------------------------------------------------------------------------------------------------------------------------------------------------------------------------------------------------------------------------------------------------------------------|-----|
| Figure 4.5 ^1H NMR (300 MHz, CDCl_3 , 25 °C) spectra of poly(<i>n</i> -butyl vinyl ether) polymerized by (a) $\text{H}(\text{DMF})_2$ [4.1] at 19 °C, (b) $\text{H}(\text{OEt}_2)_2$ [4.2] at 16 °C and (c) $\text{H}(\text{OEt}_2)_2$ [4.2] at -78 °C..... | 73 |
| Figure 4.6 $^{13}\text{C}\{^1\text{H}\}$ NMR (101 MHz, CDCl_3 , 25 °C) spectrum of $\text{H}(\text{OEt}_2)_2$ [4.2] initiated polyisoprene..... | 77 |
| Figure 4.7 Refractive index traces of (a) poly(<i>n</i> -butyl vinyl ether), (b) polystyrene and (c) polyisoprene in Table 4.4 with varying monomer to initiator ratio. | 79 |
| Figure 5.1 Photograph of the flammability test chamber designed following the TAPPI (Technical Association of Pulp and Paper Industry) Standard Method T461 cm-00 (L = 76.5 cm, W = 36.0 cm, H = 31.0 cm)..... | 92 |
| Figure 5.2 Representative results of the flame retardancy test for TMP paper samples. (a) No flame retardant added. (b) Treated with 5.7 (phosphorus content = 0.723 mmol P / g paper). (c) Treated with 5.8 (phosphorus content = 0.680 mmol P / g paper). (d) Treated with $\text{NH}_4\text{H}_2\text{PO}_4$ (phosphorus content = 0.824 mmol P / g paper)..... | 93 |
| Figure 5.3 The set-up of the paper samples in the flammability test chamber. | 98 |
| Figure 6.1 $^{13}\text{C}\{^1\text{H}\}$ NMR (151 MHz, CDCl_3) spectrum of alkoxyamine initiated poly(methylenephosphine) at 25 °C. | 102 |
| Figure 6.2 $^{13}\text{C}\{^1\text{H}\}$ NMR spectra (75 MHz, CDCl_3) of (a) poly(methylenephosphine) 6.1 and (b) model compound 6.2 | 102 |
| Figure 6.3 ^{13}C APT NMR (151 MHz, CDCl_3) spectrum of alkoxyamine initiated poly(methylenephosphine) at 25 °C. | 104 |
| Figure 6.4 ^1H - ^{13}C HSQC NMR spectrum (CDCl_3) of alkoxyamine initiated poly(methylenephosphine) at 25 °C. | 104 |
| Figure 6.5 $^{13}\text{C}\{^1\text{H}\}$ NMR (101 MHz, CDCl_3) spectrum of model compound 6.8 at 25 °C..... | 106 |
| Figure 6.6 ^1H NMR (400 MHz, CDCl_3) spectrum of model compound 6.8 at 25 °C..... | 107 |

List of Schemes

| | |
|-----------------------------------------------------------------------------------------------------------|----|
| Scheme 1.1 Methyl abstraction of zirconocene dimethyl complexes with $B(C_6F_5)_3$ | 7 |
| Scheme 1.2 Methyl abstraction of a zirconocene dimethyl complex with $Ph_3C[1.15]$ | 8 |
| Scheme 1.3 Protonolysis of metal-carbon bond with $HN^tBu_3[1.15]$ | 8 |
| Scheme 1.4 Protonolysis of metal-carbon bond with $H(OEt_2)_2[1.17]$ | 9 |
| Scheme 1.5 Halide abstraction of metal-halide with $Na[1.17]$ | 9 |
| Scheme 2.1 Reaction of potassium hydride with a mixture of 2.5 and 2.6 | 22 |
| Scheme 2.2 Formation of 2.7 in $DMSO-d_6$ | 23 |
| Scheme 2.3 Synthesis of $M[2.1]$ ($M = K, Na$)..... | 24 |
| Scheme 2.4 Halide abstraction of $(dppp)PdCl_2$ with $K[2.1]$ | 30 |
| Scheme 2.5 Halide abstraction of $[(cod)RhCl]_2$ with $K[2.1]$ | 32 |
| Scheme 3.1 Synthesis of Brønsted acids $HL_2[3.1]$ ($L = DMSO, DMF$)..... | 41 |
| Scheme 3.2 Protonolysis of $(dppe)PdMe_2$ with one equivalent of $H(DMF)_2[3.1]$ | 48 |
| Scheme 3.3 Protonolysis of $(dppe)PdMe_2$ with two equivalent of $H(DMF)_2[3.1]$ | 49 |
| Scheme 4.1 Generation of active initiator (A^+B^+) for cationic polymerization..... | 59 |
| Scheme 4.2 Cationic polymerization of vinyl monomers..... | 60 |
| Scheme 4.3 $H(DMF)_2[4.1]$ initiated cationic polymerization of <i>n</i> -butyl vinyl ether..... | 62 |
| Scheme 4.4 Synthesis of Brønsted acid $H(OEt_2)_2[4.2]$ | 64 |
| Scheme 4.5 Synthesis of Brønsted acid $H(OEt_2)(NCMe)[4.2]$ | 64 |
| Scheme 4.6 Proposed dissociation of $H(OEt_2)(NCMe)[4.2]$ in solution into 4.3 | 69 |
| Scheme 4.7 $H(OEt_2)_2[4.2]$ initiated cationic polymerization of <i>n</i> -butyl vinyl ether..... | 73 |
| Scheme 4.8 $H(OEt_2)_2[4.2]$ initiated cationic polymerization of styrene..... | 74 |
| Scheme 4.9 $H(OEt_2)_2[4.2]$ initiated cationic polymerization of isoprene..... | 74 |

| | |
|--------------------------------------------------------------------------------------------------------------------------|-----|
| Scheme 5.1 Synthesis of poly(methylenephosphine) 5.7 and its oxide, 5.8 | 91 |
| Scheme 6.1 Synthesis of poly(methylenephosphine) 6.1 through addition polymerization. | 99 |
| Scheme 6.2 Synthesis of model compound 6.2 | 100 |
| Scheme 6.3 Reaction of phosphalkene 6.3 with two equivalents of TEMPO. | 100 |
| Scheme 6.4 Polymerization of MesP=CPh ₂ initiated by alkoxyamine 6.6 | 101 |
| Scheme 6.5 Synthesis of model compound 6.8 | 105 |
| Scheme 6.6 Equilibrium of radicals 6.9 and 6.10 through 1,5-hydrogen abstraction. | 108 |
| Scheme 7.1 Halide abstraction of (dppp)PdCl ₂ and [(cod)RhCl] ₂ with K[7.1]. | 113 |
| Scheme 7.2 Protonolysis of (dppe)PdMe ₂ with H(DMF) ₂ [7.1]. | 113 |
| Scheme 7.3 Alkoxyamine 7.5 initiated polymerization of MesP=CPh ₂ | 115 |

List of Symbols and Abbreviations

| | |
|-----------------|---------------------------------------------------------------------------------------|
| Å | angstrom |
| Anal. | analysis |
| Ar | aryl |
| APT | attached proton test |
| avg. | average |
| br | broad (spectra) |
| ⁿ Bu | n-butyl |
| ^t Bu | tert-butyl |
| C | Celsius |
| ca. | circa |
| Calcd. | calculated |
| CCDC | Cambridge Crystallographic Data Centre |
| CFC | chlorofluorocarbons |
| cod | 1,5-cyclooctadiene (ligand) |
| COSY | correlation spectroscopy |
| cydtbp | <i>trans</i> -1,4-dithiocyclohexanediyl-2,2'-bis(4,6-di- <i>tert</i> -butylphenolate) |
| Δ | delta (configurational) |
| ° | degree |
| δ | NMR chemical shift in parts per million (ppm) |
| d | doublet (spectra) |
| D | density |
| DMF | dimethylformamide |

| | |
|---------------|--------------------------------------------|
| DMSO | dimethyl sulfoxide |
| dn/dc | refractive index increment |
| dppe | 1,2-bis(diphenylphosphino)ethane |
| dppen | 1,2-bis(diphenylphosphino)ethene |
| dppp | 1,3-bis(diphenylphosphino)propane |
| e.g. | exempli gratia (for example) |
| EI | electron impact |
| Et | ethyl |
| <i>et al.</i> | and others |
| equiv | equivalent |
| FT | Fourier transform |
| fw | formula weight |
| GOF | goodness of fit (crystallography) |
| GPC | gel permeation chromatography |
| h | hour |
| HFC | hydrofluorocarbons |
| HPLC | high-performance liquid chromatography |
| HMBC | heteronuclear multiple bond correlation |
| HMQC | heteronuclear multiple quantum correlation |
| HSQC | heteronuclear single quantum coherence |
| <i>i</i> | ipso |
| IR | infrared |
| Λ | lambda (configurational) |
| L | generic ligand |

| | |
|------------------|--------------------------------------------------------------|
| LLS | laser light scattering |
| $\bar{\nu}$ | wavenumber |
| M | generic metal; molar (mol L ⁻¹) |
| M ⁺ | molecular ion |
| m | multiplet (spectra) |
| <i>m</i> | meta |
| MALDI-TOF | matrix-assisted laser desorption ionization - time of flight |
| Me | methyl |
| Mes | 2,4,6-trimethylphenyl |
| MHz | megahertz |
| min | minute |
| M_n | number-average molecular weight |
| mol | mole |
| MS | mass spectrometry |
| <i>m/z</i> | mass-to-charge ratio |
| NMR | nuclear magnetic resonance |
| <i>o</i> | ortho |
| OTf | triflate |
| <i>p</i> | para |
| P [^] P | generic bidentate phosphorus ligand |
| PAPTAC | Pulp and Paper Technical Association of Canada |
| PBDE | polybrominated diphenyl ether |
| PDI | polydispersity index |
| PFC | perfluorocarbons |

| | |
|-----------|--------------------------------------------------|
| Ph | phenyl |
| pH | negative logarithm of hydrogen ion concentration |
| ppm | parts per million |
| pK_a | pK for association |
| i Pr | isopropyl |
| q | quartet |
| R | generic substituent |
| r_{vdw} | van der Waals radii |
| s | second; singlet (spectra) |
| t | triplet (spectra) |
| TAPPI | Technical Association of Pulp and Paper Industry |
| TEMPO | 2,2,6,6-tetramethyl-1-piperidinyloxy |
| THF | tetrahydrofuran |
| TMEDA | N,N,N',N' -tetramethylethylenediamine |
| TMP | thermomechanical pulp |
| WCA | weakly coordinating anion |
| wt % | weight percentage |
| X | generic halogen |
| VAZO 88 | 1,1'-azobis(cyclohexanecarbonitrile) |

Acknowledgements

First and foremost, I offer my sincere gratitude to my supervisor, Prof. Derek P. Gates, for giving me the opportunity to work in his research group. I appreciate the amount of time that he has invested in me and the room that he has given me to grow. In particular, I thank him for his patience with my writing and presentation skills or rather, the lack of them in the early years of my degree.

Many thanks go to Prof. Chris Orvig for reviewing my thesis. Likewise, Dr. Eamonn Conrad, Dr. Thomas Hey, Dr. Tom Hsieh and Andrew Priegert have all proofread and provided insightful comments for my thesis chapters.

Life in the Gates group is not always easy but the people in it have definitely kept things interesting. I appreciate all the times that I have shared with the present and the past members of the Gates group: Dr. Vittorio Cappello, Dr. Ivo Krummenacher, Dr. Eamonn Conrad, Dr. Thomas Hey, Dr. Tom Hsieh, Mandy Yam, Kevin Noonan, Bronwyn Gillon, Josh Bates, Julien Dugal-Tessier, Cindy Chun, Line Christiansen, Amber Juilfs, Jiazhang Wang, Andrew Priegert, Spencer Serin, Ben Rawe, Khatera Hazin, Abby Leung, Jimmy Tian, Gawon Go. I would like to thank Josh Bates and Dr. Brian Patrick for training me in X-ray crystallography. The ability to collect and refine my own X-ray crystallographic data has been incredibly rewarding. Also, the support staff at UBC Chemistry Department have been outstanding and the depth of my thesis work would not have been possible without them.

*To my parents,
who instilled the importance of hard work and sacrifice into me.*

Chapter 1: Introduction

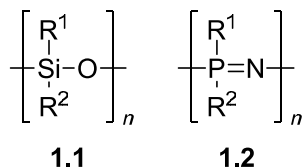
1.1 Prevalence of p-Block Elements

Underneath the umbrella of s- and p-block elements, but beyond the jurisdiction of organic chemists, lies the realm of intriguing possibilities that drives the focus of main group chemists. Over the years, intense efforts by these researchers have pushed the frontier of main group chemistry into the 21st century. In particular, application-oriented research has led to the prevalence of the p-block elements in innovations that stretch across numerous fields, including polymer materials, nanomaterials, catalysis, medicinal chemistry, chemical sensors and alternative energy sources.¹ Detailed discussion of each individual topic is beyond the scope of this thesis; thus, select examples of polymeric materials and catalysis will be discussed to highlight the importance of p-block elements in these fields.

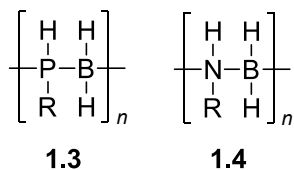
1.2 Polymeric Materials

The widespread applications of polysiloxanes (**1.1**), in particular poly(dimethylsiloxane), $[\text{Me}_2\text{Si-O}]_n$, in modern lives (e.g. lubricants, electrical insulations, fabric softeners, bakewares and contact lenses) overshadow the important advances in other inorganic polymers containing p-block elements in their backbones.²⁻⁴ Predating Kipping's fundamental discovery of polysiloxanes⁵ was Stokes' report of the first "inorganic rubber", an insoluble crosslinked polyphosphazene (**1.2**).⁶⁻⁷ This laid the foundation for the eventual discovery of the soluble non-crosslinked polyphosphazene $[\text{Cl}_2\text{P=N}]_n$ by Allcock *et al.*⁸⁻⁹ Substitution of the chlorine atoms in $[\text{Cl}_2\text{P=N}]_n$ is possible on a macromolecular level, offering a variety of polymeric structures suitable for numerous applications.¹⁰⁻¹¹ The presence of phosphorus centers in the polymeric chain attributes to the inherent flame retardant properties of many polyphosphazenes. In

particular, aryloxy-substituted polyphosphazenes, ranging from rigid materials to elastomers, have shown high flame resistance and low levels of smoke and gas toxicity upon combustion.¹¹⁻
¹² Current developments in polyphosphazenes focus on their potential applications as high-performance elastomers, biomedical materials and conductive polymers.¹⁰



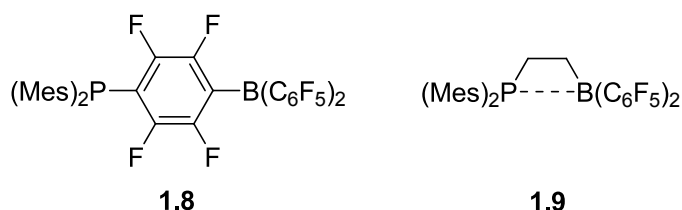
Allcock's seminal work on polyphosphazene (**1.2**) inspired a generation of phosphorus-based inorganic polymers. Recent advances in dehydrocoupling reactions have led to high molecular weight polyphosphinoboranes (**1.3**)¹³⁻¹⁴ and polyaminoboranes (**1.4**).¹⁵ These polymers are currently being investigated as precursors for BP- and BN-based ceramics.¹⁶ In addition, the phosphorus containing **1.3** is of interest for its high-temperature stability and flame retardant properties.¹³⁻¹⁴



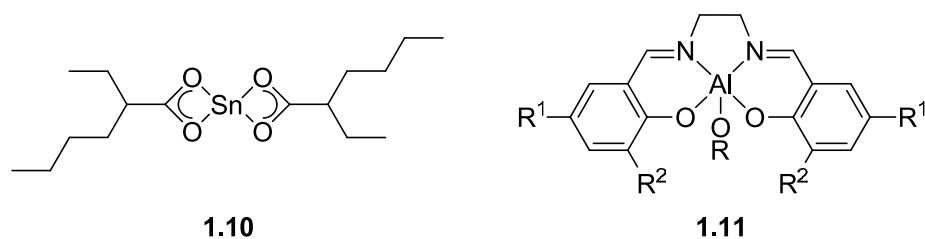
Another polymer containing phosphorus in the main chain is poly(methylenephosphine) **1.5**,¹⁷ which can be synthesized either by radical or anionic polymerizations of the phosphalkene monomer, MesP=CPh₂. This represents the first example of an inorganic polymer containing a p-block element synthesized through addition polymerization,¹⁸ a powerful synthetic method traditionally reserved for olefins to yield organic polymers. This also enabled the synthesis of random copolymers and block copolymers of MesP=CPh₂.¹⁹⁻²⁰ The phosphorus(III) centers in **1.5** readily coordinate to metal centers, making them suitable for various applications. Random copolymers of **1.5** and polystyrene are effective supports for palladium catalyzed Suzuki cross-coupling reactions.¹⁹ Amphiphilic block copolymers of

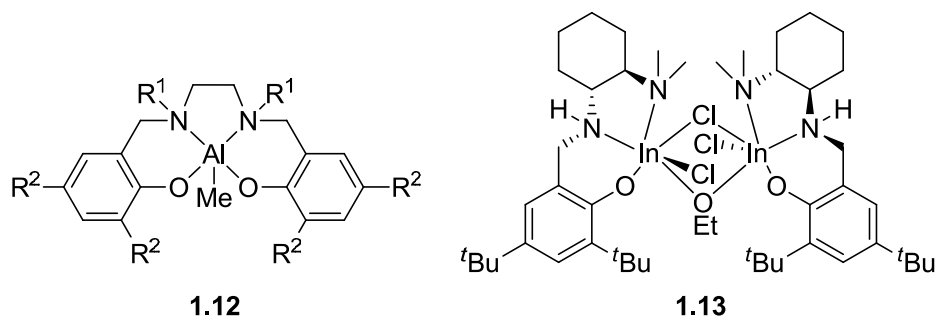
main group elements onto the center stage and a number of catalytic systems based on p-block elements have been developed.

In recent years, one of the major advancements in p-block chemistry has been the development of frustrated Lewis pairs, deceptively simple systems consisting of sterically hindered Lewis acid-base pairs that do not form adducts but are capable of activating small molecules such as alkenes, CO₂ and H₂.²⁷⁻²⁸ The activation of H₂ is regarded as a key step in hydrogenation, a highly relevant transformation in the petrochemical, agricultural and pharmaceutical industries. Frustrated Lewis pairs **1.8** and **1.9** were shown to be effective non-metal hydrogenation catalysts for imines and enamines.²⁹⁻³⁰

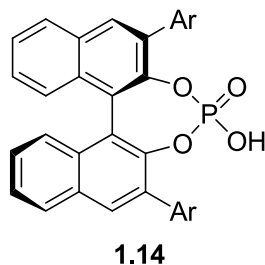


Biodegradable materials based on poly(lactic acid) are attractive green alternatives to traditional petroleum-based plastics. Currently, tin(II) octanoate (**1.10**) is the most commonly used catalyst in the ring opening polymerization of lactide in the industrial preparation of poly(lactic acid).³¹ The widely investigated aluminum-salen catalysts (**1.11**) and aluminum-salan catalysts (**1.12**) offer remarkable stereocontrol over this polymerization.³²⁻³³ More recently, there has been a growing interest in indium-based poly(lactic acid) catalysts, which have been shown to be highly active. In particular, catalyst **1.13** was reported to be an excellent catalyst for the living ring opening polymerization of lactide.³⁴





There is an emerging interest in a new class of Brønsted acid catalysts, based on the chiral phosphoric acid motif **1.14**, suitable for various asymmetric carbon-carbon bond-forming reactions.³⁵⁻³⁶ The bifunctional structure of **1.14** offers suitable acidity for catalytic transformations, while the phosphoryl oxygen functions as a Brønsted base site to mediate the necessary tight anion-substrate interactions for high enantioselectivities. Deprotonation of **1.14** yields the corresponding chiral anions, which can be incorporated into various metal catalysts. Even in the absence of chiral ligands on the metal centers, the presence of these chiral anions can still induce enantioselectivities onto various catalytic transformations.³⁷



1.4 Weakly Coordinating Anions

In general, the reactivity of a coordinatively unsaturated cation is highly dependent upon its degree of ion-pair interaction with the charge-balancing anion. In order to maintain the high electrophilicity at the cationic center, the choice of counteranion is of critical importance. A small, strongly coordinating anion will bind to the cationic center, rendering it coordinatively saturated and unreactive. However, a larger, more charge-delocalized anion will lead to weaker

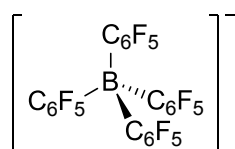
ion-pair interaction, leaving the cationic center unscathed, thus maximizing reactivity. The search for anions with minimal interaction with the cations coined the term “weakly coordinating anions” (WCAs),³⁸⁻³⁹ a topic that is of great relevance to this thesis and is dominated by p-block elements. Although the utility of WCAs spans many applications, including electrochemistry, ionic liquids, lithium-ion batteries and photoacid generators,³⁸⁻³⁹ the focus of this thesis will be on the importance of WCAs in catalysis and polymerizations.

The ubiquity of p-block elements in the field of WCAs began with $[\text{BF}_4]^-$, $[\text{PF}_6]^-$, $[\text{AsF}_6]^-$, $[\text{SbF}_6]^-$, $[\text{SO}_3\text{F}]^-$ and $[\text{SO}_3\text{CF}_3]^-$, which are now termed “classical” anions.³⁸⁻³⁹ Although they continue to play a significant role in all aspects of synthetic chemistry and catalysis, their limitations as WCAs were made evident with the advancements in X-ray crystallographic techniques. This led to the structural characterizations of various metal complexes bound by these classical WCAs.⁴⁰ The desire to generate and isolate increasingly electrophilic cationic complexes, both metal and non-metal, continues to drive researchers not only to rationally design new WCAs but also to scour the literature for previously unexplored candidates. While many p-block elements continue to play prominent roles in this area, boron- and aluminum-based anions have by far made the greatest impact.

1.4.1 Boron-Based Weakly Coordinating Anions

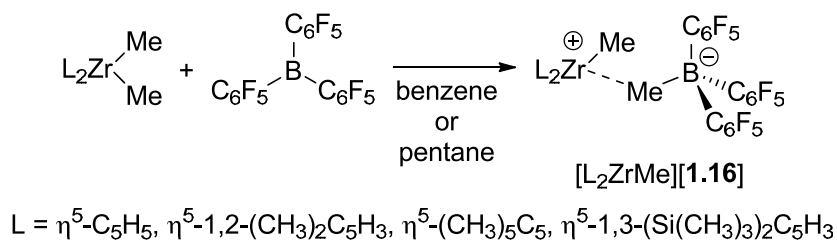
1.4.1.1 Fluoroarylborates

The early 1960s gave way to the synthesis of the lithium salt of tetrakis(pentafluorophenyl)borate, $[\mathbf{1.15}]^-$, by Massey and Park.⁴¹ For many years after, this fluorinated organoborate was perceived only as a mere obscurity to most chemists.⁴²



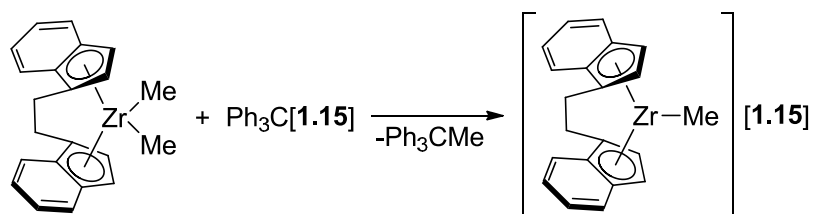
[1.15]⁻

This attitude dramatically changed beginning in 1991, when Ewen⁴³⁻⁴⁴ and Marks⁴⁵ exploited the strong Lewis acidity of the related tricoordinate $\text{B}(\text{C}_6\text{F}_5)_3$,⁴¹ and independently showed that $\text{B}(\text{C}_6\text{F}_5)_3$, in conjunction with a neutral dialkyl metallocene, is effective in α -olefin polymerizations. Specifically, Marks and coworkers showed that $\text{B}(\text{C}_6\text{F}_5)_3$ is effective in the methyl abstractions of zirconocene dimethyl complexes, generating active “cation-like” zirconocene catalysts $[\text{L}_2\text{ZrMe}]^+$ [$\text{L} = \eta^5\text{-C}_5\text{H}_5$, $\eta^5\text{-1,2-(CH}_3)_2\text{C}_5\text{H}_3$, $\eta^5\text{-(CH}_3)_5\text{C}_5$, $\eta^5\text{-1,3-(Si(CH}_3)_3)_2\text{C}_5\text{H}_3$] that are weakly coordinated by the slightly distorted tetrahedral [1.16]⁻ (Scheme 1.1).⁴⁵⁻⁴⁶ Although $\text{B}(\text{C}_6\text{F}_5)_3$ is the alkyl abstraction reagent, it is the resulting anion [1.16]⁻ that plays an essential role during the polymerization since it often tampers the cationic nature of the metal centers through weak interactions.



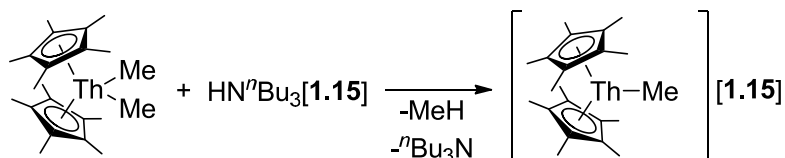
Scheme 1.1 Methyl abstraction of zirconocene dimethyl complexes with $\text{B}(\text{C}_6\text{F}_5)_3$.

This led to an immediate interest in the related tetrakis(pentafluorophenyl)borate, [1.15]⁻, as a counteranion for polymerization catalysts. In particular, Chien *et al.* synthesized $\text{Ph}_3\text{C}[1.15]$ as an alkyl abstraction reagent and incorporated [1.15]⁻ into a zirconocene complex, resulting in a highly active catalyst for propylene polymerization (Scheme 1.2).⁴⁷ In comparison to [1.16]⁻, the more symmetrical [1.15]⁻ is a weaker coordinating anion. Polymerization catalysts of [1.15]⁻ are more catalytically active and yield polypropylene with higher molecular weights.⁴⁸



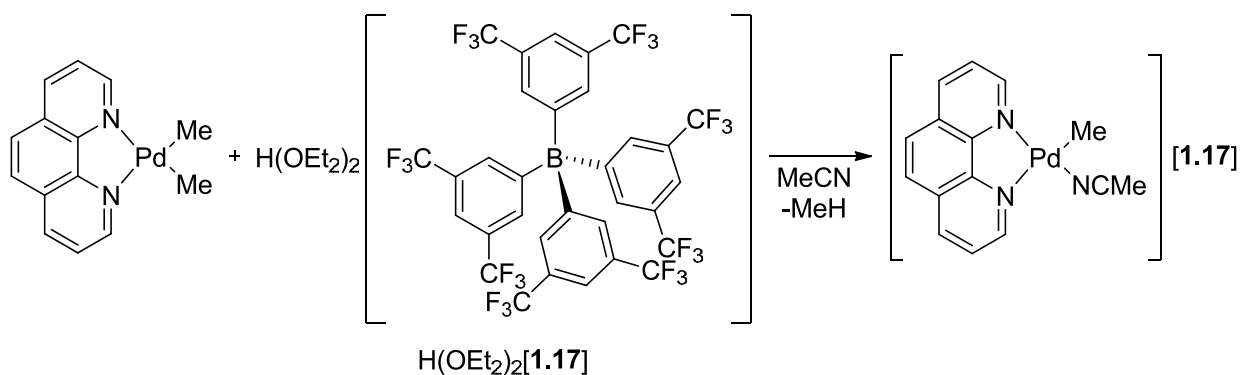
Scheme 1.2 Methyl abstraction of a zirconocene dimethyl complex with Ph₃C[1.15].

The highly polarized metal-carbon bond can also be activated through protonolytic reactions. Marks and coworkers showed that [1.15][−] can be introduced into active ethylene polymerization catalysts by using protic reagents such as HNⁿBu₃[1.15] (Scheme 1.3).⁴⁹



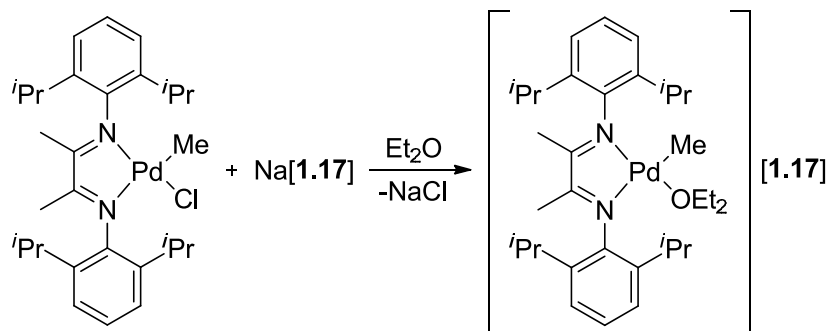
Scheme 1.3 Protonolysis of metal-carbon bond with HNⁿBu₃[1.15].

Although ammonium reagents of WCAs are effective for early transition metal-carbon bond protonolysis, they are nevertheless limited in acidity and are not sufficient for late transition metal-carbon bonds. Brookhart *et al.* overcame this limitation with an alternative fluoroarylborate-based protic reagent, H(OEt₂)₂[1.17].⁵⁰ Fluoroarylborate [1.17][−] was chosen because its sodium salt had previously been synthesized and exhibited extraordinary stability against H₂SO₄.⁵¹ As a Brønsted acid, Brookhart *et al.* showed that H(OEt₂)₂[1.17] is effective in the protonolysis of palladium-carbon bonds (Scheme 1.4), generating cationic palladium complexes that are catalytically active in the living copolymerization of olefins and carbon monoxide.⁵²



Scheme 1.4 Protonolysis of metal-carbon bond with $\text{H}(\text{OEt}_2)_2$ [1.17].

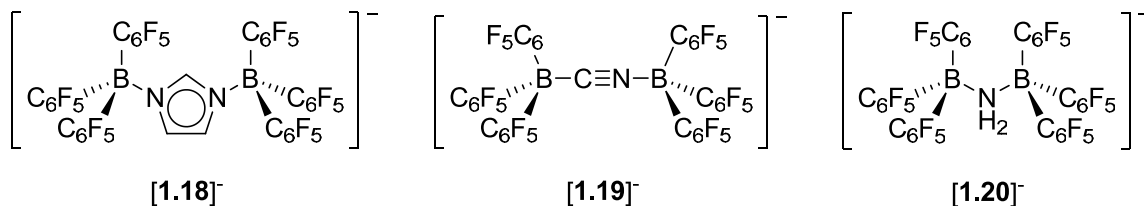
Brookhart and co-workers also showed that $\text{Na}[1.17]$ is a convenient reagent for the halide abstraction of various neutral palladium-chloride complexes (Scheme 1.5), generating active cationic metal catalysts for the copolymerization of α -olefins and methyl acrylate.⁵³ Importantly, the application of $[1.15]^-$ and $[1.17]^-$ in catalysis is not limited to olefin polymerizations. Numerous other catalytic reactions continue to be reported, including amide reduction,⁵⁴ hydroamination,⁵⁵⁻⁵⁶ hydrosilylation,⁵⁷ hydrogenation,⁵⁸⁻⁵⁹ hydroboration,⁶⁰ and Diels-Alder reaction.⁶¹



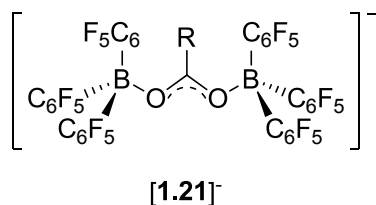
Scheme 1.5 Halide abstraction of metal-halide with $\text{Na}[1.17]$.

The success of $[1.15]^-$ and $[1.17]^-$ as integral components in catalysis, in particular for olefin polymerizations, inspired the development of larger and more electronically diffused derivatives.⁶² One particularly successful strategy is to “link” two moieties of $\text{B}(\text{C}_6\text{F}_5)_3$ with an anionic bridging group, thus delocalizing the negative charge over multiple boron centers.

WCAs, such as **[1.18]**⁻,⁶³ **[1.19]**⁻,⁶⁴ and **[1.20]**⁻,⁶⁵ are effective in generating and stabilizing various cationic metal-based olefin polymerization catalysts.^{63,65-69} Other reported catalytic reactions include ring-opening polymerization of lactides,⁷⁰⁻⁷¹ cyclopropanation and aziridination of olefins,⁷² and coupling of terminal alkynes with aldehydes and amines.⁷³



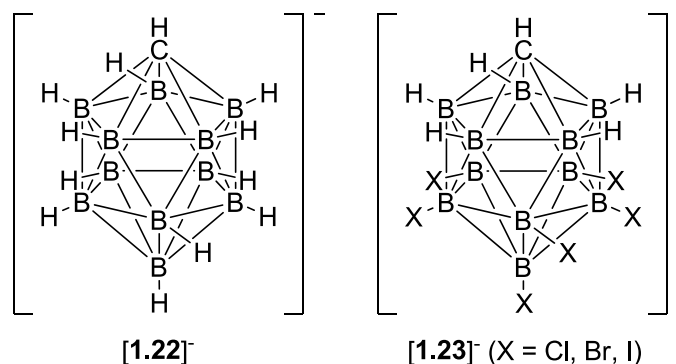
Baird and coworkers also utilized this strategy and linked two moieties of B(C₆F₅)₃ with various carboxylic acids to form Brønsted acids comprised of **[1.21]**⁻.⁷⁴⁻⁷⁵ Although these Brønsted acids were only generated *in situ*, they are nevertheless effective protic initiators for the polymerization of isobutene and copolymerization of isobutene and isoprene. In addition, Baird and coworkers were able to isolate the tetramethylammonium salt of the methyl derivative (**[1.21]**⁻, R = Me), thereby confirming the general structure of these WCAs.⁷⁶



1.4.1.2 Carborane Anions

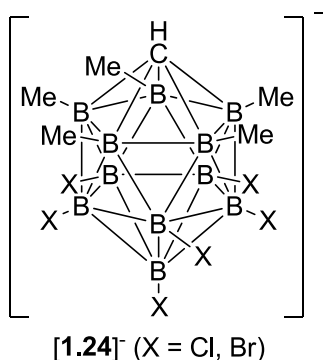
Another notably successful class of boron-based WCAs is the carborane anions. Their rise to prominence as WCAs followed a similar story as tetrakis(pentafluorophenyl)borate, **[1.15]**⁻. Although the cesium salt of the first carborane **[1.22]**⁻ was synthesized in 1967,⁷⁷ several decades would pass before the weakly coordinating properties of **[1.22]**⁻ were appreciated.³⁹ Arguably, it was Reed's group in the 1990s that propelled this class of WCAs into the spotlight by utilizing the hexahalogenated carboranes **[1.23]**⁻ to isolate complexes that are considered to

be close approximations to the highly electrophilic silylium cation, namely $[i\text{Pr}_3\text{Si}]^+$.⁷⁸⁻⁷⁹ Since then, derivatives of carborane anions have time and time again brought forth fundamental breakthroughs in chemistry and continue to be frontrunners for the title of the least coordinating anions.^{38-39,80}

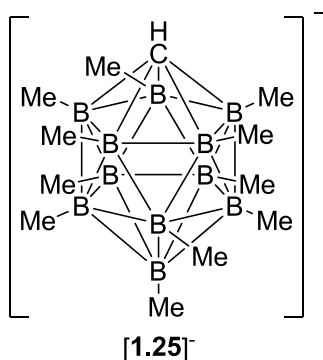


Some of the most exciting breakthroughs in recent years have been made possible by the synthesis of carborane-based silylium reagents. In particular, Ozerov and coworkers showed that *in situ* generated trialkyl silylium reagents of $[1.22]^-$ and $[1.23]^-$ (X = Cl, Br) are powerful catalysts for the hydrodehalogenation of aliphatic carbon-halogen bonds, converting C-F and C-Cl bonds to C-H bonds.⁸¹⁻⁸² This could potentially be applied to the disposal of environmental pollutants such as chlorofluorocarbons (CFC), hydrofluorocarbons (HFC) and perfluorocarbons (PFC). A related alkylative defluorination reaction was also developed, to convert C-F bonds to C-C bonds, using highly reactive catalysts comprised of dialkylaluminum cations paired with $[1.23]^-$ (X = Br).⁸³

The tendency for silylium cations to C-F activate also led Siegel and coworkers to use $i\text{Pr}_3\text{Si}[1.23]$ (X = Cl) to catalyze the Friedel-Crafts coupling of fluoroarenes.⁸⁴ Manners and Reed showed that $\text{Et}_3\text{Si}[1.23]$ (X = Br) and $\text{Et}_3\text{Si}[1.24]$ (X = Br) are potent initiators for the room temperature ring opening polymerization of the cyclic chlorophosphazene trimer, $[\text{Cl}_2\text{P}=\text{N}]_3$.⁸⁵ In the absence of these silylium catalysts, a high temperature of 250 °C is necessary for the polymerization,⁸⁻⁹ leaving little control over the molecular weight of the polymer.



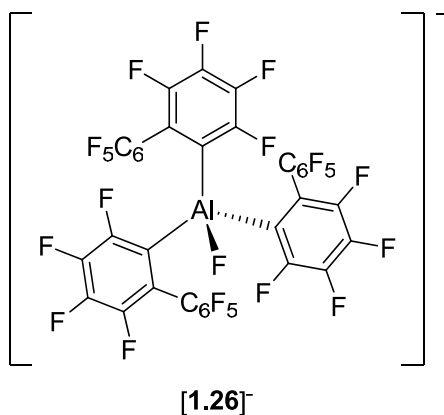
Incorporating carborane anions into transition metal-based complexes has also resulted in catalysts for a variety of catalytic transformations, including olefin polymerization,⁸⁶ olefin hydrogenation,⁸⁷ alkene and alkyne hydroacylation,⁸⁸⁻⁸⁹ and Diels-Alder reactions.⁹⁰⁻⁹¹ The lithium salt of **[1.25]⁻** can also catalyze a number of reactions, including pericyclic rearrangements,⁹² and radical polymerization of terminal alkenes.⁹³ Nevertheless, the widespread practical application of carborane anions in catalysis is currently hampered by their cost, illustrating the necessary balance between synthetic availability and effectiveness for successful WCAs.⁹⁴



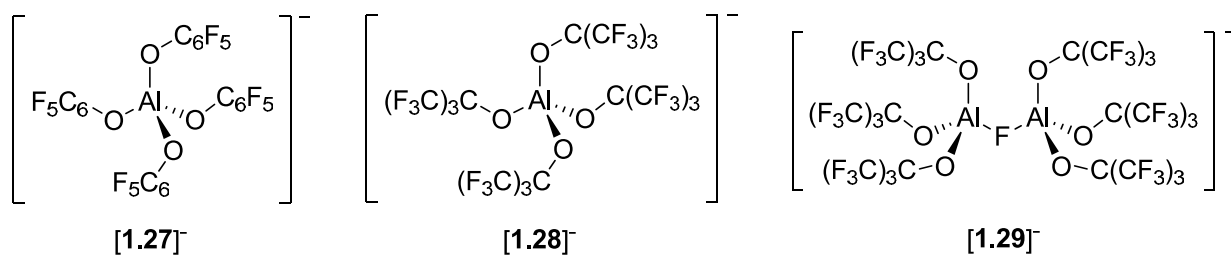
1.4.2 Aluminum- and Gallium-Based Weakly Coordinating Anions

The success of fluoroarylborates **[1.15]⁻** and **[1.17]⁻** as WCAs naturally led researchers to explore anions of heavier group 13 elements. Marks and coworkers synthesized the trityl salt of **[1.26]⁻**, a (perfluoroaryl)aluminate anion based on the nonafluorobiphenyl-substitution.⁹⁵⁻⁹⁶ Although zirconium and titanium complexes of **[1.26]⁻** are effective in olefin polymerizations,

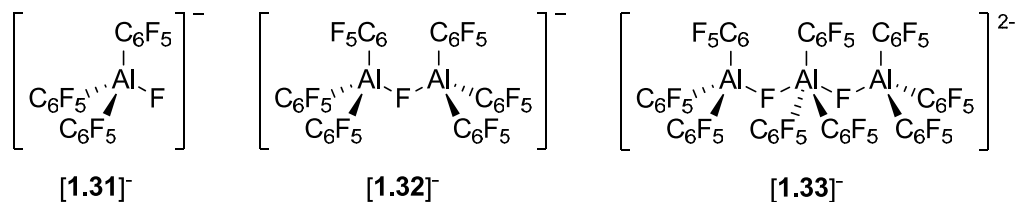
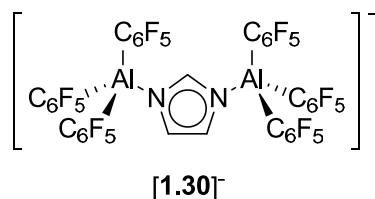
their catalytic activities are much lower than the analogous catalysts containing **[1.15]**⁻, leading to the conclusion that **[1.26]**⁻ is more coordinating than **[1.15]**⁻.⁹⁷⁻⁹⁸ The stronger affinity of **[1.26]**⁻ for the cationic metal center attributes to stabilizing the cationic charge, resulting in less erosion of syndioselectivity at elevated temperatures.



Aluminate anions bearing perfluoroalkoxide or perfluoroaryloxy substituents, such as **[1.27]**⁻ and **[1.28]**⁻, are also effective WCAs.⁹⁹⁻¹⁰⁰ Although alcohols are generally deemed poisonous for the highly oxophilic early transition metal catalysts, this disadvantage is offset by the strong aluminum-oxygen bonds. Furthermore, the nucleophilicities of the oxygen centers are circumvented by the presence of multiple electron-withdrawing fluorine groups. Zirconocene complexes of **[1.27]**⁻ and **[1.28]**⁻ are effective catalysts for ethylene polymerization.^{99,101} McGuinness *et al.* also reported a chromium complex of **[1.28]**⁻ that showed remarkable selectivity in the tetramerization of ethylene into 1-octene, a highly desirable comonomer in the production of linear low-density polyethylene.¹⁰² The larger fluoro-bridged anion **[1.29]**⁻ was expected to be more charge diffused than **[1.28]**⁻; however, studies showed that the chromium-based oligomerization catalyst of **[1.29]**⁻ yields lower catalytic activity and selectivity than **[1.28]**⁻. This was likely due to the instability of **[1.29]**⁻ in polar solvents, dissociating into its constituents $[\text{FAl}(\text{OC}(\text{CF}_3)_3)_3]^-$ and $\text{Al}(\text{OC}(\text{CF}_3)_3)_3$.

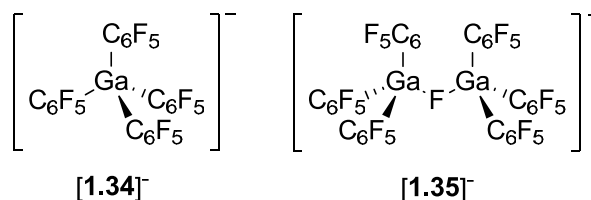


In general, delocalization of the negative charge over multiple aluminum centers is an effective strategy in designing larger and weaker coordinating anions. The titanium complex of **[1.30]⁻**, an aluminate analog of fluoroarylborate **[1.18]⁻**, catalyzes the copolymerization of ethylene and 1-octene, exhibiting higher activity and yielding higher molecular weight polymers than with the fluoroarylborates **[1.15]⁻** and **[1.18]⁻**.⁶³ Marks and coworkers synthesized a series of mono- and polynuclear fluoroarylaluminate anions, **[1.31]⁻**, **[1.32]⁻** and **[1.33]⁻**, and incorporated them into zirconocene catalysts for propylene polymerization.¹⁰³⁻¹⁰⁵ Increasing the size of the anion from **[1.31]⁻** to **[1.32]⁻** resulted in increased catalytic activity; however, in conjunction with an increased negative charge, such as from **[1.32]⁻** to **[1.33]⁻**, an expected decrease in catalytic activity was observed.



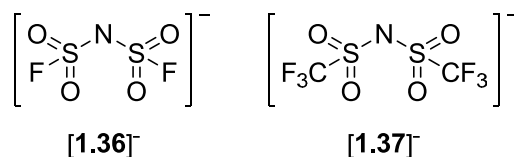
Gallium-based WCAs have also found applications in polymerizations. In particular, Neckers and coworkers have developed cyclopropenium and iodonium salts of **[1.34]⁻** that are effective photoinitiators for the cationic photopolymerization of epoxides.¹⁰⁶⁻¹⁰⁹ The fluoro-bridged derivative **[1.35]⁻** has been incorporated into zirconocene complexes, resulting in active

catalysts for propylene polymerization, albeit with lower catalytic activity than for the aluminate analog, **[1.32]**⁻.¹⁰³⁻¹⁰⁵

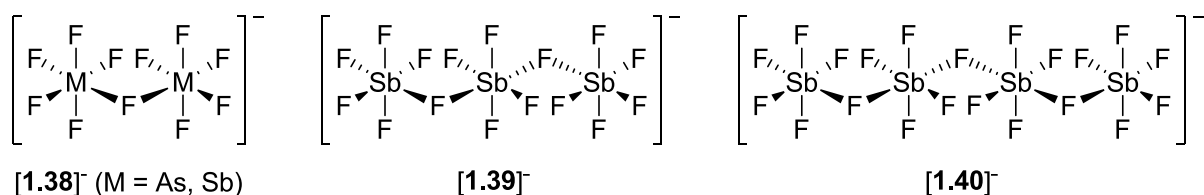


1.4.3 Weakly Coordinating Anions of Other p-Block Elements

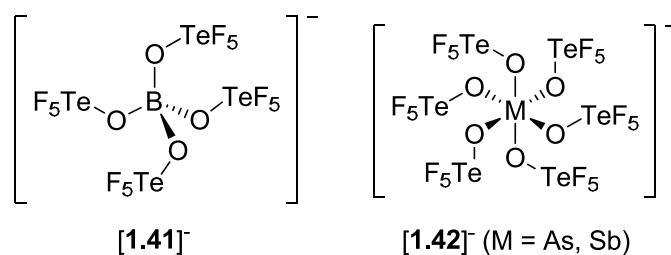
The linking strategy for designing larger WCAs has also been applied for $[\text{SO}_3\text{F}]^-$, to give **[1.36]**⁻.¹¹⁰⁻¹¹¹ However, anion **[1.36]**⁻ has only received minimal attention in catalysis.¹¹² The related triflimidate anion, **[1.37]**⁻,¹¹³ derived from the more electron-withdrawing $[\text{SO}_3\text{CF}_3]^-$, has been much more popular in catalysis.¹¹⁴ In particular, **[1.37]**⁻ has been widely studied in gold-catalyzed transformations.¹¹⁵⁻¹¹⁸ Many of the phosphine and N-heterocyclic carbene gold(I) complexes of **[1.37]**⁻ are crystalline air-stable compounds, a stark contrast to similar gold(I) complexes of classical anions (e.g. $[\text{BF}_4]^-$, $[\text{PF}_6]^-$ and $[\text{SbF}_6]^-$).¹¹⁴ The conjugate acid of **[1.37]**⁻ is a strong Brønsted acid and in the presence of silyl enol ethers, it is effective for the group transfer polymerizations of methyl methacrylate and *N,N*-dimethylacrylamide.¹¹⁹⁻¹²⁰ In conjunction with an alcohol initiator, $\text{H}[\text{1.37}]$ is also effective in the ring opening polymerization of δ -valerolactone.¹²¹



The larger fluoro-bridged derivatives of $[\text{AsF}_6]^-$ and $[\text{SbF}_6]^-$ are known in the forms of **[1.38]**⁻, **[1.39]**⁻ and **[1.40]**⁻.¹²²⁻¹³² However, their applications in catalysis have yet to be explored. It is expected that their tendency to dissociate in solution, generating Lewis acids of MF_5 ($\text{M} = \text{As}, \text{Sb}$), may lead to unwanted side reactions.



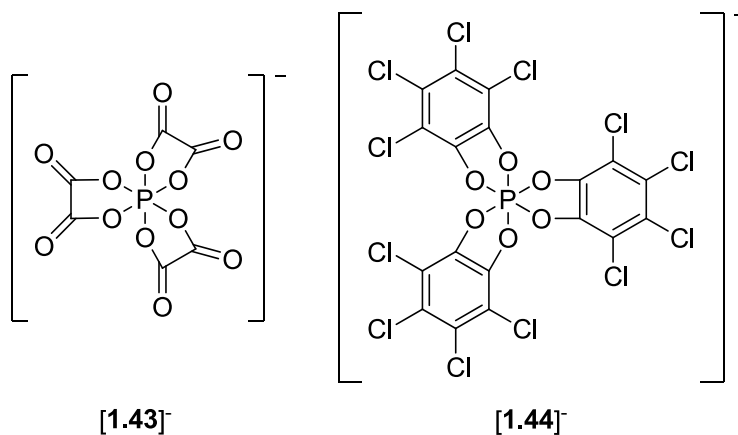
The teflate-based anions [1.41]⁻ and [1.42]⁻ were once promised to be excellent WCAs.¹³³⁻¹³⁶ Thus far, however, [1.42]⁻ (M = Sb) remains the only WCA of interest in this series and catalytic reactions involving these teflate-based WCAs have not yet been demonstrated.¹³⁷⁻¹³⁹



1.4.3.1 Phosphorus-Based Weakly Coordinating Anions

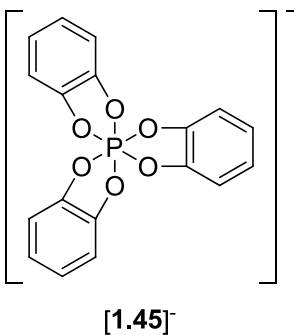
There are few examples of the larger derivatives of [PF₆]⁻ in catalysis. The protic acid of the tris(oxalate)phosphate anion, [1.43]⁻, has been shown to effectively catalyze Friedel-Crafts type alkylation reactions.¹⁴⁰ In general, octahedral hexacoordinated phosphorus anions bearing three dianionic bidentate ligands exist in either Λ or Δ configurations, thus they are chiral. To take advantage of this property, Lacour *et al.* synthesized and resolved the configurationally stable tris(tetrachlorobenzenediolato)phosphate anion, [1.44]⁻,¹⁴¹⁻¹⁴² and utilized it in various chiral anion-mediated asymmetric applications.^{37,143} Several other groups have studied the asymmetric influence of the enantiomerically pure [1.44]⁻ in transition metal-based catalysis.¹⁴⁴⁻¹⁴⁶ While ruthenium, iridium and rhodium complexes of the enantiomerically pure [1.44]⁻ are catalytically active, the chiral anion does not influence the enantioselectivity of these reactions.¹⁴⁴⁻¹⁴⁶ The trityl salt of [1.44]⁻, in conjunction with silyl ketene acetal, has been shown

to be an effective initiator system for the polymerizations of butyrolactone and methacrylate.¹⁴⁷⁻¹⁴⁸



1.5 Outline of Thesis

The main goal of this thesis was to further explore hexacoordinated phosphorus(V) anions as potential WCAs in catalysis. Since the birth of “modern” hexacoordinated phosphorus chemistry in the early 1960s, numerous hexacoordinated phosphorus(V) anions have been reported, offering a diverse library of potential WCA candidates.¹⁴⁹ It was expected that, in comparison to the tetracoordinated fluoroarylborates, the larger hexacoordinated phosphorus(V) anions would be more charge diffused, thus more weakly coordinating. The catechol-based hexacoordinated phosphorus(V) anion was an attractive motif, since the chlorinated derivative [1.44]⁻ has already found applications in several catalytic reactions. The weakly coordinating ability of the simpler non-chlorinated derivative [1.45]⁻ has not been explored,¹⁴⁹⁻¹⁵¹ thus it was chosen for initial investigation. The ability of [1.45]⁻ to stabilize cationic metal complexes would be evaluated; however, suitable precursors containing [1.45]⁻ were needed to generate these cationic metal complexes.



Chapter 2 describes the synthesis of two new alkali metal complexes of [1.45]⁻ as halide abstraction reagents. This offers a convenient route for generating cationic metal complexes through the halide abstraction of metal-halide bonds. Alternatively, cationic metal complexes can also be generated through the protonolysis of metal-carbon bonds. Although ammonium salts of [1.45]⁻ are known,¹⁵⁰⁻¹⁵¹ their low acidity would limit protonolysis to early transition metal-carbon bonds. Chapter 3 discusses the coordinating ability of [1.45]⁻ and synthesis of two strong Brønsted acids of [1.45]⁻ for the protonolysis of late transition metal-carbon bonds. Strong Brønsted acids are also of interest as initiators for polymerizations. Beginning with the Brønsted acid of [1.45]⁻ and extending to a new Brønsted acid of [1.44]⁻, Chapter 4 describes the application of these strong Brønsted acids of hexacoordinated phosphorus(V) anions as initiators for cationic polymerizations.

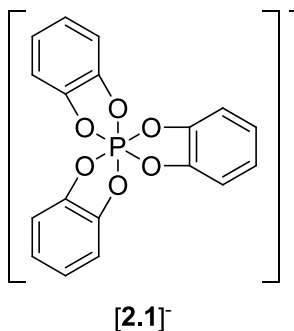
Chapter 5 changes the focus onto the inorganic polymer, poly(methylenephosphine) **1.5**. Recent advances by the Gates group have led to several potential applications for **1.5**,^{19,21} which entices further efforts to develop new applications in this area. Like polyphosphazene **1.2**, the presence of phosphorus in the main chain of **1.5** could exhibit desirable flame retardant properties for the polymer. Chapter 5 describes the investigation into the flame retardant property of **1.5** and its oxide. During this investigation, new evidence arose that questioned the connectivity of **1.5**. Chapter 6 discloses the new proposed microstructure of radically

polymerized poly(methylenephosphine). Finally, Chapter 7 summarizes the results presented in this dissertation.

Chapter 2: Synthesis, Characterization and Use of a Halide Abstraction Reagent with a Phosphorus(V)-Based Anion*

2.1 Introduction

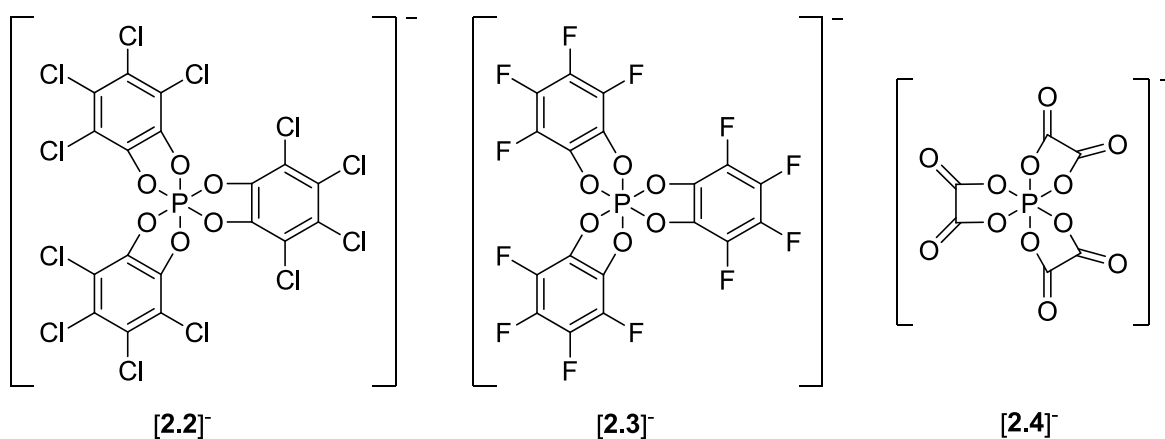
In 1963, the first example of a hexacoordinated organophosphate anion, **[2.1]⁻**, was synthesized as an ammonium salt by Allcock.^{150,152-153} This marked the birth of “modern” hexacoordinated phosphorus chemistry.¹⁴⁹ Since then, the development and investigation of hexacoordinated phosphorus compounds continue to be areas of widespread fundamental interest. Although cationic and neutral complexes of such species are now known,^{149,154-156} the most prevalent are anionic species of the type $[PX_6]^-$, led by $[PF_6]^-$ and $[PCl_6]^-$.



Recently, there is an emerging interest in the applications of hexacoordinated phosphorus(V)-based anions bearing three chelating dianionic ligands.¹⁴⁹ Anions, such as **[2.1]⁻**,^{150,152-153} **[2.2]⁻**,¹⁴¹ **[2.3]⁻**,¹⁵⁷ and **[2.4]⁻**,¹⁴⁰ are large, highly symmetrical and charge-diffused, which are ideal properties for weakly coordinating anions (WCAs). The lithium salts of **[2.1]⁻**, **[2.3]⁻** and **[2.4]⁻** are of interest as lithium battery electrolytes.^{140,157-158} They exhibit good thermal stability (up to 150 °C) and their electrochemical properties have been studied.^{140,157-158}

* A version of this chapter has been accepted for publication. Paul W. Siu and Derek P. Gates. “M[P(1,2-O₂C₆H₄)₃] (M = K or Na): Synthesis, Characterization and Use in Halide Abstraction.” *Can. J. Chem.*, **2012**, *accepted*. Copyright 2012 NRC Canada.

This subclass of hexacoordinated phosphorus(V) anions are also chiral. Of these, perhaps the most widely studied is $[2.2]^-$,¹⁴¹ which can be resolved into pure enantiomers and is employed in NMR enantiodifferentiation and resolution of chiral cations.^{37,143} Interestingly, the non-halogenated $[2.1]^-$ cannot be resolved into pure enantiomers due to acid-catalyzed racemization.¹⁵⁹



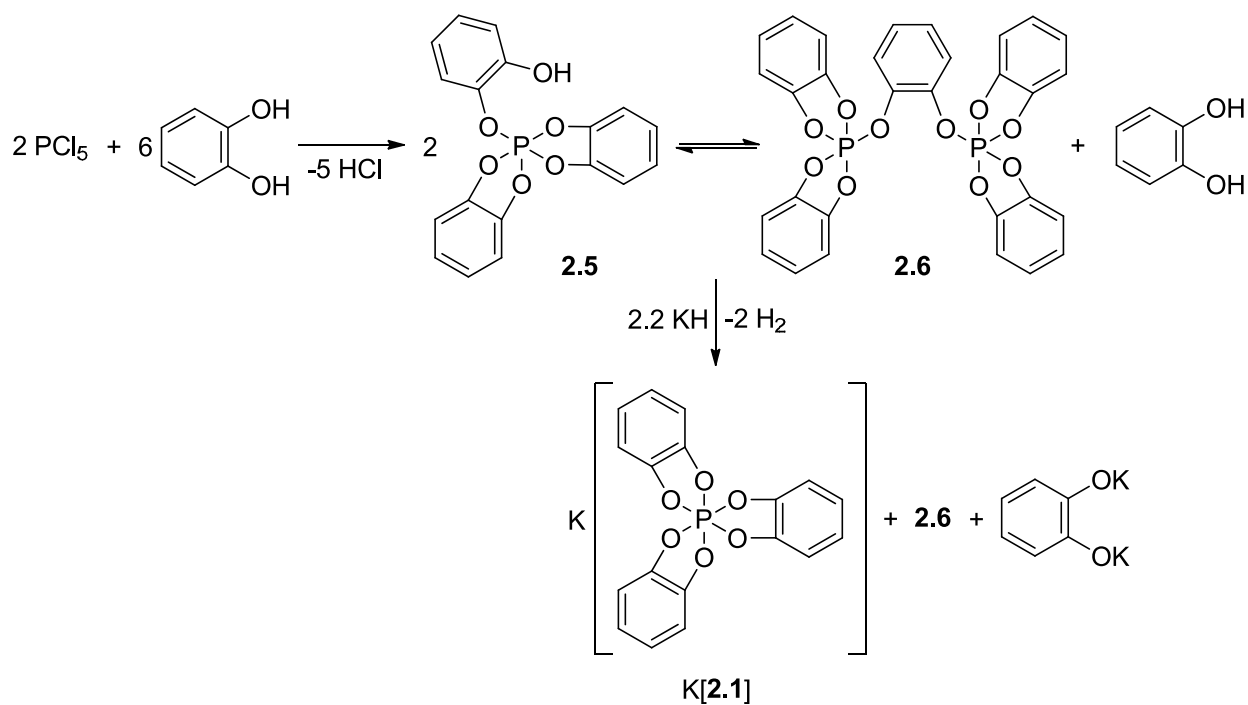
Anion $[2.2]^-$ has been employed as a counteranion in transition metal-based catalysis;¹⁴⁴⁻¹⁴⁶ however, the ability of $[2.1]^-$ to stabilize cationic transition metal complexes has yet to be explored. Alkali metal salts of $[2.1]^-$ are of particular interest due to their potential application as halide abstracting reagents to generate reactive cations. Although $\text{Li}[2.1]$ has been prepared,¹⁵⁸ the heavier alkali salts of $[2.1]^-$ have not been reported. In this chapter, the synthesis and characterization of sodium and potassium salts of $[2.1]^-$ will be discussed. Preliminary investigation showed that $\text{K}[2.1]$ is an effective halide abstracting reagent, in particular for $(\text{dppp})\text{PdCl}_2$ [$\text{dppp} = 1,3\text{-bis}(\text{diphenylphosphino})\text{propane}$] and $[(\text{cod})\text{RhCl}]_2$.

2.2 Results and Discussion

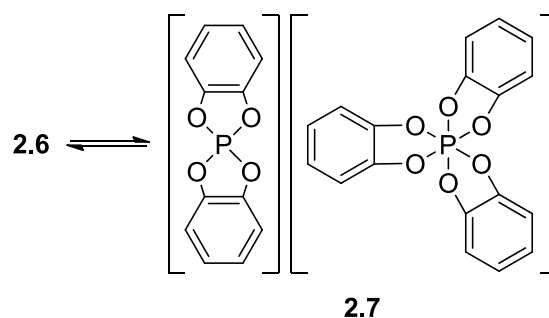
2.2.1 Synthesis and Characterization of Alkali Metals Salts of $[2.1]^-$

It is well established that the reaction of phosphorus(V) chloride with catechol (3 equiv) affords a mixture of **2.5** and **2.6** (Scheme 2.1).¹⁶⁰ The lithium salt of $[2.1]^-$ has previously been

prepared by treating this mixture with ${}^n\text{BuLi}$.¹⁵⁷⁻¹⁵⁸ Since ${}^n\text{BuK}$ is not readily available, the preparation of $\text{K}[\mathbf{2.1}]$ was attempted by treating this mixture of $\mathbf{2.5}$ and $\mathbf{2.6}$ in THF with potassium hydride. The ${}^{31}\text{P}$ NMR spectrum of the reaction mixture exhibits signals assigned to starting material $\mathbf{2.6}$ ($\delta = -27$)¹⁶⁰⁻¹⁶¹ and to a product with a chemical shift consistent with $[\mathbf{2.1}]^-$ ($\delta = -83$),^{158,162-164} tentatively assigned as $\text{K}[\mathbf{2.1}]$. Interestingly, upon isolation and redissolution of the crude product in $\text{DMSO-}d_6$, the ${}^{31}\text{P}$ NMR spectrum showed signals at 13 ppm and -83 ppm, suggesting the formation of the known $\mathbf{2.7}$ (Scheme 2.2).¹⁶⁰ Unfortunately, isolation of $\text{K}[\mathbf{2.1}]$ from this mixture has thus far been unsuccessful.

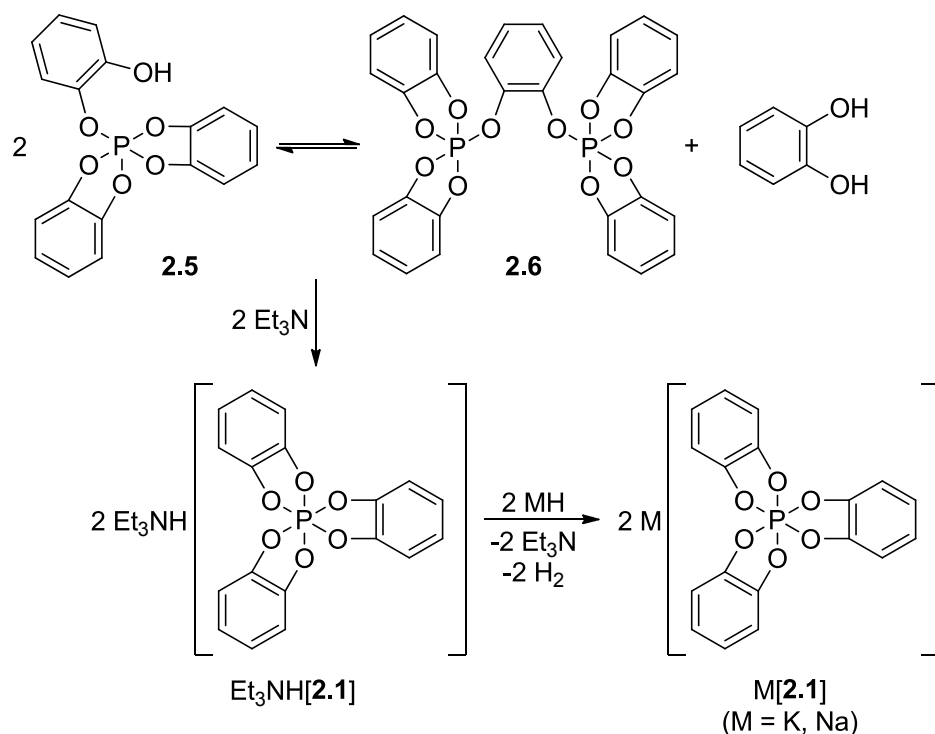


Scheme 2.1 Reaction of potassium hydride with a mixture of $\mathbf{2.5}$ and $\mathbf{2.6}$.



Scheme 2.2 Formation of **2.7** in DMSO- d_6 .

As an alternate strategy to synthesize K[**2.1**], the known ammonium salt, Et₃NH[**2.1**],^{150,152-153} was deprotonated with a slurry of potassium hydride (1.1 equiv) in acetonitrile (Scheme 2.3). After workup, the desired product, K[**2.1**], was isolated as a white solid. Characterization by ³¹P NMR spectroscopy in CD₂Cl₂ revealed a singlet resonance at -86.1 ppm, consistent with the presence of [**2.1**]⁻. The ¹H and ¹³C{¹H} NMR spectra show only signals in the aromatic region as expected for K[**2.1**], free of coordinated solvents. In particular, three signals are observed in the ¹³C{¹H} NMR spectrum, which is consistent with the symmetrical [**2.1**]⁻. Satisfactory elemental microanalysis was obtained for K[**2.1**]. Following an analogous procedure, the sodium salt, Na[**2.1**], was prepared and characterized by ³¹P, ¹H and ¹³C{¹H} NMR spectroscopy and elemental analysis.



Scheme 2.3 Synthesis of $\text{M}[\mathbf{2.1}]$ ($\text{M} = \text{K}, \text{Na}$).

Efforts to obtain single crystals of $\text{K}[\mathbf{2.1}]$ from CH_2Cl_2 proved unsuccessful; however, crystals obtained from slow diffusion of toluene into a DMSO solution of the crude product were suitable for X-ray diffraction. The molecular structure is shown in Figure 2.1 and reveals a dimeric structure of formulation $\text{K}_2(\text{DMSO})_6[\mathbf{1}]_2 \cdot \text{C}_7\text{H}_8$. Within the asymmetric unit, the two $[\mathbf{2.1}]^-$ anions are of the same stereochemistry; thus, the dimer exists either as $\Delta, \Delta\text{-K}_2(\text{DMSO})_6[\mathbf{1}]_2 \cdot \text{C}_7\text{H}_8$ or $\Lambda, \Lambda\text{-K}_2(\text{DMSO})_6[\mathbf{1}]_2 \cdot \text{C}_7\text{H}_8$. Both enantiomers are present within the crystal and are related by symmetry in the $P\bar{1}$ space group. Each of the potassium cations [$\text{K}(1)$ and $\text{K}(2)$] is seven-coordinate, bound by two terminal DMSO ligands, two bridging DMSO ligands and three oxygen atoms of $[\mathbf{2.1}]^-$. The $[\mathbf{2.1}]^-$ anions are slightly perturbed from binding to the potassium cations, with the bound P–O bonds [avg. 1.721(3) Å; range 1.715(1) to 1.735(1) Å] being slightly longer than the unbound P–O bonds [avg. 1.709(3) Å; range 1.707(1) to 1.714(1) Å]. Overall, the average P–O bond [1.715(5) Å] is longer

than those typically observed for P-O single bonds in triarylphosphates [1.59(1) Å]¹⁶⁵ but is similar to those found in previously reported Et₃NH[**2.1**] [1.708(4) Å].¹⁵³ The phosphorus atoms, P(1) and P(2), show only minor deviation from perfect octahedral geometry. The largest deviation from octahedral angles is 3.68(7)° [O(4)-P(1)-O(5)]. The average endocyclic O-P-O angle [90.9(2)°] within [**2.1**]⁻ is similar to those found in previously reported Et₃NH[**2.1**] [91.4(2)°].¹⁵³ The K-O distances involving [**2.1**]⁻ [avg. 2.855(3) Å] are longer than those involving the DMSO moiety [avg._{terminal} = 2.741(2) Å; avg._{bridging} = 2.680(3) Å].

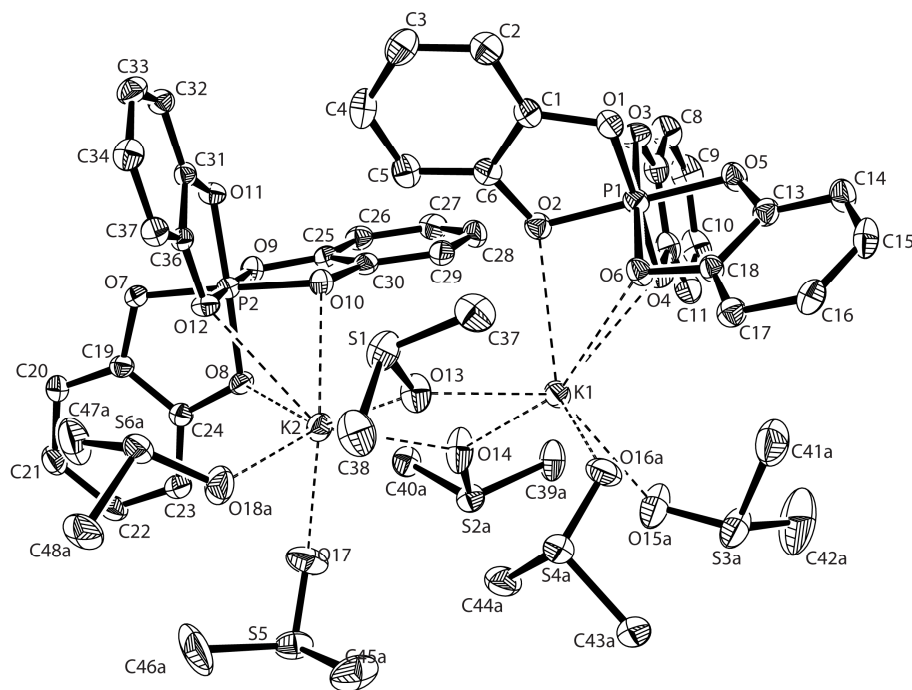


Figure 2.1 Molecular structure of Δ,Δ -K₂(DMSO)₆[**2.1**]₂. Ellipsoids are drawn at the 50% probability level. All hydrogen atoms and the solvent of crystallization (C₇H₈) are omitted for clarity. Selected bond lengths (Å): P(1)-O(1) = 1.714(1); P(1)-O(2) = 1.722(1); P(1)-O(3) = 1.707(1); P(1)-O(4) = 1.721(1); P(1)-O(5) = 1.708(1); P(1)-O(6) = 1.717(1); P(2)-O(7) = 1.710(1); P(2)-O(8) = 1.718(1); P(2)-O(9) = 1.708(1); P(2)-O(10) = 1.715(1); P(2)-O(11) = 1.708(1); P(2)-O(12) = 1.735(1); K(1)-O(2) = 2.876(1); K(1)-O(4) = 2.846(1); K(1)-O(6) = 2.801(1); K(1)-O(13) = 2.696(2); K(1)-O(14) = 2.666(2); K(1)-O(15A) = 2.766(5); K(1)-O(16A) = 2.779(7); K(2)-O(8) = 2.754(1); K(2)-O(10) = 2.965(1); K(2)-O(12) = 2.887(1); K(2)-O(13) = 2.678(2); K(2)-O(14) = 2.681(2); K(2)-O(17) = 2.670(2); K(2)-O(18A) = 2.729(8). Selected bond angles (°): O(1)-P(1)-O(2) = 90.88(6); O(3)-P(1)-O(4) = 91.04(6); O(5)-P(1)-O(6) = 90.67(6); O(7)-P(2)-O(8) = 90.51(6); O(9)-P(2)-O(10) = 91.44(6); O(11)-P(2)-O(12) = 90.76(6).

Recrystallization of K[**2.1**] from acetonitrile gave a different structure (Figure 2.2). Remarkably, the molecular structure consists of macrocyclic hexamers of formulation $\{K(\text{MeCN})_2[\mathbf{2.1}]\}_6$ with S_6 point group symmetry. The potassium cations [K(1) and K(1*)] bridge two κ^3 -bound $[\mathbf{2.1}]^-$ anions and are further coordinated by two acetonitrile ligands, making the K^+ cations eight coordinate. The K–O distances [avg. 2.883(2) Å] are slightly longer than the corresponding K–O distances in $K_2(\text{DMSO})_6[\mathbf{1}]_2 \cdot \text{C}_7\text{H}_8$ [avg. 2.855(3) Å]. The $[\mathbf{2.1}]^-$ anions are situated at the vertices of a hexagon and their stereochemistry alternates between Λ and Δ around the ring. The phosphorus atoms, P(1) and P(1*), show only minor deviation from perfect octahedral geometry. The largest deviation from octahedral angles is 3.86(6)° [O(4)-P(1)-O(5)]. The metrical parameters within $[\mathbf{2.1}]^-$ [avg. P–O = 1.712(2) Å and avg. O–P–O = 91.23(8)°] are comparable to those found in $K_2(\text{DMSO})_6[\mathbf{2.1}]_2 \cdot \text{C}_7\text{H}_8$ [avg. P–O = 1.715(5) Å and avg. O–P–O = 90.9(2)°]. Each of the hexagonal $\{K(\text{MeCN})_2[\mathbf{2.1}]\}_6$ macrocycles has an outside diameter of ca. 25 Å and a very small hole (≤ 2.5 Å). In the crystalline lattice, these macrocycles are organized into a one-dimensional array with spacing of ca. 9.4 Å (Figure 2.3).

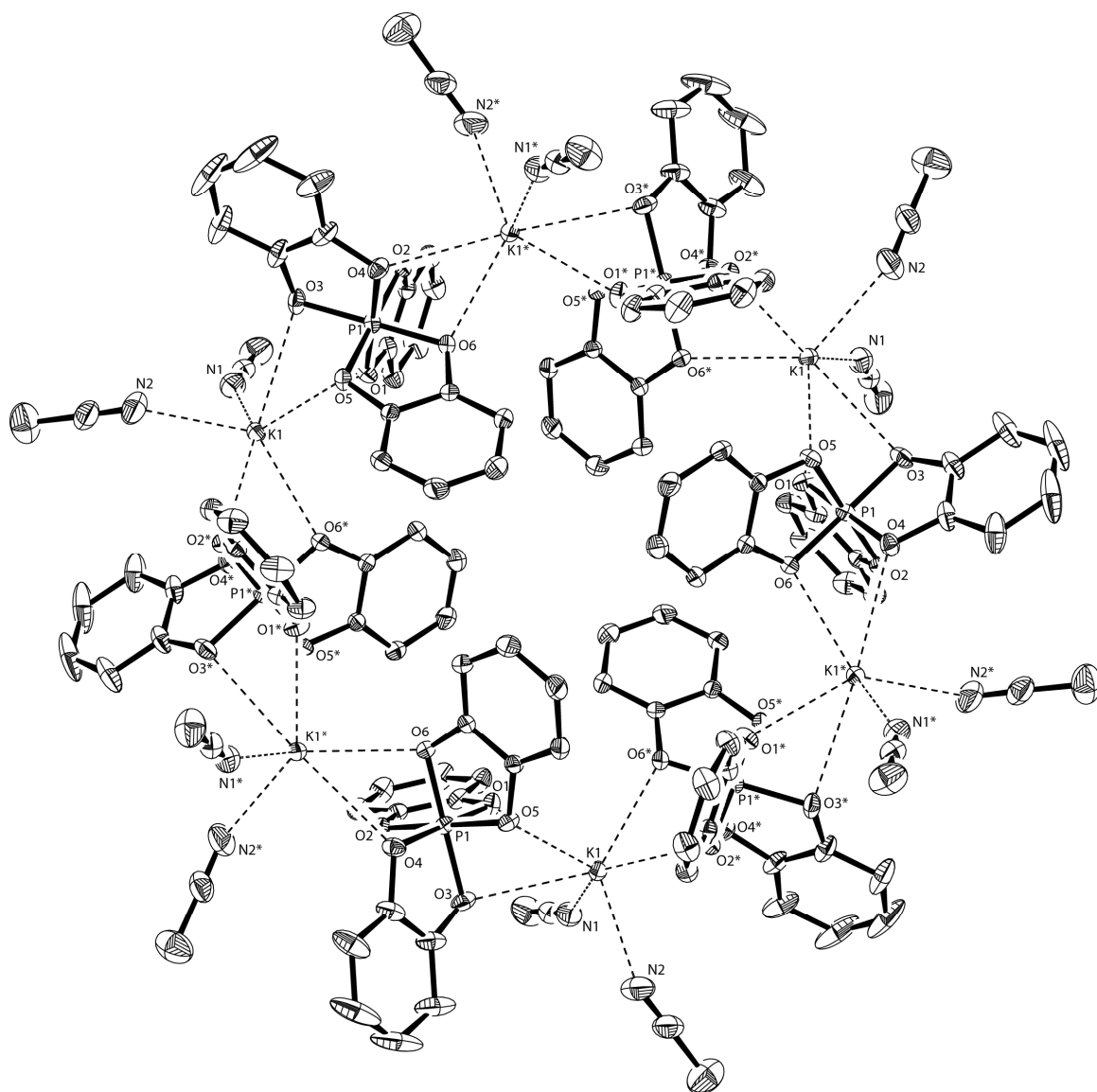


Figure 2.2 Molecular structure of $\{K(\text{MeCN})_2[2.1]\}_6$. Ellipsoids are drawn at the 50% probability level. All hydrogen atoms are omitted for clarity. Selected bond lengths (Å): O(1)-P(1) = 1.7149(9); O(2)-P(1) = 1.7111(9); O(3)-P(1) = 1.7189(9); O(4)-P(1) = 1.7207(9); O(5)-P(1) = 1.7058(9); O(6)-P(1) = 1.7024(9); K(1)-O(1) = 2.7770(9); K(1)-O(3) = 3.019(1); K(1)-O(5) = 2.8244(9); K(1*)-O(2) = 2.8832(9); K(1*)-O(4) = 3.024(1); K(1*)-O(6) = 2.7705(9). Selected bond angles (°): O(1)-P(1)-O(2) = 91.06(4); O(3)-P(1)-O(4) = 91.11(5); O(5)-P(1)-O(6) = 91.53(4).

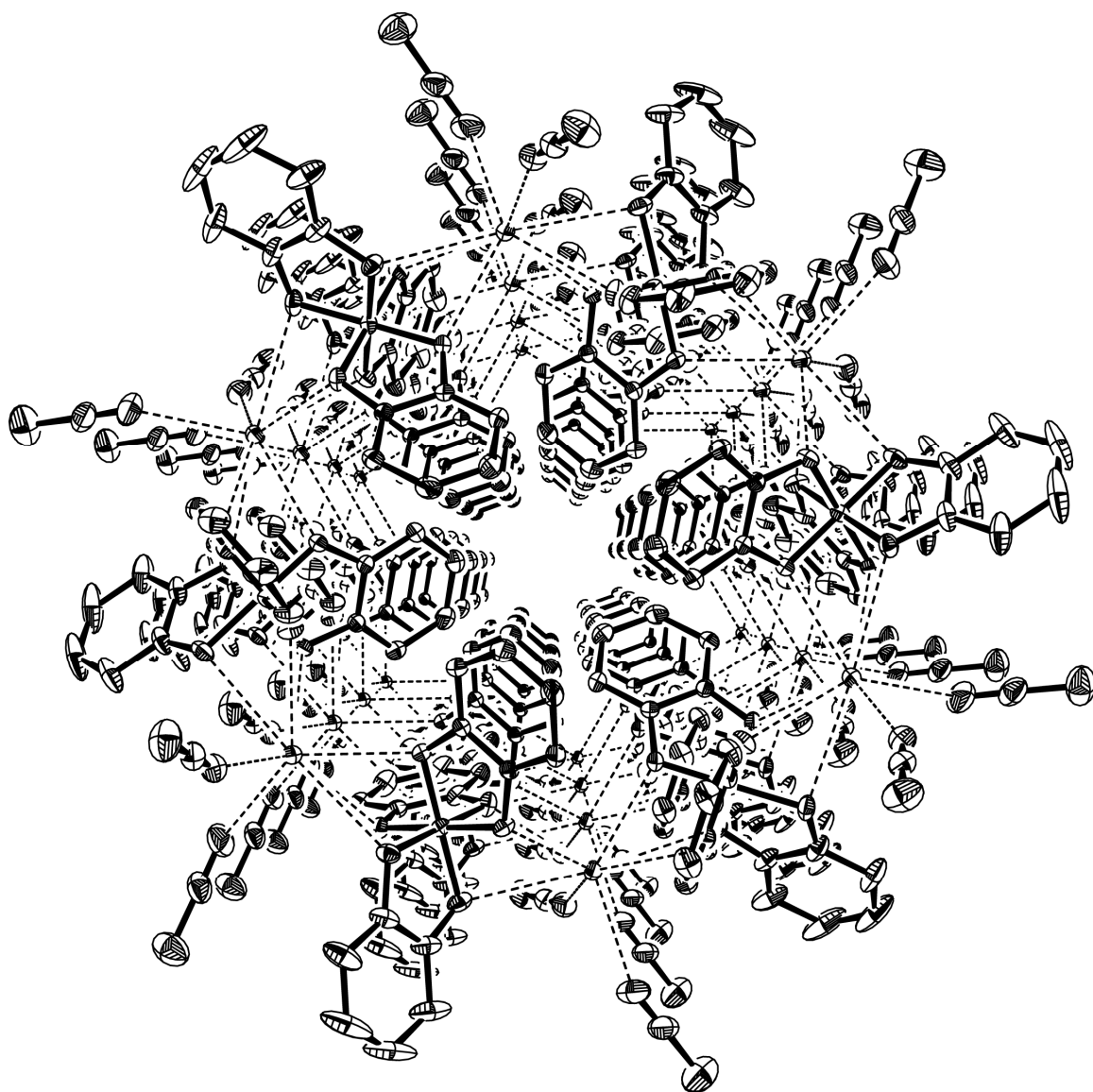
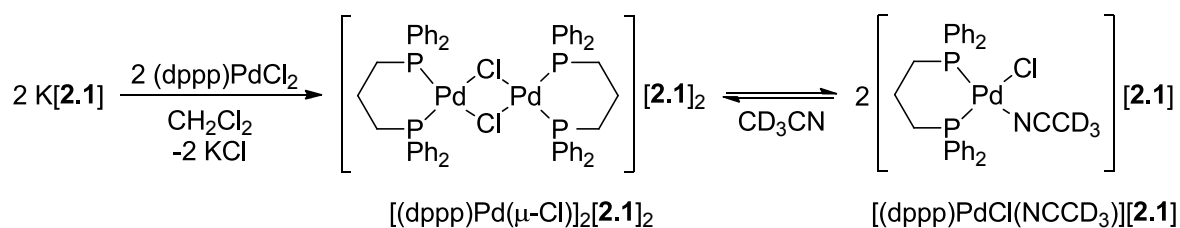


Figure 2.3 Three dimensional stacking of the $\{K(MeCN)_2[2.1]\}_6$. Ellipsoids are drawn at the 50% probability level. All hydrogen atoms are omitted for clarity.

2.2.2 Application of K[2.1] in Metal-Halide Abstraction

As a starting point to testing the efficacy of K[2.1] as a halide abstracting reagent, a mixture of $(dppp)PdCl_2$ [$dppp = 1,3$ -bis(diphenylphosphino)propane] and K[2.1] was dissolved in chloroform (Scheme 2.4). The ^{31}P NMR spectrum of the yellow reaction solution, after filtration to remove KCl, showed singlet resonances at 12.4 and -84.2 ppm. Single crystals suitable for X-ray diffraction were obtained upon slow evaporation of the reaction mixture. The

molecular structure of the chloro-bridged dimer $[(\text{dppp})\text{Pd}(\mu\text{-Cl})_2][\mathbf{2.1}]_2$ is shown in Figure 2.4 and confirms the successful abstraction of a Cl^- ion with $\text{K}[\mathbf{2.1}]$. There is a crystallographically imposed inversion center between the Pd atoms [Pd(1) and Pd(1*)]. The metrical parameters of $[(\text{dppp})\text{Pd}(\mu\text{-Cl})_2][\mathbf{2.1}]_2$ are unremarkable, being similar to those of related dimeric structures, such as $[(\text{dppp})\text{Pd}(\mu\text{-Cl})_2][\text{SO}_4]_2$,¹⁶⁶ $[(\text{dppe})\text{Pd}(\mu\text{-Cl})_2][\text{X}]_2$ ($\text{X} = \text{ClO}_4^-$, BF_4^-),¹⁶⁷⁻¹⁶⁸ $[(\text{dppen})\text{Pd}(\mu\text{-Cl})_2][\text{CF}_3\text{SO}_3]_2$ [$\text{dppen} = 1,2\text{-bis}(\text{diphenylphosphino})\text{ethene}$],¹⁶⁹ $[(o\text{-C}_6\text{H}_4(\text{CH}_2\text{PPh}_2)_2)\text{Pd}(\mu\text{-Cl})_2][\text{PF}_6]_2$,¹⁷⁰ and $[(\text{Ph}_3\text{P})_2\text{Pd}(\mu\text{-Cl})_2][\text{BF}_4]_2$.¹⁷¹ Significantly, the molecular structure suggests weak ion-pair interactions are present between the $[(\text{dppp})\text{Pd}(\mu\text{-Cl})_2]^{2+}$ cation and the $[\mathbf{2.1}]^-$ anions. The closest contact is between an oxygen of the $[\mathbf{2.1}]^-$ anion and a hydrogen of the CH_2 moiety within the dppp ligand [$\text{O}(1)\cdots\text{H}(33\text{b}) = 2.208(1) \text{ \AA}$] and it is within the sum of the van der Waals radii for oxygen and hydrogen [$r_{\text{vdw}} = 2.72 \text{ \AA}$].¹⁷² The phosphorus atom in $[\mathbf{2.1}]^-$, P(1), shows only minor deviation from perfect octahedral geometry. The largest deviation from octahedral angles is $3.57(8)^\circ$ [$\text{O}(2)\text{-P}(1)\text{-O}(3)$]. The metrical parameters within $[\mathbf{2.1}]^-$ [avg. P–O = $1.715(4) \text{ \AA}$ and avg. O–P–O = $91.0(1)^\circ$] are consistent with those found in $\text{K}_2(\text{DMSO})_6[\mathbf{2.1}]_2 \cdot \text{C}_7\text{H}_8$ and $\{\text{K}(\text{MeCN})_2[\mathbf{2.1}]\}_6$. Noteworthy is the fact that the molecular structure is consistent with the aforementioned ^{31}P NMR spectroscopic data for the reaction mixture with equivalent phosphine moieties of dppp ($\delta = 12.4$) and $[\mathbf{2.1}]^-$ ($\delta = -84.2$). It was not possible to dissolve the crystals in weakly-coordinating solvents (e.g. CDCl_3 or CD_2Cl_2). As such, crystals of $[(\text{dppp})\text{Pd}(\mu\text{-Cl})_2][\mathbf{2.1}]_2$ were dissolved in acetonitrile- d_3 for further spectroscopic analysis. Interestingly, the CD_3CN solution showed inequivalent phosphine moieties [$\delta = 15.1$ (br s), 10.3 (br s)] and $[\mathbf{2.1}]^-$ ($\delta = -81.7$) (Figure 2.5). These data are consistent with the solution structure being $[(\text{dppp})\text{PdCl}(\text{NCCD}_3)][\mathbf{2.1}]$ which appears to be in equilibrium with $[(\text{dppp})\text{Pd}(\mu\text{-Cl})_2][\mathbf{2.1}]_2$ (Scheme 2.4), since in some instances signals attributed to both species are observed.



Scheme 2.4 Halide abstraction of (dppp)PdCl₂ with K[**2.1**].

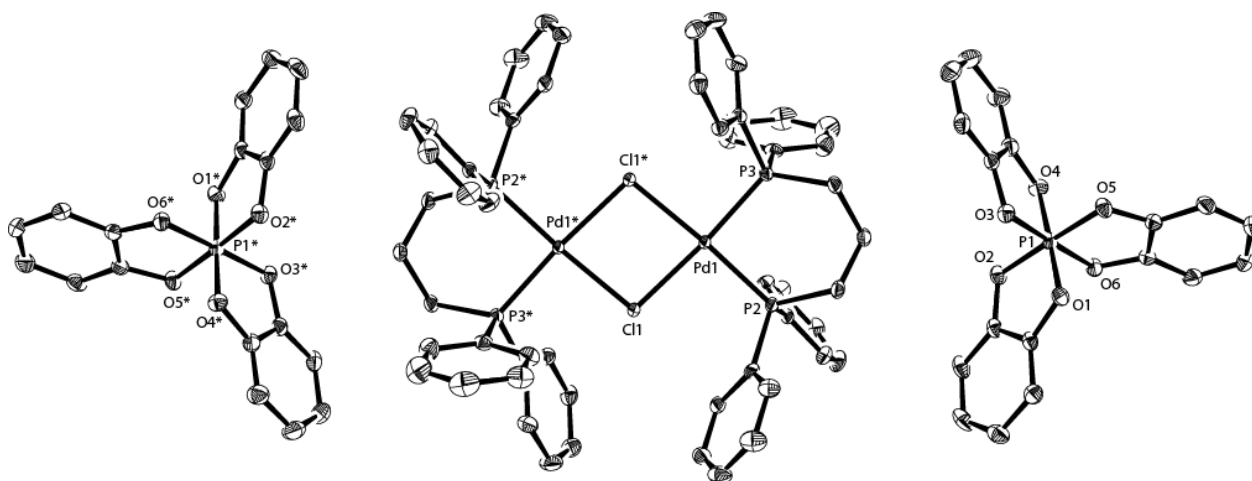


Figure 2.4 Molecular structure of $[(\text{dppp})\text{Pd}(\mu_2\text{-Cl})_2][\mathbf{2.1}]_2$. Ellipsoids are drawn at the 50% probability level. All hydrogen atoms and the solvent of crystallization ($2 \times \text{CHCl}_3$) are omitted for clarity. Selected bond lengths (Å): P(1)-O(1) = 1.713(2); P(1)-O(2) = 1.710(2); P(1)-O(3) = 1.713(2); P(1)-O(4) = 1.708(2); P(1)-O(5) = 1.724(2); P(1)-O(6) = 1.720(2); Pd(1)-P(2) = 2.2489(5); Pd(1)-P(3) = 2.2598(5); Pd(1)-Cl(1) = 2.4024(5); Pd(1)-Cl(1*) = 2.4004(5). Selected bond angles (°): O(1)-P(1)-O(2) = 90.88(7); O(3)-P(1)-O(4) = 91.24(7); O(5)-P(1)-O(6) = 90.93(7); P(2)-Pd(1)-P(3) = 91.10(2); Cl(1)-Pd(1)-Cl(1*) = 83.22(2).

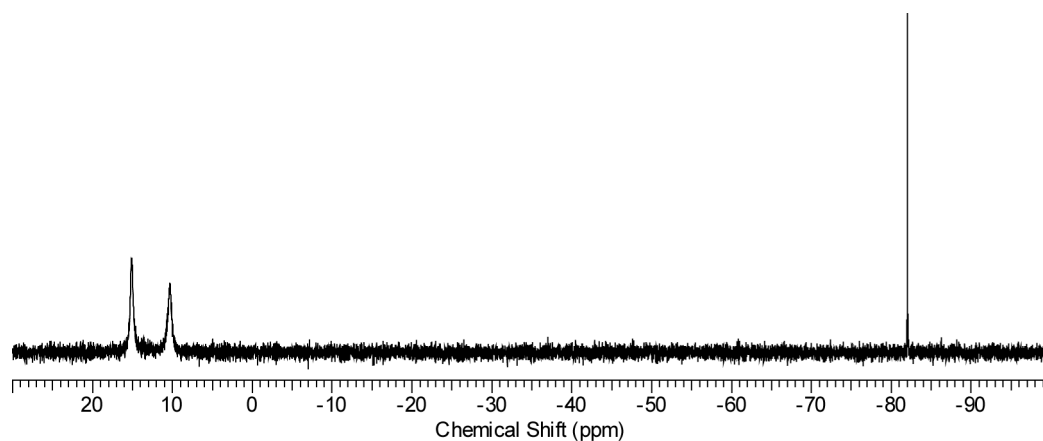
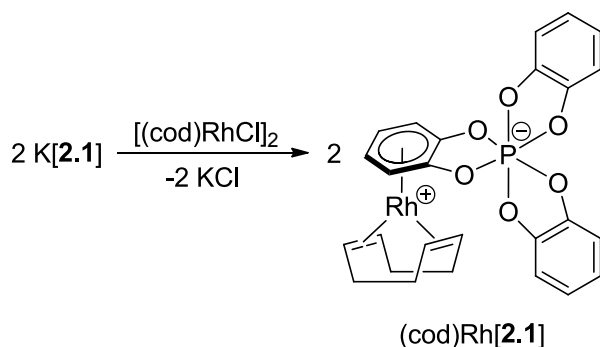


Figure 2.5 ^{31}P NMR (162 MHz, CD_3CN) spectrum of $[(\text{dppp})\text{PdCl}(\text{NCCD}_3)][\mathbf{2.1}]$ at 25 °C.

Given that K[**2.1**] was an effective halide abstraction reagent for palladium(II)-chloride bonds, we further examined the efficacy of K[**2.1**] as a halide abstraction reagent with the rhodium(I) dimer, [(cod)RhCl]₂. To a mixture of [(cod)RhCl]₂ and K[**2.1**] (2 equiv) was added acetonitrile and the yellow mixture was stirred overnight (Scheme 2.5). Recrystallization of the crude product from dichloromethane afforded orange crystals. The molecular structure is shown in Figure 2.6 and reveals that [**2.1**][−] is η⁶-bound to the rhodium(I) center to afford the zwitterionic (cod)Rh[**2.1**]. Similar cation-anion interactions have been noted in the solid-state structures of similar rhodium(I) complexes containing the weakly coordinating anions [BPh₄][−] and [B(3,5-C₆H₃(CF₃)₂)₄][−].¹⁷³⁻¹⁷⁴ The distances between the centroid of the η⁶-bound aromatic ring and the rhodium(I) center are 1.859(6) for Rh(1) and 1.867(5) Å for Rh(2) [avg. 1.863(8) Å]. For comparison, the analogous distance in Rh(dppe)[BPh₄] is 1.860(1) Å whereas this distance in (cod)Rh[B(3,5-C₆H₃(CF₃)₂)₄] is 1.836(4) Å. The anion-cation interaction results in a lowering of the symmetry about phosphorus with the four P–O bonds of the uncoordinated catechol [avg. 1.700(7) Å] being shorter than the P–O bonds of the coordinated catechol [avg. 1.745(4) Å]. The crystals were further characterized by ¹H and ³¹P NMR spectroscopy and elemental microanalysis. The ³¹P NMR spectrum (CD₂Cl₂) displayed a singlet resonance at −79.9 ppm, which is shifted downfield compared to K[**2.1**] (δ = −86.1) and is consistent with the retention of coordination complex in solution. Comparison of the ¹H NMR spectra (CD₂Cl₂) of K[**2.1**] and (cod)Rh[**1**] in the aromatic region show a loss of symmetry for the aryl-*H* moieties in (cod)Rh[**1**] and provides further evidence that the complex structure of (cod)Rh[**1**] is retained in solution (Figure 2.7).



Scheme 2.5 Halide abstraction of $[(\text{cod})\text{RhCl}]_2$ with K[2.1] .

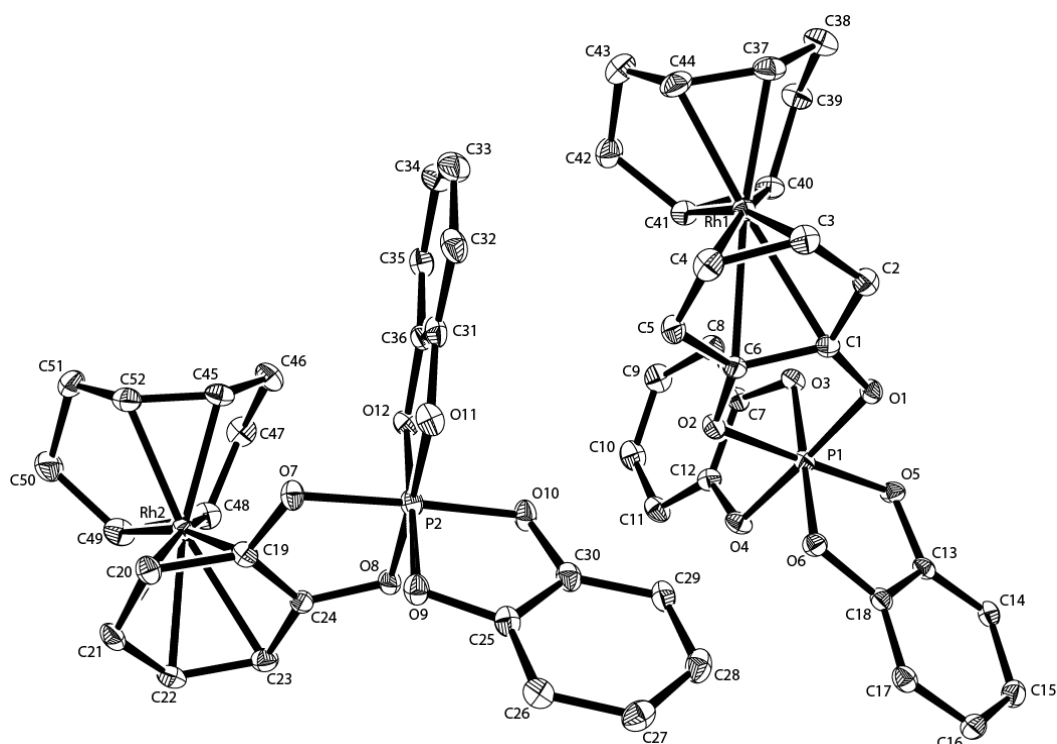


Figure 2.6 Molecular structure of (cod)Rh[2.1]. Ellipsoids are drawn at the 50% probability level. All hydrogen atoms and solvents of crystallization ($2.5 \times \text{CH}_2\text{Cl}_2$) are omitted for clarity. Selected bond lengths (Å): P(1)-O(1) = 1.747(3); P(1)-O(2) = 1.746(3); P(1)-O(3) = 1.695(2); P(1)-O(4) = 1.699(3); P(1)-O(5) = 1.706(3); P(1)-O(6) = 1.702(2); P(2)-O(7) = 1.746(3); P(2)-O(8) = 1.739(3); P(2)-O(9) = 1.703(2); P(2)-O(10) = 1.702(3); P(2)-O(11) = 1.697(3); P(2)-O(12) = 1.697(2); Rh(1)-C(1) = 2.405(4); Rh(1)-C(2) = 2.373(4); Rh(1)-C(3) = 2.262(3); Rh(1)-C(4) = 2.280(3); Rh(1)-C(5) = 2.355(4); Rh(1)-C(6) = 2.371(4); Rh(1)-C(37) = 2.127(5); Rh(1)-C(40) = 2.151(3); Rh(1)-C(41) = 2.136(3); Rh(1)-C(44) = 2.130(5); Rh(2)-C(19) = 2.364(3); Rh(2)-C(20) = 2.307(3); Rh(2)-C(21) = 2.286(3); Rh(2)-C(22) = 2.254(4); Rh(2)-C(23) = 2.357(5); Rh(2)-C(24) = 2.431(3); Rh(2)-C(45) = 2.125(4); Rh(2)-C(48) = 2.136(3); Rh(2)-C(49) = 2.124(3); Rh(2)-C(52) = 2.146(5). Selected bond angles (°): O(1)-P(1)-O(2) = 89.4(1); O(3)-P(1)-O(4) = 91.7(1); O(5)-P(1)-O(6) = 91.7(1); O(7)-P(2)-O(8) = 89.7(1); O(9)-P(2)-O(10) = 91.6(1); O(11)-P(2)-O(12) = 91.8(1).

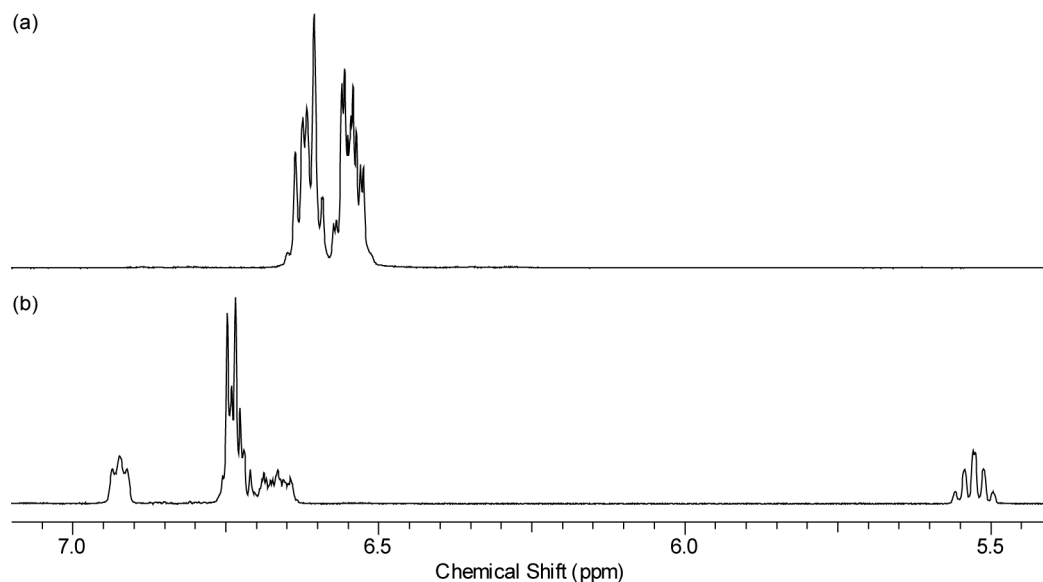


Figure 2.7 (a) ^1H NMR (300 MHz, CD_2Cl_2) spectrum of $\text{K}[\mathbf{2.1}]$ at 25 $^\circ\text{C}$. (b) ^1H NMR (400 MHz, CD_2Cl_2) spectrum of $(\text{cod})\text{Rh}[\mathbf{2.1}]$ at 25 $^\circ\text{C}$.

2.3 Summary

Synthetic procedures to access alkali metal salts of the hexacoordinated phosphorus(V)-based $[\mathbf{2.1}]^-$, namely $\text{K}[\mathbf{2.1}]$ and $\text{Na}[\mathbf{2.1}]$, have been presented. Both compounds were characterized spectroscopically. In addition, X-ray crystallographic analysis of $\text{K}[\mathbf{2.1}]$, recrystallized in the presence of either DMSO or MeCN, revealed two distinct crystal structures: a dimeric structure of formulation $\text{K}_2(\text{DMSO})_6[\mathbf{2.1}]_2 \cdot \text{C}_7\text{H}_8$ and a hexagonal macrocycle with formulation $\{\text{K}(\text{MeCN})_2[\mathbf{2.1}]\}_6$. Solvent-free $\text{K}[\mathbf{2.1}]$ was shown to be an effective halide abstractor for $(\text{dppp})\text{PdCl}_2$ [$\text{dppp} = 1,3\text{-bis}(\text{diphenylphosphino})\text{propane}$] (1:1 ratio) and $[(\text{cod})\text{RhCl}]_2$ (2:1 ratio) to generate the dimeric $[(\text{dppp})\text{Pd}(\mu\text{-Cl})]_2[\mathbf{2.1}]_2$ and the zwitterionic $(\text{cod})\text{Rh}[\mathbf{2.1}]$, both of which were structurally characterized.

2.4 Experimental Section

2.4.1 General Procedures

All manipulations were performed using standard Schlenk or glove box techniques under nitrogen atmosphere. THF was dried over sodium/benzophenone ketyl and distilled prior to use. Triethylamine, dichloromethane, acetonitrile and CD₃CN (Cambridge Isotope Laboratories Inc.) were dried over calcium hydride and distilled prior to use. DMSO was dried over 3Å molecular sieves and distilled prior to use. Et₂O and toluene were deoxygenated with nitrogen and dried by passing through a column containing activated alumina. PCl₅ (Aldrich) was sublimed prior to use. Potassium hydride (30 wt % dispersion in mineral oil) was purchased from Aldrich, washed with hexanes and dried *in vacuo* prior to use. Sodium hydride (Aldrich, dry 95%), catechol (Aldrich), CD₂Cl₂ (Cambridge Isotope Laboratories Inc. in 1 g sealed ampules) and [(cod)RhCl]₂ (Strem) were used as received. Mixture **2.5** / **2.6**¹⁶⁰ and [(dppp)PdCl₂]¹⁷⁵ [dppp = 1,3-bis(diphenylphosphino)propane] were prepared following literature procedures. ¹H, ¹³C{¹H} and ³¹P NMR spectra were recorded at 25 °C on Bruker Avance 300 or 400 MHz spectrometers. 85% H₃PO₄ was used as an external standard (δ 0.0) for ³¹P NMR spectra. ¹H NMR spectra were referenced to residual protonated solvent, and ¹³C{¹H} NMR spectra were referenced to the deuterated solvent. Elemental analyses were performed in the University of British Columbia Chemistry Microanalysis Facility.

2.4.2 Synthesis of K[2.1]

To a stirred mixture of **2.5** and **2.6** (1.8 g, 5.1 mmol) in THF (15 mL) was added triethylamine (0.58 g, 5.7 mmol). An immediate precipitate was observed. After the reaction mixture was stirred for 30 min, the precipitate was isolated by centrifugation and the solid was dried *in vacuo*. To a suspension of this colorless solid in acetonitrile (10 mL) was added

potassium hydride (0.23 g, 5.7 mmol). The evolution of a gas was observed. After the mixture was stirred for 30 min, the solvent was removed *in vacuo* and the resultant white residue was dissolved in THF (40 mL). The solution was filtered to remove insoluble salts and the filtrate was evaporated to dryness to afford a white solid. The solid was dissolved in minimal dichloromethane (3 mL) and Et₂O (100 mL) was added to precipitate the product, which was collected by filtration and dried *in vacuo* at 130 °C. Yield = 1.4 g (70%).

³¹P NMR (121 MHz, CD₂Cl₂): δ -86.1 (s); ¹H NMR (300 MHz, CD₂Cl₂): δ 6.65-6.59 (m, 6H, Ar-H), 6.57-6.53 (m, 6H, Ar-H); ¹³C{¹H} NMR (101 MHz, CD₂Cl₂): δ 144.5 (d, *J*_{CP} = 4 Hz), 121.3 (s), 110.8 (d, *J*_{CP} = 16 Hz). Anal. Calcd. for C₁₈H₁₂KO₆P: C, 54.82; H, 3.07. Found: C, 54.58; H, 3.20. X-ray quality crystals of K₂(DMSO)₆[**2.1**]₂, were obtained from slow diffusion of toluene into a DMSO solution of K[**2.1**] for ca. 1 week. X-ray quality crystals of {K(NCMe)₂[**2.1**]}₆, were obtained from slow evaporation of a concentrated solution of K[**2.1**] in toluene/MeCN for 8 days.

2.4.3 Synthesis of Na[**2.1**]

To a stirred mixture of **2.5** and **2.6** (0.55 g, 1.5 mmol) in THF (5 mL) was added triethylamine (0.18 g, 1.8 mmol). An immediate precipitate was observed. After the reaction mixture was stirred for 15 min, the precipitate was isolated by centrifugation and the solid was dried *in vacuo*. To a suspension of this white solid in acetonitrile (10 mL) was added sodium hydride (0.039 g, 1.6 mmol). The evolution of a gas was observed. After the mixture was refluxed for 30 min, the solvent was removed *in vacuo* and the resultant white residue was dissolved in THF (15 mL). The solution was filtered to remove insoluble salts and the filtrate was evaporated to dryness to afford a white solid. The solid was dried *in vacuo* at 120 °C. Yield = 0.47 g (80%).

^{31}P NMR (162 MHz, CD_3CN): δ -82.9 (s); ^1H NMR (400 MHz, CD_3CN): δ 6.67-6.65 (m, 12H, Ar-H); $^{13}\text{C}\{^1\text{H}\}$ NMR (101 MHz, CD_2Cl_2): δ 146.4 (d, $J_{\text{CP}} = 5$ Hz), 120.5 (s), 110.5 (d, $J_{\text{CP}} = 17$ Hz). Anal. Calcd. for $\text{C}_{18}\text{H}_{12}\text{NaO}_6\text{P}$: C, 57.16; H, 3.20. Found: C, 57.50; H, 3.44.

2.4.4 Synthesis of [(dppp)Pd(μ -Cl)]₂[2.1]₂

To a solid mixture of (dppp)PdCl₂ (50 mg, 0.085 mmol) and K[2.1] (34 mg, 0.086 mmol) was added chloroform (2 mL). The yellow reaction solution was stirred overnight and filtered through celite. The ^{31}P NMR spectrum of the reaction mixture showed singlet resonances at 12.4 and -84.2 ppm. Slow evaporation of the yellow solution afforded yellow crystals suitable for X-ray diffraction. Yield = 32 mg (41%).

^{31}P NMR (162 MHz, CD_3CN): δ 15.1 (br s, dppp), 10.3 (br s, dppp), -81.7 (s, [2.1]⁻); ^1H NMR (400 MHz, CD_3CN): δ 7.69-7.45 (m, 20H, Ar-H of dppp), 6.64-6.58 (m, 12H, Ar-H of anion), 2.67 (br s, 4H, PCH₂), 2.15-1.99 (m, 2H, CH₂CH₂CH₂); $^{13}\text{C}\{^1\text{H}\}$ NMR (101 MHz, CD_3CN): δ 146.9 (d, $J_{\text{CP}} = 5$ Hz), 134.3 (d, $J_{\text{CP}} = 11$ Hz), 133.4 (s), 130.18 (s), 128.5 (s), 127.9 (s), 120.0 (s), 110.9 (d, $J_{\text{CP}} = 17$ Hz), 24.1 (br s), 19.2 (s). Anal. Calcd. for $\text{C}_{45}\text{H}_{38}\text{ClO}_6\text{P}_3\text{Pd}$: C, 59.42; H, 4.21. Found: C, 59.06; H, 4.00.

2.4.5 Synthesis of (cod)Rh[2.1]

To solid mixture of K[2.1] (83 mg, 0.21 mmol) and [(cod)RhCl]₂ (51 mg, 0.10 mmol) was added acetonitrile (3 mL). The resulting cloudy yellow mixture was stirred overnight, followed by the removal of all volatiles *in vacuo*. The yellow residue was dissolved in dichloromethane (3 mL) and filtered to remove a small amount of insoluble material. Slow evaporation of the solution yield orange crystals suitable for X-ray diffraction. Yield = 33 mg (52%).

^{31}P NMR (161 MHz, CD_2Cl_2): δ -79.9 (s); ^1H NMR (400 MHz, CD_2Cl_2): δ 6.94-6.91 (m, 2H, Ar-*H*), 6.76-6.64 (m, 8H, Ar-*H*), 5.56-5.50 (m, 2H, Ar-*H*), 5.33 (s, 1.25H, CH_2Cl_2), 4.69-4.39 (m, 4H, $\text{HC}=\text{CH}$ in COD), 2.44-2.03 (m, 8H, CH_2 in COD); Anal. Calcd. for $\text{C}_{26}\text{H}_{24}\text{O}_6\text{PRh}\cdot 1.25\text{CH}_2\text{Cl}_2$: C, 48.67; H, 3.97. Found: C, 48.53; H, 3.95.

2.4.6 X-ray Crystallography

All single crystals were immersed in oil and were mounted on a glass fiber. Data were collected on a Bruker X8 APEX II diffractometer with graphite-monochromated Mo $\text{K}\alpha$ radiation. Data were collected and integrated using the Bruker SAINT¹⁷⁶ software package and corrected for absorption effect using SADABS.¹⁷⁷ All structures were solved by direct methods and subsequent Fourier difference techniques. Unless noted, all non-hydrogen atoms were refined anisotropically, whereas all hydrogen atoms were included in calculated positions but not refined. All data sets were corrected for Lorentz and polarization effects. All refinements were performed using the SHELXTL¹⁷⁸⁻¹⁷⁹ crystallographic software package from Bruker-AXS.

Compounds $\{\text{K}(\text{NCMe})_2[\mathbf{2.1}]\}_6$ and $(\text{cod})\text{Rh}[\mathbf{2.1}]$ did not show any crystallographic complexity. The molecular structure of $\text{K}_2(\text{DMSO})_6[\mathbf{1}]_2$ contains five disordered molecules of DMSO bound to K(1) and K(2). Each of the disordered DMSO molecules was modeled in two orientations and refined with combinations of SADI, DANG, SIMU and EADP where needed. Their respective populations were refined and the final occupancy of the major orientations are 0.802(2), 0.822(2), 0.855(2), 0.73(3), and 0.922(2). $(\text{cod})\text{Rh}[\mathbf{2.1}]$ crystallizes with two molecules of $(\text{cod})\text{Rh}[\mathbf{2.1}]$ and 2.5 equivalent of dichloromethane per asymmetric unit. The other half equivalent of dichloromethane is related through an inversion center. Crystal data and refinement parameters are listed in Table 2.1. CIF files giving supplementary crystallographic data for the

structures reported in this chapter are available from Cambridge Crystallographic Data Centre (CCDC 866633 – 866636).

Table 2.1 X-ray crystallographic data for $K_2(\text{DMSO})_6[\mathbf{2.1}]_2$, $\{[\text{K}(\text{MeCN})_2][\mathbf{2.1}]\}_6$, $[(\text{dppp})\text{Pd}(\mu_2\text{-Cl})_2][\mathbf{2.1}]_2$ and $(\text{cod})\text{Rh}[\mathbf{2.1}]$.

| | $K_2(\text{DMSO})_6[\mathbf{2.1}]_2$ $\cdot \text{C}_7\text{H}_8$ | $\{[\text{K}(\text{MeCN})_2][\mathbf{2.1}]\}_6$ | $[(\text{dppp})\text{Pd}(\mu_2\text{-Cl})_2][\mathbf{2.1}]_2 \cdot 2\text{CHCl}_3$ | $2(\text{cod})\text{Rh}[\mathbf{2.1}]$ $\cdot 2.5\text{CH}_2\text{Cl}_2$ |
|----------------------------------------------|-------------------------------------------------------------------------|------------------------------------------------------------------------------|------------------------------------------------------------------------------------|-----------------------------------------------------------------------------|
| formula | $\text{C}_{55}\text{H}_{68}\text{K}_2\text{O}_{18}\text{P}_2\text{S}_6$ | $\text{C}_{132}\text{H}_{108}\text{K}_6\text{N}_{12}\text{O}_{36}\text{P}_6$ | $\text{C}_{94}\text{H}_{80}\text{Cl}_{14}\text{O}_{12}\text{P}_6\text{Pd}_2$ | $\text{C}_{54.5}\text{H}_{53}\text{Cl}_5\text{O}_{12}\text{P}_2\text{Rh}_2$ |
| fw | 1349.59 | 2858.72 | 2296.50 | 1344.98 |
| cryst syst | triclinic | trigonal | triclinic | triclinic |
| space group | $P\bar{1}$ | $R\bar{3}$ | $P\bar{1}$ | $P\bar{1}$ |
| color | colorless | colorless | yellow | yellow |
| a (Å) | 11.145(1) | 35.6003(9) | 13.6136(5) | 13.479(1) |
| b (Å) | 15.992(2) | 35.6003(9) | 14.0099(5) | 14.978(2) |
| c (Å) | 19.375(2) | 9.3796(2) | 14.3587(5) | 15.072(1) |
| α (deg) | 75.155(6) | 90 | 67.568(2) | 106.636(4) |
| β (deg) | 75.710(6) | 90 | 87.784(2) | 116.413(3) |
| γ (deg) | 86.784(6) | 120 | 77.725(2) | 90.610(4) |
| V (Å ³) | 3234.6(6) | 10294.9(4) | 2470.7(2) | 2577.2(4) |
| T (K) | 173(2) | 173(2) | 173(2) | 173(2) |
| Z | 2 | 3 | 1 | 2 |
| $\mu(\text{Mo K}\alpha)$ (mm ⁻¹) | 0.456 | 0.342 | 0.898 | 1.027 |
| cryst size (mm ³) | $0.50 \times 0.45 \times 0.40$ | $0.75 \times 0.70 \times 0.65$ | $0.60 \times 0.15 \times 0.05$ | $0.45 \times 0.45 \times 0.10$ |
| $D_{\text{calcd.}}$ (Mg m ⁻³) | 1.386 | 1.383 | 1.543 | 1.733 |
| $2\theta(\text{max})$ (°) | 55.8 | 60.0 | 60.0 | 55.8 |
| no. of reflns | 50394 | 36207 | 78226 | 61859 |
| no. of unique data | 15240 | 6660 | 14338 | 12176 |
| R(int) | 0.0389 | 0.0231 | 0.0312 | 0.0296 |
| refln/param ratio | 16.62 | 22.89 | 24.85 | 17.78 |
| R_1 [$I > 2\sigma(I)$] ^a | 0.0410 | 0.0349 | 0.0337 | 0.0371 |
| wR_2 [all data] ^b | 0.0952 | 0.0914 | 0.0810 | 0.1040 |
| GOF | 1.028 | 1.030 | 1.048 | 1.168 |

^a $R_1 = \frac{\sum ||F_o| - |F_c||}{\sum |F_o|}$. ^b $wR_2(F^2[\text{all data}]) = \left\{ \frac{\sum [w(F_o^2 - F_c^2)^2]}{\sum [w(F_o^2)^2]} \right\}^{1/2}$.

Chapter 3: Solid Brønsted Acids with a Weakly Basic Phosphorus(V) Anion*

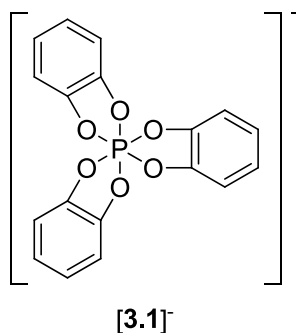
3.1 Introduction

The stabilization of coordinatively unsaturated cations, which are often found as reactive intermediates or active catalysts, necessitates the presence of charge-balancing anions with minimal nucleophilicity, the so-called weakly coordinating anions (WCAs).^{38-39,180} Amongst the number of sophisticated approaches that have been designed to prepare large, charge-delocalized WCAs (e.g. carboranes,^{80,82,94,180-185} fluoroalkoxyaluminates,¹⁸⁶⁻¹⁸⁹ and teflates),^{139,190} the most popular remains to be the fluoroarylborates.^{62-63,65,191-193} Specifically, the diversity of starting materials available for $[\text{B}(3,5\text{-(CF}_3)_2\text{C}_6\text{H}_3)_4]^-$ and $[\text{B}(\text{C}_6\text{F}_5)_4]^-$ (e.g. alkali metal,^{41,51} silver(I),¹⁹⁴⁻¹⁹⁵ thallium(I),¹⁹⁶⁻¹⁹⁷ trityl,^{47,198} dimethylanilinium,¹⁹⁹⁻²⁰⁰ and $[\text{H}(\text{OEt}_2)_2]^+$ salts)^{50,201} have helped to facilitate numerous important advancements in both fundamental²⁰²⁻²¹² and applied chemistry.²¹³⁻²¹⁶

Hexacoordinated phosphorus(V) anions, such as $[\mathbf{3.1}]^-$ and its derivatives, are large, highly symmetrical and charge diffused, which are ideal properties for WCAs. In Chapter 2, preliminary investigation into the efficacy of $[\mathbf{3.1}]^-$ to stabilize reactive cations has led to the synthesis of two new alkali metal salts, namely $\text{K}[\mathbf{3.1}]$ and $\text{Na}[\mathbf{3.1}]$. It was shown that $\text{K}[\mathbf{3.1}]$ is an effective halide abstraction reagent for metal-halide bonds, leading to the isolation of $[(\text{dppp})\text{Pd}(\mu\text{-Cl})_2][\mathbf{3.1}]_2$ [dppp = 1,3-bis(diphenylphosphino)propane] and $(\text{cod})\text{Rh}[\mathbf{3.1}]$. To further facilitate the evaluation of $[\mathbf{3.1}]^-$ as a WCA, Brønsted acids of $[\mathbf{3.1}]^-$ were highly desired for their potential to serve as catalyst activators through the protonolysis of metal-alkyl bonds.

* A version of this chapter has been published. Paul W. Siu and Derek P. Gates. "HL₂[P(1,2-O₂C₆H₄)₃] (L = DMSO or DMF): A Convenient Proton Source with a Weakly Basic Phosphorus(V) Anion" *Organometallics* **2009**, 28, 4491. Copyright 2009 American Chemical Society.

Although ammonium salts of $[3.1]^-$ are known,¹⁵⁰⁻¹⁵¹ their low acidity would limit protonolysis to early transition metal-carbon bonds. In this chapter, the preparation and characterization of solid Brønsted acids $H(DMF)_2[3.1]$ and $H(DMSO)_2[3.1]$ will be described. Preliminary investigation showed that $H(DMF)_2[3.1]$ is effective in the stoichiometric activation of the metal-alkyl bonds of $(dppe)PdMe_2$ [$dppe = 1,2$ -bis(diphenylphosphino)ethane]. The coordinating nature of the anion $[3.1]^-$ will also be discussed.

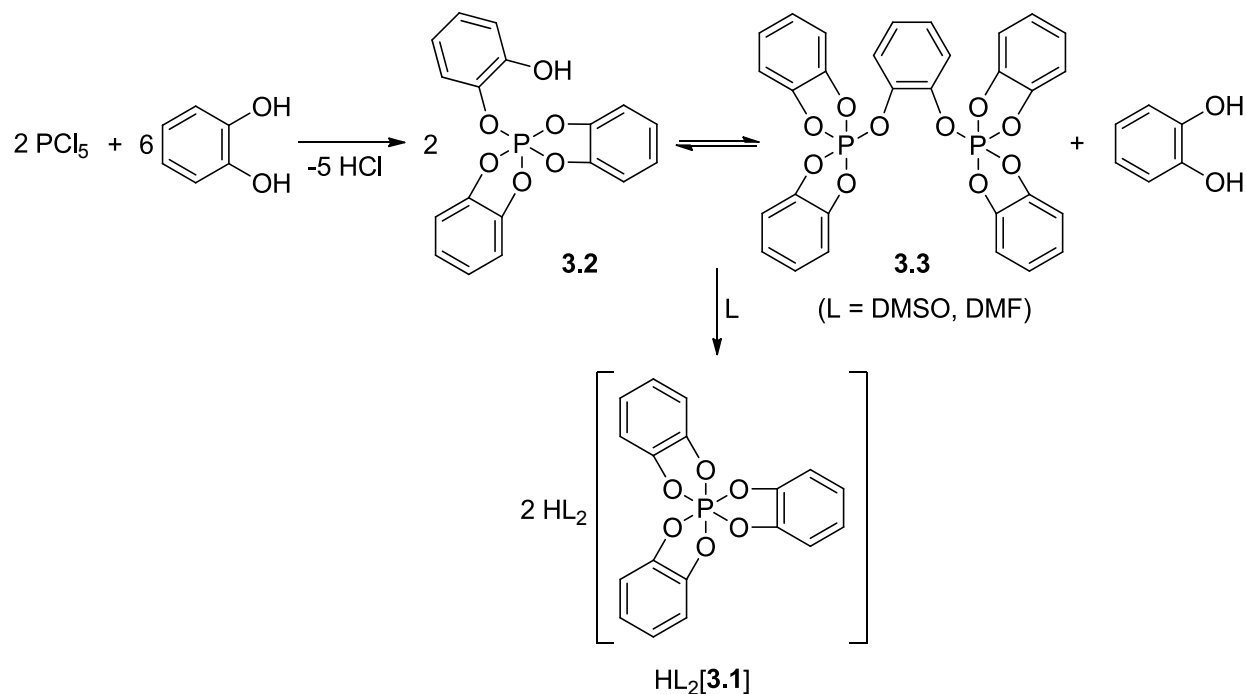


3.2 Results and Discussion

3.2.1 Synthesis and Characterization of Brønsted Acids of $[3.1]^-$

It has been reported that the treatment of PCl_5 with catechol (3 equiv) affords an equilibrium mixture of **3.2** and **3.3**.¹⁶⁰ Interestingly, previous studies of these catechol-containing phosphorus(V) compounds in DMF or DMSO provided evidence for the formation of Brønsted acids of $[3.1]^-$, although no compounds were isolated nor was structural data obtained. The presence of $HL[3.1]$ ($L = DMSO$ or DMF) was inferred on the basis of ^{31}P NMR spectroscopic data which suggested the presence of hexacoordinated $[3.1]^-$ ($\delta = -83.5$).^{164,217} Inspired by this previous work, a mixture of **3.2** and **3.3** was prepared and, subsequently, the mixture was dissolved in DMSO (Scheme 3.1). Following an identical procedure, the mixture of **3.2** and **3.3** was dissolved in DMF. Analysis of each reaction mixture using ^{31}P NMR spectroscopy revealed that the resonances at -28.8 and -29.4 ppm, attributed to **3.2** and **3.3**, respectively, had been

diminished and were replaced by a signal at ca. -80 ppm (DMSO: $\delta = -80.5$; DMF: $\delta = -80.0$) which is similar to those reported previously.^{164,217}



Scheme 3.1 Synthesis of Brønsted acids $\text{HL}_2[\mathbf{3.1}]$ ($\text{L} = \text{DMSO}, \text{DMF}$).

In contrast to previous studies, the Brønsted acids of $[\mathbf{3.1}]^-$ were successfully isolated as analytically pure white solids and spectroscopically characterized. In addition to ^{31}P NMR spectroscopy, each compound was characterized using ^1H and $^{13}\text{C}\{^1\text{H}\}$ NMR spectroscopy and elemental analysis. The ^1H NMR spectra (CD_3CN) of the crystalline solids are shown in Figure 3.1 and Figure 3.2. Of particular importance is the broad downfield signal that is assigned to the acidic proton of $H(\text{DMSO})_2[\mathbf{3.1}]$ ($\delta = 13.3$) and $H(\text{DMF})_2[\mathbf{3.1}]$ ($\delta = 15.3$). In addition, the integrated ratio of the signal assigned to acidic proton and the DMSO protons ($\delta = 2.83$) or the DMF protons ($\delta = 8.06, 3.07$ and 2.95) are consistent with proposed formulations. The slight downfield shift observed for the complex in comparison to free DMSO ($\delta = 2.50$)²¹⁸ or free DMF ($\delta = 7.92, 2.89$ and 2.77)²¹⁸ provides evidence that the $[\text{HL}_2]^+$ moiety is retained in solution ($\text{L} = \text{DMSO}$ or DMF). Remarkably, $\text{H}(\text{DMF})_2[\mathbf{3.1}]$ exhibits excellent stability. At room

temperature, a solid sample of $\text{H}(\text{DMF})_2[\mathbf{3.1}]$ and a solution of $\text{H}(\text{DMF})_2[\mathbf{3.1}]$ in CD_3CN were stored in a glovebox and showed no change in their ^1H and ^{31}P NMR spectra when monitored for over one month. In contrast, the ^{31}P NMR spectrum of a solution of $\text{H}(\text{DMSO})_2[\mathbf{3.1}]$ in CD_3CN shows evidence of decomposition after several hours.

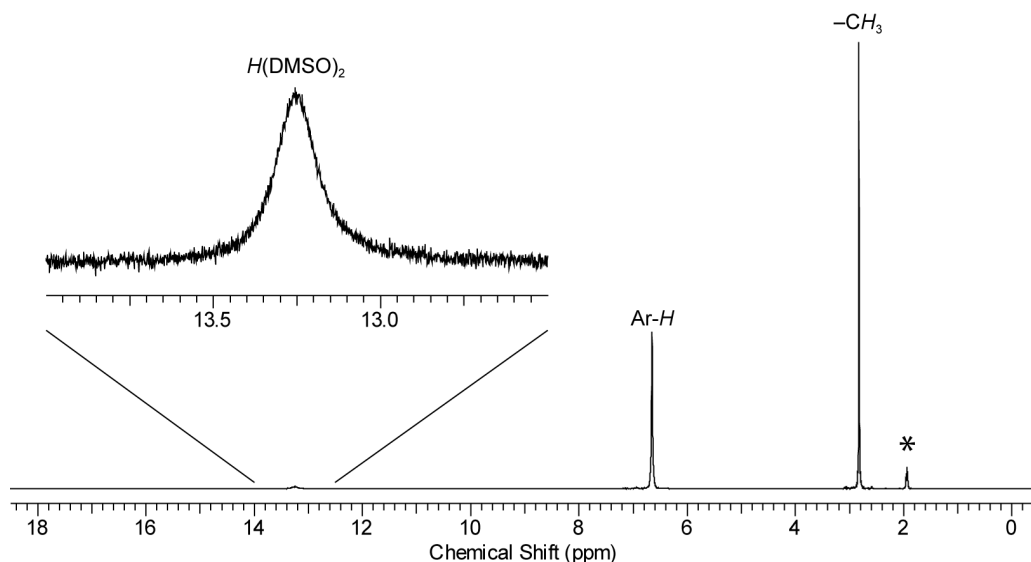


Figure 3.1 ^1H NMR (300 MHz, CD_3CN) spectrum of $\text{H}(\text{DMSO})_2[\mathbf{3.1}]$ at 25 °C. (* = residual protonated solvent) Adapted with permission from *Organometallics* **2009**, 28, 4491. Copyright 2009 American Chemical Society.

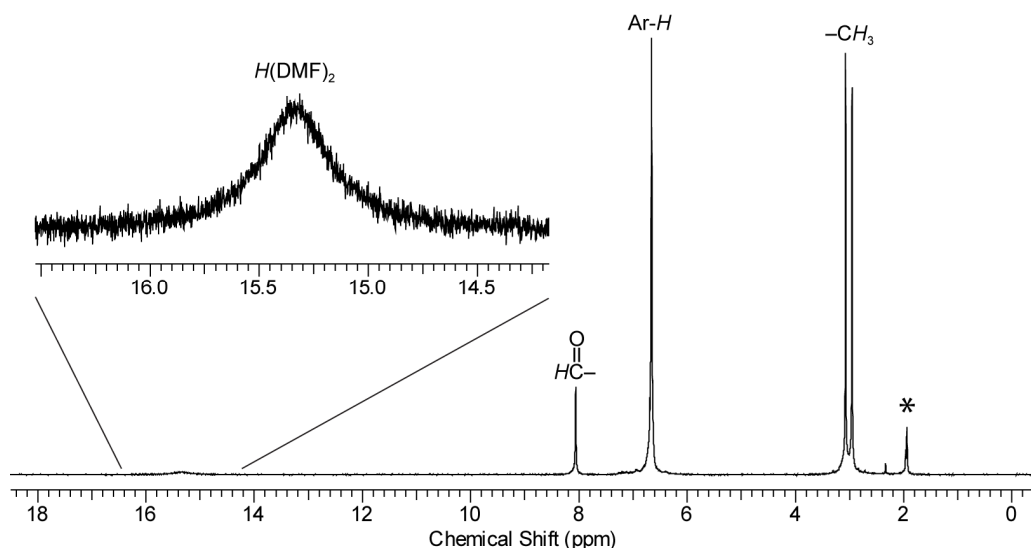


Figure 3.2 ^1H NMR (300 MHz, CD_3CN) spectrum of $\text{H}(\text{DMF})_2[\mathbf{3.1}]$ at 25 °C. (* = residual protonated solvent) Adapted with permission from *Organometallics* **2009**, 28, 4491. Copyright 2009 American Chemical Society.

A rough indication of the acidity of the *H* in the $[\text{H}(\text{DMSO})_2]^+$ and $[\text{H}(\text{DMF})_2]^+$ cations and the innocence of the $[\mathbf{3.1}]^-$ anion may be obtained from the ^1H NMR chemical shift for the acidic proton. At 25 °C, the chemical shift for $[\text{H}(\text{DMSO})_2]^+$ is 13.3 ppm whereas for $[\text{H}(\text{DMF})_2]^+$ it is observed further downfield at 15.3 ppm, suggesting a higher acidity for the latter. This is inconsistent with the relative $\text{p}K_a$ values of $[\text{H}(\text{DMSO})]^+$ ($\text{p}K_a = -2.01$)²¹⁹ and $[\text{H}(\text{DMF})]^+$ ($\text{p}K_a = -1.2 \pm 0.5$),²²⁰ however, it has been proposed previously that the positive charge in monosolvated protons is better delocalized through resonance stabilization than for disolvated protons.²²¹ The significant deshielding of the acidic proton is consistent with that observed for acids of other WCAs. For comparison, chemical shifts of the acidic proton in related compounds such as $\text{H}_2(\text{DMF})_4[\text{TeBr}_6]$ and $\text{H}(\text{DMF})_2[\text{OTf}]$ are 16.8 and 16.9 ppm, respectively,²²² whereas those of the widely used $[\text{H}(\text{OEt}_2)_2][\text{B}(3,5\text{-}(\text{CF}_3)_2\text{C}_6\text{H}_3)_4]$ and $[\text{H}(\text{OEt}_2)_2][\text{B}(\text{C}_6\text{F}_5)_4]$ are 11.1 and 15.5 ppm, respectively.^{50,201}

The Brønsted acids $[\text{H}(\text{DMSO})_2][\mathbf{3.1}]$ and $\text{H}(\text{DMF})_2[\mathbf{3.1}]$ were also crystallographically characterized. The molecular structures are presented in Figure 3.3 and Figure 3.4 and confirm the presence of a hexacoordinated $[\mathbf{3.1}]^-$ in each complex. The P(1) atom of $[\mathbf{3.1}]^-$ in each compound shows minor deviation from perfect octahedral geometry. The largest deviation from octahedral angles for the anion in $\text{H}(\text{DMSO})_2[\mathbf{3.1}]$ is $3.42(5)^\circ$ [O(2)-P(1)-O(5)] and for $\text{H}(\text{DMF})_2[\mathbf{3.1}]$ is $2.66(7)^\circ$ [O(2)-P(1)-O(4)]. The P-O bond lengths in $\text{HL}_2[\mathbf{3.1}]$ [avg. 1.711(3) Å, L = DMF; 1.716(3) Å, L = DMSO] are longer than those typically observed for P-O single bonds in triarylphosphates [1.59(1) Å]¹⁶⁵ but are similar to those found in $\text{Et}_3\text{NH}[\mathbf{3.1}]$ [avg. 1.715(6)]¹⁵³ and other complexes of $[\mathbf{3.1}]^-$ that were described in Chapter 2, namely $\text{K}_2(\text{DMSO})_6[\mathbf{3.1}]_2$ [avg. 1.715(5) Å], $\{\text{K}(\text{MeCN})_2[\mathbf{3.1}]\}_6$ [avg. 1.712(2) Å], $[(\text{dppp})\text{Pd}(\mu\text{-Cl})_2[\mathbf{3.1}]_2$ [avg. 1.715(4) Å] and $(\text{cod})\text{Rh}[\mathbf{3.1}]$ [avg. 1.715(9) Å].

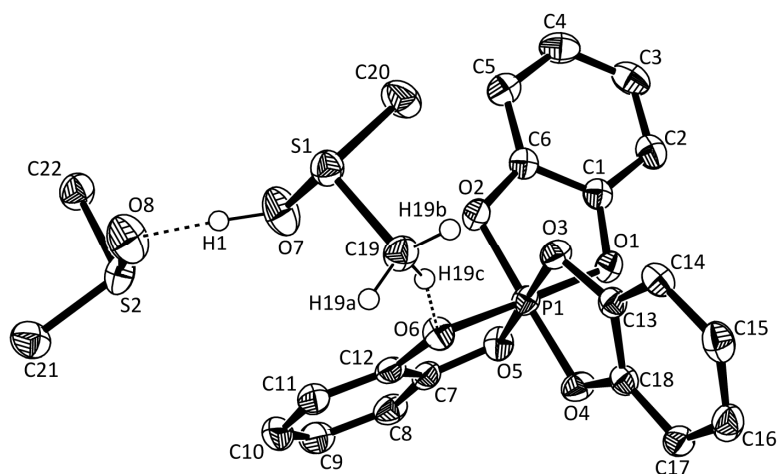


Figure 3.3 Molecular structure of $\text{H(DMSO)}_2[\mathbf{3.1}]$. Ellipsoids are drawn at the 50% probability level. All hydrogen atoms are omitted for clarity, except for H(1), H(19a), H(19b) and H(19c). Selected bond lengths (Å): O(1)-P(1) = 1.726(1); O(2)-P(1) = 1.716(1); O(3)-P(1) = 1.725(1); O(4)-P(1) = 1.709(1); O(5)-P(1) = 1.705(1); O(6)-P(1) = 1.713(1); O(7)-H(1) = 1.00(3); O(8)-H(1) = 1.45(3); O(7)-O(8) = 2.445(6); O(6)-H(19c) = 2.421(1). Selected bond angles (°): O(1)-P(1)-O(2) = 90.85(5); O(3)-P(1)-O(4) = 90.60(5); O(5)-P(1)-O(6) = 91.27(5); O(7)-H(1)-O(8) = 171(3). Adapted with permission from *Organometallics* **2009**, 28, 4491. Copyright 2009 American Chemical Society.

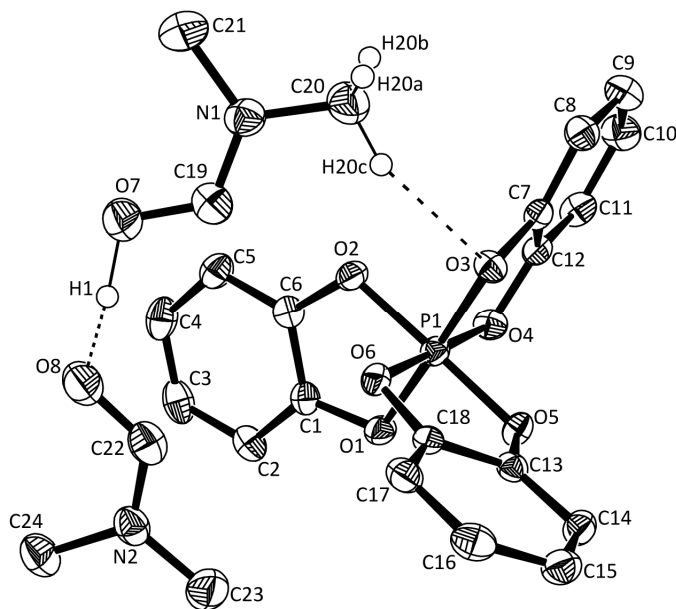


Figure 3.4 Molecular structure of $\text{H(DMF)}_2[\mathbf{3.1}]$. Ellipsoids are drawn at the 50% probability level. All hydrogen atoms are omitted for clarity, except for H(1), H(20a), H(20b) and H(20c). Selected bond lengths (Å): O(1)-P(1) = 1.706(1); O(2)-P(1) = 1.715(1); O(3)-P(1) = 1.708(1); O(4)-P(1) = 1.708(1); O(5)-P(1) = 1.700(1); O(6)-P(1) = 1.730(1); O(7)-H(1) = 1.13(4); O(8)-H(1) = 1.31(4); O(7)-O(8) = 2.438(2); O(3)-H(20c) = 2.375(1). Selected bond angles (°): O(1)-P(1)-O(2) = 90.96(6); O(3)-P(1)-O(4) = 91.05(6); O(5)-P(1)-O(6) = 90.46(6); O(7)-H(1)-O(8) = 176(4). Adapted with permission from *Organometallics* **2009**, 28, 4491. Copyright 2009 American Chemical Society.

Importantly, the molecular structures of the Brønsted acids of **[3.1]⁻** are consistent with their ¹H NMR spectroscopic data and confirm that their cationic components consist of a single proton coordinated through the oxygen atom of two ligand molecules. In each case, the acidic hydrogen atom, H(1), was located in the difference map and was refined isotropically. The O-H bond lengths in the [H(DMSO)₂]⁺ cation differ considerably [O(7)-H(1) = 1.00(3); O(8)-H(1) = 1.45(3) Å], which are consistent with that observed in related compounds: [H(DMSO)₂]₂[TeCl₆], H(DMSO)₂[7,8-C₂B₉H₁₂] and H(DMSO)₂[*trans*-RuCl₄(DMSO)₂] [O-H = 0.9(1), and 1.5(1) Å;²²³ 0.95(4) and 1.45(4) Å;²²⁴ 1.12(6) and 1.30(6) Å,²²⁵ respectively]. Similarly, the acidic hydrogen in the [H(DMF)₂]⁺ cation is also bound asymmetrically [O(7)-H(1) = 1.13(4); O(8)-H(1) = 1.31(4) Å]. Asymmetric hydrogen bonding is quite common for protons bound by oxygen donors such as DMF and DMSO.²²³⁻²²⁴ The O...O distance in the O-H-O moiety of the [HL₂]⁺ cation is generally accepted as being more indicative of the strength of hydrogen bonding than the O-H distance, which is difficult to determine accurately.^{223,225-229} The O...O distances for the O-H-O moiety in H(DMSO)₂**[3.1]** [O(7)...O(8) = 2.445(6) Å] and H(DMF)₂**[3.1]** [O(7)...O(8) = 2.438(2) Å] are significantly shorter than the sum of van der Waals radii for oxygen and oxygen [*r*_{vdw} = 3.04 Å],¹⁷² which is consistent with strong hydrogen bonding for the O-H-O moiety in the [H(DMSO)₂]⁺ and the [H(DMF)₂]⁺ cations.^{227,230} The O...O distances are also comparable to those observed in related compounds {H(DMSO)₂[*trans*-RuCl₄(DMSO)₂]: 2.423(5) Å;²²⁵ [H(DMSO)₂]₂[TeBr₆]: 2.448(4) Å;²²⁹ [H(DMF)₂]₂[TeBr₆]: 2.44(2) Å;²²² and the partially chlorinated derivative, H(DMF)₂[P(1,2-O₂C₆H₄)(1,2-O₂C₆Cl₄)₂]: 2.413(5) Å}.²³¹

The metrical parameters for H(DMSO)₂**[3.1]** and H(DMF)₂**[3.1]** reveal the presence of weak interactions between the cation and anion **[3.1]⁻**. Specifically, the closest contact between [H(DMSO)₂]⁺ and **[3.1]⁻** involves an oxygen atom in the catecholate anion and an H-atom of the methyl group of DMSO [O(6)...H(19c) = 2.421(1) Å]. Likewise, the closest contact between

$[\text{H}(\text{DMF})_2]^+$ and $[\mathbf{3.1}]^-$ involves a methyl group of DMF and an oxygen atom of $[\mathbf{3.1}]^-$ [$\text{O}(3)\cdots\text{H}(20\text{c}) = 2.375(1) \text{ \AA}$]. In both cases, the closest ion-pair distances are within the sum of van der Waals radii for oxygen and hydrogen [$r_{\text{vdw}} = 2.72 \text{ \AA}$],¹⁷² consistent with weak cation-anion interactions.

3.2.2 Placement of $[\mathbf{3.1}]^-$ on Infrared Scale for Weakly Basic Anions

To further investigate the potential use of $[\mathbf{3.1}]^-$ as a WCA, it was necessary to compare the coordinating ability of $[\mathbf{3.1}]^-$ with other anions. A convenient scale for evaluating the basicity of anions in solution has been proposed which involves measuring the N-H stretching frequency for ammonium salts of various anions.²³² In an effort to place $[\mathbf{3.1}]^-$ on this scale, the trioctylammonium salt of $[\mathbf{3.1}]^-$ was synthesized and characterized. Following the literature protocol, analysis of a CCl_4 solution of $(\text{C}_8\text{H}_{17})_3\text{NH}[\mathbf{3.1}]$ by infrared spectroscopy revealed a N-H stretching frequency of 3129 cm^{-1} . Interestingly, this value is comparable to $(\text{C}_8\text{H}_{17})_3\text{NH}[\text{BF}_4]^-$ [$\bar{\nu}_{\text{N-H}} = 3133 \text{ cm}^{-1}$,²³² 3129 cm^{-1} (our data)] suggesting that $[\mathbf{3.1}]^-$ has a similar basicity to $[\text{BF}_4]^-$. In comparison, the most likely candidates for the title of “weakest coordinating anion”, $[\text{B}(\text{C}_6\text{F}_5)_4]^-$ and $[\text{CMeB}_{11}\text{F}_{11}]^-$, have N-H stretching frequency of 3233 and 3219 cm^{-1} , respectively.²³² In contrast, the chloride anion is the most basic of those previously measured and $(\text{C}_8\text{H}_{17})_3\text{NHCl}$ possesses an N-H stretching frequency of 2330 cm^{-1} .²³²

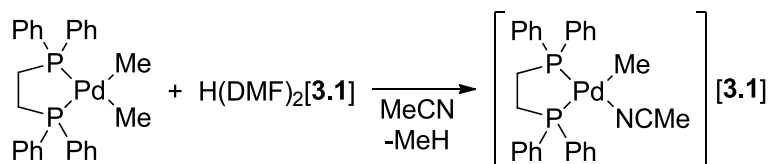
3.2.3 Application of $\text{H}(\text{DMF})_2[\mathbf{3.1}]$ in Metal-Carbon Bond Protonolysis

The results from the previous section suggest that the coordinating ability of $[\mathbf{3.1}]^-$ should be comparable to tetrafluoroborate. Although more coordinating than the perfluoroarylborate and the carborane anions, the relative ease of synthesis for $\text{H}(\text{DMSO})_2[\mathbf{3.1}]$ and $\text{H}(\text{DMF})_2[\mathbf{3.1}]$, compared to protic salts of fluoroarylborates or carboranes, makes them attractive as catalyst

activators where a moderately coordinating anion can be tolerated. Moreover, they represent convenient protic reagents because they are isolable in solid form and may be readily weighed.²³³ Protic acids of WCAs are important for the protonolysis of metal-alkyls to generate active catalysts. Readily available anhydrous Brønsted acids, such as HOSO₂CF₃, HOSO₂F, HBF₄/Et₂O and HF·SbF₅, can be effective in metal-alkyl bond activation; however, they are available only in solution or in liquid form. Weighable solid Brønsted acids of moderate molecular weight, such as H(DMSO)₂[**3.1**] and H(DMF)₂[**3.1**], are less common. They are, nevertheless, attractive for catalytic applications, since due to the small amount of catalyst typically used, they enable more precise control of stoichiometry.⁵⁰ In this section, the activation of palladium(II)-methyl bonds using H(DMF)₂[**3.1**] will be discussed.

It is known that the reaction of (P[^]P)PdMe₂ (where P[^]P is a bidentate ligand) with H(OEt)₂[B(3,5-(CF₃)₂C₆H₃)₄] affords [(P[^]P)Pd(solvent)Me][B(3,5-(CF₃)₂C₆H₃)₄],²³⁴⁻²³⁵ an active catalyst for alternating polymerization of carbon monoxide and ethylene.²³⁶⁻²³⁸ Consequently, the reaction of (dppe)PdMe₂ with H(DMF)₂[**3.1**] in Et₂O/CH₃CN was investigated as a starting point to test the effectiveness of the Brønsted acids of [**3.1**]⁻ to protonate metal-alkyl moieties (Scheme 3.2). Brønsted acid H(DMF)₂[**3.1**] was chosen rather than H(DMSO)₂[**3.1**] due to the greater stability of the former at room temperature. Cooling the reaction mixture to -30 °C resulted in the precipitation of a colorless solid. The ³¹P{¹H} NMR spectrum of a CD₃CN solution of the powder is shown in Figure 3.5 and is consistent with the successful formation of [(dppe)Pd(NCMe)Me][**3.1**]. Importantly, the spectrum reveals two coupled doublet resonances [δ = 62.5, 40.7; ²J_{PP} = 28 Hz] that arise from two inequivalent coupled phosphine moieties and a singlet resonance assigned to [**3.1**]⁻ [δ = -82.0]. For comparison, similar resonances are observed for the phosphine moieties in [(dppe)Pd(NCMe)Me][OTf] [δ = 60.4, 35.2; ²J_{PP} = 27 Hz]²³⁹ and [(dppe)Pd(NCMe)Me][PF₆] [δ = 61.2, 39.5; ²J_{PP} = 27 Hz].²⁴⁰ Additional analysis of the product

by ^1H and $^{13}\text{C}\{^1\text{H}\}$ NMR spectroscopy provided further evidence for the formulation of the product as $[(\text{dppe})\text{Pd}(\text{NCMe})\text{Me}][\mathbf{3.1}]$.



Scheme 3.2 Protonolysis of $(\text{dppe})\text{PdMe}_2$ with one equivalent of $\text{H}(\text{DMF})_2[\mathbf{3.1}]$.

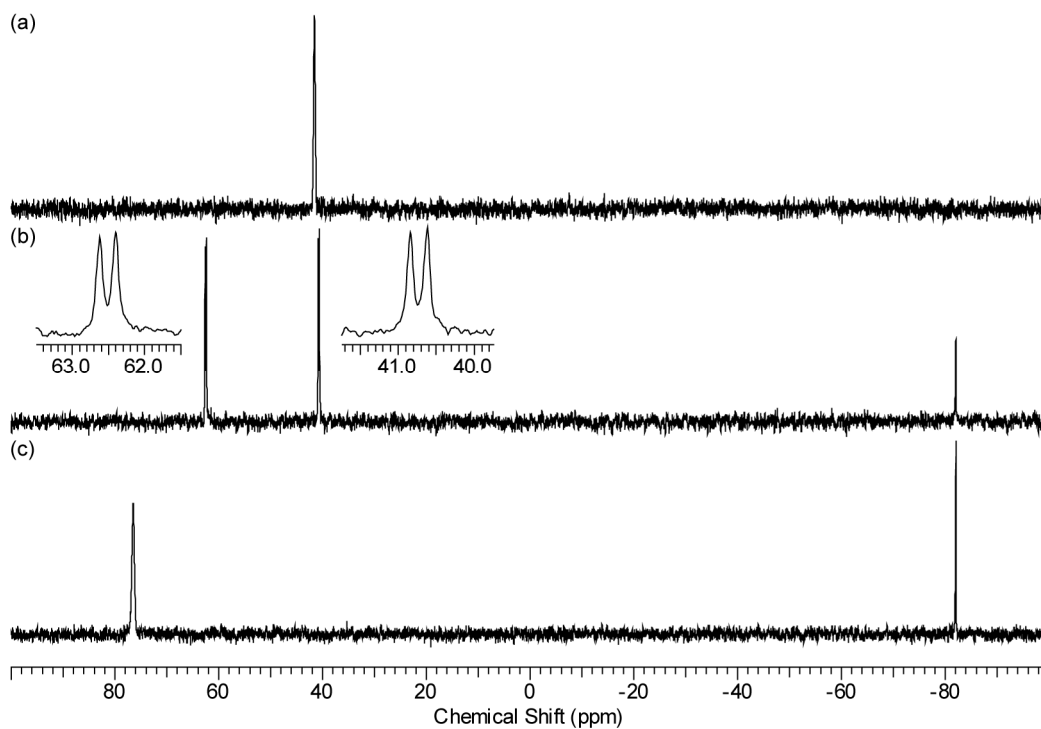
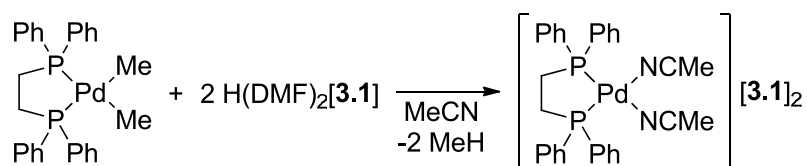


Figure 3.5 (a) ^{31}P NMR (162 MHz, CD_3CN) spectrum of $(\text{dppe})\text{PdMe}_2$ at 25 °C. (b) $^{31}\text{P}\{^1\text{H}\}$ NMR (121 MHz, CD_3CN) spectrum of $[(\text{dppe})\text{Pd}(\text{NCMe})\text{Me}][\mathbf{3.1}]$ at 25 °C. (c) ^{31}P NMR (162 MHz, CD_3CN) spectrum of $[(\text{dppe})\text{Pd}(\text{NCMe})_2][\mathbf{3.1}]_2$ at 25 °C. Adapted with permission from *Organometallics* **2009**, 28, 4491. Copyright 2009 American Chemical Society.

It was also of interest to investigate the ability of $\text{H}(\text{DMF})_2[\mathbf{3.1}]$ to doubly activate $(\text{dppe})\text{PdMe}_2$ and to determine the stability of the resulting dicationic $[(\text{dppe})\text{Pd}(\text{NCMe})_2]^{2+}$ in the presence of $[\mathbf{3.1}]^-$. Complexes containing the $[(\text{dppe})\text{Pd}(\text{solvent})_2]^{2+}$ are effective for various catalytic transformations, including polymerization of norbornene,²⁴¹⁻²⁴² hydrosulfination of propene,²⁴³⁻²⁴⁴ and hydrogenation of olefins.²⁴⁵⁻²⁴⁶ A mixture of $(\text{dppe})\text{PdMe}_2$ and $\text{H}(\text{DMF})_2[\mathbf{3.1}]$

(2 equiv) was dissolved in CH₃CN and an immediate color change to yellow was observed (Scheme 3.3). After the reaction mixture was stirred for a total of 3 h, analysis by ³¹P NMR spectroscopy revealed the quantitative formation of [(dppe)Pd(NCMe)₂][**3.1**]₂ [δ = 76.5 (s), -82.1 (s)] (Figure 3.5). Upon standing, a pale yellow solid precipitated from the reaction solution and the solid was separated, washed and dried. Analysis of a DMSO-*d*₆ solution of the solid product by ³¹P, ¹H and ¹³C{¹H} NMR spectroscopy was consistent with the dication salt [(dppe)Pd(NCMe)₂][**3.1**]₂. For comparison, a solution of (dppe)PdMe₂ in acetonitrile was treated with hydrogen chloride which afforded (dppe)PdCl₂ rather than [(dppe)Pd(NCMe)₂]Cl₂.



Scheme 3.3 Protonolysis of (dppe)PdMe₂ with two equivalent of H(DMF)₂[**3.1**].

The molecular structures of [(dppe)Pd(NCMe)Me][**3.1**] and [(dppe)Pd(NCMe)₂][**3.1**]₂ were determined using X-ray crystallography (Figure 3.6 and Figure 3.7, respectively) and confirmed the formulations proposed from NMR spectroscopy. The metrical parameters within [**3.1**]⁻ in each molecular structure are similar to those found in the HL₂⁺ salts discussed above and will not be discussed further. Noteworthy is the fact that [(dppe)Pd(NCMe)Me][**3.1**] crystallizes in a chiral space group, *P*2₁. Remarkably, the analysis of two different crystals revealed that the Λ- and Δ-isomers of [**3.1**]⁻ are resolved in the presence of [(dppe)Pd(NCMe)Me]⁺. Careful comparison of the molecular structures of [(dppe)Pd(NCMe)Me][Λ-**3.1**] with [(dppe)Pd(NCMe)Me][Δ-**3.1**] reveals an asymmetrical twist in the conformation of the palladacycle, which results in the opposite enantiomer for the cation in each structure. Such twisting is commonly observed for square planar palladium(II) compounds containing the dppe ligand.²⁴⁷⁻²⁵⁰ The molecular structure of

$[(dppe)Pd(NCMe)_2][\mathbf{3.1}]_2$ shows similar behavior, however, both enantiomers of the cation and anion are present and are related by symmetry in the $P\bar{1}$ space group.²⁵¹

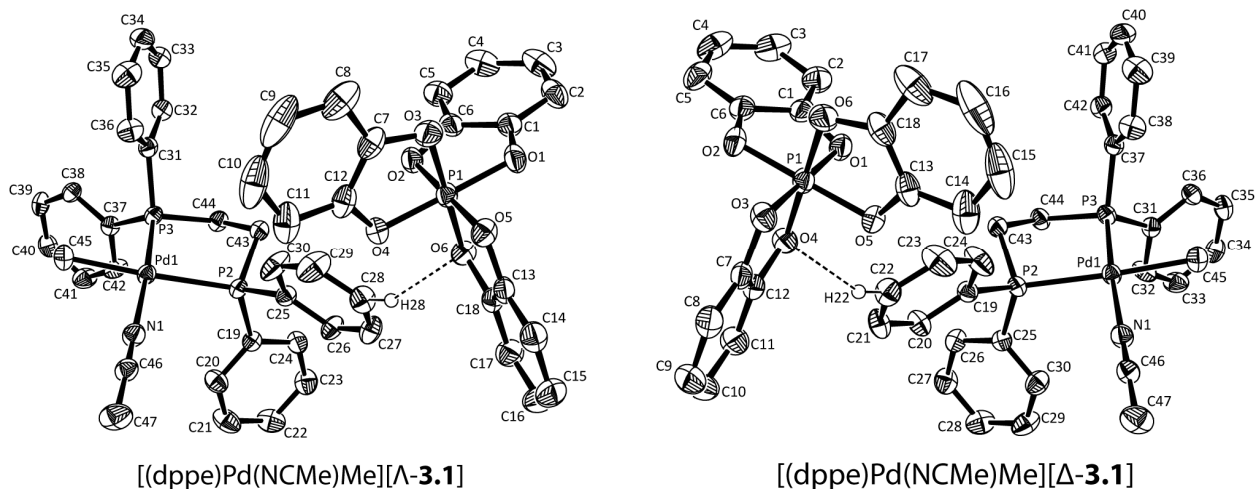


Figure 3.6 Molecular structures of Λ - and Δ -isomers of $[(dppe)Pd(NCMe)Me][\mathbf{3.1}]$. Ellipsoids are drawn at the 50% probability level. All hydrogen atoms are omitted for clarity, except for H(28) for $[(dppe)Pd(NCMe)Me][\Lambda\text{-}\mathbf{3.1}]$ and H(22) for $[(dppe)Pd(NCMe)Me][\Delta\text{-}\mathbf{3.1}]$. In both cases, solvents of crystallization (CH_3CN) are also omitted for clarity.

$[(dppe)Pd(NCMe)Me][\Lambda\text{-}\mathbf{3.1}]$: O(1)-P(1) = 1.705(2); O(2)-P(1) = 1.703(2); O(3)-P(1) = 1.712(2); O(4)-P(1) = 1.708(2); O(5)-P(1) = 1.712(2); O(6)-P(1) = 1.707(2); P(2)-Pd(1) = 2.3368(6); P(3)-Pd(1) = 2.2022(6); N(1)-Pd(1) = 2.063(2); C(45)-Pd(1) = 2.084(2); O(6)-H(28) = 2.551(2); O(1)-P(1)-O(2) = 91.28(8); O(3)-P(1)-O(4) = 90.74(8); O(5)-P(1)-O(6) = 91.17(8); N(1)-Pd(1)-C(45) = 89.17(9); C(45)-Pd(1)-P(3) = 87.26(7); N(1)-Pd(1)-P(2) = 96.76(6); P(3)-Pd(1)-P(2) = 86.73(2).

$[(dppe)Pd(NCMe)Me][\Delta\text{-}\mathbf{3.1}]$: O(1)-P(1) = 1.706(1); O(2)-P(1) = 1.708(1); O(3)-P(1) = 1.716(1); O(4)-P(1) = 1.711(1); O(5)-P(1) = 1.710(1); O(6)-P(1) = 1.714(2); P(2)-Pd(1) = 2.3381(6); P(3)-Pd(1) = 2.2076(6); N(1)-Pd(1) = 2.069(2); C(45)-Pd(1) = 2.087(2); O(4)-H(22) = 2.550(1); O(1)-P(1)-O(2) = 91.06(7); O(3)-P(1)-O(4) = 90.99(7); O(5)-P(1)-O(6) = 90.87(7); N(1)-Pd(1)-C(45) = 89.36(7); C(45)-Pd(1)-P(3) = 87.31(6); N(1)-Pd(1)-P(2) = 96.52(5); P(3)-Pd(1)-P(2) = 86.75(2). Adapted with permission from *Organometallics* **2009**, 28, 4491. Copyright 2009 American Chemical Society.

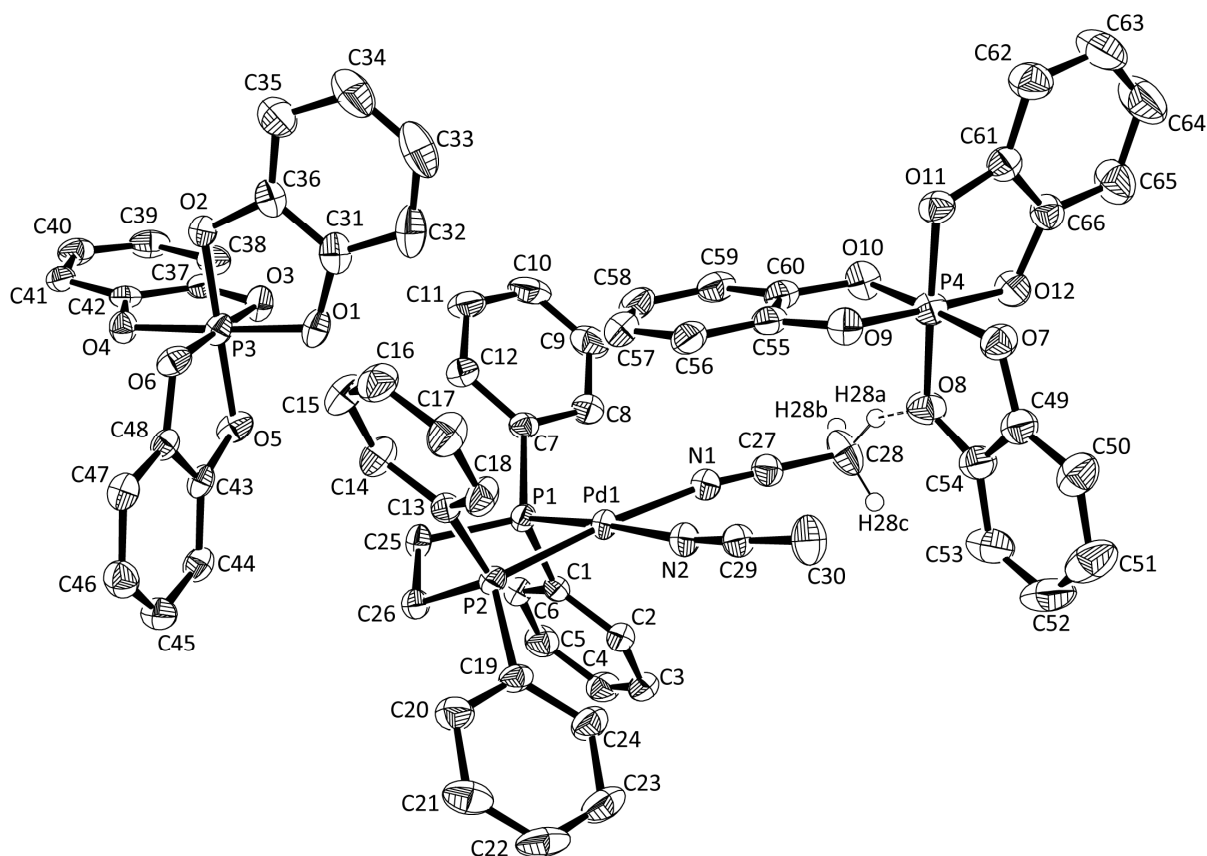


Figure 3.7 Molecular structure of $[(dppe)Pd(NCMe)_2][\mathbf{3.1}]_2$. Ellipsoids are drawn at the 50% probability level. All hydrogen atoms are omitted for clarity, except for H(28a), H(28b) and H(28c). Solvents of crystallization ($2 \times CH_3CN$) are also omitted for clarity. Selected bond lengths (Å): O(1)-P(3) = 1.708(2); O(2)-P(3) = 1.709(2); O(3)-P(3) = 1.715(2); O(4)-P(3) = 1.708(2); O(5)-P(3) = 1.720(2); O(6)-P(3) = 1.723(2); O(7)-P(4) = 1.711(2); O(8)-P(4) = 1.713(2); O(9)-P(4) = 1.703(2); O(10)-P(4) = 1.717(2); O(11)-P(4) = 1.717(2); O(12)-P(4) = 1.711(2); P(1)-Pd(1) = 2.2492(6); P(2)-Pd(1) = 2.2370(7); N(1)-Pd(1) = 2.080(2); N(2)-Pd(1) = 2.093(2); O(8)-H(28a) = 2.318(2). Selected bond angles ($^\circ$): O(1)-P(3)-O(2) = 90.84(8); O(3)-P(3)-O(4) = 91.17(8); O(5)-P(3)-O(6) = 90.24(7); O(7)-P(4)-O(8) = 90.85(8); O(9)-P(4)-O(10) = 91.02(8); O(11)-P(4)-O(12) = 90.47(8); O(12)-P(4)-O(7) = 92.53(9); O(12)-P(4)-O(8) = 88.26(8); N(1)-Pd(1)-N(2) = 87.38(8); N(2)-Pd(1)-P(2) = 93.50(6); N(1)-Pd(1)-P(1) = 93.74(6); P(2)-Pd(1)-P(1) = 85.09(2). Adapted with permission from *Organometallics* **2009**, 28, 4491. Copyright 2009 American Chemical Society.

The metrical parameters within the $[(dppe)Pd(NCMe)Me]^+$ and $[(dppe)Pd(NCMe)_2]^{2+}$ cations are comparable to those observed in analogous species. As represented by a dashed line in Figure 3.6, the closest ion contact in $[(dppe)Pd(NCMe)Me][\Delta\text{-}\mathbf{3.1}]$ and $[(dppe)Pd(NCMe)Me][\Delta\text{-}\mathbf{3.1}]$ is between a phenyl-H of the dppe ligand and an oxygen atom from the catecholate anion $\{[(dppe)Pd(NCMe)Me][\Delta\text{-}\mathbf{3.1}]: O(6)-H(28) = 2.551(2) \text{ \AA};$

[(dppe)Pd(NCMe)Me][Δ -**3.1**]: O(4)-H(22) = 2.550(1) Å}. In contrast, Figure 3.7 shows that the closest contact in [(dppe)Pd(NCMe)₂][**3.1**]₂ is between an acetonitrile hydrogen and an oxygen atom of [**3.1**]⁻ [O(8)-H(28a) = 2.318(2) Å]. In both compounds, these approaches are slightly less than the sum of the van der Waals radii for oxygen and hydrogen [$r_{\text{vdw}} = 2.72$ Å]¹⁷² and suggest weak interactions between the cation and the anion.

3.3 Summary

The preparation of two new Brønsted acids containing the hexacoordinated phosphorus(V) anion [**3.1**]⁻, H(DMF)₂[**3.1**] and H(DMSO)₂[**3.1**], was accomplished following a straightforward procedure from PCl₅, catechol and the appropriate solvent (DMF or DMSO). Both compounds were characterized spectroscopically and through X-ray crystallography. Their high acidities were suggested by the downfield shifts of the acidic proton in their ¹H NMR spectra. The basicity of [**3.1**]⁻ was determined to be similar to that of the classical weakly coordinating anion, [BF₄]⁻, based on a similar N-H stretching frequency for (C₈H₁₇)₃NH[**1**] and to that observed for (C₈H₁₇)₃NH[BF₄]. Brønsted acid H(DMF)₂[**3.1**] was shown to be effective in the stoichiometric activation of the metal-alkyl bonds of (dppe)PdMe₂ to afford either [(dppe)Pd(NCMe)Me][**3.1**] (1:1 ratio) or [(dppe)Pd(NCMe)₂][**3.1**]₂ (1:2 ratio), both of which were structurally characterized.

3.4 Experimental Section

3.4.1 General Procedures

All manipulations were performed using standard Schlenk or glove box techniques under nitrogen atmosphere. Toluene and Et₂O were deoxygenated with nitrogen and dried by passing through a column containing activated alumina. CD₃CN, CD₂Cl₂, and DMSO-*d*₆ were purchased

from Cambridge Isotope Laboratories Inc. in 1 g sealed ampules and dried over 3Å molecular sieves before use. Trioctylamine and HPLC grade carbon tetrachloride were purchased from Aldrich and dried over 3Å molecular sieves before use. DMSO and DMF were dried over 3Å molecular sieves and distilled before use. Acetonitrile was distilled from CaH₂ before use. PCl₅ (Aldrich) was sublimed prior to use. Anhydrous HCl (BOC Gases) and catechol (Aldrich) were used as received. Mixture **3.2** / **3.3**¹⁶⁰ and [(dpppe)PdMe₂]²⁵² were prepared following literature procedures. ¹H, ¹³C{¹H}, ³¹P and ³¹P{¹H} NMR spectra were recorded at 25 °C on Bruker Avance 300 or 400 MHz spectrometers. 85% H₃PO₄ was used as an external standard (δ 0.0) for ³¹P and ³¹P{¹H} NMR spectra. ¹H NMR spectra were referenced to residual protonated solvent, and ¹³C{¹H} NMR spectra were referenced to the deuterated solvent. Elemental analyses were performed in the University of British Columbia Chemistry Microanalysis Facility. Infrared spectra were recorded on a Thermo Nicolet Nexus 670 FT-IR spectrometer equipped with an inlet attached to a nitrogen supply. The sample chamber was purged with nitrogen until a constant concentration level of moisture and carbon dioxide was obtained for the background. IR spectra of 0.005-0.01 M solutions of trioctylammonium salts in carbon tetrachloride were obtained using a cell with KBr windows and recorded in the 4000-500 cm⁻¹ range under a flow of nitrogen.

3.4.2 Synthesis of H(DMSO)₂[**3.1**]

To a solid mixture of **3.2** and **3.3** (1.0 g, 2.8 mmol) was added DMSO (5.0 g, 64 mmol) and the resultant pale purple solution was stirred for 20 min. Subsequently, toluene (90 mL) was added to afford a colorless precipitate which was collected by filtration. The solid was redissolved in CH₃CN (10 mL), reprecipitated with toluene (90 mL) and collected by filtration. The crude product was dried *in vacuo*. Yield = 1.4 g (98%). Crystals suitable for X-ray

crystallography were obtained from slow diffusion of toluene into a DMSO solution of $\text{H}(\text{DMSO})_2[\mathbf{3.1}]$ (ca. 5 days).

^{31}P NMR (162 MHz, CH_3CN): δ -80.5; ^1H NMR (300 MHz, CD_3CN): δ 13.3 (br s, 1H, *H*-DMSO₂), 6.65 (s, 12H, Ar-*H*), 2.83 (s, 12H, CH₃); $^{13}\text{C}\{^1\text{H}\}$ NMR (101 MHz, DMSO-*d*₆): 145.4 (d, $J_{\text{CP}} = 4$ Hz), 118.6 (s), 108.9 (d, $J_{\text{CP}} = 17$ Hz), 40.4 (s). Anal. Calcd. for $\text{C}_{22}\text{H}_{25}\text{O}_8\text{PS}_2$: C, 51.55; H, 4.92. Found: C, 51.68; H, 4.93.

3.4.3 Synthesis of $\text{H}(\text{DMF})_2[\mathbf{3.1}]$

To a solid mixture of **3.2** and **3.3** (1.0 g, 2.8 mmol) was added DMF (5.0 g, 68 mmol) and the resultant white suspension was stirred for 60 min. Subsequently, toluene (40 mL) was added and the colorless precipitate was collected by filtration. The solid was redissolved in CH_3CN (10 mL), reprecipitated with toluene (90 mL) and collected by filtration. The crude product was dried *in vacuo*. Yield = 1.1 g (78%). Crystals suitable for X-ray diffraction were obtained from slow diffusion of toluene into a solution of $\text{H}(\text{DMF})_2[\mathbf{3.1}]$ in DMF.

^{31}P NMR (162 MHz, CH_3CN): δ -80.0; ^1H NMR (300 MHz, CD_3CN): δ 15.3 (br s, 1H, *H*-DMF₂), 8.06 (s, 2H, HC=O), 6.69-6.65 (m, 12H, Ar-*H*), 3.07 (s, 6H, CH₃), 2.95 (s, 6H, CH₃); $^{13}\text{C}\{^1\text{H}\}$ NMR (101 MHz, CD_3CN): 165.5 (s), 146.6 (d, $J_{\text{CP}} = 4$ Hz), 120.3 (s), 110.4 (d, $J_{\text{CP}} = 16$ Hz), 39.3 (s), 33.8 (s). Anal. Calcd. for $\text{C}_{24}\text{H}_{27}\text{N}_2\text{O}_8\text{P}$: C, 57.37; H, 5.42; N, 5.58. Found: C, 57.52; H, 5.45; N, 5.64.

3.4.4 Synthesis of $(\text{C}_8\text{H}_{17})_3\text{NH}[\mathbf{3.1}]$

Triethylamine (1.7 g, 2.8 mmol) and solid mixture of **3.2** and **3.3** (1.0 g, 4.8 mmol) were dissolved in CH_2Cl_2 (5 mL). After 3 h, the solvent was removed *in vacuo* and the resultant colorless oil was heated *in vacuo* at 140 °C. Subsequently, hexanes (15 mL) was added to the

colorless oil and this mixture was ultrasonicated for 15 min. to afford a white solid. $(C_8H_{17})_3NH[3.1]$ was isolated by filtration, washed with hexanes (10 mL) and dried *in vacuo*. Yield = 1.3 g (65%).

^{31}P NMR (121 MHz, $CDCl_3$): δ -83.8; 1H NMR (300 MHz, $CDCl_3$): δ 8.61 (br s, 1H, *H-N*), 6.70 (s, 12H, *Ar-H*), 3.20-3.12 (m, 6H, *N-CH₂*), 1.74-1.63 (m, 6H, *NCH₂-CH₂*), 1.26-1.17 (m, 30H, *NC₂H₄-C₅H₁₀*), 0.87 (t, $^3J_{HH} = 7$ Hz, 9H, *CH₃*); $^{13}C\{^1H\}$ NMR (101 MHz, $CDCl_3$): 145.0 (d, $J_{CP} = 4$ Hz), 119.5 (s), 109.7 (d, $J_{CP} = 19$ Hz), 53.4 (s), 31.5 (s), 28.8 (s), 28.7 (s), 26.5 (s), 23.1 (s), 22.4 (s), 14.0 (s). Anal. Calcd. for $C_{42}H_{64}NO_6P$: C, 71.06; H, 9.09; N, 1.97. Found: C, 71.12; H, 9.21; N, 2.12.

3.4.5 Synthesis of [(dppe)Pd(NCMe)Me][3.1]

To a solid mixture of (dppe)PdMe₂ (50 mg, 0.093 mmol) and H(DMF)₂[3.1] (47 mg, 0.094 mmol) was added Et₂O (ca. 1 mL). Acetonitrile was added dropwise to the stirred suspension until all the solid was dissolved (ca. 10 drops). The solution was stirred at room temperature for 15 min, where after the mixture was cooled to -30 °C to afford a colorless precipitate. The supernatant liquid was decanted from the precipitate and the solid was dried *in vacuo*. Yield = 72 mg (85%). Crystals suitable for X-ray diffraction were grown by slow evaporation of a solution of [(dppe)Pd(NCMe)Me][3.1] in Et₂O:CH₃CN.

$^{31}P\{^1H\}$ NMR (121 MHz, CD_3CN): δ 62.5 (d, $^2J_{PP} = 28$ Hz, dppe), 40.7 (d, $^2J_{PP} = 28$ Hz, dppe), -82.0 (s, anion); 1H NMR (300 MHz, CD_3CN): δ 7.69-7.52 (m, 20H, *Ar-H* of dppe), 6.65-6.58 (m, 12H, *Ar-H* of anion), 2.73-2.55, 2.41-2.24 (m, 4H, *CH₂CH₂*), 1.96 (s, 3H, Pd-*NCCH₃*), 0.52 (dd, $^3J_{HP} = 6$ Hz, $^3J_{HP} = 3$ Hz, 3H, Pd-*CH₃*); $^{13}C\{^1H\}$ NMR (101 MHz, CD_2Cl_2): 146.3 (d, $J_{CP} = 5$ Hz), 133.8 (d, $J_{CP} = 12$ Hz), 133.2 (d, $J_{CP} = 14$ Hz), 132.8 (d, $J_{CP} = 3$ Hz), 132.3 (s), 130.1 (d, $J_{CP} = 9$ Hz), 130.4 (d, $J_{CP} = 34$ Hz), 130.0 (d, $J_{CP} = 12$ Hz), 127.9 (d, $J_{CP} =$

57 Hz), 123.7 (s), 119.4 (s), 109.9 (d, $J_{CP} = 18$ Hz), 31.3 (dd, $J_{CP} = 35$ Hz, $J_{CP} = 21$ Hz), 24.2 (dd, $J_{CP} = 28$ Hz, $J_{CP} = 8.1$ Hz), 8.6 (d, $J_{CP} = 88$ Hz), 3.0 (s).

3.4.6 Synthesis of [(dppe)Pd(NCMe)₂][3.1]₂

To a solid mixture of (dppe)PdMe₂ (45 mg, 0.084 mmol) and H(DMF)₂[3.1] (85 mg, 0.17 mmol) was added CH₃CN (2 mL). The resulting cloudy yellow mixture was stirred for 3 h, and the supernatant was decanted off. The remaining yellow solid was washed with cold CH₃CN (3 × 2 mL) and dried *in vacuo*. Yield = 66 mg (61%). Crystals suitable for X-ray diffraction, were obtained after a concentrated solution of [(dppe)Pd(NCMe)₂][3.1]₂ in CH₃CN was left in the glovebox overnight.

³¹P NMR (162 MHz, CH₃CN): δ 76.5 (s, dppe), -82.1 (s, anion). ¹H NMR (400 MHz, CD₃CN): δ 7.79-7.61 (m, 20H, Ar-*H* on dppe), 6.64-6.58 (m, 24H, Ar-*H* on anion), 2.92-2.77 (m, 4H, CH₂CH₂ on dppe), 1.96 (s, 6H, PdNCCH₃); ¹³C{¹H} NMR (101 MHz, DMSO-*d*₆): 145.5 (d, $J_{CP} = 4$ Hz), 133.5 (d, $J_{CP} = 12$ Hz), 129.7 (d, $J_{CP} = 12$ Hz), 125.3 (d, $J_{CP} = 55$ Hz), 118.6 (s), 118.0 (s), 108.9 (d, $J_{CP} = 17$ Hz), 26.9 (dd, $J_{CP} = 39$ Hz, $J_{CP} = 8$ Hz), 1.1 (s).

3.4.7 Reaction of (dppe)PdMe₂ with HCl

Anhydrous HCl was bubbled through a stirred solution of (dppe)PdMe₂ in CH₃CN (10 mL) at 0 °C for a few minutes. The solvent was removed *in vacuo* to afford a white solid. The ³¹P NMR spectrum of the isolated solid was identical to that of an authentic sample of (dppe)PdCl₂ [$\delta = 68.1$ in CH₃CN].²⁵³

3.4.8 X-ray Crystallography

All single crystals were immersed in oil and were mounted on a glass fiber. Data were collected on a Bruker X8 APEX II diffractometer with graphite-monochromated Mo K α radiation. Data were collected and integrated using the Bruker SAINT¹⁷⁶ software package and corrected for absorption effect using SADABS.¹⁷⁷ All structures were solved by direct methods and subsequent Fourier difference techniques. Unless noted, all non-hydrogen atoms were refined anisotropically, whereas all hydrogen atoms were included in calculated positions but not refined. All data sets were corrected for Lorentz and polarization effects. All refinements were performed using the SHELXTL¹⁷⁸⁻¹⁷⁹ crystallographic software package from Bruker-AXS.

Compound H(DMSO)₂[**3.1**] has two disordered molecules of DMSO bound to H(1). H(1) was located using the difference map and refined isotropically. Each of the disordered DMSO molecules was modeled in two orientations. Their respective populations were refined to the final occupancy of 0.926(2), 0.074(2), 0.8570(16) and 0.1430(16). Due to the low occupancy values (0.074(2)) for C(19b) and C(20b), they were refined isotropically. Compound H(DMF)₂[**3.1**] has two molecules of DMF bound to H(1). H(1) was located using the difference map and refined isotropically. Compounds [(dppe)Pd(NCMe)Me][Λ -**3.1**], [(dppe)Pd(NCMe)Me][Δ -**3.1**] and [(dppe)Pd(NCMe)₂][**3.1**]₂ did not show any crystallographic complexity. Crystal data and refinement parameters are listed in Table 3.1. CIF files giving supplementary crystallographic data for the structures reported in this chapter are available from Cambridge Crystallographic Data Centre (CCDC 727172 – 727176).

Table 3.1 X-ray crystallographic data of H(DMSO)₂[**3.1**], H(DMF)₂[**3.1**], [(dppe)Pd(NCMe)Me][Λ -**3.1**], [(dppe)Pd(NCMe)Me][Δ -**3.1**] and [(dppe)Pd(NCMe)₂][**3.1**]₂.

| | H(DMSO) ₂ [3.1] | H(DMF) ₂ [3.1] | [(dppe)Pd(NCMe)Me][Λ - 3.1] ·CH ₃ CN | [(dppe)Pd(NCMe)Me][Δ - 3.1] ·CH ₃ CN | [(dppe)Pd(NCMe) ₂][3.1] ₂ ·2CH ₃ CN |
|--------------------------------------------------------------------------|----------------------------------------------------------------|-----------------------------------------------------------------|---------------------------------------------------------------------------------|---------------------------------------------------------------------------------|-----------------------------------------------------------------------------------|
| formula | C ₂₂ H ₂₅ O ₈ PS ₂ | C ₂₄ H ₂₇ N ₂ O ₈ P | C ₄₉ H ₄₅ N ₂ O ₆ P ₃ Pd | C ₄₉ H ₄₅ N ₂ O ₆ P ₃ Pd | C ₇₀ H ₆₀ N ₄ O ₁₂ P ₄ Pd |
| fw | 512.51 | 502.45 | 957.18 | 957.18 | 1379.50 |
| cryst syst | monoclinic | monoclinic | monoclinic | monoclinic | triclinic |
| space group | <i>P</i> 2 ₁ / <i>n</i> | <i>P</i> 2 ₁ / <i>n</i> | <i>P</i> 2 ₁ | <i>P</i> 2 ₁ | <i>P</i> $\bar{1}$ |
| color | colorless | colorless | colorless | colorless | yellow |
| <i>a</i> (Å) | 12.767(3) | 11.5961(9) | 10.036(1) | 10.030(2) | 12.173(1) |
| <i>b</i> (Å) | 13.932(3) | 14.877(1) | 17.318(2) | 17.331(3) | 15.673(2) |
| <i>c</i> (Å) | 13.625(3) | 13.831(1) | 13.035(2) | 13.073(3) | 18.048(2) |
| α (deg) | 90 | 90 | 90 | 90 | 81.711(5) |
| β (deg) | 108.507(7) | 97.807(4) | 95.200(5) | 95.079(7) | 83.998(5) |
| γ (deg) | 90 | 90 | 90 | 90 | 68.021(5) |
| <i>V</i> (Å ³) | 2298.2(9) | 2364.0(3) | 2256.2(5) | 2263.6(8) | 3154.8(6) |
| <i>T</i> (K) | 173(2) | 173(2) | 173(2) | 173(2) | 173(2) |
| <i>Z</i> | 4 | 4 | 2 | 2 | 2 |
| μ (Mo K α) (mm ⁻¹) | 0.349 | 0.169 | 0.569 | 0.567 | 0.463 |
| cryst size (mm ³) | 1.1 × 0.7 × 0.5 | 0.5 × 0.3 × 0.2 | 0.9 × 0.8 × 0.3 | 0.8 × 0.6 × 0.5 | 0.40 × 0.35 × 0.15 |
| <i>D</i> _{calcd.} (Mg m ⁻³) | 1.481 | 1.406 | 1.409 | 1.404 | 1.452 |
| 2 θ (max) (°) | 55.8 | 55.88 | 56.0 | 55.82 | 56.7 |
| no. of reflns | 39445 | 38168 | 19836 | 37561 | 67930 |
| no. of unique data | 5373 | 5664 | 9813 | 10816 | 15158 |
| <i>R</i> (int) | 0.0319 | 0.0493 | 0.0205 | 0.0216 | 0.0476 |
| refln/param ratio | 14.37 | 17.48 | 17.75 | 19.56 | 18.40 |
| <i>R</i> ₁ [<i>I</i> > 2 σ (<i>I</i>)] ^a | 0.0324 | 0.0423 | 0.0245 | 0.0216 | 0.0375 |
| <i>wR</i> ₂ [all data] ^b | 0.0836 | 0.1131 | 0.0621 | 0.0518 | 0.0816 |
| GOF | 1.019 | 1.020 | 1.042 | 1.032 | 1.004 |

^a $R_1 = \frac{\sum |F_o| - |F_c|}{\sum |F_o|}$. ^b $wR_2(F^2[\text{all data}]) = \left\{ \frac{\sum [w(F_o^2 - F_c^2)^2]}{\sum [w(F_o^2)^2]} \right\}^{1/2}$. Adapted with permission from *Organometallics* **2009**, *28*, 4491. Copyright 2009 American Chemical Society.

Chapter 4: Novel Cationic Polymerization Initiators for Vinyl Monomers*

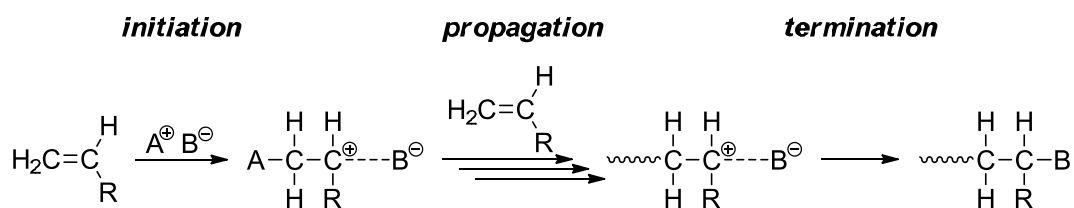
4.1 Introduction

Effective cationic polymerization of vinyl monomers necessitates highly reactive initiators that are often too unstable to isolate. Thus, active initiators (A^+B^-) are commonly generated *in situ* by binary systems, typically comprised of a proton donor (HX) or a cationogen (cation donor, RX) activated by a neutral Lewis acid (MX_n), such as BF_3 , $AlCl_3$, $SnCl_4$, $TiCl_4$ and $ZnCl_2$ (Scheme 4.1).²⁵⁴⁻²⁵⁹ The activation of proton donors (HX), such as hydrohalic acids,²⁶⁰⁻²⁶⁴ carboxylic acids,²⁶⁵⁻²⁷⁰ and water,²⁷¹ liberates H^+ as the active cationic initiator. While the activation of cationogens (RX), such as alkyl halides,²⁷²⁻²⁷⁷ alkylaryl halides,²⁷⁸⁻²⁷⁹ esters,²⁸⁰⁻²⁸³ and alcohols,²⁸⁴⁻²⁹⁰ results in the formation of a carbenium ion as the active cationic initiator. Subsequent initiation of polymerization forms a propagating carbenium ion, which is charge-balanced by the corresponding anion (B^-), derived from the Lewis acid activator (MX_n) (Scheme 4.2). Due to the highly electrophilic nature of the propagating carbenium, the role of counteranion (B^-) is of crucial importance.²⁵⁴⁻²⁵⁹ The nucleophilicity of the anion can influence the degree of dissociation between the ion-pair. If the anion is too nucleophilic, propagation will be suppressed, thereby effectively terminating polymerization. In addition, the rates of chain transfer are also highly affected by the nature of the counteranion.²⁹¹⁻²⁹³



Scheme 4.1 Generation of active initiator (A^+B^-) for cationic polymerization.

* A version of this chapter will be submitted for publication. Paul W. Siu and Derek P. Gates.



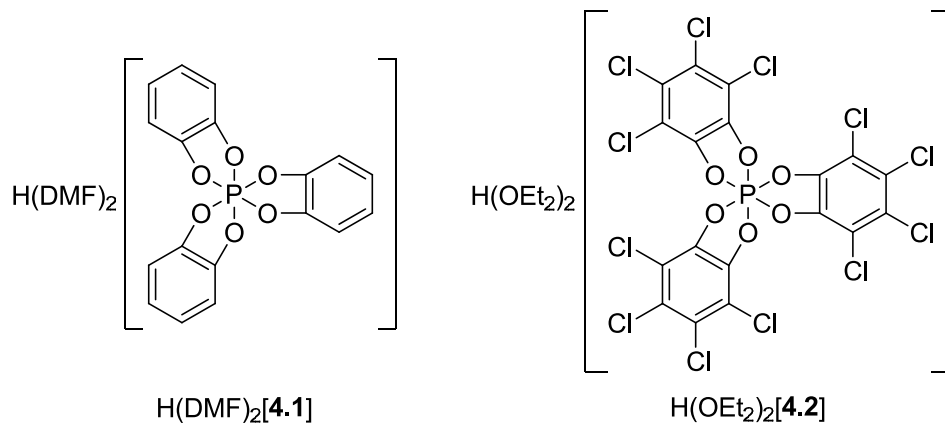
Scheme 4.2 Cationic polymerization of vinyl monomers.

For binary initiator systems, the choice of Lewis acid activator has a direct effect on the nature of the *in situ* counteranion. The use of highly electrophilic Lewis acids, such as $\text{B}(\text{C}_6\text{F}_5)_3$,²⁹³⁻³⁰⁰ $o\text{-C}_6\text{F}_4\{\text{B}(\text{C}_6\text{F}_5)_2\}_2$,^{191,301} and $o\text{-C}_6\text{F}_4(9\text{-BC}_{12}\text{F}_8)_2$ ($9\text{-BC}_{12}\text{F}_8 = 1,2,3,4,5,6,7,8\text{-octafluoro-9-borabluorene}$),¹⁹¹ in conjunction with an appropriate cationogen, enables the *in situ* preparation of active carbenium initiators stabilized by the corresponding weakly nucleophilic anions. For proton donors, the activation of water or carboxylic acids by $\text{B}(\text{C}_6\text{F}_5)_3$,^{74-75,293,298-300} $o\text{-C}_6\text{F}_4\{\text{B}(\text{C}_6\text{F}_5)_2\}_2$,³⁰² $o\text{-C}_6\text{F}_4(9\text{-BC}_{12}\text{F}_8)_2$,³⁰² $\text{Al}(\text{C}_6\text{F}_5)_3$,³⁰³ and $\text{Ga}(\text{C}_6\text{F}_5)_3$ ³⁰³ has been shown to generate protic initiators in solution. Although the active initiators are presumed to be a strong Brønsted acid containing the corresponding weakly nucleophilic anion, their structures tend to be somewhat ill-defined. Likewise, in the presence of water or other protogens, silylium and trityl salts of the weakly nucleophilic $[\text{B}(\text{C}_6\text{F}_5)_4]^-$ have been shown to initiate cationic polymerization.^{292,304-305} The active initiator is presumed to be the protic acid of $[\text{B}(\text{C}_6\text{F}_5)_4]^-$. The activation of neutral metallocene complexes {e.g. $[(\text{C}_5\text{H}_5)_2\text{YMe}]_2$, $[(\text{C}_5\text{H}_4\text{SiMe}_3)_2\text{YMe}]_2$, $[(\text{C}_5\text{H}_4\text{SiMe}_3)_2\text{ZrH}_2]_2$, $(\text{C}_5\text{Me}_5)\text{TiMe}_3$ } by trityl salts of weakly nucleophilic anions, such as $[\text{B}(\text{C}_6\text{F}_5)_4]^-$,^{68,306-308} $[\text{H}_2\text{N}\{\text{B}(\text{C}_6\text{F}_5)_3\}_2]^-$,⁶⁸ $[\text{CN}\{\text{B}(\text{C}_6\text{F}_5)_3\}_2]^-$,⁶⁸ and $[\text{B}\{\text{C}_6\text{F}_4(\text{Si}^i\text{Pr}_3)_4\}]^-$,³⁰⁷ can also generate highly effective *in situ* initiators for cationic polymerization.³⁰⁹⁻³¹⁰

In contrast to binary initiator systems, isolable protic initiators containing weakly nucleophilic anions are somewhat less well established. Solid Brønsted acids, such as $[\text{H}(\text{OEt}_2)_2][\text{Al}\{\text{OC}(\text{CF}_3)_3\}_4]$,³¹¹ $[\text{H}(\text{OEt}_2)_2][\text{B}(\text{C}_6\text{F}_5)_4]$,³¹² $[\text{Na}(\text{H}_2\text{O})_2][\text{B}(3,5\text{-}(\text{CF}_3)_2\text{C}_6\text{H}_3)_4]$,³¹³ and $\text{H}[\text{B}(\text{C}_2\text{O}_4)_2]$ ($\text{C}_2\text{O}_4 = \text{oxalate}$),³¹⁴⁻³¹⁵ have been studied as cationic polymerization initiators. In

addition, heteropolyacids such as 12-tungstophosphoric acid ($\text{H}_3\text{PW}_{12}\text{O}_{40}$),³¹⁶ 12-molybdophosphoric acid ($\text{H}_3\text{PMo}_{12}\text{O}_{40}$),³¹⁶⁻³¹⁷ and $\text{M}_{0.5}\text{H}_{0.5}\text{PW}_{12}\text{O}_{40}$ ($\text{M} = \text{Cs}, \text{NH}_4$)³¹⁸ have received some attention as heterogeneous initiators.

In Chapter 3, the convenient synthesis of solid Brønsted acid $\text{H}(\text{DMF})_2[\mathbf{4.1}]$ was described. The high acidity of this reagent was evidenced by its efficacy to protonate late transition metal-alkyl bonds, a key step in the generation of numerous active catalyst species. Based on the IR stretching frequencies of the ammonium salts, the basicity of $[\mathbf{4.1}]^-$ is similar to $[\text{BF}_4]^-$; thus, their nucleophilicity may also be similar. Therefore, $\text{H}(\text{DMF})_2[\mathbf{4.1}]$ is of interest as an initiator for the cationic polymerization of vinyl monomers. In this chapter, the preliminary investigation into the efficacy of $\text{H}(\text{DMF})_2[\mathbf{4.1}]$ and its chlorinated derivative, $\text{H}(\text{OEt}_2)_2[\mathbf{4.2}]$, to initiate the cationic polymerizations of *n*-butyl vinyl ether, styrene and isoprene will be discussed. Although the ammonium salts of $[\mathbf{4.2}]^-$ are known,^{141,319} strong Brønsted acids of $[\mathbf{4.2}]^-$ have not been reported.



4.2 Results and Discussion

4.2.1 $\text{H}(\text{DMF})_2[\mathbf{4.1}]$ Initiated Cationic Polymerizations

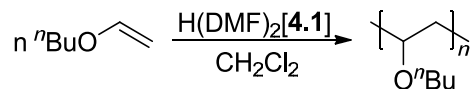
Brønsted acid $\text{H}(\text{DMF})_2[\mathbf{4.1}]$ was readily synthesized following procedures outlined in Chapter 3. The efficacy of $\text{H}(\text{DMF})_2[\mathbf{4.1}]$ as a cationic polymerization initiator for *n*-butyl vinyl

ether, styrene and isoprene was investigated at 17 °C (Table 4.1). *n*-Butyl vinyl ether was polymerized by H(DMF)₂[**4.1**] in dichloromethane to afford poly(*n*-butyl vinyl ether) as a brown oil, albeit in low yield (15%) (Table 4.1, entry 1). The coloration of the resultant polymer is common among the cationically polymerized poly(vinyl ether)s reported in the literature.^{262,277,320-323} Analysis of the polymer by triple detection gel permeation chromatography (GPC-LLS) revealed it is of moderate molecular weight ($M_n = 10,000 \text{ g mol}^{-1}$) and high polydispersity index (PDI = 2.80).

Table 4.1 H(DMF)₂[**4.1**] initiated cationic polymerizations of *n*-butyl vinyl ether, styrene and isoprene in CH₂Cl₂ at 17 °C.

| entry | initiator | monomer | temp (°C) | time (min) | [M]:[I] ^a | yield (%) | M_n obsd ^b (g mol ⁻¹) | PDI |
|-------|------------------------------------|-----------------------------|-----------|------------|----------------------|----------------|------------------------------------------------|------|
| 1 | H(DMF) ₂ [4.1] | <i>n</i> -butyl vinyl ether | 19 | 15 | 410 | 15 | 10,000 | 2.80 |
| 2 | H(DMF) ₂ [4.1] | styrene | 17 | 15 | 239 | 0 ^c | | |
| 3 | H(DMF) ₂ [4.1] | isoprene | 17 | 15 | 271 | 0 ^c | | |

^a [monomer]:[initiator]. ^b Absolute molecular weights were determined using triple-detection GPC. ^c No polymer was isolated.



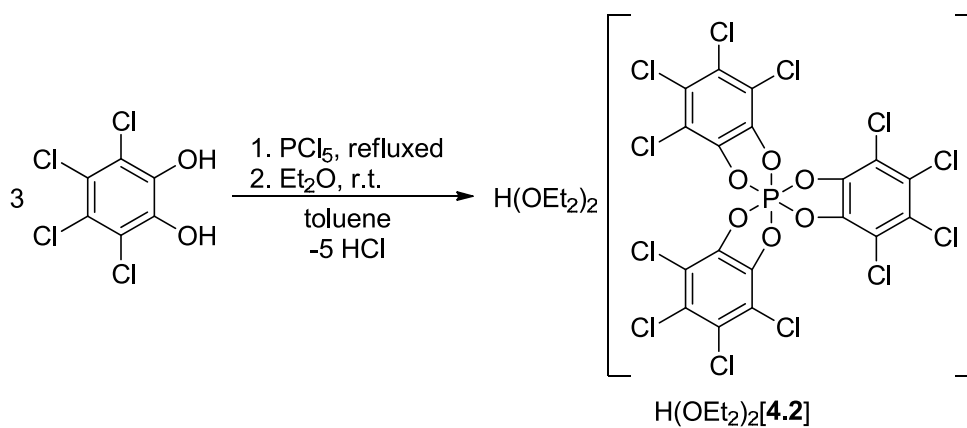
Scheme 4.3 H(DMF)₂[**4.1**] initiated cationic polymerization of *n*-butyl vinyl ether.

Furthermore, the treatment of Brønsted acid H(DMF)₂[**4.1**] in dichloromethane with styrene or isoprene at 17 °C did not afford any polymers (Table 4.1, entry 2-3). This indicates that H(DMF)₂[**4.1**] is not an effective initiator for these less reactive vinyl monomers and suggests that [H(DMF)₂]⁺ might not be sufficiently acidic to initiate cationic polymerization. Alternatively, anion [**4.1**]⁻ might be too nucleophilic, thus propagation is sequestered, leading to the termination of polymerization. Nevertheless, the ability of H(DMF)₂[**4.1**] to initiate the cationic polymerization of *n*-butyl vinyl ether is encouraging; however, a stronger Brønsted acid containing a less nucleophilic anion would be desirable.

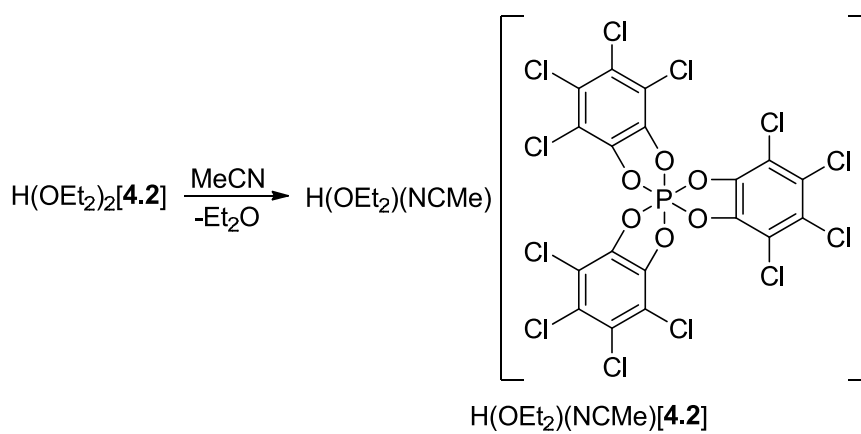
4.2.2 Synthesis and Characterization of Brønsted Acids of [4.2]⁻

It is well-understood that increasing the number of electron-withdrawing substituents on the anion would lead to increased charge delocalization and decreased nucleophilicity.³⁸⁻³⁹ Therefore, it was expected that the chlorinated [4.2]⁻ should be less nucleophilic than [4.1]⁻. Although the ammonium salts of [4.2]⁻ are known,^{141,319} strong Brønsted acids of [4.2]⁻ have yet to be reported. In particular, [H(OEt₂)₂]⁺ acids of [4.2]⁻ are of great interest as cationic polymerization initiators, since [H(OEt₂)₂]⁺ (pK_a = -3.6 ± 0.1)³²⁴ is more acidic than [H(DMF)]⁺ (pK_a = -1.2 ± 0.5).²²⁰

It has been reported that treatment of PCl₅ with tetrachlorocatechol (3 equiv) in hot toluene, followed by addition of an amine, readily affords the ammonium salt of [4.2]⁻.¹⁴¹ Inspired by this previous work, it was speculated that if a weaker base, such as Et₂O, was employed in the reaction, a stronger Brønsted acid of [4.2]⁻ could be synthesized. Hence, PCl₅ and tetrachlorocatechol (3 equiv) were refluxed together in toluene, followed by the addition of excess Et₂O, to afford an off-white precipitate that was presumed to be crude H(OEt₂)₂[4.2] (Scheme 4.4). Subsequent work-up and recrystallization (CH₂Cl₂/Et₂O) afforded the Brønsted acid H(OEt₂)₂[4.2] as a white crystalline solid, suitable for X-ray diffraction. Interestingly, recrystallization of H(OEt₂)₂[4.2] from acetonitrile gave a different crystal structure, H(OEt₂)(NCMe)[4.2], as determined by X-ray diffraction (Scheme 4.5). The molecular structures of H(OEt₂)₂[4.2] and H(OEt₂)(NCMe)[4.2] are presented in Figure 4.1 and Figure 4.2, respectively. For H(OEt₂)(NCMe)[4.2], there are two crystallographically independent compounds per asymmetric unit. For clarity, only one of them is shown in Figure 4.2. The metrical parameters for H(OEt₂)₂[4.2] and H(OEt₂)(NCMe)[4.2] will be discussed later.



Scheme 4.4 Synthesis of Brønsted acid $\text{H}(\text{OEt}_2)_2[4.2]$.



Scheme 4.5 Synthesis of Brønsted acid $\text{H}(\text{OEt}_2)(\text{NCMe})[4.2]$.

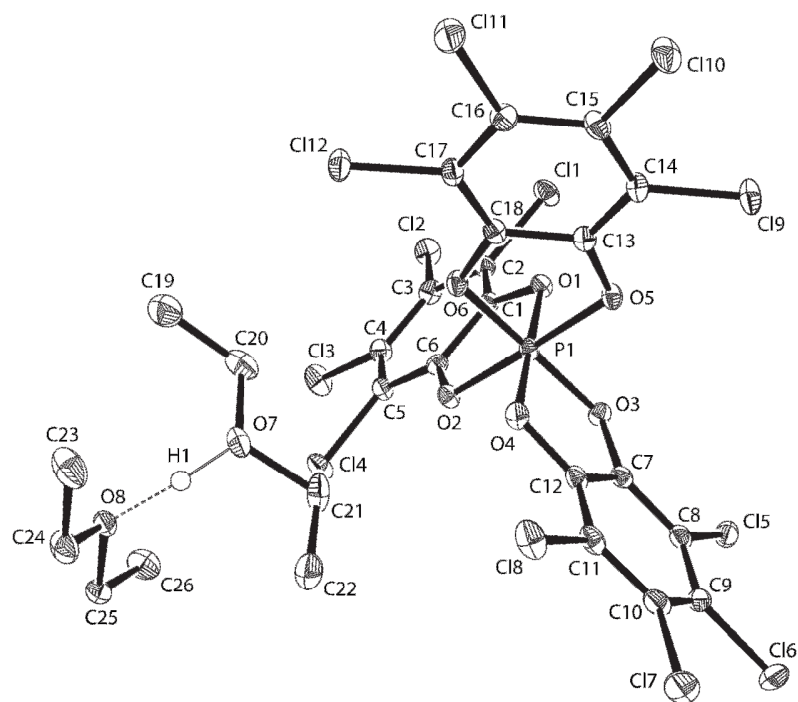


Figure 4.1 Molecular structure of $\text{H}(\text{OEt}_2)_2[\mathbf{4.2}]$. Ellipsoids are drawn at the 50% probability level. Solvents of crystallization ($1.5 \times \text{CH}_2\text{Cl}_2$) and hydrogen atoms are omitted for clarity, except for H(1). Selected bond lengths (\AA): O(1)-P(1) = 1.704(1); O(2)-P(1) = 1.709(1); O(3)-P(1) = 1.717(1); O(4)-P(1) = 1.717(1); O(5)-P(1) = 1.722(1); O(6)-P(1) = 1.722(1); H(1)-O(7) = 1.09(4); H(1)-O(8) = 1.34(4); O(7)-O(8) = 2.429(2). Selected bond angles ($^\circ$): O(1)-P(1)-O(2) = 91.44(6); O(3)-P(1)-O(4) = 90.89(6); O(5)-P(1)-O(6) = 90.79(6); O(7)-H(1)-O(8) = 173(3).

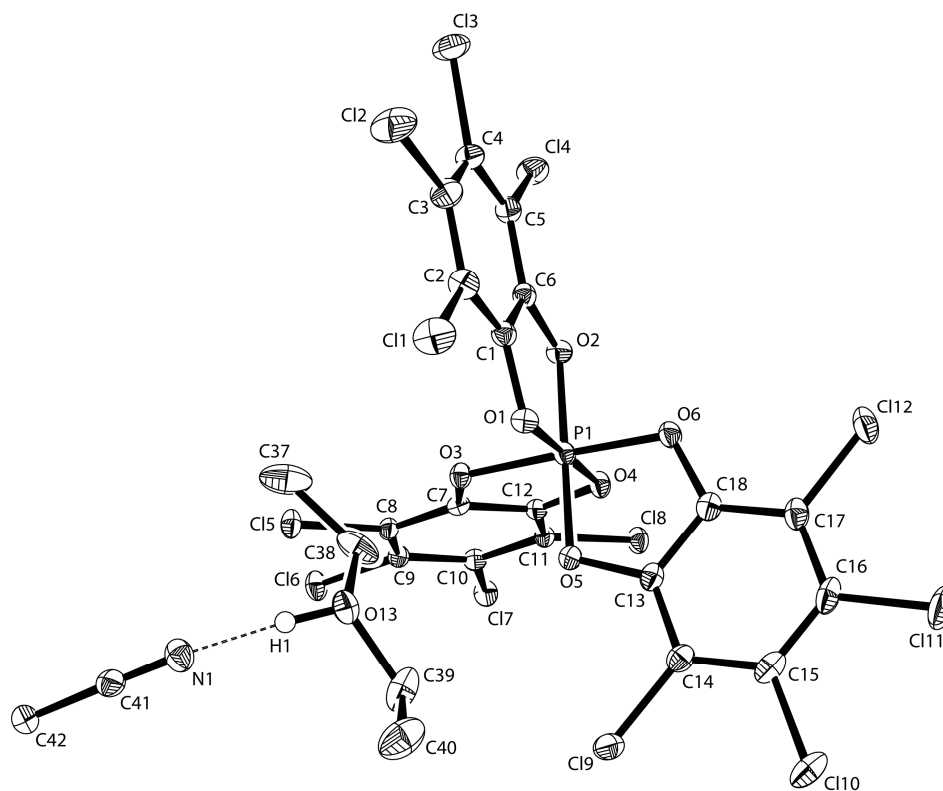


Figure 4.2 Molecular structure of $\text{H}(\text{OEt}_2)(\text{NCMe})[\mathbf{4.2}]$. Only one of two molecules in the asymmetric unit is shown. Ellipsoids are drawn at the 50% probability level. Solvents of crystallization ($1.5 \times \text{CH}_3\text{CN}$) and hydrogen atoms are omitted for clarity, except for H(1). Selected bond lengths (\AA): O(1)-P(1) = 1.720(1); O(2)-P(1) = 1.708(1); O(3)-P(1) = 1.724(1); O(4)-P(1) = 1.714(1); O(5)-P(1) = 1.726(2); O(6)-P(1) = 1.712(1); H(1)-O(13) = 0.91(3); H(1)-N(1) = 1.63(4); O(13)-N(1) = 2.536(3). Selected bond angles ($^\circ$): O(1)-P(1)-O(2) = 90.92(6); O(3)-P(1)-O(4) = 90.95(6); O(5)-P(1)-O(6) = 90.93(6); O(13)-H(1)-N(1) = 175(3).

Analysis of a CD_3CN solution of $\text{H}(\text{OEt}_2)_2[\mathbf{4.2}]$ using ^{31}P NMR spectroscopy revealed a singlet resonance at -79.9 ppm, consistent with the ammonium salts reported previously,¹⁴¹ thus confirming the presence of hexacoordinated $[\mathbf{4.2}]^-$ in solution. In addition, $\text{H}(\text{OEt}_2)_2[\mathbf{4.2}]$ was characterized by ^1H and $^{13}\text{C}\{^1\text{H}\}$ NMR spectroscopy. At 25 $^\circ\text{C}$, the ^1H NMR spectrum (CD_3CN) of the crystalline solid revealed a broad signal at 13.2 ppm, which was assigned to the acidic $[\text{H}(\text{OEt}_2)_2]^+$ (Figure 4.3). At -80 $^\circ\text{C}$ (CD_2Cl_2), this signal shifts further downfield to 16.7 ppm (Figure 4.4). Such a downfield signal is comparable to the chemical shifts of the acidic proton in $\text{H}(\text{DMSO})_2[\mathbf{4.1}]$ (Chapter 3: $\delta = 13.3$, CD_3CN), $\text{H}(\text{DMF})_2[\mathbf{4.1}]$ (Chapter 3: $\delta = 15.3$, CD_3CN) and other $[\text{H}(\text{OEt}_2)_2]^+$ acids at room temperature, such as $[\text{H}(\text{OEt}_2)_2][\text{B}(3,5\text{-}(\text{CF}_3)_2\text{C}_6\text{H}_3)_4]$

($\delta = 11.1$, CD_2Cl_2),⁵⁰ $[\text{H}(\text{OEt}_2)_2][\text{B}(\text{C}_6\text{F}_5)_4]$ ($\delta = 15.5$, CD_2Cl_2),²⁰¹ $[\text{H}(\text{OEt}_2)_2][\text{H}_2\text{N}\{\text{B}(\text{C}_6\text{F}_5)_3\}]$ ($\delta = 16.6$, CD_2Cl_2),⁶⁵ $[\text{H}(\text{OEt}_2)_2][(\text{C}_3\text{H}_3\text{N}_2)\{\text{B}(\text{C}_6\text{F}_5)_3\}_2]$ ($\delta = 16.3$, CD_2Cl_2),³²⁵ $[\text{H}(\text{OEt}_2)_2][\text{C}_6\text{F}_4-1,2-\{\text{B}(\text{C}_6\text{F}_5)_2\}_2(\mu\text{-OCH}_3)]$ ($\delta = 16.4$, CD_2Cl_2),³²⁶ $[\text{H}(\text{OEt}_2)_2][\text{CHB}_{11}\text{Me}_5\text{X}_6]$ (X = Cl, $\delta = 13.8$; X = Br, $\delta = 11.7$, C_6D_6),²³³ $[\text{H}(\text{OEt}_2)_2][\text{Al}\{\text{OC}(\text{CF}_3)_3\}_4]$ ($\delta = 14.7$, C_6D_6),¹⁸⁶ and $[\text{H}(\text{OEt}_2)_2][\text{P}(\text{C}_2\text{O}_4)_3]$ ($\text{C}_2\text{O}_4 = \text{oxalate}$, $\delta = 15.5$, CDCl_3).¹⁴⁰ Importantly, the integration ratio of the signal assigned to the acidic proton ($\delta = 13.2$) and the signals assigned to Et_2O ($\delta = 3.90$ and 1.28) in Figure 4.3 are consistent with the proposed structure. The slight downfield shift observed for the complex, in comparison to free Et_2O ($\delta = 3.42$ and 1.12),²¹⁸ provides evidence that the $[\text{H}(\text{OEt}_2)_2]^+$ moiety is retained in solution. The ^1H NMR spectrum (CD_3CN) also revealed the presence of 0.5 equivalent of residual CH_2Cl_2 from recrystallization, based on the integration ratio of its signal at 5.44 ppm and the signal assigned to acidic proton. This is consistent with data obtained from elemental analysis.

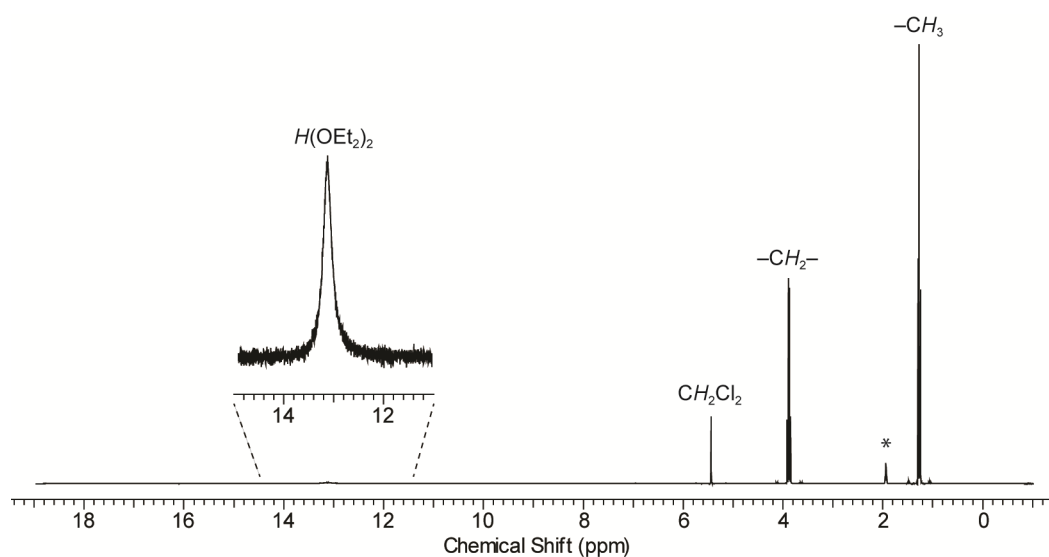


Figure 4.3 ^1H NMR (400 MHz, CD_3CN) spectrum of $\text{H}(\text{OEt}_2)_2[\mathbf{4.2}]$ at 25 °C. (* = residual protonated solvent)

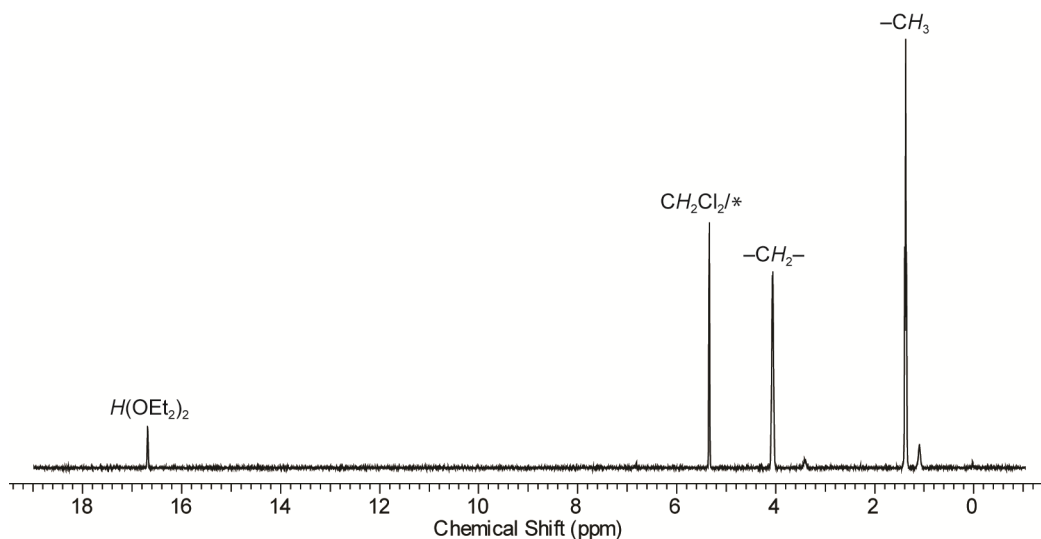
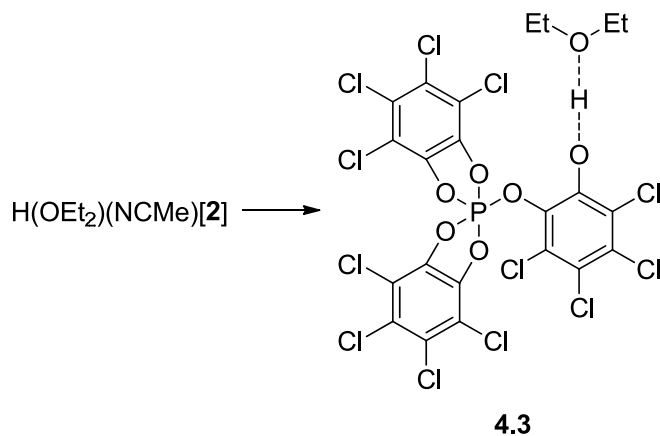


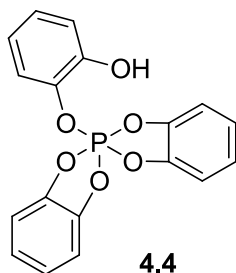
Figure 4.4 ^1H NMR (400 MHz, CD_2Cl_2) spectrum of $\text{H}(\text{OEt}_2)_2[\mathbf{4.2}]$ at $-80\text{ }^\circ\text{C}$. (* = residual protonated solvent)

Interestingly, the ^{31}P and ^1H NMR spectra of crystalline $\text{H}(\text{OEt}_2)(\text{NCMe})[\mathbf{4.2}]$ in CD_2Cl_2 suggest a different structure in solution than in solid-state and provide evidence for the proposed structure **4.3** (Scheme 4.6). ^{31}P NMR spectroscopy revealed only one singlet at ca. -26 ppm ($25\text{ }^\circ\text{C}$: $\delta = -25.5$; $-80\text{ }^\circ\text{C}$: $\delta = -27.3$), consistent with the proposed pentacoordinated structure **4.3** and the related pentacoordinated **4.4** ($\delta = -29$).¹⁶⁰ Typically, complexes of hexacoordinated $[\mathbf{4.2}]^-$ give rise to a singlet at ca. -80 ppm;¹⁴¹ however, no resonance was observed in this region, suggesting the absence of $[\mathbf{4.2}]^-$ in solution. At $25\text{ }^\circ\text{C}$, the ^1H NMR spectrum revealed the presence of free MeCN ($\delta = 1.98$). More importantly, the signals assigned to Et_2O were observed as a doublet of quartets at 4.24 ppm ($^3J_{\text{HH}} = 11$ Hz, $^3J_{\text{HH}} = 7$ Hz) and a doublet of triplets at 1.28 ppm ($^3J_{\text{HH}} = 7$ Hz, $^4J_{\text{HH}} = 2$ Hz). The fine couplings can be attributed to the acidic proton in the proposed structure **4.3**, strongly bound to the Et_2O molecule in solution. The strong interaction between the acidic proton and the Et_2O molecule likely contributes to the observed doublet of quartets ($\delta = 4.24$) being shifted downfield in comparison to the quartet for $\text{H}(\text{OEt}_2)_2[\mathbf{4.2}]$ ($\delta = 3.90$), which is further downfield than for the free Et_2O [$\delta = 3.42$].²¹⁸ The resonance for the

acidic proton of the proposed structure **4.3** was not observed in the ^1H NMR spectra at 25 °C and -80 °C. However, the above spectroscopic data do suggest that the dissolution of $\text{H}(\text{OEt}_2)(\text{NCMe})[\mathbf{4.2}]$ in CH_2Cl_2 results in the dissociation of hexacoordinated $[\mathbf{4.2}]^-$ into a pentacoordinated species that is likely to be **4.3**. Thus, $\text{H}(\text{OEt}_2)(\text{NCMe})[\mathbf{4.2}]$ was not investigated as a cationic polymerization initiator.



Scheme 4.6 Proposed dissociation of $\text{H}(\text{OEt}_2)(\text{NCMe})[\mathbf{4.2}]$ in solution into **4.3**.



4.2.3 Molecular Structures of $\text{H}(\text{OEt}_2)_2[\mathbf{4.2}]$ and $\text{H}(\text{OEt}_2)(\text{NCMe})[\mathbf{4.2}]$.

The phosphorus atom of $[\mathbf{4.2}]^-$, in $\text{H}(\text{OEt}_2)_2[\mathbf{4.2}]$ (Figure 4.1) and $\text{H}(\text{OEt}_2)(\text{NCMe})[\mathbf{4.2}]$ (Figure 4.2), shows only minor deviation from perfect octahedral geometry. The largest deviation from octahedral angles is $3.39(6)^\circ$ for $\text{H}(\text{OEt}_2)_2[\mathbf{4.2}]$ and $3.55(7)^\circ$ for $\text{H}(\text{OEt}_2)(\text{NCMe})[\mathbf{4.2}]$. The average P-O bond lengths $\{\text{H}(\text{OEt}_2)_2[\mathbf{4.2}]$: 1.715(2) Å; $\text{H}(\text{OEt}_2)(\text{NCMe})[\mathbf{4.2}]$: 1.717(5) Å} are longer than those typically observed for P-O single bonds

in triarylphosphates [1.59(1) Å]¹⁶⁵ but are similar to those found in previously isolated complexes of **[4.2]**, such as [diethylammonium][**4.2**] [avg. 1.713(8) Å],³¹⁹ [cinchonidinium][**Δ-4.2**] [avg. 1.71(2) Å],¹⁴¹ and [tris(4-dimethylaminobenzene)carbenium][**4.2**] [avg. 1.72(2) Å].³²⁷

In the molecular structure of Brønsted acid H(OEt₂)₂**[4.2]** (Figure 4.1), the acidic hydrogen atom, H(1), was located in the difference map and refined isotropically. H(1) is coordinated asymmetrically by two Et₂O molecules through their oxygen atoms [H(1)-O(7) = 1.09(4) Å; H(1)-O(8) = 1.34(4) Å]. Similar asymmetric hydrogen bonding has been observed in related [H(OEt₂)₂]⁺ acids, including [H(OEt₂)₂][B(C₆F₅)₄] [0.93(1) and 1.52(1) Å],²⁰¹ [H(OEt₂)₂][CHB₁₁Me₅Cl₆] [1.08(3) and 1.59(3) Å; 0.80(3) and 1.45(3) Å],²³³ and [H(OEt₂)₂][Al{OC(CF₃)₃}₄] [0.75(5) and 1.76(5) Å].¹⁸⁶ However, the exact position of the hydrogen atom as determined by X-ray diffraction is generally considered to be unreliable.^{186,201,328} The O...O distance in [H(OEt₂)₂]⁺ is more accurately measured by X-ray diffraction. For H(OEt₂)₂**[4.2]**, the distance between the oxygen atoms of the two Et₂O molecules [O(7)...O(8) = 2.429(2) Å] is significantly shorter than the sum of their van der Waals radii [*r*_{vdw} = 3.04 Å],¹⁷² which is consistent with strong hydrogen bonding for the O-H-O moiety in the [H(OEt₂)₂]⁺ cation.^{227,230} The O(7)...O(8) distance is similar to that found in [H(OEt₂)₂][B(C₆F₅)₄] [2.446(9) Å],²⁰¹ [H(OEt₂)₂][CHB₁₁Me₅Cl₆] [avg. 2.40(1) Å],²³³ [H(OEt₂)₂][Al{OC(CF₃)₃}₄] [2.424(5) Å]¹⁸⁶ and [H(OEt₂)₂][P(C₂O₄)₃] [avg. 2.37(3) Å]¹⁴⁰ but is slightly longer than those found in [H(OEt₂)₂][(C₃H₃N₂){B(C₆F₅)₃}₂] [2.395(8) Å]³²⁵ and [H(OEt₂)₂][C₆F₄-1,2-{B(C₆F₅)₂}₂(μ-OCH₃)] [2.394(7) Å].³²⁶

Analogous to that described for H(OEt₂)₂**[4.2]**, in the molecular structure of H(OEt₂)(NCMe)**[4.2]** (Figure 4.2), hydrogen atom H(1) was also located in the difference map and refined isotropically. Remarkably, H(1) is coordinated by one Et₂O molecule through the oxygen atom [H(1)-O(13) = 0.91(3) Å] and one acetonitrile molecule through the nitrogen atom

[H(1)-N(1) = 1.63(4) Å]. Notably, this is believed to be the first example of a crystallographically characterized [H(OEt₂)(NCMe)]⁺. The more reliable distance from X-ray diffraction is the O⋯N distance in [H(OEt₂)(NCMe)]⁺ [O(13)⋯N(1) = 2.536(3) Å], which is significantly shorter than their sum of van der Waals radii for oxygen and nitrogen [$r_{\text{vdw}} = 3.07$ Å].¹⁷² Similar to the Brønsted acid H(OEt₂)₂[**4.2**] discussed above, this is also consistent with strong hydrogen bonding for the O-H-N moiety in [H(OEt₂)(NCMe)]⁺.²²⁷ In addition, the O(13)⋯N(1) distance is similar to those found in other complexes containing strong O-H-N hydrogen bonds, such as pentachlorophenol with 4-methylpyridine [2.515(4) Å],³²⁹⁻³³⁰ pentachlorophenol with 3-oxo-azabicyclo[2.2.2]octane [2.514(5) Å],³³¹ 3,5-dinitrobenzoic acid with 4-methylpyridine [2.525(2) Å],³³² and 3,5-dinitrobenzoic acid with 3,5-dimethylpyridine [2.529(2) Å].³³³

Notably, the molecular structures of H(OEt₂)₂[**4.2**] and H(OEt₂)(NCMe)[**4.2**] suggest weak ion-pair interactions are present between each of the cation and [**4.2**]⁻. In each compound, the closest contact is between an oxygen of the [**4.2**]⁻ anion and a hydrogen of the CH₂ moiety within Et₂O {H(OEt₂)₂[**4.2**], Figure 4.1: O(4)⋯H(21a) = 2.429(1) Å; H(OEt₂)(NCMe)[**4.2**], Figure 4.2: O(1)⋯H(38b) = 2.236(2) Å}. In both cases, the closest ion-pair distances are within the sum of the van der Waals radii for oxygen and hydrogen [$r_{\text{vdw}} = 2.72$ Å].¹⁷²

4.2.4 H(OEt₂)₂[**4.2**] Initiated Cationic Polymerizations

4.2.4.1 Cationic Polymerizations at 17 °C

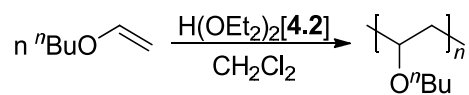
Initial studies into the efficacy of H(OEt₂)₂[**4.2**] as a cationic polymerization initiator were carried out in similar polymerization conditions to those for H(DMF)₂[**4.1**] (Table 4.2). *n*-Butyl vinyl ether was polymerized by H(OEt₂)₂[**4.2**] in dichloromethane at 19 °C and 16 °C to afford poly(*n*-butyl vinyl ether) (Scheme 4.7) as a brown gummy solid in reasonable yield (19

°C: 80%; 16 °C: 63%) (Table 4.2, entry 1). At these temperatures, it was difficult to achieve consistent polymerization results, as evidenced by the wide range of molecular weight of the polymers obtained (19 °C: $M_n = 35,200 \text{ g mol}^{-1}$, PDI = 1.31; 16 °C: $M_n = 90,800 \text{ g mol}^{-1}$, PDI = 2.57). Such inconsistency might be due to the difficulties in dissipating heat when the polymerizations were carried out at these higher temperatures. Nevertheless, these polymers are of higher molecular weight than the polymer initiated by H(DMF)₂[**4.1**] (Table 4.1, entry 1: $M_n = 10,000 \text{ g mol}^{-1}$, PDI = 2.80). At ambient temperature, other cationic polymerization initiator systems (e.g. AlHCl₂³³⁴ and EtAlCl₂/1-butoxyethyl-acetate³³⁵) for *n*-butyl vinyl ether can also afford polymers of moderate molecular weight. The brown color of the H(OEt₂)₂[**4.2**] initiated poly(*n*-butyl vinyl ether) is similar to that of the H(DMF)₂[**4.1**] initiated poly(*n*-butyl vinyl ether). Upon close inspection, the ¹H NMR spectra of the polymer initiated by H(DMF)₂[**4.1**] (Figure 4.5a) and H(OEt₂)₂[**4.2**] (Figure 4.5b) revealed several weak broad resonances in the vinylic region, consistent with the presence of a small amount of terminal conjugated polyene moieties.³³⁶ The formation of terminal conjugated polyenes during the cationic polymerization of vinyl ethers has previously been rationalized through β-proton elimination followed by dealcoholation.³³⁶

Table 4.2 H(OEt₂)₂[**4.2**] initiated cationic polymerizations of *n*-butyl vinyl ether, styrene and isoprene in CH₂Cl₂ at 17 °C.

| entry | initiator | monomer | temp (°C) | time (min) | [M]:[I] ^a | yield (%) | M_n obsd ^b (g mol ⁻¹) | PDI |
|-------|--------------------------------------------------|-----------------------------|--------------|---------------|----------------------|--------------|---------------------------------------------------|------|
| 1 | H(OEt ₂) ₂ [4.2] | <i>n</i> -butyl vinyl ether | 19 | 15 | 411 | 80 | 35,200 | 1.31 |
| | | | 16 | 15 | 418 | 63 | 90,800 | 2.57 |
| 2 | H(OEt ₂) ₂ [4.2] | styrene | 17 | 15 | 233 | 74 | 5,200 | 2.36 |
| 3 | H(OEt ₂) ₂ [4.2] | isoprene | 17 | 15 | 267 | 36 | 5,500 | 1.63 |

^a [monomer]:[initiator]. ^b Absolute molecular weights were determined using triple-detection GPC.



Scheme 4.7 H(OEt₂)₂[4.2] initiated cationic polymerization of *n*-butyl vinyl ether.

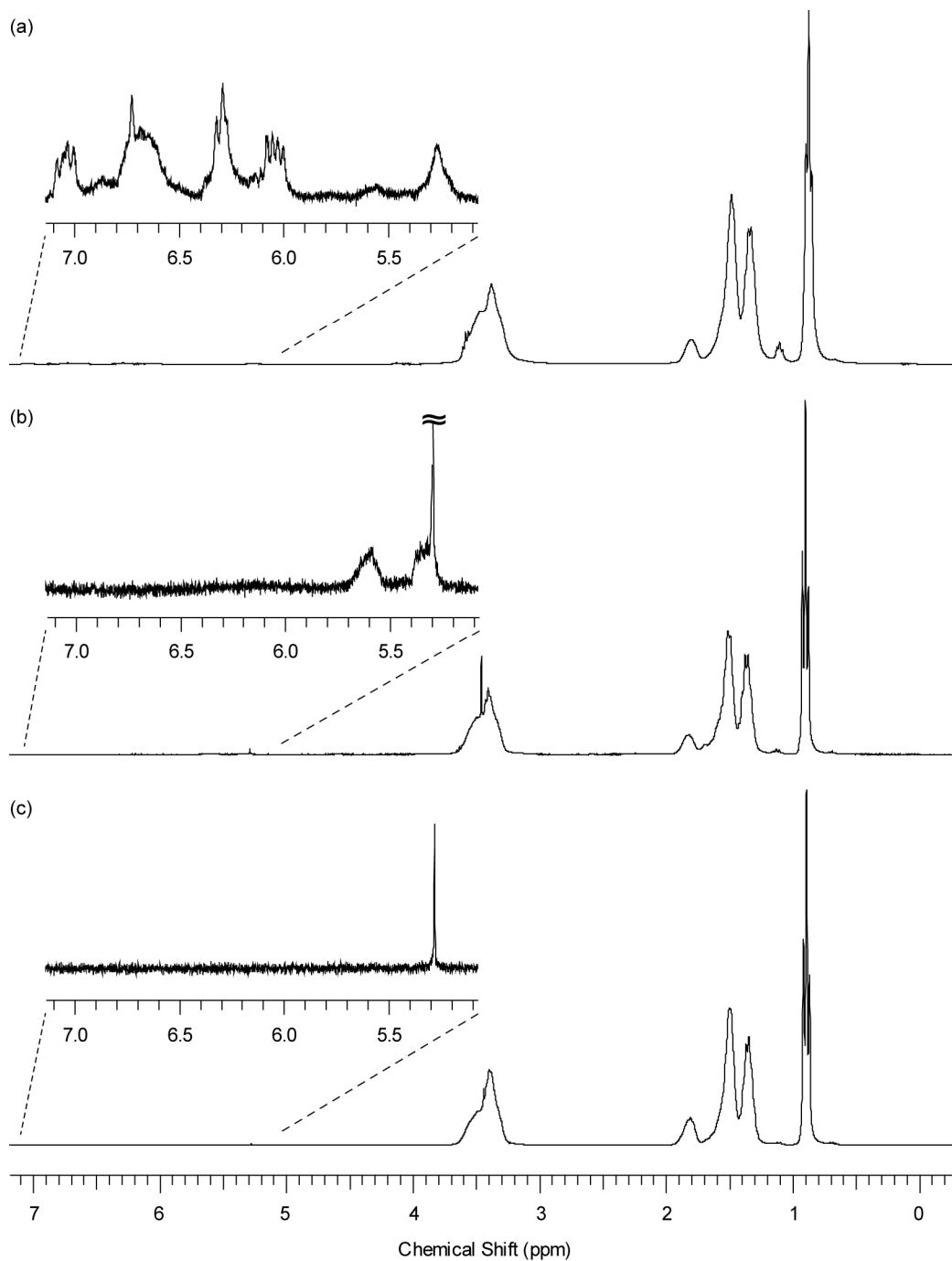
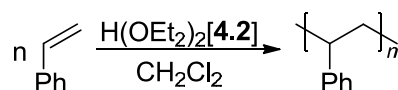
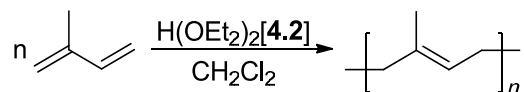


Figure 4.5 ¹H NMR (300 MHz, CDCl₃, 25 °C) spectra of poly(*n*-butyl vinyl ether) polymerized by (a) H(DMF)₂[4.1] at 19 °C, (b) H(OEt₂)₂[4.2] at 16 °C and (c) H(OEt₂)₂[4.2] at -78 °C.

In contrast to H(DMF)₂[4.1], Brønsted acid H(OEt₂)₂[4.2] is also an effective initiator for the cationic polymerization of styrene (Scheme 4.8) and isoprene (Scheme 4.9) at 17 °C (Table 4.2, entry 2-3). The polymerizations at 17 °C afford polystyrene as a white solid (Table 4.2, entry 2: $M_n = 5,200 \text{ g mol}^{-1}$, PDI = 2.36) and polyisoprene as a pale yellow solid (Table 4.2, entry 3: $M_n = 5,500 \text{ g mol}^{-1}$, PDI = 1.63) of low molecular weight and moderate polydispersity index. At such high polymerization temperature, other cationic polymerization initiator systems for styrene {e.g. AlCl₃³¹⁵ and H[B(C₂O₄)₂]³¹⁵} and isoprene {e.g. BF₃·OEt₂/trichloroacetic acid²⁶⁸ and TiCl₄/trichloroacetic acid²⁶⁹⁻²⁷⁰} also only afford oligomeric or low molecular weight polymeric products. Thus, the results obtained from H(OEt₂)₂[4.2] initiated cationic polymerizations of styrene and isoprene are nonetheless promising and warranted further investigations.



Scheme 4.8 H(OEt₂)₂[4.2] initiated cationic polymerization of styrene.



Scheme 4.9 H(OEt₂)₂[4.2] initiated cationic polymerization of isoprene.

4.2.4.2 Cationic Polymerizations at Low Temperatures

It is well-established that chain transfer processes in cationic polymerizations are suppressed at lower temperatures, thereby resulting in polymers of higher molecular weight.²⁵⁸ The temperature dependencies of H(OEt₂)₂[4.2] initiated polymerizations of *n*-butyl vinyl ether, styrene and isoprene were examined. The results of the polymerizations are summarized in Table 4.3.

Table 4.3 Temperature dependencies of H(OEt₂)₂[**4.2**] initiated cationic polymerizations of *n*-butyl vinyl ether, styrene and isoprene in CH₂Cl₂.

| entry | initiator | monomer | temp (°C) | time (min) | [M]:[I] ^a | yield (%) | M _n obsd ^b (g mol ⁻¹) | PDI |
|-------|--------------------------------------------------|-----------------------------|-----------|------------|----------------------|----------------|---------------------------------------------------------|------|
| 1 | H(OEt ₂) ₂ [4.2] | <i>n</i> -butyl vinyl ether | 19 | 15 | 411 | 80 | 35,200 | 1.31 |
| | | | 16 | 15 | 418 | 63 | 90,800 | 2.57 |
| 2 | H(OEt ₂) ₂ [4.2] | <i>n</i> -butyl vinyl ether | 0 | 15 | 411 | 69 | 35,300 | 1.91 |
| 3 | H(OEt ₂) ₂ [4.2] | <i>n</i> -butyl vinyl ether | -15 | 15 | 401 | 67 | 19,300 | 2.09 |
| 4 | H(OEt ₂) ₂ [4.2] | <i>n</i> -butyl vinyl ether | -38 | 15 | 406 | 81 | 24,200 | 2.11 |
| 5 | H(OEt ₂) ₂ [4.2] | <i>n</i> -butyl vinyl ether | -50 | 15 | 414 | 86 | 29,300 | 1.83 |
| 6 | H(OEt ₂) ₂ [4.2] | <i>n</i> -butyl vinyl ether | -78 | 15 | 407 | 88 | 41,600 | 1.11 |
| 7 | H(OEt ₂) ₂ [4.2] | styrene | 17 | 15 | 233 | 74 | 5,200 | 2.36 |
| 8 | H(OEt ₂) ₂ [4.2] | styrene | 0 | 15 | 241 | 85 | 9,300 | 2.26 |
| 9 | H(OEt ₂) ₂ [4.2] | styrene | -15 | 15 | 232 | 84 | 17,700 | 2.05 |
| 10 | H(OEt ₂) ₂ [4.2] | styrene | -38 | 15 | 239 | 80 | 34,900 | 1.82 |
| 11 | H(OEt ₂) ₂ [4.2] | styrene | -50 | 15 | 241 | 68 | 55,400 | 1.62 |
| 12 | H(OEt ₂) ₂ [4.2] | styrene | -78 | 15 | 238 | 7 | 163,000 | 1.25 |
| 13 | H(OEt ₂) ₂ [4.2] | isoprene | 17 | 15 | 267 | 36 | 5,500 | 1.63 |
| 14 | H(OEt ₂) ₂ [4.2] | isoprene | 0 | 15 | 266 | 37 | 4,700 | 1.67 |
| 15 | H(OEt ₂) ₂ [4.2] | isoprene | -15 | 15 | 272 | 38 | 6,700 | 1.68 |
| 16 | H(OEt ₂) ₂ [4.2] | isoprene | -38 | 15 | 272 | 56 | 11,600 | 1.89 |
| 17 | H(OEt ₂) ₂ [4.2] | isoprene | -50 | 15 | 232 | 2 | n.d. ^c | |
| 18 | H(OEt ₂) ₂ [4.2] | isoprene | -78 | 15 | 269 | 0 ^d | | |

^a [monomer]:[initiator]. ^b Absolute molecular weights were determined using triple-detection GPC. ^c Not determined. ^d No polymer was isolated.

As the temperature of the *n*-butyl vinyl ether polymerization is decreased, the isolated yield of the resultant polymer is increased (Table 4.3, entry 1-6). The appearance of the resultant poly(*n*-butyl vinyl ether) changed from a brown gummy solid at 16 °C (Table 4.3, entry 1) to an orange gummy solid at -38 °C (Table 4.3, entry 4) to colorless gummy solid at -78 °C (Table 4.3, entry 6). No resonances were observed in vinylic region of the ¹H NMR spectrum for the colorless polymer (Figure 4.5c), suggesting that conjugated polyene moieties are absent when polymerization of *n*-butyl vinyl ether is carried out at -78 °C. Poly(*n*-butyl vinyl ether) of moderate molecular weight and low polydispersity index was obtained at this temperature (Table 4.3, entry 6: M_n = 41,600 g mol⁻¹, PDI = 1.11). In addition to the narrow molecular weight distribution, the observed M_n (41,600 g mol⁻¹) is also consistent with the expected M_n (40,800 g mol⁻¹), which suggests the polymerization might be living; however, the “living”

aspect of this polymerization was not investigated further. At $-78\text{ }^{\circ}\text{C}$, numerous Lewis acids (e.g. SnCl_4 , EtAlCl_2 and TiCl_4) in conjunction with a proton donor (e.g. triflic acid and various phosphoric acids) have been shown to be effective in the polymerization of isobutyl vinyl ether to afford polymer of moderate molecular weight.²⁶⁷ Above $-78\text{ }^{\circ}\text{C}$, the polydispersity index of the $\text{H}(\text{OEt}_2)_2$ [4.2] initiated poly(*n*-butyl vinyl ether) is much higher and the molecular weight exhibits no definitive trend (Table 4.3, entry 1-5). The difficulty in obtaining consistent results at higher temperature is likely due to insufficient heat dissipation during polymerization.

For the polymerization of styrene, decreasing the temperature of polymerization resulted in polymer of higher molecular weight and lower polydispersity index (Table 4.3, entry 7-12). At $-78\text{ }^{\circ}\text{C}$, high molecular weight polystyrene with low polydispersity index was obtained (Table 4.3, entry 12: $M_n = 163,000\text{ g mol}^{-1}$, PDI = 1.25), albeit in low yield (7%). Polymer of moderate molecular weight and polydispersity index was obtained in reasonable yield (68%) at $-50\text{ }^{\circ}\text{C}$ (Table 4.3, entry 11: $M_n = 55,400\text{ g mol}^{-1}$, PDI = 1.62). Polystyrene of moderate molecular weight has also been reported for the cationic polymerization of styrene initiated by binary systems (e.g. $\text{AlCl}_3 \cdot \text{OBu}_2$ /2-phenyl-2-propanol²⁸⁹ and TiCl_4 /2-chloro-2,4,4-trimethylpentane²⁷⁶) at low temperature. Analysis of the $\text{H}(\text{OEt}_2)_2$ [4.2] initiated polystyrene (Table 4.3, entry 11) by $^{13}\text{C}\{^1\text{H}\}$ NMR spectroscopy (CDCl_3) at $55\text{ }^{\circ}\text{C}$ revealed that the resonances observed in the aromatic and methylene carbon regions are consistent with that of an atactic polystyrene sample.³³⁷

As the isoprene polymerization temperature decreased from $17\text{ }^{\circ}\text{C}$ to $-38\text{ }^{\circ}\text{C}$, the polymerization afforded polyisoprene of increased molecular weight and polydispersity index (Table 4.3, entry 13-18). Polymer of moderate molecular weight and polydispersity index was isolated at $-38\text{ }^{\circ}\text{C}$ (Table 4.3, entry 16: $M_n = 11,600\text{ g mol}^{-1}$, PDI = 1.89). Similar molecular weight and polydispersity index has been reported for the resultant polymer from $\text{B}(\text{C}_6\text{F}_5)_3$

initiated polymerization of isoprene at $-30\text{ }^{\circ}\text{C}$.²⁹⁵ Whereas the low temperature polymerizations of isoprene by $\text{BF}_3\cdot\text{OEt}_2/\text{trichloroacetic acid}$ ²⁶⁸ and $\text{TiCl}_4/\text{trichloroacetic acid}$ ²⁶⁹⁻²⁷⁰ afford lower molecular weight polymer with much higher polydispersity index. Analysis of the $\text{H}(\text{OEt}_2)_2[\mathbf{4.2}]$ initiated polyisoprene (Table 4.3, entry 16) by $^{13}\text{C}\{^1\text{H}\}$ NMR spectroscopy (CDCl_3) revealed signals consistent with the presence of *cis*-1,4-unit ($\delta = 23$), 1,2-unit ($\delta = 22$), 3,4-unit ($\delta = 19$) and *trans*-1,4-unit ($\delta = 16$) (Figure 4.6).^{268-269,290,295,338-339} Since the major signal is attributed to the *trans*-1,4-unit, the polymer can be described as predominately *trans*-polyisoprene. These characteristic signals are situated on broad overlapping signals in the 55-10 ppm region, which can be attributed to the presence of branched and cyclic structures.^{268,290} This is commonly observed for cationic polymerized polyisoprene and is consistent with the presence of a characteristic broad resonance at 0.8 ppm in the ^1H NMR spectrum.^{268-269,288,290,295,338,340-343} At $-50\text{ }^{\circ}\text{C}$ and below, no appreciable amount of polyisoprene was isolated (Table 4.3, entry 17-18).

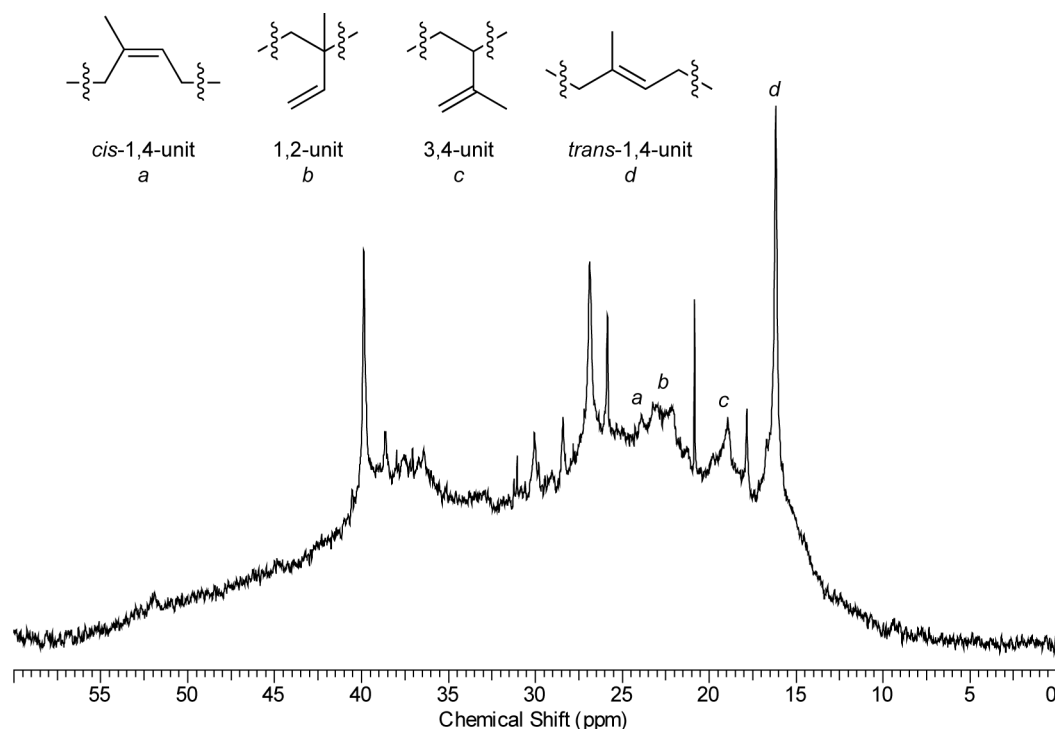


Figure 4.6 $^{13}\text{C}\{^1\text{H}\}$ NMR (101 MHz, CDCl_3 , $25\text{ }^{\circ}\text{C}$) spectrum of $\text{H}(\text{OEt}_2)_2[\mathbf{4.2}]$ initiated polyisoprene.

Cationic Polymerizations at Varying Monomer to Initiator Ratio

For the homo-polymerizations of *n*-butyl vinyl ether (Table 4.4, entry 1-3) and isoprene (Table 4.4, entry 7-9), increasing the monomer to initiator ratio notably increased the molecular weight of the resultant polymer. Poly(*n*-butyl vinyl ether) of high molecular weight and low polydispersity index was isolated from polymerization at $-78\text{ }^{\circ}\text{C}$ (Table 4.4, entry 3: $M_n = 122,000\text{ g mol}^{-1}$, PDI = 1.19). The GPC traces (differential refractive index) of the resultant poly(*n*-butyl vinyl ether) polymerized at $-78\text{ }^{\circ}\text{C}$ are narrow and symmetrical (Figure 4.7a for Table 4.4, entry 1-3). At $-38\text{ }^{\circ}\text{C}$, the polymerization of isoprene afforded polyisoprene of molecular weight up to $77,000\text{ g mol}^{-1}$ (Table 4.4, entry 9). The refractive index trace of the resultant polyisoprene suggests that the molecular weight distribution is not monomodal (Figure 4.7c for Table 4.4, entry 9).

Table 4.4 H(OEt₂)₂[**4.2**] initiated cationic polymerization of *n*-butyl vinyl ether, styrene and isoprene in CH₂Cl₂ with varying monomer to initiator ratio.

| entry | initiator | monomer | temp ($^{\circ}\text{C}$) | time (min) | [M]:[I] ^a | yield (%) | M_n obsd ^b (g mol^{-1}) | PDI |
|-------|--------------------------------------------------|-----------------------------|--------------------------------|---------------|----------------------|--------------|----------------------------------------------------|------|
| 1 | H(OEt ₂) ₂ [4.2] | <i>n</i> -butyl vinyl ether | -78 | 15 | 407 | 88 | 41,600 | 1.11 |
| 2 | H(OEt ₂) ₂ [4.2] | <i>n</i> -butyl vinyl ether | -78 | 15 | 825 | 85 | 111,000 | 1.15 |
| 3 | H(OEt ₂) ₂ [4.2] | <i>n</i> -butyl vinyl ether | -78 | 15 | 1240 | 89 | 122,000 | 1.19 |
| 4 | H(OEt ₂) ₂ [4.2] | styrene | -50 | 15 | 241 | 68 | 55,400 | 1.62 |
| 5 | H(OEt ₂) ₂ [4.2] | styrene | -50 | 15 | 493 | 89 | 37,800 | 1.88 |
| 6 | H(OEt ₂) ₂ [4.2] | styrene | -50 | 15 | 819 | 79 | 44,100 | 1.80 |
| 7 | H(OEt ₂) ₂ [4.2] | isoprene | -38 | 15 | 272 | 54 | 11,600 | 1.89 |
| 8 | H(OEt ₂) ₂ [4.2] | isoprene | -38 | 15 | 402 | 55 | 26,300 | 1.42 |
| 9 | H(OEt ₂) ₂ [4.2] | isoprene | -38 | 15 | 787 | 47 | 77,000 | 1.34 |

^a [monomer]:[initiator]. ^b Absolute molecular weights were determined using triple-detection GPC.

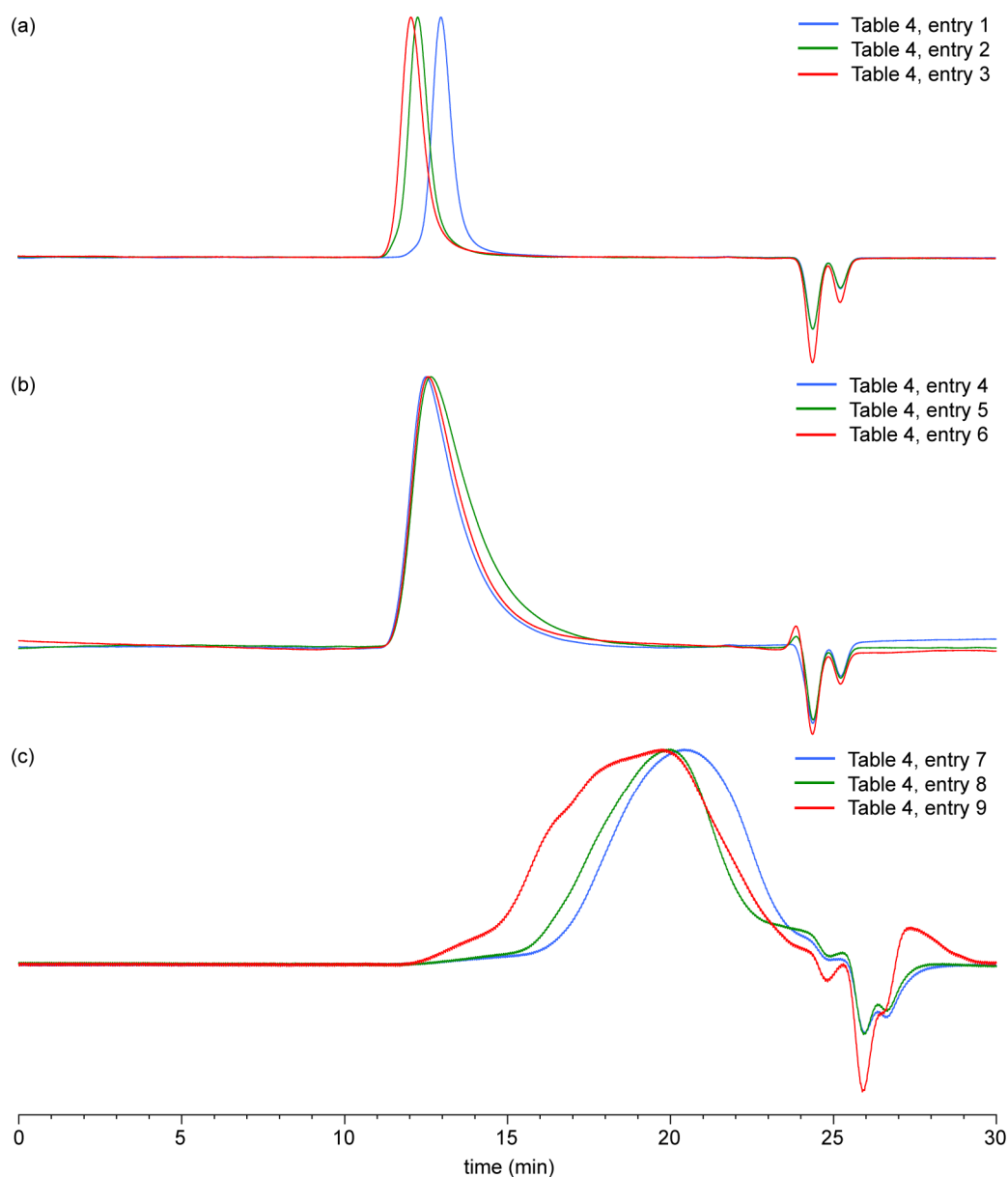


Figure 4.7 Refractive index traces of (a) poly(*n*-butyl vinyl ether), (b) polystyrene and (c) polyisoprene in Table 4.4 with varying monomer to initiator ratio. Poly(*n*-butyl vinyl ether) and polystyrene samples were analyzed using a different column set than the polyisoprene samples. See General Procedures section for more detail.

For the polymerization of styrene at $-50\text{ }^{\circ}\text{C}$, increasing the monomer to initiator ratio did not result in the increase in molecular weight of the isolated polystyrene (Table 4.4, entry 4-6). This suggests the occurrence of chain transfer to monomer is significant, thereby limiting the maximum molecular weight of polystyrene obtained at this temperature. The refractive index traces of the resultant polystyrene polymerized at $-50\text{ }^{\circ}\text{C}$ exhibit low molecular weight tailing

(Figure 4.7b for Table 4.4, entry 4-6). Varying the polymerization time also did not have a significant effect on the molecular weight of the resultant polystyrene (Table 4.5, entry 1-4); however, higher yield and polydispersity index were observed with increased polymerization time.

Table 4.5 Polymerization time dependence for H(OEt₂)₂[**4.2**] initiated cationic polymerization of styrene in CH₂Cl₂.

| entry | initiator | monomer | temp (°C) | time (min) | [M]:[I] ^a | yield (%) | <i>M_n</i> obsd ^b (g mol ⁻¹) | PDI |
|-------|--------------------------------------------------|---------|-----------|------------|----------------------|-----------|---------------------------------------------------------------|------|
| 1 | H(OEt ₂) ₂ [4.2] | styrene | -50 | 5 | 241 | 60 | 55,000 | 1.62 |
| 2 | H(OEt ₂) ₂ [4.2] | styrene | -50 | 15 | 241 | 68 | 55,400 | 1.62 |
| 3 | H(OEt ₂) ₂ [4.2] | styrene | -50 | 30 | 237 | 76 | 53,700 | 1.70 |
| 4 | H(OEt ₂) ₂ [4.2] | styrene | -50 | 60 | 236 | 83 | 50,200 | 1.85 |

^a [styrene]:[H(OEt₂)₂[**2**]]. ^b Absolute molecular weights were determined using triple-detection GPC.

4.3 Summary

The preparation of an isolable solid Brønsted acid, H(OEt₂)₂[**4.2**], was presented. The compound was characterized by NMR spectroscopy and X-ray crystallography. In addition, H(OEt₂)(NCMe)[**4.2**] was isolated from the recrystallization of H(OEt₂)₂[**4.2**] in acetonitrile. Brønsted acid H(OEt₂)(NCMe)[**4.2**] was also characterized through X-ray crystallography; however, evidence from NMR spectroscopy suggests that it is not stable in solution. Although, the non-chlorinated derivative, H(DMF)₂[**4.1**], initiates the cationic polymerization of *n*-butyl vinyl ether at 17 °C to afford moderate molecular weight polymer, it did not initiate polymerization for styrene and isoprene. In contrast, H(OEt₂)₂[**4.2**] was an effective initiator for the cationic polymerizations of *n*-butyl vinyl ether, styrene and isoprene to afford polymers of moderate molecular weight.

4.4 Experimental

4.4.1 General Procedures

All manipulations were performed using standard Schlenk or glove box techniques under nitrogen atmosphere. NH_4OH was purchased from Fisher Scientific and used as received. Toluene was dried over sodium/benzophenone ketyl and distilled prior to use. Dichloromethane, acetonitrile, CD_3CN (Cambridge Isotope Laboratories Inc.), styrene (Aldrich) and isoprene (Aldrich) were dried over calcium hydride and distilled prior to use. *n*-Butyl vinyl ether was purchased from Aldrich, dried over sodium and distilled prior to use. Et_2O was deoxygenated with nitrogen and dried by passing through a column containing activated alumina. PCl_5 (Aldrich) was sublimed prior to use. $\text{H}(\text{DMF})_2[\mathbf{2.1}]$ was prepared following procedures in Chapter 3. Tetrachlorocatechol³⁴⁴ were prepared following literature procedures, azeotropically distilled with benzene and recrystallized from hot toluene prior to use.

Unless noted, ^1H , $^{13}\text{C}\{^1\text{H}\}$ and ^{31}P NMR spectra were recorded at room temperature on Bruker Avance 300 or 400 MHz spectrometers. 85% H_3PO_4 was used as an external standard (δ 0.0) for ^{31}P NMR spectra. ^1H NMR spectra were referenced to residual protonated solvent and $^{13}\text{C}\{^1\text{H}\}$ NMR spectra were referenced to the deuterated solvent. Elemental analyses were performed in the University of British Columbia Chemistry Microanalysis Facility.

Molecular weights of poly(*n*-butyl vinyl ether) and polystyrene were determined by triple detection gel permeation chromatography (GPC-LLS) using a Agilent liquid chromatograph equipped with a Agilent 1200 Series isocratic pump, Agilent 1200 Series standard autosampler, Phenomenex Phenogel 5 μm narrow bore columns (4.6 \times 300 mm) 10^4 Å (5000-500,000), 500 Å (1,000-15,000), and 10^3 Å (1,000-75,000), Wyatt Optilab rEx differential refractometer (λ = 658 nm, 40 °C), Wyatt tristar miniDAWN (laser light scattering detector at λ = 690 nm) and a Wyatt

ViscoStar viscometer. A flow rate of 0.5 mL min^{-1} was used and samples were dissolved in THF (ca. 2 mg mL^{-1}).

Molecular weights of polyisoprene were determined by triple detection gel permeation chromatography (GPC-LLS) using a Waters liquid chromatograph equipped with a Waters 515 HPLC pump, Waters 717 plus autosampler, Waters Styragel columns ($4.6 \times 300 \text{ mm}$) HR5E (2000-4,000,000), HR4 (5000-500,000), and HR2 (500-20,000), Waters 2410 differential refractometer ($\lambda = 940 \text{ nm}$, $40 \text{ }^\circ\text{C}$), Wyatt tristar miniDAWN (laser light scattering detector at $\lambda = 690 \text{ nm}$) and a Wyatt ViscoStar viscometer. A flow rate of 0.5 mL min^{-1} was used and samples were dissolved in THF (ca. 2 mg mL^{-1}).

The dn/dc value of poly(*n*-butyl vinyl ether) was calculated using 100% mass recovery methods from ASTRA software version 5 ($dn/dc = 0.063 \text{ mL g}^{-1}$). The dn/dc values of polystyrene (0.185 mL g^{-1})³⁴⁵ and polyisoprene (0.129 mL g^{-1})³⁴⁶ in THF have been previously reported.

4.4.2 Synthesis of H(OEt₂)₂[4.2]

PCl₅ (0.30 g, 1.4 mmol) and tetrachlorocatechol (1.1 g, 4.4 mmol) were vigorously stirred in toluene (10 mL). The reaction mixture was slowly heated to reflux. After 2 h, the resulting solution was cooled to room temperature and Et₂O (20 mL) was added to afford an off-white precipitate. The solid was collected by filtration, dried *in vacuo*. Slow diffusion of Et₂O vapor into a concentration solution of the crude product in dichloromethane ($-30 \text{ }^\circ\text{C}$, ca. 7 days) yield colorless crystals suitable for X-ray diffraction. The crystals were collected by filtration at $0 \text{ }^\circ\text{C}$, washed with cold Et₂O (5 mL) and dried *in vacuo* at $0 \text{ }^\circ\text{C}$ for 30 min. Yield = 0.93 g (69%).

^{31}P NMR (162 MHz, CD_3CN): δ -79.9; ^1H NMR (400 MHz, CD_3CN): δ 13.2 (s, 1H, H - $(\text{OEt}_2)_2$), 5.44 (s, 1H, CH_2Cl_2), 3.90 (q, 8H, CH_2), 1.28 (t, 12H, CH_3); $^{13}\text{C}\{^1\text{H}\}$ NMR (101 MHz, CD_3CN): 142.6 (d, $J_{\text{CP}} = 6$ Hz), 123.7 (s), 144.8 (d, $J_{\text{CP}} = 18$ Hz), 69.9 (s), 55.4 (s), 14.7 (s).
Anal. Calcd. for $\text{C}_{26}\text{H}_{21}\text{Cl}_{12}\text{O}_8\text{P}\cdot\frac{1}{2}\text{CH}_2\text{Cl}_2$: C, 33.14; H, 2.31. Found: C, 32.93; H, 2.34.

4.4.3 Synthesis of $\text{H}(\text{OEt}_2)(\text{NCMe})[\mathbf{4.2}]$

$\text{H}(\text{OEt}_2)_2[\mathbf{4.2}]$ was dissolved in acetonitrile and colorless crystals suitable for X-ray diffraction were formed overnight. After the solvent was decanted, the solid was washed with cold dichloromethane and dried *in vacuo* at 0 °C for 30 min.

^{31}P NMR (162 MHz, CD_2Cl_2): δ -25.5; ^1H NMR (400 MHz, CD_2Cl_2): δ 4.24 (dq, $^3J_{\text{HH}} = 11$ Hz, $^3J_{\text{HH}} = 7$ Hz, 4H, CH_2CH_3), 1.98 (s, 6H, CH_3CN), 1.28 (dt, $^3J_{\text{HH}} = 7$ Hz, $^4J_{\text{HH}} = 2$ Hz, 8H, CH_2CH_3).

4.4.4 $\text{H}(\text{DMF})_2[\mathbf{4.1}]$ Initiated Cationic Polymerizations of *n*-Butyl Vinyl Ether

To a stirred solution of $\text{H}(\text{DMF})_2[\mathbf{4.1}]$ (0.010 g, 0.020 mmol) in dichloromethane (4 mL) at 19 °C was added *n*-butyl vinyl ether (0.82 g, 8.2 mmol). After stirring for 15 min, the reaction was quenched with a solution of NH_4OH in MeOH (0.2 mL, 10 vol %), followed by the removal of all volatiles *in vacuo*. The crude polymer was redissolved in dichloromethane (ca. 2 mL) and precipitated by addition to stirred MeOH (ca. 40 mL) to yield brown oil. The polymer was collected by centrifugation and dried *in vacuo*. The ^1H NMR (300 MHz, CDCl_3) spectrum of the isolated polymer is comparable to that reported in the literature.³³⁴ Yield = 0.12 g (15%).

GPC-LLS (THF): $M_n = 10,000$ g mol $^{-1}$, PDI = 2.80.

4.4.5 H(OEt₂)₂[4.2] Initiated Cationic Polymerizations of *n*-Butyl Vinyl Ether

To a stirred solution of H(OEt₂)₂[4.2] (0.010 g, 0.010 mmol) in dichloromethane (4 mL) at -78 °C was added *n*-butyl vinyl ether (0.41 g, 4.1 mmol). After stirring for 15 min, the reaction was quenched with a solution of NH₄OH in MeOH (0.2 mL, 10 vol %), followed by the removal of all volatiles *in vacuo*. The crude polymer was redissolved in dichloromethane (ca. 3 mL) and precipitated by addition to stirred MeOH (ca. 40 mL) to yield colorless gummy solid. The polymer was collected by centrifugation and dried *in vacuo*. ¹H NMR (300 MHz, CDCl₃) spectrum of the isolated polymer is comparable to that in reported the literature.³³⁴ Yield = 0.36 g (88%).

GPC-LLS (THF): $M_n = 41,600 \text{ g mol}^{-1}$, PDI = 1.11.

4.4.6 H(OEt₂)₂[4.2] Initiated Cationic Polymerizations of Styrene

To a stirred solution of H(OEt₂)₂[4.2] (0.010 g, 0.010 mmol) in dichloromethane (2 mL) at -50 °C was added styrene (0.25 g, 2.4 mmol). After stirring for 15 min, the reaction was quenched with a solution of NH₄OH in MeOH (0.2 mL, 10 vol %), followed by the removal of all volatiles *in vacuo*. The crude polymer was redissolved in dichloromethane (ca. 2 mL) and precipitated by addition to stirred MeOH (ca. 40 mL) to yield a white solid. The polymer was collected by filtration and dried *in vacuo*. The ¹³C{¹H} NMR (101 MHz, CDCl₃, 55 °C) spectrum of the isolated polymer is comparable to that of atactic polystyrene reported in the literature.³³⁷ Yield = 0.17 g (68%).

GPC-LLS (THF): $M_n = 55,400 \text{ g mol}^{-1}$, PDI = 1.62.

4.4.7 H(OEt₂)₂[4.2] Initiated Cationic Polymerizations of Isoprene.

To a stirred solution of H(OEt₂)₂[4.2] (0.010 g, 0.010 mmol) in dichloromethane (2 mL) at -38 °C was added isoprene (0.27 g, 4.0 mmol). After stirring for 15 min, the reaction was quenched with a solution of NH₄OH in MeOH (0.2 mL, 10 vol %), followed by the removal of all volatiles *in vacuo*. The crude polymer was redissolved in dichloromethane (ca. 2 mL) and precipitated by addition to stirred acetone (ca. 40 mL) to yield a yellow solid. The polymer was collected by centrifugation and dried *in vacuo*. The ¹³C{¹H} NMR (101 MHz, CDCl₃, 25 °C) spectrum of the isolated polymer is comparable to that of *trans*-polyisoprene reported in the literature.^{268-269,290,295,338-339} Yield = 0.15 g (56%).

GPC-LLS (THF): $M_n = 26,300 \text{ g mol}^{-1}$, PDI = 1.42.

4.4.8 X-ray Crystallography

All single crystals were immersed in oil and mounted on a glass fiber. Data were collected on a Bruker X8 APEX II diffractometer with graphite-monochromated Mo K α radiation. Data were collected and integrated using the Bruker SAINT¹⁷⁶ software package and corrected for absorption effect using SADABS.¹⁷⁷ All structures were solved by direct methods and subsequent Fourier difference techniques. Unless noted, all non-hydrogen atoms were refined anisotropically, whereas all hydrogen atoms were included in calculated positions but not refined. All data sets were corrected for Lorentz and polarization effects. All refinements were performed using the SHELXL-97^{179,347} via the WinGX interface.³⁴⁸

Compound H(OEt₂)₂[4.2] co-crystallizes with one CH₂Cl₂ solvate molecule disordered over an inversion center, which was modeled in two orientations. EADP constraint was applied and the occupancy was set to 0.5. A second disordered CH₂Cl₂ solvate molecule was modeled in

two orientations with final occupancy of 0.63(1) and 0.37(1). H(1) is bound by two molecules of Et₂O and was located using the difference map and refined isotropically.

Compound H(OEt₂)(NCMe)[**4.2**] crystallizes with two crystallographically independent complexes per asymmetric unit. H(1) is bound by one molecule of Et₂O and one molecule of CH₃CN. H(1) was located using the difference map and refined isotropically. H(2) is bound by one disordered molecule of Et₂O and one molecule of CH₃CN. The disordered Et₂O molecule was modeled in two orientations, restrained with SADI and refined to the final occupancy of 0.692(4) and 0.308(4). H(2) was located using the difference map; however, due to the disordered bound Et₂O molecule, it was restrained with DFIX. One of the CH₃CN solvate molecules in the asymmetric unit exhibited higher than expected thermal motion. Improvement to the refinement model was made by applying DELU restraint and setting site-occupancy factors of the CH₃CN molecule to 0.5. Crystal data and refinement parameters are listed in Table 4.6. CIF files giving supplementary crystallographic data for the structures reported in this chapter are available from Cambridge Crystallographic Data Centre (CCDC 875227 – 875228).

Table 4.6 X-ray crystallographic data of H(OEt₂)₂[**4.2**] and H(OEt₂)(NCMe)[**4.2**].

| | H(OEt ₂) ₂ [4.2]·1.5CH ₂ Cl ₂ | 2{H(OEt ₂)(NCMe)[4.2]}·1.5MeCN |
|--------------------------------------------------------------------------|-------------------------------------------------------------------------------------|----------------------------------------------------------------------------------------------------|
| formula | C _{27.5} H ₂₄ Cl _{1.5} O ₈ P | C ₅₁ H _{32.5} Cl ₂₄ N _{3.5} O ₁₄ P ₂ |
| fw | 1045.19 | 1831.05 |
| cryst syst | monoclinic | triclinic |
| space group | <i>P</i> 2 ₁ / <i>c</i> | <i>P</i> $\bar{1}$ |
| color | colorless | colorless |
| <i>a</i> (Å) | 14.419(1) | 16.080(1) |
| <i>b</i> (Å) | 12.9132(9) | 16.2759(8) |
| <i>c</i> (Å) | 22.703(2) | 17.1068(8) |
| α (deg) | 90 | 117.697(2) |
| β (deg) | 107.385(3) | 94.320(3) |
| γ (deg) | 90 | 113.619(3) |
| <i>V</i> (Å ³) | 4034.1(5) | 3438.0(4) |
| <i>T</i> (K) | 173(2) | 173(2) |
| <i>Z</i> | 4 | 2 |
| μ (Mo K α) (mm ⁻¹) | 1.108 | 1.060 |
| cryst size (mm ³) | 0.65 × 0.55 × 0.50 | 0.60 × 0.20 × 0.15 |
| <i>D</i> _{calcd.} (Mg m ⁻³) | 1.721 | 1.769 |
| 2 θ (max) (°) | 55.8 | 55.8 |
| no. of reflns | 66766 | 89242 |
| no. of unique data | 9625 | 16354 |
| <i>R</i> (int) | 0.0151 | 0.0170 |
| refln/param ratio | 18.80 | 17.60 |
| <i>R</i> ₁ [<i>I</i> > 2 σ (<i>I</i>)] ^a | 0.0286 | 0.0246 |
| <i>wR</i> ₂ [all data] ^b | 0.0657 | 0.0653 |
| GOF | 1.157 | 1.051 |

^a $R_1 = \frac{\sum ||F_o| - |F_c||}{\sum |F_o|}$. ^b $wR_2(F^2[\text{all data}]) = \left\{ \frac{\sum [w(F_o^2 - F_c^2)^2]}{\sum [w(F_o^2)^2]} \right\}^{1/2}$.

Chapter 5: Poly(methylenephosphine)s as Macromolecular Flame Retardant Additives for Paper*

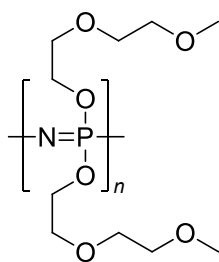
5.1 Introduction

Flame retardant additives are often added to commercial products (e.g. plastics, rubbers, fibers, synthetic and natural textiles) in order to suppress their inherent flammability and to permit their safe usage.³⁴⁹⁻³⁵¹ Traditional halogenated organic flame retardants are under growing scrutiny, due to their high toxicity and their environmental impact.³⁵² In particular, polybrominated diphenyl ethers (PBDEs) have been listed under the Stockholm Convention as persistent organic pollutants.³⁵³ This has led to the restriction of PBDEs in electronic and electrical equipment in the European Union.³⁵⁴ In addition, PBDEs are in the process of being phased out in Canada³⁵⁵ and United States;³⁵⁶ thus, there is a pressing need for new non-halogenated flame-retardants. Particularly attractive are flame retardants based on phosphorus-containing compounds, since they tend to offer much lower toxicities than their halogenated counterparts, whilst maintaining effective flame retardant properties.^{350-351,357-362}

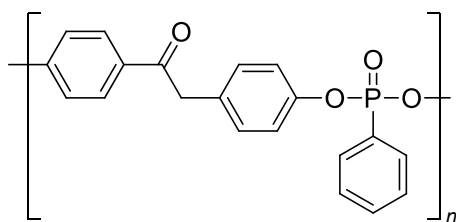
Molecular and ionic phosphorus-based flame retardants (e.g. ammonium phosphates, phosphonium salts, phosphonates, phosphines, red phosphorus) have been added to natural and synthetic polymer-based products for many years,^{350-351,357-362} however, they suffer from either appreciable volatility (due to their low molecular weight) or water solubility. These drawbacks result in their tendency to leach out of the product over time.³⁶³⁻³⁶⁴ Non-water soluble polymeric phosphorus-based flame retardant additives of moderate molecular weight offer the distinct advantage of reduced leachability when compared to their molecular counterparts. However, the

* A version of this chapter will be submitted for publication. Paul W. Siu, Thomas Q. Hu and Derek P. Gates.

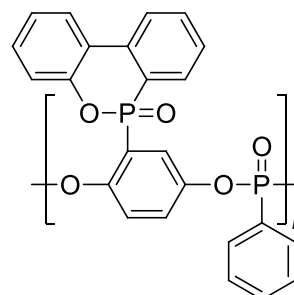
use of phosphorus-based polymers as fire retardants remains limited, due to the synthetic difficulty of incorporating phosphorus moieties into macromolecules. Perhaps the most well-studied polymeric phosphorus-based flame retardants are the polyphosphazenes, $[R_2P=N]_n$, which have been developed for commercial use.^{10-12,365-367} Recent efforts have resulted in polymeric flame retardants featuring a variety of phosphorus moieties in the backbone, including phosphazenes (**5.1**),³⁶⁸ phosphonates (**5.2** and **5.3**),³⁶⁹⁻³⁷⁰ phosphates (**5.4** and **5.5**)³⁷¹⁻³⁷³ and phosphine oxides (**5.6**).³⁷⁴



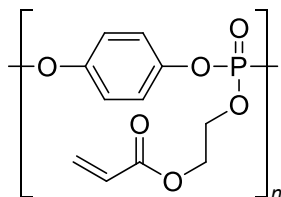
5.1



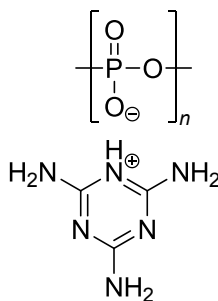
5.2



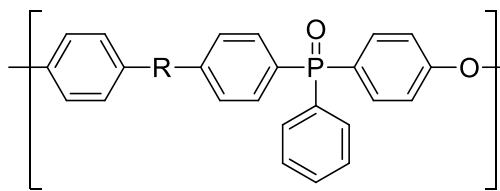
5.3



5.4



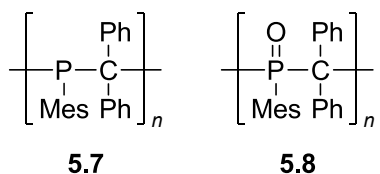
5.5



5.6 (R = SO₂ or CO)

Another recently developed phosphorus-based polymer is the poly(methylenephosphine) **5.7**,¹⁷ which can be synthesized either by radical or anionic polymerizations of the phosphalkene monomer, MesP=CPh₂. Given the presence of phosphorus centers in the backbone, **5.7** could find potential application as a flame retardant; however, its flame retardant property has not been studied. Although polymer **5.7** is reasonably resistant toward oxidation in air, the flame retardant property of its oxide, **5.8**, is also of interest. In this chapter, the preliminary investigation of **5.7** and **5.8** as polymeric flame retardant additives for paper will be

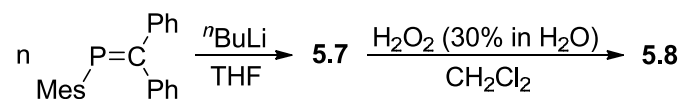
described. Cellulose-based products, derived from wood, are inherently “green” due to their renewable nature; however, their inherent flammability makes them unsuitable for many specialty applications. Thus, the development of effective flame-retardants for cellulose-based products could open up new commercial applications for wood-based products.



5.2 Results and Discussion

5.2.1 Synthesis of Poly(methylenephosphine)s **5.7** and **5.8**

The phosphalkene monomer, MesP=CPh₂, was synthesized following literature procedures.³⁷⁵⁻³⁷⁶ The anionic polymerization of MesP=CPh₂ (16.3 g) in THF was initiated by ⁿBuLi (0.015 equiv) to afford the pale yellow poly(methylenephosphine) **5.7** in good yield (91%) after workup (Scheme 5.1). In contrast to the small scale polymerizations of MesP=CPh₂ (ca. 1 g) previously reported,^{18,20-21,377-380} this illustrates that the addition polymerization of MesP=CPh₂ is amenable to moderate scale-up. Analysis of the isolated polymer by triple detection gel permeation chromatography (GPC-LLS) revealed a moderate molecular weight ($M_n = 27,000 \text{ g mol}^{-1}$) and a moderate polydispersity index (PDI = 1.47). Subsequent oxidation of **5.7** with an aqueous solution of H₂O₂ yields the oxidized polymer **5.8** after workup (Scheme 5.1). As anticipated, the analysis by GPC-LLS revealed a moderate increase in molecular weight ($M_n = 30,000 \text{ g mol}^{-1}$) for **5.8** in comparison to **5.7**. A slight decrease in polydispersity index for **5.8** (PDI = 1.24) was observed. Presumably, this arose from the fractionation of the polymer sample during the precipitation process.



Scheme 5.1 Synthesis of poly(methylenephosphine) **5.7** and its oxide, **5.8**.

5.2.2 Flame Retardancy Tests

The phosphorus-based polymers, **5.7** and **5.8**, were coated onto paper samples (70 × 151 mm) to approximately equal phosphorus content. The paper samples were made from thermomechanical pulp (TMP)³⁸¹ produced in a pilot-plant from a mixture of spruce, balsam fir and maple wood chips collected from an eastern Canadian pulp mill.³⁸² Paper samples made from TMP were chosen for this study because TMP is produced from wood chips in typical yields of ~98% and contains all the major wood components, including lignin and its functional groups.³⁸³ Thus, paper samples made from TMP can serve as an excellent model, in terms of flammability and chemical reactivity, for various wood and wood fiber products.

The flame retardancy of the polymer treated paper samples was examined using a paper flammability test chamber (Figure 5.1), built to the specifications of TAPPI (Technical Association of Pulp and Paper Industry) Standard Method T461 cm-00.³⁸⁴ During the flame test, the time that the specimen continues to flame after the burner flame is removed (flame time) and the time that the specimen continues to glow after it has ceased to flame (glow time) were measured. The results were compared to paper samples treated with the well-known molecular phosphorus-based flame retardant additive, monobasic ammonium phosphate (NH₄H₂PO₄),³⁸⁵⁻³⁸⁶ and samples of the non-treated paper. Figure 5.2 shows the paper residue after burning and is representative of multiple trials. The results are summarized in Table 5.1. In all cases, the paper samples treated with **5.7**, **5.8**, NH₄H₂PO₄ and the non-treated paper samples were ignited upon contact with a Bunsen flame. As expected, the samples without any flame retardant additive burned completely and resulted in minimal charred residue (Figure 5.2a). Importantly, samples

coated with **5.7** (Figure 5.2b) and **5.8** (Figure 5.2c) did not burn completely but rather they resulted in a significant amount of charred residue. The **5.7** and **5.8** treated paper samples flamed briefly after the Bunsen flame was removed, but were quickly extinguished and showed no subsequent glowing. In contrast, non-treated paper samples were fully combusted during the 12 s exposure to the Bunsen flame required by the TAPPI test method; thus, it showed no flame time but its edges continued to glow for 34 s after the Bunsen flame was removed. These results suggest that phosphorus-based polymers, **5.7** and **5.8**, have good efficacy as flame retardants. Admittedly, they did not perform as well as the paper samples that had been treated with the commercial flame retardant additive, $\text{NH}_4\text{H}_2\text{PO}_4$ (Figure 5.2d). The significant charring observed suggests that **5.7**, **5.8** and $\text{NH}_4\text{H}_2\text{PO}_4$ coated paper samples burn at lower temperature, through the reduction of heat of combustion, than paper samples without any flame retardant. In addition, char formation is known to reduce the amount of smoke produced during combustion;³⁸⁷⁻³⁸⁸ however, further tests on **5.7** and **5.8** are necessary to fully investigate their smoke reduction properties.



Figure 5.1 Photograph of the flammability test chamber designed following the TAPPI (Technical Association of Pulp and Paper Industry) Standard Method T461 cm-00 (L = 76.5 cm, W = 36.0 cm, H = 31.0 cm).

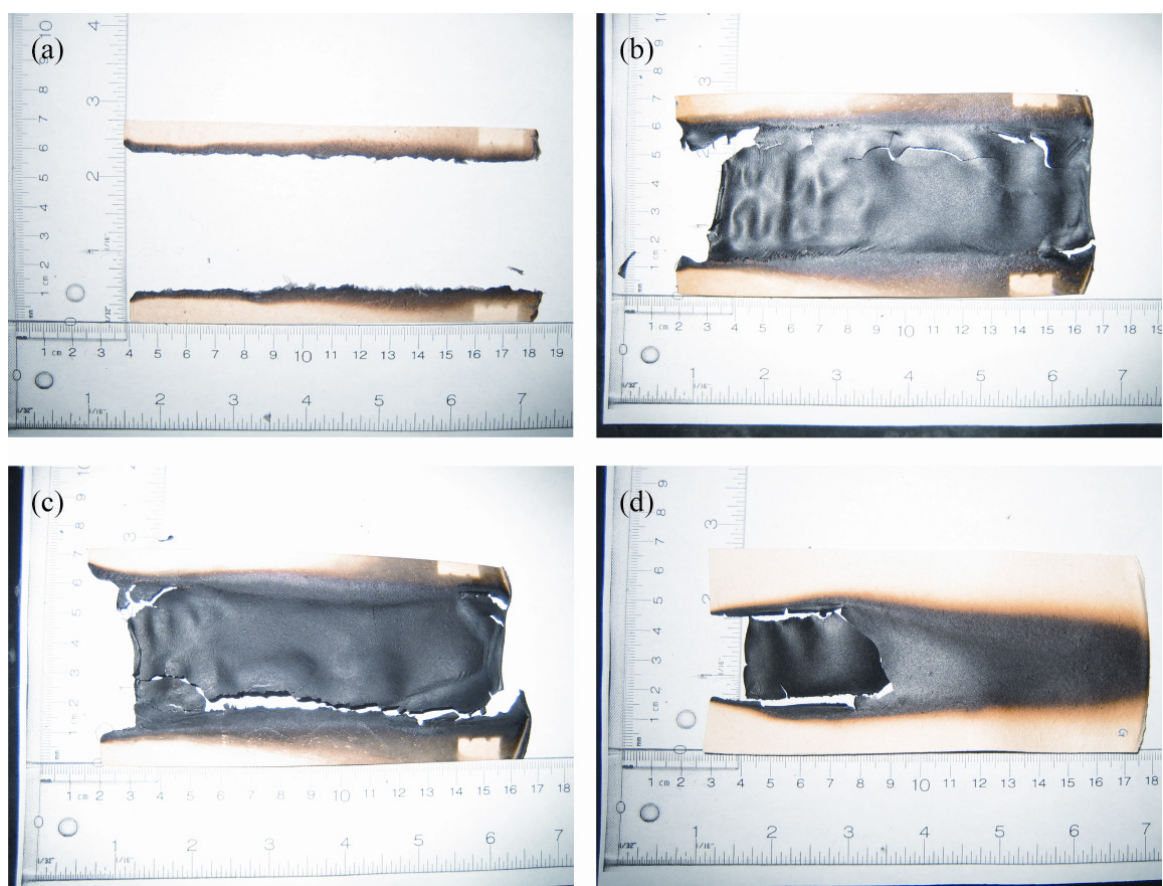


Figure 5.2 Representative results of the flame retardancy test for TMP paper samples. (a) No flame retardant added. (b) Treated with **5.7** (phosphorus content = 0.723 mmol P / g paper). (c) Treated with **5.8** (phosphorus content = 0.680 mmol P / g paper). (d) Treated with $\text{NH}_4\text{H}_2\text{PO}_4$ (phosphorus content = 0.824 mmol P / g paper).

Table 5.1 Flame retardancy test results.

| paper samples | flame time ^a (s) | glow time ^b (s) | pH of burnt residues of paper sample ^d |
|-------------------------------------------------|--------------------------------|-------------------------------|------------------------------------------------------|
| non-treated | ≤ 1 ^c | 34 | 10.47 |
| treated with 5.7 | 7 | 0 | 4.86 |
| treated with 5.8 | 6 | 0 | 5.22 |
| treated with $\text{NH}_4\text{H}_2\text{PO}_4$ | 0 | 0 | 4.00 |

^aThe time that the specimen continues to flame after the burner flame is removed. ^bThe time that the specimen continues to glow after it has ceased to flame. ^c The paper was already fully combusted when the Bunsen flame was removed. ^d The char residue was extracted with water (50 mL) and the pH was measured.

5.2.3 pH Measurements of Burnt Paper Samples

During combustion, phosphorus-based flame retardants generally decompose to phosphoric acid,³⁸⁹⁻³⁹² which is believed to promote char formation and is essential in the general flame retardant mechanism of cellulose.^{388,393} To gain insight into the flame retardant mechanism of **5.7** and **5.8**, the charred residues of the post-test samples were stirred in water (50 mL) for 30 min and their pH measured. The results are shown in Table 5.1. Interestingly, the non-treated paper sample gave a basic solution (pH 10.47), whereas samples treated with **5.7**, **5.8** and $\text{NH}_4\text{H}_2\text{PO}_4$ all resulted in acidic solutions. For the paper sample treated with $\text{NH}_4\text{H}_2\text{PO}_4$, its char residue was measured at pH 4.00. Likewise, for paper samples treated with **5.7** and **5.8**, their residues were measured at pH 4.86 and 5.22, respectively. Importantly, the similar pH measurements for the **5.7**, **5.8** and $\text{NH}_4\text{H}_2\text{PO}_4$ treated samples are consistent with the expected formation of phosphoric acid during the combustion. This implies that the flame retardancy mechanism of **5.7** and **5.8** that leads to the promotion of char formation on cellulose is likely to be similar to that of $\text{NH}_4\text{H}_2\text{PO}_4$.

5.3 Summary

Poly(methylenephosphine)s **5.7** and **5.8** were effective as polymeric phosphorus-based flame retardant additives for papers made from TMP. The results clearly demonstrated the ability of **5.7** and **5.8** to promote the formation of char and inhibit burning. Measurements of pH are consistent with the hypothesis that phosphoric acid was generated during combustion, which is commonly believed to be essential for the general flame retardant mechanism of cellulose.

5.4 Experimental Section

5.4.1 General Procedures

All manipulations of air- and/or water-sensitive compounds were performed using standard Schlenk or glovebox techniques under nitrogen atmosphere. Monobasic ammonium phosphate ($\text{NH}_4\text{H}_2\text{PO}_4$) was purchased from Aldrich and used as received. For the preparation of **5.7**, THF was dried over sodium/benzophenone ketyl and distilled prior to use. $n\text{-BuLi}$ (1.6 M in hexanes) was purchased from Aldrich and titrated prior to use. $\text{MesP}=\text{CPh}_2$ was synthesized in accordance to literature procedures.³⁷⁵⁻³⁷⁶ ^{31}P NMR spectra were recorded on Bruker Avance 300 MHz or 400 MHz spectrometers at 25 °C. Chemical shifts for ^{31}P spectra are reported relative to H_3PO_4 as an external standard (85% in H_2O , $\delta = 0$).

Molecular weights were determined by triple detection gel permeation chromatography (GPC-LLS) using a Waters liquid chromatograph equipped with a Waters 515 HPLC pump, Waters 717 plus autosampler, Waters Styragel columns (4.6 × 300 mm) HR5E (2000-4,000,000), HR4 (5000-500,000), and HR2 (500-20,000), Waters 2410 differential refractometer ($\lambda = 940$ nm, 40 °C), Wyatt tristar miniDAWN (laser light scattering detector at $\lambda = 690$ nm) and a Wyatt ViscoStar viscometer. A flow rate of 0.5 mL min^{-1} was used and samples were dissolved in THF (ca. 2 mg mL^{-1}). The dn/dc value of **5.7** in THF has been previously reported ($dn/dc = 0.223 \text{ mL g}^{-1}$).³⁷⁷

Paper sheets (70 × 151 mm) were cut from 160-mm diameter, $\sim 200 \text{ g/m}^2$ sheets prepared on a laboratory British Sheet Machine from a thermomechanical pulp (TMP)³⁸² in accordance to PAPTAC (Pulp and Paper Technical Association of Canada) Standard Method C.5.³⁹⁴ The apparatus for the flame retardancy tests was built to the specifications outlined in TAPPI (Technical Association of Pulp and Paper Industry) Standard Method T461 cm-00.³⁸⁴ pH measurements of the charred residues were obtained using an Orion pH meter (model 520A).

5.4.2 Synthesis of Poly(methylenephosphine) **5.7**

Poly(methylenephosphine) **5.7** was prepared from a modified procedure by Noonan and Gates.²⁰ In a glovebox, a solution of ⁿBuLi (0.48 mL, 0.77 mmol, 1.60 M) in hexanes was added to a stirred pale yellow solution of MesP=CPh₂ (16.3 g, 51.5 mmol) in THF (50 mL), resulting in an immediate color change to deep red. The reaction mixture was stirred at room temperature. After several days, an aliquot was removed from the reaction mixture and analyzed by ³¹P NMR spectroscopy, which showed that the signal assigned to MesP=CPh₂ (ca. 234 ppm) was completely consumed and replaced by a broad signal at -8 ppm. The reaction mixture was removed from the glovebox and **5.7** was isolated as a pale yellow solid by precipitation into hexanes (500 mL) in air. The polymer was subsequently washed with additional hexanes (2 × 250 mL) and dried *in vacuo*. Yield = 14.9 g (91%).

GPC (absolute): $M_n = 27,000 \text{ g mol}^{-1}$, PDI = 1.47; ³¹P NMR (162 MHz, THF): $\delta = -8$ (br s). ¹H and ¹³C{¹H} NMR data are available from previous work by Tsang *et al.*¹⁸

5.4.3 Synthesis of Poly(methylenephosphine) Oxide **5.8**

An aqueous solution of H₂O₂ (10 mL, 30 wt. %) was added slowly to a vigorously stirred solution of **5.7** (7.0 g, 22 mmol) in dichloromethane (120 mL). The organic layer of the reaction mixture was separated from the aqueous layer and dried with MgSO₄. The solvent was then removed *in vacuo* to afford **5.8** as a yellow solid. Yield = 4.5 g (61%).

GPC (absolute): $M_n = 30,000 \text{ g mol}^{-1}$, PDI = 1.24; ³¹P NMR (121 MHz, THF): $\delta = 45$ (br s). ¹H NMR data are available from previous work by Tsang *et al.*¹⁸

5.4.4 Preparation of $\text{NH}_4\text{H}_2\text{PO}_4$ Treated Paper

An aqueous solution of $\text{NH}_4\text{H}_2\text{PO}_4$ (8 mL, ca. $0.24 \text{ mol}\cdot\text{L}^{-1}$) was drip coated onto a sheet of paper (1.972 g), made from the TMP. Both sides of the paper were thoroughly coated to ensure an even distribution of the flame retardant additive. The paper sample was then air dried until a constant weight was observed. Final weight measured for the paper sample was 2.159 g. The amount of phosphorus content was calculated to be 0.824 mmol P / g paper.

5.4.5 Preparation of **5.7** Treated Paper

A solution of **5.7** in THF (8 mL, ca. $0.20 \text{ mol}\cdot\text{L}^{-1}$) was drip coated onto a sheet of paper (2.034 g), made from the TMP. Both sides of the paper were thoroughly coated to ensure an even distribution of the flame retardant. The paper sample was then air dried until a constant weight was observed. Final weight measured for the paper sample was 2.499 g. The amount of phosphorus content was calculated to be 0.723 mmol P / g paper.

5.4.6 Preparation of **5.8** Treated Paper

A solution of **5.8** in THF (8 mL, ca. $0.19 \text{ mol}\cdot\text{L}^{-1}$) was drip coated onto a sheet of paper (2.161 g), made from the TMP. Both sides of the paper were thoroughly coated to ensure an even distribution of the flame retardant. The paper sample was then air dried until a constant weight was observed. Final weight measured for the paper sample was 2.650 g. The amount of phosphorus content was calculated to be 0.680 mmol P / g paper.

5.4.7 Flame Retardancy Test of Paper Samples

The flame retardancy of the treated paper samples were examined based on TAPPI (Technical Association of Pulp and Paper Industry) Standard Method T461 cm-00.³⁸⁴ The general procedure is as follows:

A paper sample was clamped vertically onto the inverted U-shaped metal holder, exposing an area of 70 × 151 mm (Figure 5.3). The height of the holder was adjusted so that the lower edge of the sample would be 19 mm above the natural gas (methane)-fueled Bunsen burner. The oxygen supply of the Bunsen burner was adjusted to give a flame 40 mm high. The metal cabinet door was then closed. Using the external handle attached to the Bunsen burner, the burner was moved until flame was directly underneath the bottom edge of the sample. The flame was held there for 12 sec, and then withdrawn. The sample was carefully removed from the U-shaped metal holder and photographed.

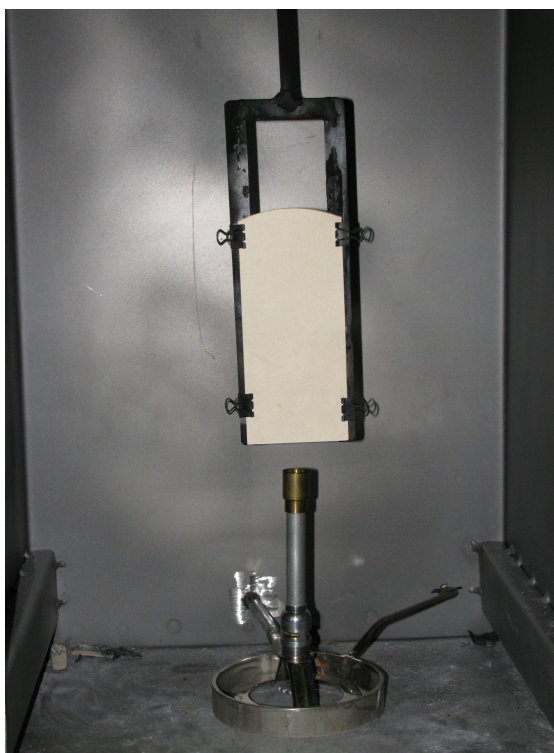
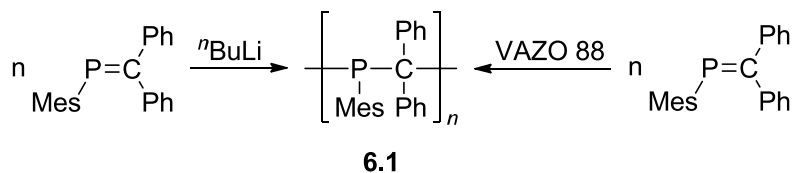


Figure 5.3 The set-up of the paper samples in the flammability test chamber.

Chapter 6: The Unexpected Microstructure of Poly(methylenephosphine)*

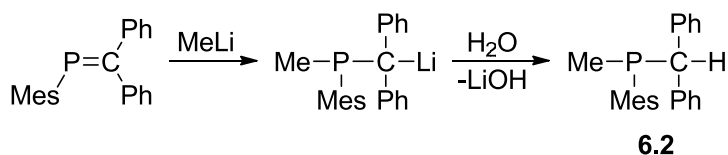
6.1 Introduction

In 2003, efforts from the Gates group led to the discovery of radical and anionic polymerizations of phosphalkene MesP=CPh₂ to afford poly(methylenephosphine) **6.1** (Scheme 6.1), thereby extending addition polymerization from C=C bonds to P=C bonds.^{17-18,395} The proposed microstructure of poly(methylenephosphine) **6.1** was elucidated based on the similarity between its ¹³C{¹H} NMR spectrum and that of the model compound Mes(Me)PCPh₂H (**6.2**) (Scheme 6.2).¹⁸ Other molecular model compounds were also synthesized to gain insights into the initiation and termination steps of the anionic polymerization.³⁹⁶ In addition, the anionic initiated oligomer of MesP=CPh₂ was studied using MALDI-TOF mass spectrometry. This suggests that the mechanism of anionic polymerization of MesP=CPh₂ is parallel to that of olefins.³⁸⁰ These studies paved the foundation for the subsequent discovery of living anionic polymerization of MesP=CPh₂ and enabled the synthesis of well-defined homo- and copolymers of MesP=CPh₂ with controlled architectures.^{20-21,377} In contrast, the mechanism of the radical initiated polymerization of MesP=CPh₂ has been much less developed.



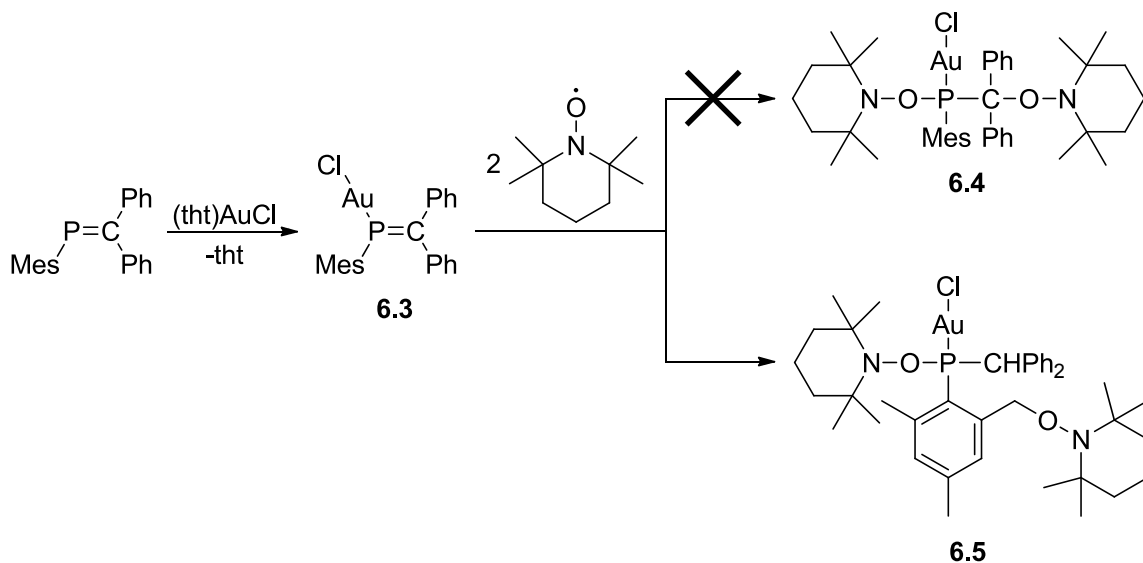
Scheme 6.1 Synthesis of poly(methylenephosphine) **6.1** through addition polymerization.

* A version of this chapter will be submitted for publication. Paul W. Siu, Ivo Krummenacher and Derek P. Gates.



Scheme 6.2 Synthesis of model compound **6.2**.

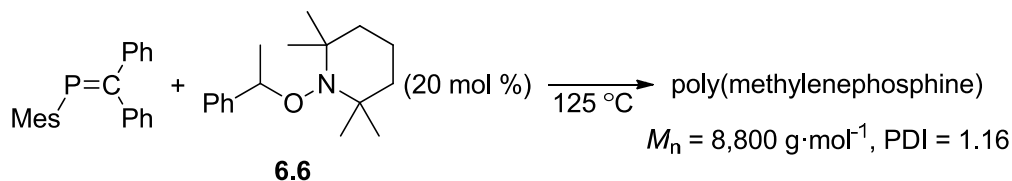
In an effort to understand the mode of activation of P=C bonds with radical reagents, Dr. Ivo Krummenacher of the Gates group investigated the reaction of phosphalkene **6.3** with two equivalents of 2,2,6,6-tetramethyl-1-piperidinyloxy (TEMPO), a stable radical reagent (Scheme 6.3).³⁹⁷⁻³⁹⁸ Surprisingly, the two TEMPO molecules did not add across the P=C bond to afford the expected **6.4**. Instead, one of the TEMPO molecules reacted at one of the *ortho*-methyl mesityl carbons to afford the unexpected **6.5**, which was crystallographically characterized by X-ray diffraction.



Scheme 6.3 Reaction of phosphalkene **6.3** with two equivalents of TEMPO.

The unexpected structure of **6.5** prompted Dr. Ivo Krummenacher to investigate the related alkoxyamine **6.6** as a radical initiator for the polymerization of MesP=CPh₂ (Scheme 6.4).³⁹⁷⁻³⁹⁸ Alkoxyamine **6.6** is commonly used as an initiator for nitroxide-mediated polymerization, a method of controlled radical polymerization.³⁹⁹⁻⁴⁰³ The molecular weight and

the polydispersity index (PDI) of the resultant poly(methylenephosphine) ($M_n = 8,800 \text{ g mol}^{-1}$, PDI = 1.16) were determined by triple detection gel permeation chromatography (GPC-LLS). Interestingly, the resultant polymer exhibited an identical $^{31}\text{P}\{^1\text{H}\}$ NMR spectrum as the previously reported **6.1**.¹⁸ The subsequent departure of Dr. Ivo Krummenacher for University of Würzburg left questions in regard to the microstructure of this polymer unanswered. Considering the unexpected structure of **6.5**, further investigation into the microstructure of this polymer was of great interest. Therefore, as part of the work of this thesis, NMR spectroscopic studies were undertaken, along with the synthesis of a molecular model compound, to elucidate the possible microstructure of the alkoxyamine (**6.6**) initiated poly(methylenephosphine).



Scheme 6.4 Polymerization of $\text{MesP}=\text{CPh}_2$ initiated by alkoxyamine **6.6**.

6.2 Results and Discussion

6.2.1 The Microstructure of Alkoxyamine Initiated Poly(methylenephosphine)

In addition to $^{31}\text{P}\{^1\text{H}\}$ NMR spectroscopy, the alkoxyamine (**6.6**) initiated poly(methylenephosphine) was also analyzed by ^1H NMR (600 MHz) and $^{13}\text{C}\{^1\text{H}\}$ NMR (151 MHz) spectroscopy. The chemical shifts observed in these spectra were identical to those in the previously reported ^1H NMR (300 MHz) and $^{13}\text{C}\{^1\text{H}\}$ NMR (75 MHz) spectra of poly(methylenephosphine) **6.1**.¹⁸ In particular, the $^{13}\text{C}\{^1\text{H}\}$ NMR (151 MHz) spectrum of the alkoxyamine initiated poly(methylenephosphine) revealed a broad resonance at 52.4 ppm (Figure 6.1), which matches well with the broad resonance at 52.2 ppm in the $^{13}\text{C}\{^1\text{H}\}$ NMR (75 MHz) spectrum of **6.1** (Figure 6.2a), previously assigned to the backbone quaternary

P-C(Ph)₂-P carbon.¹⁸ However, these resonances are also consistent with the chemical shift observed for the -CHPh₂ carbon in the ¹³C{¹H} NMR (75 MHz, CDCl₃) spectrum of model compound **6.2** [Figure 6.2b, δ = 51.3 (d)].¹⁸

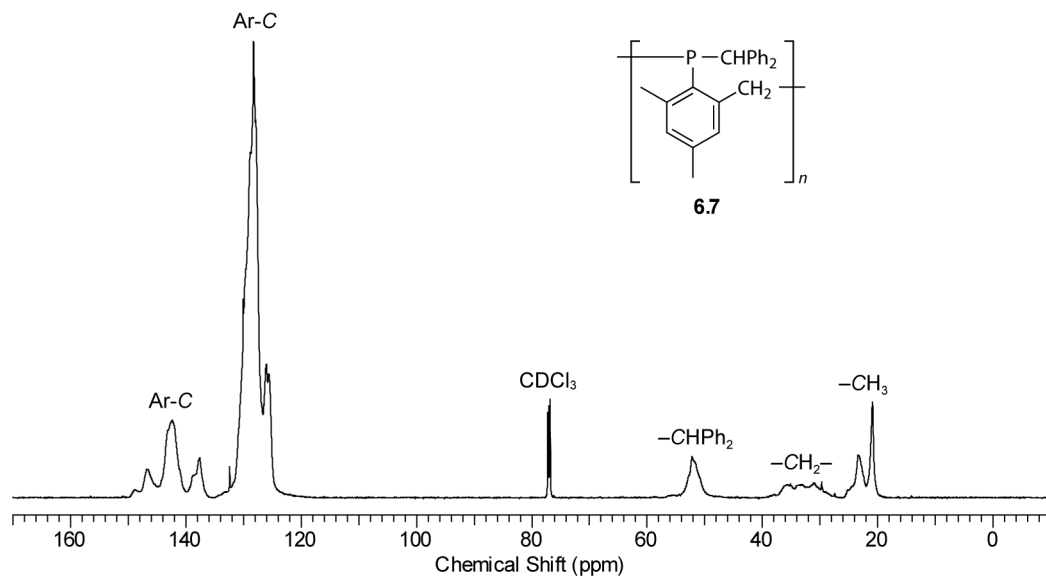


Figure 6.1 ¹³C{¹H} NMR (151 MHz, CDCl₃) spectrum of alkoxyamine initiated poly(methylenephosphine) at 25 °C.

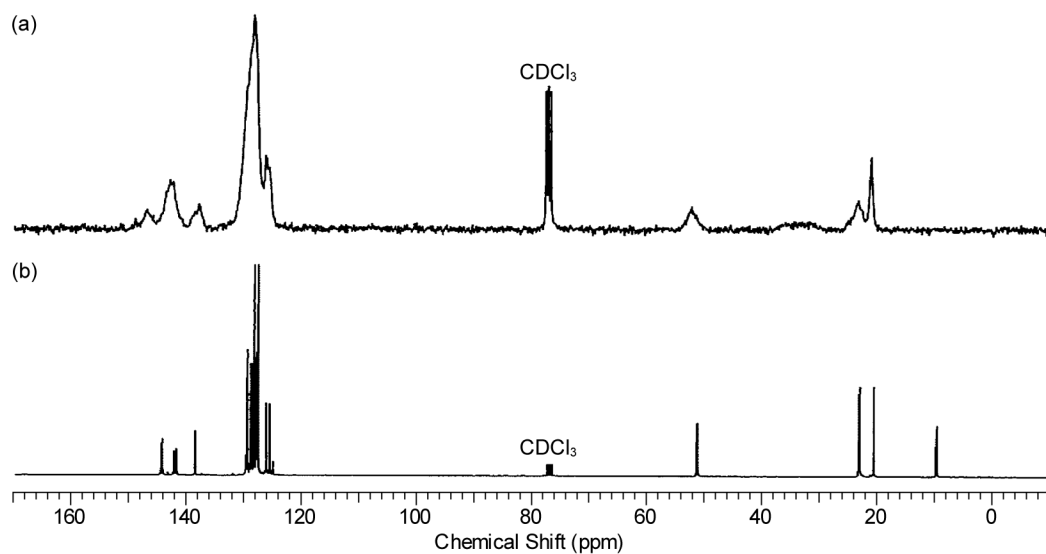


Figure 6.2 ¹³C{¹H} NMR spectra (75 MHz, CDCl₃) of (a) poly(methylenephosphine) **6.1** and (b) model compound **6.2**. Adapted with permission from *J. Am. Chem. Soc.* **2003**, *125*, 1480. Copyright 2003 American Chemical Society.

A broad resonance centered at 33.0 ppm was observed in the $^{13}\text{C}\{^1\text{H}\}$ NMR (151 MHz) spectrum of the alkoxyamine initiated poly(methylenephosphine) (Figure 6.1), which is in the region typically observed for a $-\text{CH}_2-$ carbon. Albeit much weaker, this broad resonance was also detected in the $^{13}\text{C}\{^1\text{H}\}$ NMR (75 MHz) spectrum of **6.1** (Figure 6.2a).¹⁸ This has been previously attributed to the *ortho*-methyl mesityl carbons, broadened due to restricted rotation about the P- $\text{C}_{\text{ipso-mesityl}}$ bond.³⁹⁷ In light of the unexpected structure of **6.5**, these $^{13}\text{C}\{^1\text{H}\}$ NMR spectroscopic data are consistent with an alternative possible microstructure to that of **6.1**. The proposed microstructure (**6.7**) for the alkoxyamine initiated poly(methylenephosphine) is shown in Figure 6.1. Furthermore, no resonance attributed to the $-\text{CH}_2-$ carbon was observed in the $^{13}\text{C}\{^1\text{H}\}$ NMR spectrum of model compound **6.2** (Figure 6.2b).¹⁸

Additional NMR spectroscopic experiments were carried out to provide further evidence for the proposed microstructure **6.7**. Analysis of alkoxyamine (**6.6**) initiated poly(methylenephosphine) by ^{13}C APT (Attached Proton Test) NMR spectroscopy revealed that the phasing of the broad resonance at 52.4 ppm is positive, coinciding with the phasing of the methyl resonances at 23.5 and 21.2 ppm (Figure 6.3). This indicates that the resonance at 52.4 ppm is attributed to either a primary $-\text{CH}_3$ carbon or a tertiary $-\text{CHR}_2$ carbon and is unlikely to be attributed to a quaternary $-\text{CR}_2-$ carbon such as a P- $\text{C}(\text{Ph})_2$ -P moiety. Whereas, the phasing of the broad resonance at 33.0 ppm is negative, coinciding with the phasing of the resonance attributed to the quaternary carbon of CDCl_3 . This indicates that the resonance at 33.0 ppm is attributed to either a quaternary $-\text{CR}_2-$ carbon or a secondary $-\text{CH}_2-$ carbon. Further analysis by ^1H - ^{13}C HSQC (Heteronuclear Single Quantum Coherence) NMR spectroscopy revealed cross-peaks attributed to the carbons at 51.3 and 33.0 ppm directly coupled to the protons at 4.8 and 3.6 ppm, respectively (Figure 6.4), thus providing further evidence for the proposed microstructure **6.7**.

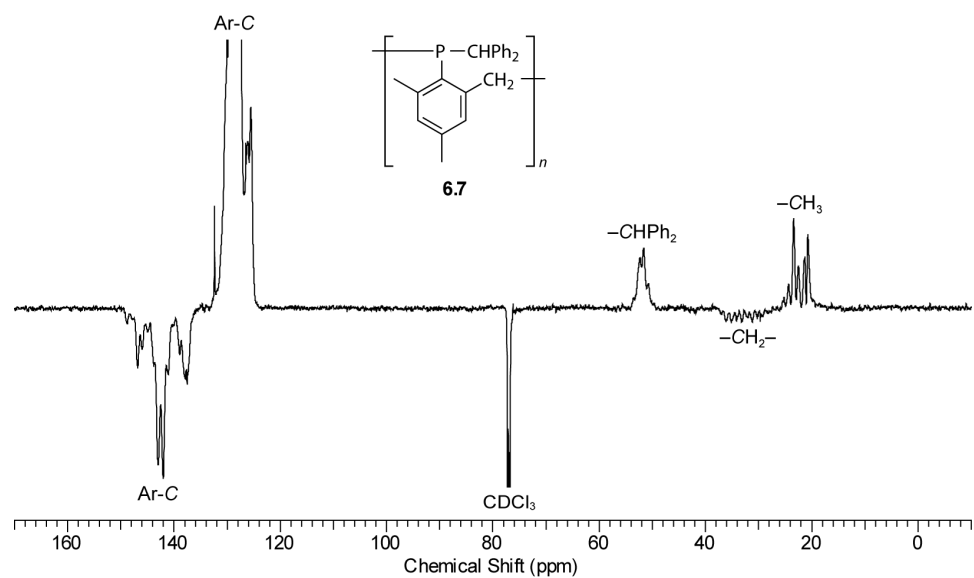


Figure 6.3 ^{13}C APT NMR (151 MHz, CDCl_3) spectrum of alkoxyamine initiated poly(methylenephosphine) at 25 °C.

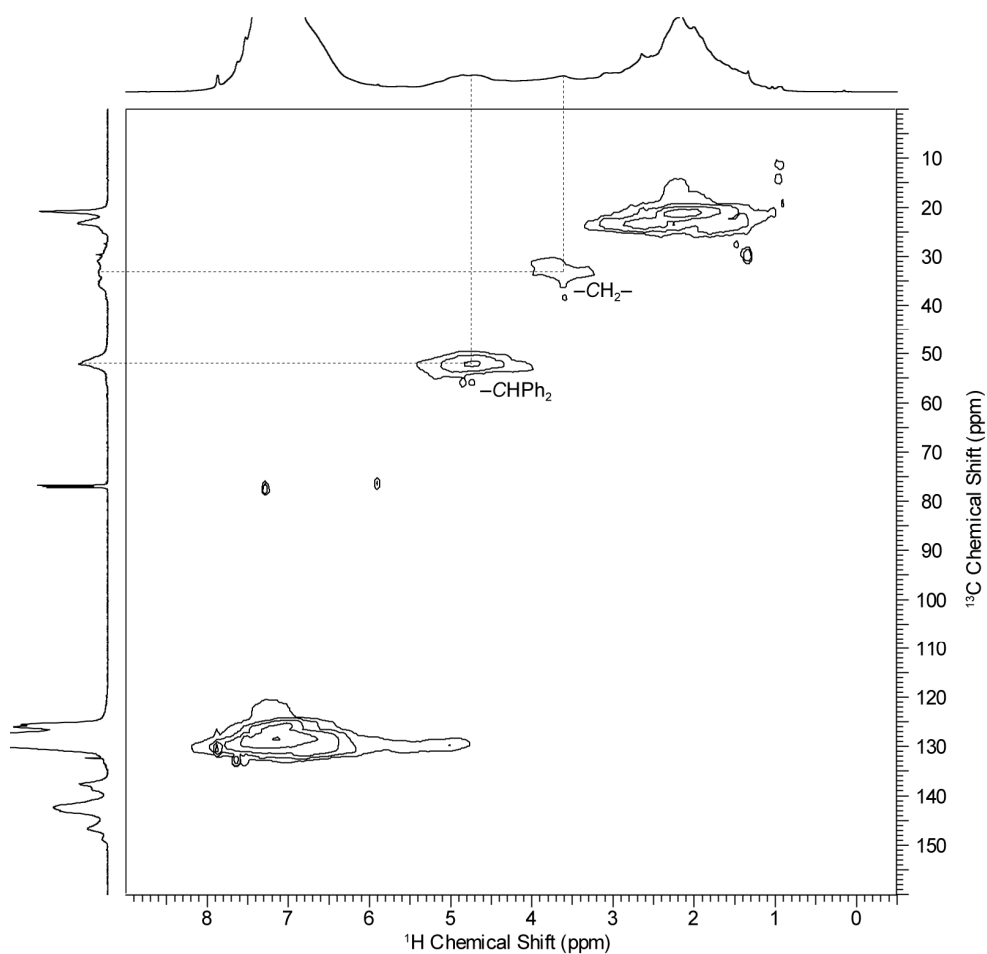
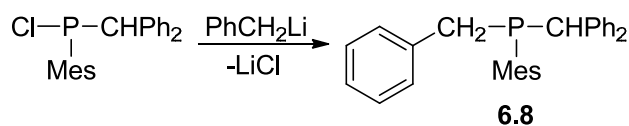


Figure 6.4 ^1H - ^{13}C HSQC NMR spectrum (CDCl_3) of alkoxyamine initiated poly(methylenephosphine) at 25 °C.

6.2.2 Synthesis and Characterization of Model Compound 6.8

The NMR spectra discussed thus far are consistent with the proposed microstructure (6.7) for the alkoxyamine initiated poly(methylenephosphine). Further comparison with an appropriate molecular model compound would provide additional evidence. Although the structure of model compound 6.2 resembles the proposed microstructure 6.7, 6.2 nevertheless lacks a $-\text{CH}_2-$ moiety adjacent to its phosphorus center. Therefore, the structurally related model compound 6.8 was synthesized by treating a solution of $\text{Mes}(\text{Cl})\text{PCPh}_2\text{H}$ with PhCH_2Li in THF (Scheme 6.5). After workup, the desired product, 6.8, was isolated as a white solid. Significantly, characterization by $^{13}\text{C}\{^1\text{H}\}$ NMR (101 MHz) spectroscopy in CDCl_3 revealed doublet resonances at 51.1 and 32.5 ppm (Figure 6.5), arising from the $-\text{CHPh}_2$ and $-\text{CH}_2-$ carbons, respectively. These resonances are coupled to the adjacent phosphorus center and are consistent with the chemical shifts assigned to the $-\text{CHPh}_2$ and $-\text{CH}_2-$ moieties in the proposed microstructure 6.7 ($\delta = 51.3$ and 33.0, respectively). Noteworthy is the broad signal centered at 23.5 ppm, attributed to the *ortho*-methyl mesityl carbons in 6.8. Such broadening is likely a consequence of restricted rotation about the $\text{P}-\text{C}_{\text{ipso-mesityl}}$ bond and has been observed for the related $\text{Mes}(^n\text{Bu})\text{PCPh}_2\text{H}$.³⁹⁶ These assignments were made with the aid of $^1\text{H}-^{13}\text{C}$ HMQC (Heteronuclear Multiple Quantum Correlation), $^1\text{H}-^{13}\text{C}$ HMBC (Heteronuclear Multiple Bond Correlation) and ^{13}C APT NMR spectroscopy.



Scheme 6.5 Synthesis of model compound 6.8.

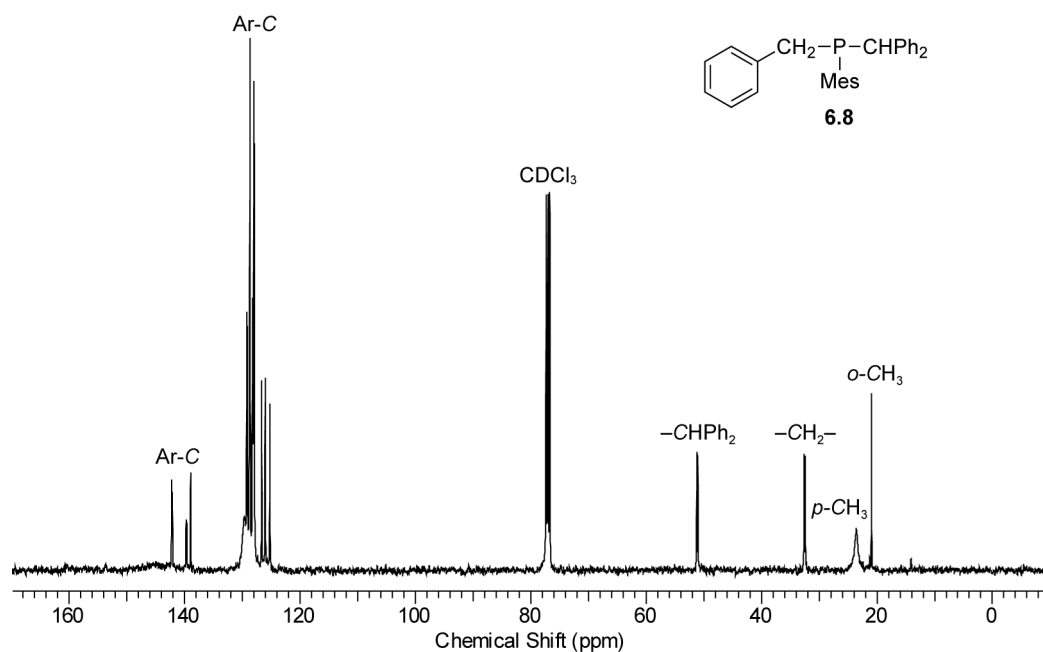


Figure 6.5 $^{13}\text{C}\{^1\text{H}\}$ NMR (101 MHz, CDCl_3) spectrum of model compound **6.8** at 25 °C.

In the ^1H NMR (400 MHz, CDCl_3) spectrum of model compound **6.8**, there is also considerable broadening of the resonance assigned to the *ortho*-methyl mesityl protons at 2.49 ppm (Figure 6.6). A doublet resonance at 5.06 ppm is attributed to the $-\text{CHPh}_2$ proton and is consistent with the chemical shift assigned to the $-\text{CHPh}_2$ proton in proposed microstructure **6.7** ($\delta = 4.8$). The diastereotopic $-\text{CH}_2-$ protons adjacent to the stereogenic phosphorus center give rise to two sets of doublets of doublets at 3.40 and 2.93 ppm, which are in the region observed for the broad resonance assigned to the $-\text{CH}_2-$ protons in **6.7** ($\delta = 3.6$). These assignments were made with the aid of $^1\text{H}\{^{31}\text{P}\}$ and $^1\text{H}-^1\text{H}$ COSY (Correlation Spectroscopy) NMR spectroscopy. In addition, the ^{31}P NMR (162 MHz, CDCl_3) spectrum of **6.8** contains a singlet resonance at -4.7 ppm. This is closer to the center of the broad resonance observed for **6.7** ($\delta = -10$) than for the previously reported model compound **6.2** ($\delta = -24.6$).¹⁸

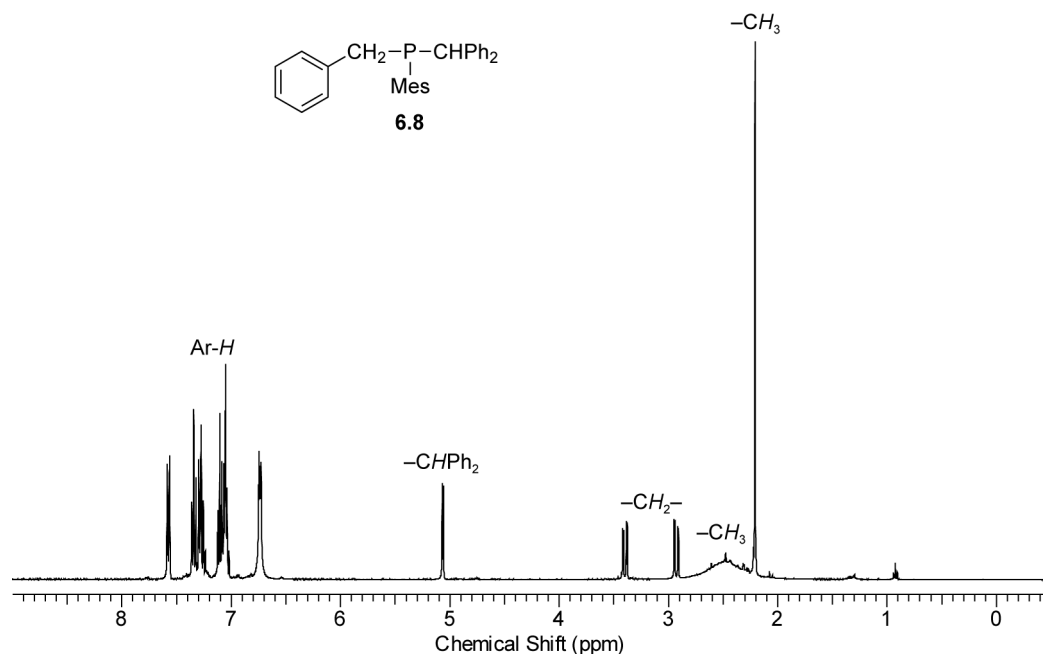
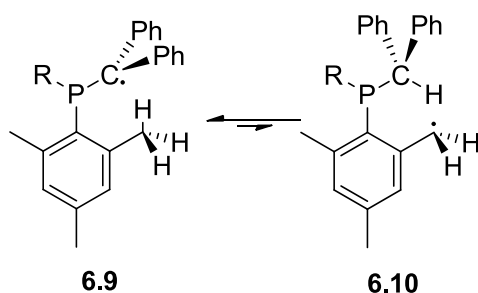


Figure 6.6 ^1H NMR (400 MHz, CDCl_3) spectrum of model compound **6.8** at 25 °C.

6.2.3 Rationalization for the Proposed Microstructure 6.7

Based on the evidence for the unexpected microstructure **6.7**, the alkoxyamine (**6.6**) initiated polymerization of $\text{MesP}=\text{CPh}_2$ is unlikely to propagate through a simple 1,2-addition across the $\text{P}=\text{C}$ bond. Although the initiation step of polymerization is likely to form the radical intermediate **6.9**, this radical intermediate is poised to rearrange to **6.10** through 1,5-hydrogen abstraction (Scheme 6.6). The tertiary radical of **6.9** is expected to be more stable than the primary radical of **6.10**; thus, the equilibrium of this arrangement should lie towards **6.9**. However, the tertiary radical of **6.9** is resonance stabilized and sterically hindered by two aryl substituents, whereas the primary radical of **6.10** is less sterically hindered and resonance stabilized by only one aryl substituent. Thus, it can be rationalized that **6.9** is less reactive than **6.10** towards additional molecules of $\text{MesP}=\text{CPh}_2$, resulting in the propagation through **6.10** to afford poly(methylenephosphine) of microstructure **6.7**.



Scheme 6.6 Equilibrium of radicals **6.9** and **6.10** through 1,5-hydrogen abstraction.

6.3 Summary

In this chapter, strong NMR spectroscopic evidence was provided for the unexpected microstructure (**6.7**) of alkoxyamine initiated poly(methylenephosphine). Model compound **6.8** was synthesized. Its NMR spectra are remarkably similar to those of alkoxyamine initiated poly(methylenephosphine), providing further support for the proposed microstructure **6.7**. The formation of this unexpected microstructure was rationalized through a proposed 1,5-hydrogen abstraction rearrangement during the propagation step of polymerization.

6.4 Experimental Section

6.4.1 General Procedures

All manipulations were performed using standard Schlenk or glovebox techniques under nitrogen atmosphere. Toluene, CH_2Cl_2 and hexanes were deoxygenated with nitrogen and dried by passing through a column containing activated alumina. THF was dried over sodium/benzophenone ketyl and distilled prior to use. *n*-Pentane was dried over 3Å molecular sieves and degassed before use. Distilled H_2O was sparged with N_2 for 30 min prior to use. *N,N,N',N'*-Tetramethylethylenediamine (TMEDA) was purchased from Acros Organics, dried over $n\text{-BuLi}$ and distilled before use. *n*-Butyllithium (1.6 M in hexanes) and *N*-benzylbenzamide were purchased from Aldrich and used as received. $\text{MesP}=\text{CPh}_2$,³⁷⁵⁻³⁷⁶ 1-(2,2,6,6-

tetramethylpiperidinyloxy)-1-phenylethane,³⁹⁹ and Mes(Cl)PHCPh₂⁴⁰⁴⁻⁴⁰⁵ were prepared following literature procedures. CDCl₃ was purchased from Cambridge Isotope Laboratories Inc. and dried over 3 Å molecular sieves before use.

¹H, ¹³C{¹H} and ³¹P NMR spectra were recorded at 25 °C on Bruker Avance 300, Avance 400 or Avance 600 MHz spectrometers. 85% H₃PO₄ was used as an external standard (δ 0.0) for ³¹P NMR spectra. ¹H NMR spectra were referenced to residual protonated solvent and ¹³C{¹H} NMR spectra were referenced to the deuterated solvent. Mass spectra were recorded on a Kratos MS 50 instrument in EI mode (70 eV). Elemental analyses were performed in the University of British Columbia Chemistry Microanalysis Facility.

Molecular weights were determined by triple detection gel permeation chromatography (GPC-LLS) using a Waters liquid chromatograph equipped with a Waters 515 HPLC pump, Waters 717 plus autosampler, Waters Styragel columns (4.6 × 300 mm) HR5E (2000-4,000,000), HR4 (5000-500,000), and HR2 (500-20,000), Waters 2410 differential refractometer (λ = 940 nm, 40 °C), Wyatt tristar miniDAWN (laser light scattering detector at λ = 690 nm) and a Wyatt ViscoStar viscometer. A flow rate of 0.5 mL min⁻¹ was used and samples were dissolved in THF (ca. 2 mg mL⁻¹). The dn/dc value of poly(methylenephosphine) in THF has been previously reported (dn/dc = 0.223 mL g⁻¹).³⁷⁷

6.4.2 Synthesis of Poly(methylenephosphine) 6.6

Poly(methylenephosphine) **6.6** was synthesized by Dr. Krummenacher.³⁹⁷ In a glove box, a Pyrex tube was charged with MesP=CPh₂ (0.80 g, 2.5 mmol) and 1-(2,2,6,6-tetramethylpiperidinyloxy)-1-phenylethane (0.013 g, 0.05 mmol) and the tube was flame sealed *in vacuo*. The mixture was heated at 125 °C for 14 h in an oven equipped with a rocking tray.

The resultant viscous mixture was dissolved in CH_2Cl_2 and the polymer was isolated by repeated precipitation into hexanes ($\times 3$).

$^{31}\text{P}\{^1\text{H}\}$ NMR (121 MHz, CDCl_3): δ -10 (br); ^1H NMR (600 MHz, CDCl_3): δ 7.1 (br, Ar-H), 4.8 (br, CHPh_2), 3.6 (br, CH_2), 2.1 (br, CH_3); $^{13}\text{C}\{^1\text{H}\}$ NMR (151 MHz, CDCl_3) (assignments made with the aid of ^1H - ^{13}C HSQC/ ^{13}C APT experiments): δ 146.9 (br, Ar-C), 142.2 (br, Ar-C), 137.9 (br, Ar-C), 128.2 (br, Ar-C), 126.3 (br, Ar-C), 52.4 (br, CHPh_2), 33.0 (br, CH_2) 23.5 (br, CH_3), 21.2 (br, CH_3). GPC (absolute): $M_n = 8,800 \text{ g mol}^{-1}$, PDI = 1.16.

6.4.3 Synthesis of PhCH_2Li

To a stirred colorless solution of TMEDA (2.03 g, 17.4 mmol) in toluene (20 mL) was added a solution of $n\text{BuLi}$ in hexanes (8.25 mL, 1.6 M, 13.2 mmol). The mixture turned red upon addition and was heated at $90 \text{ }^\circ\text{C}$ for 2 h. Subsequently, the solution was cooled to room temperature. Addition of hexanes (50 mL), followed by cooling to $-78 \text{ }^\circ\text{C}$, resulted in the precipitation of PhCH_2Li as a yellow solid, which was isolated by filtration at $-78 \text{ }^\circ\text{C}$ and washed with additional cold hexanes ($2 \times 25 \text{ mL}$) at $-78 \text{ }^\circ\text{C}$. The yellow solid was dissolved in THF (40 mL), resulting in a dark red solution of PhCH_2Li which was titrated against *N*-benzylbenzamide. The concentration was determined to be 0.156 M.

6.4.4 Synthesis of Model Compound 6.7

One equivalent of the PhCH_2Li solution in THF (18.5 mL, 0.156 M, 2.89 mmol) was added slowly to a stirred solution of $\text{Mes}(\text{Cl})\text{PCHPh}_2$ (1.02 g, 2.89 mmol) in THF (10 mL) at $-78 \text{ }^\circ\text{C}$, resulting in an orange solution. After several minutes, several drops of distilled H_2O were added at $-78 \text{ }^\circ\text{C}$ and the reaction mixture turned light brown with the formation of a white precipitate. The reaction was warmed to room temperature and the solvent was removed *in*

vacuo. The resultant white residue was dissolved in toluene (5 mL), filtered to remove insoluble salts and the filtrate was evaporated to dryness to afford a brown oil. The oil was dissolved in *n*-pentane (5 mL), cooled to $-20\text{ }^{\circ}\text{C}$ and filtered to remove an insoluble brown residue. The colorless filtrate was chilled at $-78\text{ }^{\circ}\text{C}$, resulting in the precipitation of a white solid that was isolated by filtration. Upon warming to room temperature the solid melted into slightly yellow oil. The oil was dissolved in *n*-pentane (5 mL) and chilled at $-30\text{ }^{\circ}\text{C}$ for 4 days to yield a white solid. The supernatant was decanted and the solid residue was washed with cold *n*-pentane ($3 \times 1\text{ mL}$). Residual solvent was removed *in vacuo* to afford the desired product. Yield = 414 mg (35%).

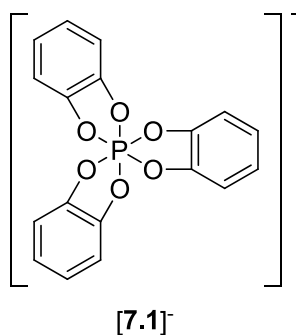
^{31}P NMR (162 MHz, CDCl_3): δ -4.7 (s); ^1H NMR (400 MHz, CDCl_3) (assignments made with the aid of $^1\text{H}\{^{31}\text{P}\}/^1\text{H}-^1\text{H}$ COSY experiments): δ 7.58-7.56 (m, 2H, Ph-*H*), 7.36-7.24 (m, 5H, Ph-*H*), 7.12-7.02 (m, 6H, Ph-*H*), 6.75-6.72 (m, 4H, Mes-*H* and Ph-*H*), 5.06 (d, $^2J_{\text{PH}} = 4\text{ Hz}$, 1H, *CHPh*₂), 3.40 (dd, $^2J_{\text{HH}} = 13\text{ Hz}$, $^2J_{\text{PH}} = 3\text{ Hz}$, 1H, P-*CHH*), 2.93 (dd, $^2J_{\text{HH}} = 13\text{ Hz}$, $^2J_{\text{PH}} = 3\text{ Hz}$, 1H, P-*CHH*), 2.49 (br s, 6H, *o*-Mes-*CH*₃), 2.20 (s, 3H, *p*-Mes-*CH*₃); $^{13}\text{C}\{^1\text{H}\}$ NMR (101 MHz, CDCl_3) (assignments made with the aid of $^1\text{H}-^{13}\text{C}$ HMQC/ $^1\text{H}-^{13}\text{C}$ HMBC/ ^{13}C APT experiments): δ 145.3 (br, *o*-Mes-*C*), 142.2 (d, $^2J_{\text{CP}} = 3\text{ Hz}$, *i*-Ph-*C*), 142.1 (d, $^2J_{\text{CP}} = 3\text{ Hz}$, *i*-Ph-*C*), 139.7 (d, $^1J_{\text{CP}} = 12\text{ Hz}$, *i*-Mes-*C*), 138.9 (s, *p*-Mes-*C*), 129.7 (br, *m*-Mes-*C*), 129.2 (d, $J_{\text{CP}} = 9\text{ Hz}$, Ph-*C*), 128.9-128.6 (m, Ph-*C*), 128.2 (d, $J_{\text{CP}} = 9\text{ Hz}$, Ph-*C*), 128.0 (d, $J_{\text{CP}} = 8\text{ Hz}$, Ph-*C*), 126.6 (s, Ph-*C*), 126.0 (d, $J_{\text{CP}} = 3\text{ Hz}$, Ph-*C*), 125.2 (d, $J_{\text{CP}} = 3\text{ Hz}$, Ph-*C*), 51.1 (d, $^1J_{\text{CP}} = 20\text{ Hz}$, *CHPh*₂), 32.5 (d, $^1J_{\text{CP}} = 20\text{ Hz}$, *CH*₂Ph), 23.5 (br s, *o*-Mes-*CH*₃), 20.9 (s, *p*-Mes-*CH*₃). MS (EI) *m/z* (%): 408 (44) [*M*⁺], 317 (13) [MesP*CHPh*₂⁺], 241 (40) [Ph*CH*₂P*Mes*⁺], 167 (100) [Ph₂*CH*⁺], 119 (6) [Mes⁺], 91 (21) [Ph*CH*₂⁺]. Anal. Calcd. for C₂₉H₂₉P: C, 85.26; H, 7.16. Found: C, 84.95; H, 7.21.

Chapter 7: Conclusion

7.1 Summary of Thesis Work

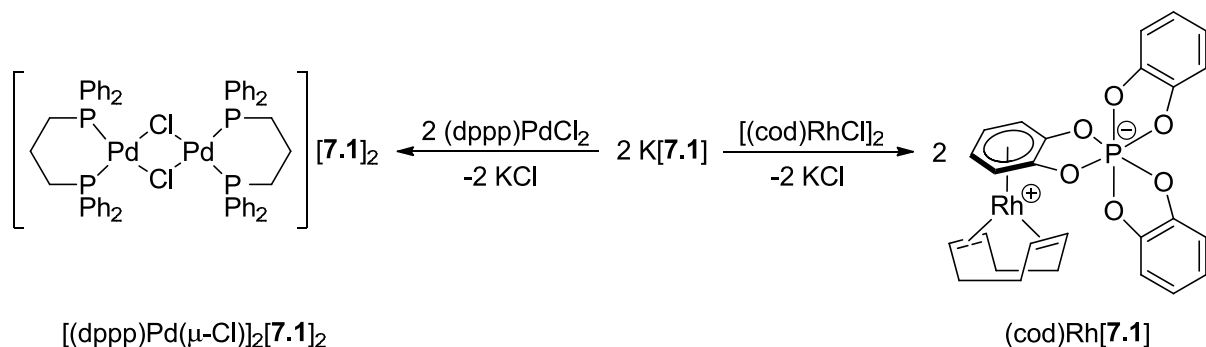
7.1.1 Hexacoordinated Phosphorus(V) Anions

Traditionally, the field of weakly coordinating anions (WCAs) has largely been dominated by boron- and aluminum-based anions.^{38-39,180} Yet, it is well-understood that larger, more charge-delocalized anions are generally less nucleophilic. Therefore, it was expected that, in comparison to the tetracoordinated borates, the larger hexacoordinated phosphorus(V) anions might be more charge-diffused, thus more weakly coordinating. The main goal of this thesis was to explore hexacoordinated phosphorus(V) anions as potential WCAs in catalysis. In particular, the catechol-based **[7.1]**⁻ was of great historical significance since it was the first example of a hexacoordinated organophosphate anion.^{150,152-153} However, its ability to stabilize cationic transition metal complexes has yet to be explored.



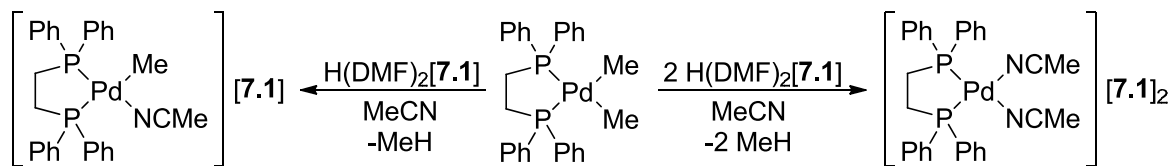
Chapter 2 described the synthesis of two new alkali metal salts of **[7.1]**⁻, specifically **K[7.1]** and **Na[7.1]**. These reagents offered a convenient route to cationic metal complexes through the halide abstraction of metal-halide bonds. The efficacy of **K[7.1]** as a halide abstraction reagent was demonstrated through its reactions with **(dppp)PdCl₂** [**dppp** = 1,3-bis(diphenylphosphino)propane] (1:1 ratio) and **[(cod)RhCl]₂** (2:1 ratio) to generate the dimeric

$[(\text{dppp})\text{Pd}(\mu\text{-Cl})_2][\mathbf{7.1}]_2$ and the zwitterionic $(\text{cod})\text{Rh}[\mathbf{7.1}]$ (Scheme 7.1). These preliminary results show that late transition metal cations can be stabilized by $[\mathbf{7.1}]^-$.



Scheme 7.1 Halide abstraction of $(\text{dppp})\text{PdCl}_2$ and $[(\text{cod})\text{RhCl}]_2$ with $\text{K}[\mathbf{7.1}]$.

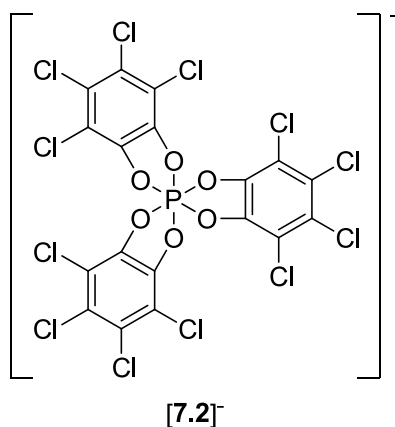
Alternatively, cationic metal complexes can be generated through the protonolysis of metal-carbon bonds. Chapter 3 described the convenient preparation of solid Brønsted acids $\text{H}(\text{DMF})_2[\mathbf{7.1}]$ and $\text{H}(\text{DMSO})_2[\mathbf{7.1}]$. The isolation of highly acidic $[\text{H}(\text{DMF})_2]^+$ and $[\text{H}(\text{DMSO})_2]^+$ is a testament to the stability of $[\mathbf{7.1}]^-$. Furthermore, the basicity of $[\mathbf{7.1}]^-$ was determined to be similar to that of the classical weakly coordinating anion, $[\text{BF}_4]^-$, based on a similar N-H stretching frequency for $(\text{C}_8\text{H}_{17})_3\text{NH}[\mathbf{7.1}]$ and to that observed for $(\text{C}_8\text{H}_{17})_3\text{NH}[\text{BF}_4]$. The efficacy of $\text{H}(\text{DMF})_2[\mathbf{7.1}]$ to activate late transition metal-alkyl bonds was evidenced by the stoichiometric activation of $(\text{dppe})\text{PdMe}_2$ to afford either $[(\text{dppe})\text{Pd}(\text{NCMe})\text{Me}][\mathbf{7.1}]$ (1:1 ratio) or $[(\text{dppe})\text{Pd}(\text{NCMe})_2][\mathbf{7.1}]_2$ (1:2 ratio) (Scheme 7.2).



Scheme 7.2 Protonolysis of $(\text{dppe})\text{PdMe}_2$ with $\text{H}(\text{DMF})_2[\mathbf{7.1}]$.

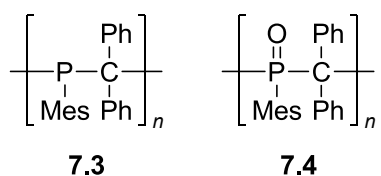
Strong Brønsted acids are also of interest as initiators for cationic polymerization. It was demonstrated in Chapter 4 that $\text{H}(\text{DMF})_2[\mathbf{7.1}]$ initiates the cationic polymerization of *n*-butyl vinyl ether at 17 °C to afford moderate molecular weight polymer. However, $\text{H}(\text{DMF})_2[\mathbf{7.1}]$ was

not an effective initiator for the polymerization of styrene and isoprene. This is likely due to the moderate nucleophilicity of [7.1]⁻, which might have hindered these polymerizations. Thus, solid Brønsted acids of the more charge-delocalized [7.2]⁻ were prepared, namely H(OEt₂)₂[7.2] and H(OEt₂)(NCMe)[7.2]. Brønsted acid H(OEt₂)₂[7.2] was shown to be an effective initiator for the cationic polymerizations of *n*-butyl vinyl ether, styrene and isoprene to afford polymers of moderate molecular weight. The investigation of H(DMF)₂[7.1] and H(OEt₂)₂[7.2] as cationic polymerization initiators has helped to broaden the general application of hexacoordinated phosphorus(V) anions.

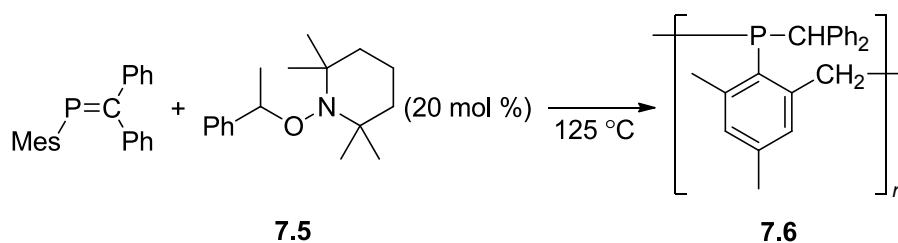


7.1.2 Poly(methylenephosphine)s

Chapter 5 changed the focus of this thesis onto the phosphorus-based polymers, poly(methylenephosphine)s **7.3** and **7.4**. Given the presence of phosphorus centers in the backbone of **7.3** and **7.4**, it was of great interest to investigate their flame retardant property. It was shown that **7.3** and **7.4** were effective polymeric phosphorus-based flame retardant additives for papers made from thermomechanical pulp through the promotion of char formation. The development of effective flame-retardants for cellulose-based products could open up new commercial applications for wood-based products.



Recently in the Gates group, alkoxyamine **7.5** was investigated as an radical initiator for the polymerization of MesP=CPh₂ (Scheme 7.3).³⁹⁷⁻³⁹⁸ Chapter 6 discussed the results from the NMR spectroscopic analysis of the resultant poly(methylenephosphine). Strong evidence was provided for the unexpected microstructure **7.6**. The formation of this unexpected microstructure was rationalized through a proposed 1,5-hydrogen abstraction rearrangement during the propagation step of polymerization. Results from this investigation could potentially lead to a better understanding of the mechanism of radical and anionic polymerizations of MesP=CPh₂.



Scheme 7.3 Alkoxyamine **7.5** initiated polymerization of MesP=CPh₂.

References

- (1) Chivers, T.; Konu, J. *Comm. Inorg. Chem.* **2009**, *30*, 131.
- (2) Seyferth, D. *Organometallics* **2001**, *20*, 4978.
- (3) Mark, J. E. *Acc. Chem. Res.* **2004**, *37*, 946.
- (4) Fink, J. K. *Reactive Polymers Fundamentals and Applications: A Concise Guide to Industrial Polymers*; William Andrew Publishing: New York, 2005.
- (5) Kipping, F. S. *Proc. R. Soc. (London)*, A **1937**, *159*, 139.
- (6) Stokes, H. N. *Am. Chem. J.* **1895**, *17*, 275.
- (7) Stokes, H. N. *Am. Chem. J.* **1897**, *19*, 782.
- (8) Allcock, H. R.; Kugel, R. L. *J. Am. Chem. Soc.* **1965**, *87*, 4216.
- (9) Allcock, H. R.; Kugel, R. L.; Valan, K. J. *Inorg. Chem.* **1966**, *5*, 1709.
- (10) Allcock, H. R. *J. Inorg. Organomet. Polym. Mater.* **2006**, *16*, 277.
- (11) Gleria, M.; De Jaeger, R. *Top. Curr. Chem.* **2005**, *250*, 165.
- (12) Allen, C. W. *J. Fire Sci.* **1993**, *11*, 320.
- (13) Dorn, H.; Rodezno, J. M.; Brunnhofer, B.; Rivard, E.; Massey, J. A.; Manners, I. *Macromolecules* **2003**, *36*, 291.
- (14) Dorn, H.; Singh, R. A.; Massey, J. A.; Nelson, J. M.; Jaska, C. A.; Lough, A. J.; Manners, I. *J. Am. Chem. Soc.* **2000**, *122*, 6669.
- (15) Staubitz, A.; Soto, A. P.; Manners, I. *Angew. Chem., Int. Ed.* **2008**, *47*, 6212.
- (16) Staubitz, A.; Robertson, A. P. M.; Sloan, M. E.; Manners, I. *Chem. Rev.* **2010**, *110*, 4023.
- (17) Bates, J. I.; Dugal-Tessier, J.; Gates, D. P. *Dalton Trans.* **2010**, *39*, 3151.
- (18) Tsang, C. W.; Yam, M.; Gates, D. P. *J. Am. Chem. Soc.* **2003**, *125*, 1480.
- (19) Tsang, C. W.; Baharloo, B.; Riendl, D.; Yam, M.; Gates, D. P. *Angew. Chem., Int. Ed.* **2004**, *43*, 5682.

- (20) Noonan, K. J. T.; Gates, D. P. *Angew. Chem., Int. Ed.* **2006**, *45*, 7271.
- (21) Noonan, K. J. T.; Gillon, B. H.; Cappello, V.; Gates, D. P. *J. Am. Chem. Soc.* **2008**, *130*, 12876.
- (22) Chen, J. W.; Cao, Y. *Acc. Chem. Res.* **2009**, *42*, 1709.
- (23) Pron, A.; Rannou, P. *Prog. Polym. Sci.* **2002**, *27*, 135.
- (24) McQuade, D. T.; Pullen, A. E.; Swager, T. M. *Chem. Rev.* **2000**, *100*, 2537.
- (25) Crassous, J.; Réau, R. *Dalton Trans.* **2008**, 6865.
- (26) Hobbs, M. G.; Baumgartner, T. *Eur. J. Inorg. Chem.* **2007**, 3611.
- (27) Welch, G. C.; Juan, R. R. S.; Masuda, J. D.; Stephan, D. W. *Science* **2006**, *314*, 1124.
- (28) Stephan, D. W.; Erker, G. *Angew. Chem., Int. Ed.* **2010**, *49*, 46.
- (29) Chase, P. A.; Welch, G. C.; Jurca, T.; Stephan, D. W. *Angew. Chem., Int. Ed.* **2007**, *46*, 8050.
- (30) Spies, P.; Schwendemann, S.; Lange, S.; Kehr, G.; Fröhlich, R.; Erker, G. *Angew. Chem., Int. Ed.* **2008**, *47*, 7543.
- (31) Dechy-Cabaret, O.; Martin-Vaca, B.; Bourissou, D. *Chem. Rev.* **2004**, *104*, 6147.
- (32) Stanford, M. J.; Dove, A. P. *Chem. Soc. Rev.* **2010**, *39*, 486.
- (33) Thomas, C. M. *Chem. Soc. Rev.* **2010**, *39*, 165.
- (34) Douglas, A. F.; Patrick, B. O.; Mehrkhodavandi, P. *Angew. Chem., Int. Ed.* **2008**, *47*, 2290.
- (35) Akiyama, T. *Chem. Rev.* **2007**, *107*, 5744.
- (36) Terada, M. *Chem. Commun.* **2008**, 4097.
- (37) Lacour, J.; Moraleda, D. *Chem. Commun.* **2009**, 7073.
- (38) Krossing, I.; Raabe, I. *Angew. Chem., Int. Ed.* **2004**, *43*, 2066.
- (39) Strauss, S. H. *Chem. Rev.* **1993**, *93*, 927.

- (40) Beck, W.; Sünkel, K. *Chem. Rev.* **1988**, *88*, 1405.
- (41) Massey, A. G.; Park, A. J. *J. Organomet. Chem.* **1964**, *2*, 245.
- (42) Piers, W. E.; Chivers, T. *Chem. Soc. Rev.* **1997**, *26*, 345.
- (43) Ewen, J. A.; Elder, M. J., Eur. Patent. Appl. 0,427,697, 1991.
- (44) Ewen, J. A.; Elder, M. J., U.S. Pat. 5,561,092, 1996.
- (45) Yang, X. M.; Stern, C. L.; Marks, T. J. *J. Am. Chem. Soc.* **1991**, *113*, 3623.
- (46) Yang, X. M.; Stern, C. L.; Marks, T. J. *J. Am. Chem. Soc.* **1994**, *116*, 10015.
- (47) Chien, J. C. W.; Tsai, W. M.; Rausch, M. D. *J. Am. Chem. Soc.* **1991**, *113*, 8570.
- (48) Chien, J. C. W.; Song, W.; Rausch, M. D. *Macromolecules* **1993**, *26*, 3239.
- (49) Yang, X. M.; Stern, C. L.; Marks, T. J. *Organometallics* **1991**, *10*, 840.
- (50) Brookhart, M.; Grant, B.; Volpe, A. F. *Organometallics* **1992**, *11*, 3920.
- (51) Nishida, H.; Takada, N.; Yoshimura, M.; Sonoda, T.; Kobayashi, H. *Bull. Chem. Soc. Jpn.* **1984**, *57*, 2600.
- (52) Brookhart, M.; Rix, F. C.; Desimone, J. M.; Barborak, J. C. *J. Am. Chem. Soc.* **1992**, *114*, 5894.
- (53) Mecking, S.; Johnson, L. K.; Wang, L.; Brookhart, M. *J. Am. Chem. Soc.* **1998**, *120*, 888.
- (54) Park, S.; Brookhart, M. *J. Am. Chem. Soc.* **2012**, *134*, 640.
- (55) Mukherjee, A.; Nembenna, S.; Sen, T. K.; Sarish, S. P.; Ghorai, P. K.; Ott, H.; Stalke, D.; Mandal, S. K.; Roesky, H. W. *Angew. Chem., Int. Ed.* **2011**, *50*, 3968.
- (56) Kinjo, R.; Donnadieu, B.; Bertrand, G. *Angew. Chem., Int. Ed.* **2011**, *50*, 5560.
- (57) Park, S.; Brookhart, M. *Chem. Commun.* **2011**, *47*, 3643.
- (58) Schumacher, A.; Schrems, M. G.; Pfaltz, A. *Chem.-Eur. J.* **2011**, *17*, 13502.
- (59) Chen, F.; Ding, Z. Y.; Qin, J.; Wang, T. L.; He, Y. M.; Fan, Q. H. *Org. Lett.* **2011**, *13*, 4348.

- (60) Sewell, L. J.; Chaplin, A. B.; Weller, A. S. *Dalton Trans.* **2011**, *40*, 7499.
- (61) Schreiber, D. F.; Ortin, Y.; Muller-Bunz, H.; Phillips, A. D. *Organometallics* **2011**, *30*, 5381.
- (62) Chen, E. Y. X.; Marks, T. J. *Chem. Rev.* **2000**, *100*, 1391.
- (63) LaPointe, R. E.; Roof, G. R.; Abboud, K. A.; Klosin, J. *J. Am. Chem. Soc.* **2000**, *122*, 9560.
- (64) Lancaster, S. J.; Walker, D. A.; Thornton-Pett, M.; Bochmann, M. *Chem. Commun.* **1999**, 1533.
- (65) Lancaster, S. J.; Rodriguez, A.; Lara-Sanchez, A.; Hannant, M. D.; Walker, D. A.; Hughes, D. H.; Bochmann, M. *Organometallics* **2002**, *21*, 451.
- (66) Vierle, M.; Zhang, Y. M.; Herdtweck, E.; Bohnenpoll, M.; Nuyken, O.; Kuhn, F. E. *Angew. Chem., Int. Ed.* **2003**, *42*, 1307.
- (67) Hijazi, A. K.; Radhakrishnan, N.; Jain, K. R.; Herdtweck, E.; Nuyken, O.; Walter, H. M.; Hanefeld, P.; Voit, B.; Kuhn, F. E. *Angew. Chem., Int. Ed.* **2007**, *46*, 7290.
- (68) Garratt, S.; Carr, A. G.; Langstein, G.; Bochmann, M. *Macromolecules* **2003**, *36*, 4276.
- (69) Rodriguez-Delgado, A.; Hannant, M. D.; Lancaster, S. J.; Bochmann, M. *Macromol. Chem. Phys.* **2004**, *205*, 334.
- (70) Sarazin, Y.; Poirier, V.; Roisnel, T.; Carpentier, J. F. *Eur. J. Inorg. Chem.* **2010**, 3423.
- (71) Sarazin, Y.; Liu, B.; Roisnel, T.; Maron, L.; Carpentier, J. F. *J. Am. Chem. Soc.* **2011**, *133*, 9069.
- (72) Zhang, Y. M.; Sun, W.; Santos, A. M.; Kuhn, F. E. *Catal. Lett.* **2005**, *101*, 35.
- (73) Zhang, Y. M.; Santos, A. M.; Herdtweck, E.; Mink, J.; Kuhn, F. E. *New J. Chem.* **2005**, *29*, 366.
- (74) McInenly, P. J.; Drewitt, M. J.; Baird, M. C. *Macromol. Chem. Phys.* **2004**, *205*, 1707.

- (75) Tse, C. K. W.; Penciu, A.; McInenly, P. J.; Kumar, K. R.; Drewitt, M. J.; Baird, M. C. *Eur. Polym. J.* **2004**, *40*, 2653.
- (76) Mitu, S.; Baird, M. C. *Can. J. Chem.* **2006**, *84*, 225.
- (77) Knoth, W. H. *J. Am. Chem. Soc.* **1967**, *89*, 1274.
- (78) Xie, Z. W.; Manning, J.; Reed, R. W.; Mathur, R.; Boyd, P. D. W.; Benesi, A.; Reed, C. A. *J. Am. Chem. Soc.* **1996**, *118*, 2922.
- (79) Reed, C. A.; Xie, Z. W.; Bau, R.; Benesi, A. *Science* **1993**, *262*, 402.
- (80) Reed, C. A. *Acc. Chem. Res.* **2010**, *43*, 121.
- (81) Douvris, C.; Ozerov, O. V. *Science* **2008**, *321*, 1188.
- (82) Douvris, C.; Nagaraja, C. M.; Chen, C. H.; Foxman, B. M.; Ozerov, O. V. *J. Am. Chem. Soc.* **2010**, *132*, 4946.
- (83) Gu, W. X.; Haneline, M. R.; Douvris, C.; Ozerov, O. V. *J. Am. Chem. Soc.* **2009**, *131*, 11203.
- (84) Allemann, O.; Duttwyler, S.; Romanato, P.; Baldrige, K. K.; Siegel, J. S. *Science* **2011**, *332*, 574.
- (85) Zhang, Y.; Huynh, K.; Manners, I.; Reed, C. A. *Chem. Commun.* **2008**, 494.
- (86) Crowther, D. J.; Borkowsky, S. L.; Swenson, D.; Meyer, T. Y.; Jordan, R. F. *Organometallics* **1993**, *12*, 2897.
- (87) Rifat, A.; Patmore, N. J.; Mahon, M. F.; Weller, A. S. *Organometallics* **2002**, *21*, 2856.
- (88) Moxham, G. L.; Randell-Sly, H. E.; Brayshaw, S. K.; Woodward, R. L.; Weller, A. S.; Willis, M. C. *Angew. Chem., Int. Ed.* **2006**, *45*, 7618.
- (89) Moxham, G. L.; Randell-Sly, H.; Brayshaw, S. K.; Weller, A. S.; Willis, M. C. *Chem.-Eur. J.* **2008**, *14*, 8383.

- (90) Hague, C.; Patmore, N. J.; Frost, C. G.; Mahon, M. F.; Weller, A. S. *Chem. Commun.* **2001**, 2286.
- (91) Patmore, N. J.; Hague, C.; Cotgreave, J. H.; Mahon, M. F.; Frost, C. G.; Weller, A. S. *Chem.-Eur. J.* **2002**, *8*, 2088.
- (92) Moss, S.; King, B. T.; de Meijere, A.; Kozhushkov, S. I.; Eaton, P. E.; Michl, J. *Org. Lett.* **2001**, *3*, 2375.
- (93) Vyakaranam, K.; Barbour, J. B.; Michl, J. *J. Am. Chem. Soc.* **2006**, *128*, 5610.
- (94) Körbe, S.; Schreiber, P. J.; Michl, J. *Chem. Rev.* **2006**, *106*, 5208.
- (95) Chen, Y. X.; Stern, C. L.; Marks, T. J. *J. Am. Chem. Soc.* **1997**, *119*, 2582.
- (96) Chen, Y. X.; Metz, M. V.; Li, L. T.; Stern, C. L.; Marks, T. J. *J. Am. Chem. Soc.* **1998**, *120*, 6287.
- (97) Chen, M. C.; Roberts, J. A. S.; Marks, T. J. *J. Am. Chem. Soc.* **2004**, *126*, 4605.
- (98) Chen, M. C.; Marks, T. J. *J. Am. Chem. Soc.* **2001**, *123*, 11803.
- (99) Sun, Y. M.; Metz, M. V.; Stern, C. L.; Marks, T. J. *Organometallics* **2000**, *19*, 1625.
- (100) Krossing, I. *Chem.-Eur. J.* **2001**, *7*, 490.
- (101) Metz, M. V.; Sun, Y. M.; Stern, C. L.; Marks, T. J. *Organometallics* **2002**, *21*, 3691.
- (102) McGuinness, D. S.; Rucklidge, A. J.; Tooze, R. P.; Slawin, A. M. Z. *Organometallics* **2007**, *26*, 2561.
- (103) Chen, M. C.; Roberts, J. A. S.; Marks, T. J. *Organometallics* **2004**, *23*, 932.
- (104) Chen, M. C.; Roberts, J. A. S.; Seyam, A. M.; Li, L. T.; Zuccaccia, C.; Stahl, N. G.; Marks, T. J. *Organometallics* **2006**, *25*, 2833.
- (105) Roberts, J. A. S.; Chen, M. C.; Seyam, A. M.; Li, L. T.; Zuccaccia, C.; Stahl, N. G.; Marks, T. J. *J. Am. Chem. Soc.* **2007**, *129*, 12713.
- (106) Li, H. Y.; Ren, K. T.; Neckers, D. C. *Macromolecules* **2001**, *34*, 8637.

- (107) Li, H. Y.; Ren, K. T.; Zhang, W. Q.; Malpert, J. H.; Neckers, D. C. *Macromolecules* **2001**, *34*, 2019.
- (108) Ren, K. T.; Malpert, J. H.; Li, H. Y.; Gu, H. Y.; Neckers, D. C. *Macromolecules* **2002**, *35*, 1632.
- (109) Ren, K. T.; Serguievski, P.; Gu, H. Y.; Grinevich, O.; Malpert, J. H.; Neckers, D. C. *Macromolecules* **2002**, *35*, 898.
- (110) Appel, R.; Eisenhauer, G. *Chem. Ber.* **1962**, *95*, 246.
- (111) Vij, A.; Kirchmeier, R. L.; Shreeve, J. M.; Verma, R. D. *Coord. Chem. Rev.* **1997**, *158*, 413.
- (112) Kaur, G.; Manju, K.; Trehan, S. *Chem. Commun.* **1996**, 581.
- (113) Foropoulos, J., Jr.; Desmarteau, D. D. *J. Am. Chem. Soc.* **1982**, *104*, 4260.
- (114) Antoniotti, S.; Dalla, V.; Duñach, E. *Angew. Chem., Int. Ed.* **2010**, *49*, 7860.
- (115) Fehr, C.; Vuagnoux, M.; Buzas, A.; Arpagaus, J.; Sommer, H. *Chem.-Eur. J.* **2011**, *17*, 6214.
- (116) Ramón, R. S.; Gaillard, S.; Poater, A.; Cavallo, L.; Slawin, A. M. Z.; Nolan, S. P. *Chem.-Eur. J.* **2011**, *17*, 1238.
- (117) Seidel, G.; Lehmann, C. W.; Furstner, A. *Angew. Chem., Int. Ed.* **2010**, *49*, 8466.
- (118) Wang, Z. J.; Benitez, D.; Tkatchouk, E.; Goddard, W. A.; Toste, F. D. *J. Am. Chem. Soc.* **2010**, *132*, 13064.
- (119) Kakuchi, R.; Chiba, K.; Fuchise, K.; Sakai, R.; Satoh, T.; Kakuchi, T. *Macromolecules* **2009**, *42*, 8747.
- (120) Fuchise, K.; Narumi, A.; Sakai, R.; Satoh, T.; Kawaguchi, S.; Kakuchi, T. *Abstr. Pap. Am. Chem. Soc.* **2010**, 240.

- (121) Kakuchi, R.; Tsuji, Y.; Chiba, K.; Fuchise, K.; Sakai, R.; Satoh, T.; Kakuchi, T. *Macromolecules* **2010**, *43*, 7090.
- (122) Dean, P. A. W.; Gillespie, R. J.; Hulme, R. *J. Chem. Soc., Chem. Commun.* **1969**, 990.
- (123) Minkwitz, R.; Neikes, F. *Inorg. Chem.* **1999**, *38*, 5960.
- (124) Christe, K. O.; Zhang, X. Z.; Bau, R.; Hegge, J.; Olah, G. A.; Prakash, G. K. S.; Sheehy, J. A. *J. Am. Chem. Soc.* **2000**, *122*, 481.
- (125) Bacon, J.; Dean, P. A. W.; Gillespie, R. J. *Can. J. Chem.* **1969**, *47*, 1655.
- (126) Bacon, J.; Dean, P. A. W.; Gillespie, R. J. *Can. J. Chem.* **1970**, *48*, 3413.
- (127) Sibi, M. P.; Ji, J. G. *Angew. Chem., Int. Ed.* **1997**, *36*, 274.
- (128) Bernhardt, I.; Drews, T.; Seppelt, K. *Angew. Chem., Int. Ed.* **1999**, *38*, 2232.
- (129) Drews, T.; Koch, W.; Seppelt, K. *J. Am. Chem. Soc.* **1999**, *121*, 4379.
- (130) Lehmann, J. F.; Riedel, S.; Schrobilgen, G. J. *Inorg. Chem.* **2008**, *47*, 8343.
- (131) Elliott, H. S.; Lehmann, J. F.; Mercier, H. P. A.; Jenkins, H. D. B.; Schrobilgen, G. J. *Inorg. Chem.* **2010**, *49*, 8504.
- (132) Hughes, M. J.; Mercier, H. P. A.; Schrobilgen, G. J. *Inorg. Chem.* **2010**, *49*, 271.
- (133) Kropshofer, H.; Leitzke, O.; Peringer, P.; Sladky, F. *Chem. Ber.* **1981**, *114*, 2644.
- (134) Noirot, M. D.; Anderson, O. P.; Strauss, S. H. *Inorg. Chem.* **1987**, *26*, 2216.
- (135) Collins, M. J.; Schrobilgen, G. J. *Inorg. Chem.* **1985**, *24*, 2608.
- (136) Mercier, H. P. A.; Sanders, J. C. P.; Schrobilgen, G. J. *J. Am. Chem. Soc.* **1994**, *116*, 2921.
- (137) Aris, D.; Beck, J.; Decken, A.; Dionne, I.; Gunne, J.; Hoffbauer, W.; Kochner, T.; Krossing, I.; Passmore, J.; Rivard, E.; Steden, F.; Wang, X. P. *Dalton Trans.* **2011**, *40*, 5865.

- (138) Mercier, H. P. A.; Moran, M. D.; Sanders, J. C. P.; Schrobilgen, G. J.; Suontamo, R. J. *Inorg. Chem.* **2005**, *44*, 49.
- (139) Mercier, H. P. A.; Moran, M. D.; Schrobilgen, G. J.; Steinberg, C.; Suontamo, R. J. *J. Am. Chem. Soc.* **2004**, *126*, 5533.
- (140) Wietelmann, U.; Bonrath, W.; Netscher, T.; Noth, H.; Panitz, J. C.; Wohlfahrt-Mehrens, M. *Chem.-Eur. J.* **2004**, *10*, 2451.
- (141) Lacour, J.; Ginglinger, C.; Grivet, C.; Bernardinelli, G. *Angew. Chem.-Int. Edit. Engl.* **1997**, *36*, 608.
- (142) Favarger, F.; Goujon-Ginglinger, C.; Monchaud, D.; Lacour, J. *J. Org. Chem.* **2004**, *69*, 8521.
- (143) Lacour, J.; Hebbe-Viton, V. *Chem. Soc. Rev.* **2003**, *32*, 373.
- (144) Chavarot, M.; Ménage, S.; Hamelin, O.; Charnay, F.; Pécaut, J.; Fontecave, M. *Inorg. Chem.* **2003**, *42*, 4810.
- (145) Smidt, S. P.; Zimmermann, N.; Studer, M.; Pfaltz, A. *Chem.-Eur. J.* **2004**, *10*, 4685.
- (146) Snelders, D. J. M.; Kunna, K.; Müller, C.; Vogt, D.; van Koten, G.; Gebbink, R. *Tetrahedron: Asymmetry* **2010**, *21*, 1411.
- (147) Miyake, G. M.; Zhang, Y.; Chen, E. Y. X. *Macromolecules* **2010**, *43*, 4902.
- (148) Zhang, Y.; Gustafson, L. O.; Chen, E. Y. X. *J. Am. Chem. Soc.* **2011**, *133*, 13674.
- (149) Constant, S.; Lacour, J. *Top. Curr. Chem.* **2005**, *250*, 1.
- (150) Allcock, H. R. *J. Am. Chem. Soc.* **1963**, *85*, 4050.
- (151) Allcock, H. R. *J. Am. Chem. Soc.* **1964**, *86*, 2591.
- (152) Allcock, H. R.; Bissell, E. C. *J. Chem. Soc., Chem. Commun.* **1972**, 676.
- (153) Allcock, H. R.; Bissell, E. C. *J. Am. Chem. Soc.* **1973**, *95*, 3154.
- (154) Holmes, R. R. *Chem. Rev.* **1996**, *96*, 927.

- (155) Holmes, R. R. *Acc. Chem. Res.* **1998**, *31*, 535.
- (156) Wong, C. Y.; Kennepohl, D. K.; Cavell, R. G. *Chem. Rev.* **1996**, *96*, 1917.
- (157) Eberwein, M.; Schmid, A.; Schmidt, M.; Zabel, M.; Burgemeister, T.; Barthel, J.; Kunz, W.; Gores, H. J. *J. Electrochem. Soc.* **2003**, *150*, A994.
- (158) Handa, M.; Suzuki, M.; Suzuki, J.; Kanematsu, H.; Sasaki, Y. *Electrochem. Solid-State Lett.* **1999**, *2*, 60.
- (159) Cavezzan, J.; Etemad-Moghadam, G.; Koenig, M.; Kläbe, A. *Tetrahedron Lett.* **1979**, 795.
- (160) Koenig, M.; Kläbe, A.; Munoz, A.; Wolf, R. *J. Chem. Soc., Perkin Trans. 2* **1979**, 40.
- (161) Schmidpeter, A.; Criegern, T. V.; Sheldrick, W. S.; Schomburg, D. *Tetrahedron Lett.* **1978**, *19*, 2857.
- (162) Gallagher, M.; Munoz, A.; Gence, G.; Koenig, M. *Chem. Commun.* **1976**, 321.
- (163) Hellwinkel, D.; Wilfinger, H. J. *Chem. Ber.* **1970**, *103*, 1056.
- (164) Munoz, A.; Gallagher, M.; Kläbe, A.; Wolf, R. *Tetrahedron Lett.* **1976**, *17*, 673.
- (165) Lide, D. R. *CRC Handbook of Chemistry and Physics*; 88th ed.; CRC Press/Taylor and Francis: Boca Raton, FL, 2008.
- (166) Pelzer, G.; Herwig, J.; Keim, W.; Goddard, R. *Russ. Chem. Bull.* **1998**, *47*, 904.
- (167) Kumar, J. S.; Singh, A. K.; Yang, J. C.; Drake, J. E. *J. Coord. Chem.* **1998**, *44*, 335.
- (168) Abu-Surrah, A. S.; Klinga, M.; Repo, T.; Leskela, M.; Debaerdemaeker, T.; Rieger, B. *Acta Crystallogr., Sect. C: Cryst. Struct. Commun.* **2000**, *56*, E44.
- (169) Devic, T.; Batail, P.; Fourmigué, M.; Avarvari, N. *Inorg. Chem.* **2004**, *43*, 3136.
- (170) Brown, M. D.; Levason, W.; Reid, G.; Watts, R. *Polyhedron* **2005**, *24*, 75.
- (171) Ganguly, S.; Georgiev, E. M.; Mague, J. T.; Roundhill, D. M. *Acta Crystallogr., Sect. C: Cryst. Struct. Commun.* **1993**, *49*, 1169.

- (172) Bondi, A. *J. Phys. Chem.* **1964**, *68*, 441.
- (173) Albano, P.; Aresta, M.; Manassero, M. *Inorg. Chem.* **1980**, *19*, 1069.
- (174) Powell, J.; Lough, A.; Saeed, T. *Dalton Trans.* **1997**, 4137.
- (175) Lassahn, P. G.; Lozan, V.; Wu, B.; Weller, A. S.; Janiak, C. *Dalton Trans.* **2003**, 4437.
- (176) *SAINT*; Version 7.60A. Bruker AXS Inc.: Madison, WI, (1997-2009).
- (177) *SADABS*; V2008/1. Bruker AXS Inc.: Madison, WI, (2008).
- (178) Sheldrick, G. M. *SHELXTL*; 5.1 ed.; Bruker AXS Inc.: Madison, WI, 1997.
- (179) Sheldrick, G. M. *Acta Crystallogr., Sect. A: Fundam. Crystallogr.* **2008**, *64*, 112.
- (180) Reed, C. A. *Acc. Chem. Res.* **1998**, *31*, 133.
- (181) Reed, C. A. *Chem. Commun.* **2005**, 1669.
- (182) Reed, C. A. *Acc. Chem. Res.* **1998**, *31*, 325.
- (183) Küppers, T.; Bernhardt, E.; Eujen, R.; Willner, H.; Lehmann, C. W. *Angew. Chem., Int. Ed.* **2007**, *46*, 6346.
- (184) Clarke, A. J.; Ingleson, M. J.; Kociok-Köhn, G.; Mahon, M. F.; Patmore, N. J.; Rourke, J. P.; Ruggiero, G. D.; Weller, A. S. *J. Am. Chem. Soc.* **2004**, *126*, 1503.
- (185) Tsang, C. W.; Yang, Q. C.; Sze, E. T. P.; Mak, T. C. W.; Chan, D. T. W.; Xie, Z. W. *Inorg. Chem.* **2000**, *39*, 5851.
- (186) Krossing, I.; Reisinger, A. *Eur. J. Inorg. Chem.* **2005**, 1979.
- (187) Timofte, T.; Pitula, S.; Mudring, A. V. *Inorg. Chem.* **2007**, *46*, 10938.
- (188) Tsujioka, S.; Nolan, B. G.; Takase, H.; Fauber, B. P.; Strauss, S. H. *J. Electrochem. Soc.* **2004**, *151*, A1418.
- (189) Ivanova, S. M.; Nolan, B. G.; Kobayashi, Y.; Miller, S. M.; Anderson, O. P.; Strauss, S. H. *Chem.-Eur. J.* **2001**, *7*, 503.
- (190) Cameron, T. S.; Krossing, I.; Passmore, J. *Inorg. Chem.* **2001**, *40*, 4488.

- (191) Chai, J. F.; Lewis, S. P.; Collins, S.; Sciarone, T. J. J.; Henderson, L. D.; Chase, P. A.; Irvine, G. J.; Piers, W. E.; Elsegood, M. R. J.; Clegg, W. *Organometallics* **2007**, *26*, 5667.
- (192) Hannant, M. H.; Wright, J. A.; Lancaster, S. J.; Hughes, D. L.; Horton, P. N.; Bochmann, M. *Dalton Trans.* **2006**, 2415.
- (193) Bavarian, N.; Baird, M. C. *Organometallics* **2005**, *24*, 2889.
- (194) Golden, J. H.; Mutolo, P. F.; Lobkovsky, E. B.; DiSalvo, F. J. *Inorg. Chem.* **1994**, *33*, 5374.
- (195) Mukaiyama, T.; Maeshima, H.; Jona, H. *Chem. Lett.* **2001**, 388.
- (196) Hughes, R. P.; Lindner, D. C.; Rheingold, A. L.; Yap, G. P. A. *Inorg. Chem.* **1997**, *36*, 1726.
- (197) Alberti, D.; Pörschke, K. R. *Organometallics* **2004**, *23*, 1459.
- (198) Bahr, S. R.; Boudjouk, P. *J. Org. Chem.* **1992**, *57*, 5545.
- (199) Taube, R.; Wache, S. *J. Organomet. Chem.* **1992**, *428*, 431.
- (200) Pellecchia, C.; Proto, A.; Longo, P.; Zambelli, A. *Makromol. Chem., Rapid Commun.* **1991**, *12*, 663.
- (201) Jutzi, P.; Müller, C.; Stammler, A.; Stammler, H. G. *Organometallics* **2000**, *19*, 1442.
- (202) Yao, S. L.; Xiong, Y.; van Wüllen, C.; Driess, M. *Organometallics* **2009**, *28*, 1610.
- (203) Avelar, A.; Tham, F. S.; Reed, C. A. *Angew. Chem., Int. Ed.* **2009**, *48*, 3491.
- (204) Yang, Y.; Panisch, R.; Bolte, M.; Müller, T. *Organometallics* **2008**, *27*, 4847.
- (205) Yang, J.; White, P. S.; Schauer, C. K.; Brookhart, M. *Angew. Chem., Int. Ed.* **2008**, *47*, 4141.
- (206) Stoyanov, E. S.; Stoyanova, I. V.; Reed, C. A. *Chem.-Eur. J.* **2008**, *14*, 7880.

- (207) Koppe, K.; Frohn, H. J.; Mercier, H. P. A.; Schrobilgen, G. J. *Inorg. Chem.* **2008**, *47*, 3205.
- (208) Bonnier, C.; Piers, W. E.; Parvez, M.; Sorensen, T. S. *Chem. Commun.* **2008**, 4593.
- (209) Brownie, J. H.; Baird, M. C. *Organometallics* **2007**, *26*, 5890.
- (210) Jones, J. N.; Moore, J. A.; Cowley, A. H.; Macdonald, C. L. B. *Dalton Trans.* **2005**, 3846.
- (211) Jutzi, P.; Mix, A.; Rummel, B.; Schoeller, W. W.; Neumann, B.; Stammler, H. G. *Science* **2004**, *305*, 849.
- (212) Filippou, A. C.; Philippopoulos, A. I.; Portius, P.; Schnakenburg, G. *Organometallics* **2004**, *23*, 4503.
- (213) Uyeda, C.; Jacobsen, E. N. *J. Am. Chem. Soc.* **2008**, *130*, 9228.
- (214) Friesen, D. M.; Piers, W. E.; Parvez, M. *Organometallics* **2008**, *27*, 6596.
- (215) Ono, T.; Sugimoto, T.; Shinkai, S.; Sada, K. *Nat. Mater.* **2007**, *6*, 429.
- (216) Broene, R. D.; Brookhart, M.; Lamanna, W. M.; Volpe, A. F., Jr. *J. Am. Chem. Soc.* **2005**, *127*, 17194.
- (217) Ramirez, F.; Nowakowski, M.; Marecek, J. F. *J. Am. Chem. Soc.* **1977**, *99*, 4515.
- (218) Fulmer, G. R.; Miller, A. J. M.; Sherden, N. H.; Gottlieb, H. E.; Nudelman, A.; Stoltz, B. M.; Bercaw, J. E.; Goldberg, K. I. *Organometallics* **2010**, *29*, 2176.
- (219) Reynolds, W. L.; Lampe, K. A. *J. Inorg. Nucl. Chem.* **1968**, *30*, 2860.
- (220) Grant, H. M.; McTigue, P.; Ward, D. G. *Aust. J. Chem.* **1983**, *36*, 2211.
- (221) Larson, J. W.; McMahan, T. B. *J. Am. Chem. Soc.* **1982**, *104*, 6255.
- (222) Behmel, P.; Jones, P. G.; Sheldrick, G. M.; Ziegler, M. *J. Mol. Struct.* **1980**, *69*, 41.
- (223) Pietkäinen, J.; Maaninen, A.; Laitinen, R. S.; Oilunkaniemi, R.; Valkonen, J. *Polyhedron* **2002**, *21*, 1089.

- (224) Buchanan, J.; Hamilton, E. J. M.; Reed, D.; Welch, A. J. *Dalton Trans.* **1990**, 677.
- (225) Jaswal, J. S.; Rettig, S. J.; James, B. R. *Can. J. Chem.* **1990**, 68, 1808.
- (226) Cartwright, P. S.; Gillard, R. D.; Sillanpaa, E. R. J.; Valkonen, J. *Polyhedron* **1988**, 7, 2143.
- (227) Emsley, J. *Chem. Soc. Rev.* **1980**, 9, 91.
- (228) Keefer, L. K.; Hrabie, J. A.; Ohannesian, L.; Flippen-Anderson, J. L.; George, C. *J. Am. Chem. Soc.* **1988**, 110, 3701.
- (229) Rudd, M. D.; Kokke, G.; Lindeman, S. V. *Acta Crystallogr., Sect. E: Struct. Rep. Online* **2008**, 64, O1161.
- (230) Steiner, T. *Angew. Chem., Int. Ed.* **2002**, 41, 48.
- (231) Krill, J.; Shevchenko, I. V.; Fischer, A.; Jones, P. G.; Schmutzler, R. *Chem. Ber.* **1997**, 130, 1479.
- (232) Stoyanov, E. S.; Kim, K. C.; Reed, C. A. *J. Am. Chem. Soc.* **2006**, 128, 8500.
- (233) Stasko, D.; Hoffmann, S. P.; Kim, K. C.; Fackler, N. L. P.; Larsen, A. S.; Drovetskaya, T.; Tham, F. S.; Reed, C. A.; Rickard, C. E. F.; Boyd, P. D. W.; Stoyanov, E. S. *J. Am. Chem. Soc.* **2002**, 124, 13869.
- (234) Ledford, J.; Shultz, C. S.; Gates, D. P.; White, P. S.; DeSimone, J. M.; Brookhart, M. *Organometallics* **2001**, 20, 5266.
- (235) Shultz, C. S.; Ledford, J.; DeSimone, J. M.; Brookhart, M. *J. Am. Chem. Soc.* **2000**, 122, 6351.
- (236) Bianchini, C.; Meli, A.; Oberhauser, W.; Segarra, A. M.; Claver, C.; Suarez, E. J. G. *J. Mol. Catal. A: Chem.* **2007**, 265, 292.
- (237) Drent, E.; Budzelaar, P. H. M. *Chem. Rev.* **1996**, 96, 663.
- (238) Drent, E.; van Broekhoven, J. A. M.; Doyle, M. J. *J. Organomet. Chem.* **1991**, 417, 235.

- (239) Dekker, G.; Elsevier, C. J.; Vrieze, K.; van Leeuwen, P. W. N. M. *Organometallics* **1992**, *11*, 1598.
- (240) Bianchini, C.; Lee, H. M.; Meli, A.; Oberhauser, W.; Peruzzini, M.; Vizza, F. *Organometallics* **2002**, *21*, 16.
- (241) Abu-Surrah, A. S.; Lappalainen, K.; Kettunen, M.; Repo, T.; Leskelä, M.; Hodali, H. A.; Rieger, B. *Macromol. Chem. Phys.* **2001**, *202*, 599.
- (242) Abu-Surrah, A. S.; Lappalainen, K.; Repo, T.; Klinga, M.; Leskelä, M.; Hodali, H. A. *Polyhedron* **2000**, *19*, 1601.
- (243) Herwig, J.; Keim, W. *Inorg. Chim. Acta* **1994**, *222*, 381.
- (244) Keim, W.; Herwig, J. *Chem. Commun.* **1993**, 1592.
- (245) Davies, J. A.; Hartley, F. R.; Murray, S. G.; Marshall, G. *J. Mol. Catal. A: Chem.* **1981**, *10*, 171.
- (246) Davies, J. A.; Hartley, F. R.; Murray, S. G. *Dalton Trans.* **1980**, 2246.
- (247) Batsanov, A. S.; Howard, J. A. K.; Robertson, G. S.; Kilner, M. *Acta Crystallogr., Sect. E: Struct. Rep. Online* **2001**, *57*, m301.
- (248) Oberhauser, W.; Bachmann, C.; Stampfl, T.; Haid, R.; Brüggeller, P. *Polyhedron* **1997**, *16*, 2827.
- (249) Capdevila, M.; Clegg, W.; González-Duarte, P.; Harris, B.; Mira, I.; Sola, J.; Taylor, I. C. *Dalton Trans.* **1992**, 2817.
- (250) Bachechi, F.; Lehmann, R.; Venanzi, L. M. *J. Crystallogr. Spectrosc. Res.* **1988**, *18*, 721.
- (251) The absolute configuration of anion [1]⁻ components of **5(Λ)** and **5(Δ)** were determined on the basis of their Flack values. Their final Flack values were refined to be 0.006(12) for **5(Λ)** and -0.012(10) for **5(Δ)**. (Flack, H. D. *Acta Crystallogr., Sect. A: Found. Crystallogr.* **1983**, *39*, 876.)

- (252) Spaniel, T.; Schmidt, H.; Wagner, C.; Merzweiler, K.; Steinborn, D. *Eur. J. Inorg. Chem.* **2002**, 2868.
- (253) Lindsay, C. H.; Benner, L. S.; Balch, A. L. *Inorg. Chem.* **1980**, *19*, 3503.
- (254) Aoshima, S.; Kanaoka, S. *Chem. Rev.* **2009**, *109*, 5245.
- (255) Goethals, E. J.; Du Prez, F. *Prog. Polym. Sci.* **2007**, *32*, 220.
- (256) Shaffer, T. D. In *Cationic Polymerization: Fundamentals and Applications*; Faust, R., Shaffer, T. D., Eds.; American Chemical Society: Washington, 1997; Vol. 665, p 1.
- (257) Sawamoto, M. *Prog. Polym. Sci.* **1991**, *16*, 111.
- (258) Kennedy, J. P.; Maréchal, E. *Carbocationic Polymerization*; John Wiley & Sons: New York, NY, 1982.
- (259) Kennedy, J. P. *Cationic Polymerization of Olefins: A Critical Inventory*; Wiley: New York, 1975.
- (260) Lanson, D.; Schappacher, M.; Borsali, R.; Deffieux, A. *Macromolecules* **2007**, *40*, 5559.
- (261) Kamigaito, M.; Sawamoto, M.; Higashimura, T. *Macromolecules* **1992**, *25*, 2587.
- (262) Kanaoka, S.; Sawamoto, M.; Higashimura, T. *Macromolecules* **1991**, *24*, 2309.
- (263) Kojima, K.; Sawamoto, M.; Higashimura, T. *Macromolecules* **1989**, *22*, 1552.
- (264) Sawamoto, M.; Okamoto, C.; Higashimura, T. *Macromolecules* **1987**, *20*, 2693.
- (265) Kamigaito, M.; Yamaoka, K.; Sawamoto, M.; Higashimura, T. *Macromolecules* **1992**, *25*, 6400.
- (266) Kamigaito, M.; Sawamoto, M.; Higashimura, T. *Macromolecules* **1991**, *24*, 3988.
- (267) Ouchi, M.; Sueoka, M.; Kamigaito, M.; Sawamoto, M. *J. Polym. Sci., Part A: Polym. Chem.* **2001**, *39*, 1067.
- (268) Rozentsvet, V. A.; Kozlov, V. G.; Ziganshina, E. F.; Boreiko, N. P. *Int. J. Polym. Anal. Charact.* **2009**, *14*, 631.

- (269) Rozentsvet, V. A.; Kozlov, V. G.; Ziganshina, E. F.; Boreiko, N. P.; Khachaturov, A. S. *Russ. J. Appl. Chem.* **2009**, *82*, 148.
- (270) Rozentsvet, V. A.; Kozlov, V. G.; Ziganshina, E. F.; Boreiko, N. P. *Polym. Sci. Ser. A* **2008**, *50*, 1038.
- (271) Nakatani, K.; Ouchi, M.; Sawamoto, M. *J. Polym. Sci., Part A: Polym. Chem.* **2009**, *47*, 4194.
- (272) Kanazawa, A.; Kanaoka, S.; Aoshima, S. *Macromolecules* **2009**, *42*, 3965.
- (273) Mizuno, N.; Satoh, K.; Kamigaito, M.; Okamoto, Y. *Macromolecules* **2006**, *39*, 5280.
- (274) Zhou, Y. H.; Faust, R.; Chen, S. J.; Gido, S. P. *Macromolecules* **2004**, *37*, 6716.
- (275) Yun, J. P.; Faust, R.; Szilagyi, L. S.; Keki, S.; Zsuga, M. *Macromolecules* **2003**, *36*, 1717.
- (276) Puskas, J. E.; Luo, W. *Macromolecules* **2003**, *36*, 6942.
- (277) Pernecker, T.; Kennedy, J. P.; Ivan, B. *Macromolecules* **1992**, *25*, 1642.
- (278) Storey, R. F.; Thomas, Q. A. *Macromolecules* **2003**, *36*, 5065.
- (279) Coca, S.; Matyjaszewski, K. *Macromolecules* **1997**, *30*, 2808.
- (280) Shibata, T.; Kanaoka, S.; Aoshima, S. *J. Am. Chem. Soc.* **2006**, *128*, 7497.
- (281) Sugihara, S.; Hashimoto, K.; Okabe, S.; Shibayama, M.; Kanaoka, S.; Aoshima, S. *Macromolecules* **2004**, *37*, 336.
- (282) Oda, Y.; Kanaoka, S.; Aoshima, S. *J. Polym. Sci., Part A: Polym. Chem.* **2010**, *48*, 1207.
- (283) Yoshida, T.; Tsujino, T.; Kanaoka, S.; Aoshima, S. *J. Polym. Sci., Part A: Polym. Chem.* **2005**, *43*, 468.
- (284) Kanazawa, A.; Kanaoka, S.; Aoshima, S. *Macromolecules* **2010**, *43*, 2739.
- (285) Vasilenko, I. V.; Frolov, A. N.; Kostjuk, S. V. *Macromolecules* **2010**, *43*, 5503.

- (286) Kamigaito, M.; Nakashima, J.; Satoh, K.; Sawamoto, M. *Macromolecules* **2003**, *36*, 3540.
- (287) Satoh, K.; Nakashima, J.; Kamigaito, I.; Sawamoto, M. *Macromolecules* **2001**, *34*, 396.
- (288) Ouardad, S.; Kostjuk, S. V.; Ganachaud, F.; Puskas, J. E.; Deffieux, A.; Peruch, F. *J. Polym. Sci., Part A: Polym. Chem.* **2011**, *49*, 4948.
- (289) Frolov, A. N.; Kostjuk, S. V.; Vasilenko, I. V.; Kaputsky, F. N. *J. Polym. Sci., Part A: Polym. Chem.* **2010**, *48*, 3736.
- (290) Puskas, J. E.; Peres, C.; Peruch, F.; Deffieux, A.; Dabney, D. E.; Wesdemiotis, C.; Hayat-Soytas, S.; Lindsay, A. *J. Polym. Sci., Part A: Polym. Chem.* **2009**, *47*, 2181.
- (291) Kennedy, J. P. *J. Polym. Sci., Part A: Polym. Chem.* **1999**, *37*, 2285.
- (292) Shaffer, T. D.; Ashbaugh, J. R. *J. Polym. Sci., Part A: Polym. Chem.* **1997**, *35*, 329.
- (293) Shaffer, T. D. In *Cationic Polymerization: Fundamentals and Applications*; Faust, R., Shaffer, T. D., Eds.; American Chemical Society: Washington, 1997; Vol. 665, p 96.
- (294) Bochmann, M.; Dawson, D. M. *Angew. Chem., Int. Ed.* **1996**, *35*, 2226.
- (295) Kostjuk, S. V.; Ouardad, S.; Peruch, F.; Deffieux, A.; Absalon, C.; Puskas, J. E.; Ganachaud, F. *Macromolecules* **2011**, *44*, 1372.
- (296) Kostjuk, S. V.; Radchenko, A. V.; Ganachaud, F. *Macromolecules* **2007**, *40*, 482.
- (297) Lian, B.; Ma, H. Y.; Spaniol, T. P.; Okuda, J. *Dalton Trans.* **2009**, 9033.
- (298) Kostjuk, S. V.; Ganachaud, F. *Macromolecules* **2006**, *39*, 3110.
- (299) Kostjuk, S. V.; Radchenko, A. V.; Ganachaud, F. *J. Polym. Sci., Part A: Polym. Chem.* **2008**, *46*, 4734.
- (300) Radchenko, A. V.; Kostjuk, S. V.; Vasilenko, I. V.; Ganachaud, F.; Kaputsky, F. N.; Guillaneuf, Y. *J. Polym. Sci., Part A: Polym. Chem.* **2008**, *46*, 6928.
- (301) Lewis, S. P.; Taylor, N. J.; Piers, W. E.; Collins, S. *J. Am. Chem. Soc.* **2003**, *125*, 14686.

- (302) Lewis, S. P.; Chai, J. F.; Collins, S.; Sciarone, T. J. J.; Henderson, L. D.; Fan, C.; Parvez, M.; Piers, W. E. *Organometallics* **2009**, *28*, 249.
- (303) Mathers, R. T.; Lewis, S. P. *J. Polym. Sci., Part A: Polym. Chem.* **2012**, *50*, 1325.
- (304) Pi, Z.; Jacob, S.; Kennedy, J. P. In *Ionic Polymerizations and Related Processes*; Puskas, J. E., Ed.; Springer: Dordrecht, 1999; Vol. 359, p 1.
- (305) Jacob, S.; Pi, Z. J.; Kennedy, J. P. *Polym. Bull.* **1998**, *41*, 503.
- (306) Barsan, F.; Karam, A. R.; Parent, M. A.; Baird, M. C. *Macromolecules* **1998**, *31*, 8439.
- (307) Carr, A. G.; Dawson, D. M.; Thornton-Pett, M.; Bochmann, M. *Organometallics* **1999**, *18*, 2933.
- (308) Song, X. J.; Thornton-Pett, M.; Bochmann, M. *Organometallics* **1998**, *17*, 1004.
- (309) Bochmann, M. *Acc. Chem. Res.* **2010**, *43*, 1267.
- (310) Baird, M. C. *Chem. Rev.* **2000**, *100*, 1471.
- (311) Huber, M.; Kurek, A.; Krossing, I.; Mulhaupt, R.; Schnoekel, H. Z. *Anorg. Allg. Chem.* **2009**, *635*, 1787.
- (312) Miyake, G. M.; DiRocco, D. A.; Liu, Q.; Oberg, K. M.; Bayram, E.; Finke, R. G.; Rovis, T.; Chen, E. Y. X. *Macromolecules* **2010**, *43*, 7504.
- (313) Chang, C. T.; Chen, C. L.; Liu, Y. H.; Peng, S. M.; Chou, P. T.; Liu, S. T. *Inorg. Chem.* **2006**, *45*, 7590.
- (314) Vijayaraghavan, R.; MacFarlane, D. R. *Macromolecules* **2007**, *40*, 6515.
- (315) Vijayaraghavan, R.; MacFarlane, D. R. *Chem. Commun.* **2004**, 700.
- (316) Aouissi, A.; Al-Othman, Z. A.; Al-Anezi, H. *Molecules* **2010**, *15*, 3319.
- (317) Chen, D. Y.; Xue, Z. G.; Su, Z. X. *J. Mol. Catal. A: Chem.* **2003**, *203*, 307.
- (318) Burrington, J. D.; Johnson, J. R.; Pudelski, J. K. *Top. Catal.* **2003**, *23*, 175.
- (319) Shevchenko, I. V.; Fischer, A.; Jones, P. G.; Schmutzler, R. *Chem. Ber.* **1992**, *125*, 1325.

- (320) Kanazawa, A.; Kanaoka, S.; Aoshima, S. *Macromolecules* **2010**, *43*, 3682.
- (321) Satoh, K.; Kamigaito, M.; Sawamoto, M. *Macromolecules* **1999**, *32*, 3827.
- (322) Bae, Y. C.; Faust, R. *Macromolecules* **1998**, *31*, 2480.
- (323) Cho, C. G.; Feit, B. A.; Webster, O. W. *Macromolecules* **1990**, *23*, 1918.
- (324) Arnett, E. M.; Wu, C. Y. *J. Am. Chem. Soc.* **1960**, *82*, 4999.
- (325) Vagedes, D.; Erker, G.; Frohlich, R. *J. Organomet. Chem.* **2002**, *641*, 148.
- (326) Henderson, L. D.; Piers, W. E.; Irvine, G. J.; McDonald, R. *Organometallics* **2002**, *21*, 340.
- (327) Lacour, J.; Bernardinelli, G.; Russell, V.; Dance, I. *Cryst. Eng. Comm.* **2002**, 165.
- (328) Cotton, F. A.; Fair, C. K.; Lewis, G. E.; Mott, G. N.; Ross, F. K.; Schultz, A. J.; Williams, J. M. *J. Am. Chem. Soc.* **1984**, *106*, 5319.
- (329) Steiner, T.; Majerz, I.; Wilson, C. C. *Angew. Chem., Int. Ed.* **2001**, *40*, 2651.
- (330) Malarski, Z.; Majerz, I.; Lis, T. *J. Mol. Struct.* **1996**, *380*, 249.
- (331) Majerz, I.; Malarski, Z.; Lis, T. *J. Mol. Struct.* **1989**, *213*, 161.
- (332) Jin, Z. M.; Hu, M. L.; Li, Z. G.; Xuan, R. C.; Yu, K. B. *J. Chem. Crystallogr.* **2004**, *34*, 657.
- (333) Jerzykiewicz, L. B.; Malarski, Z.; Sobczyk, L.; Lis, T.; Grech, E. *J. Mol. Struct.* **1998**, *440*, 175.
- (334) Kéki, S.; Nagy, M.; Deák, G.; Zsuga, M. *J. Phys. Chem. B* **2001**, *105*, 9896.
- (335) Castelvetro, V.; Pittaluga, G. B.; Ciardelli, F. *Macromol. Chem. Phys.* **2001**, *202*, 2093.
- (336) Aoshima, S.; Higashimura, T. *Polym. J.* **1984**, *16*, 249.
- (337) Kawamura, T.; Toshima, N.; Matsuzaki, K. *Macromol. Rapid Commun.* **1994**, *15*, 479.
- (338) Puskas, J. E.; Peruch, F.; Deffieux, A.; Dabney, D. E.; Wesdemiotis, C.; Li, H. B.; Lindsay, A. J. *Polym. Sci., Part A: Polym. Chem.* **2009**, *47*, 2172.

- (339) Tanaka, Y.; Sato, H.; Nakafutami, Y.; Iwasaki, H.; Taketomi, T. *Polym. J.* **1982**, *14*, 713.
- (340) Hasegawa, K.; Asami, R.; Higashimura, T. *Macromolecules* **1977**, *10*, 592.
- (341) Gaylord, N. G.; Matyska, B.; Mach, K.; Vodehnal, J. *J. Polym. Sci., Part A: Polym. Chem.* **1966**, *4*, 2493.
- (342) Matyska, B.; Petrusová, L.; Mach, K.; Švestka, M. *Collect. Czech. Chem. Commun.* **1979**, *44*, 1262.
- (343) Cooper, W. In *The Chemistry of Cationic Polymerization*; Plesch, P. H., Ed.; Pergamon Press: New York, 1963, p 349.
- (344) Lubbecke, H.; Boldt, P. *Tetrahedron* **1978**, *34*, 1577.
- (345) Hutchings, L. R.; Dodds, J. M.; Rees, D.; Kimani, S. M.; Wu, J. J.; Smith, E. *Macromolecules* **2009**, *42*, 8675.
- (346) Jackson, C.; Chen, Y. J.; Mays, J. W. *J. Appl. Polym. Sci.* **1996**, *61*, 865.
- (347) Sheldrick, G. M. *SHELXL-97 (Release 97-2)*; University of Göttingen: Germany, 1997.
- (348) Farrugia, L. J. *J. Appl. Crystallogr.* **1999**, *32*, 837.
- (349) Emsley, A. M.; Stevens, G. C. In *Advances in Fire Retardant Materials*; Horrocks, A. R., Price, D., Eds.; Woodhead Publishing Limited: Cambridge, England, 2008, p 363.
- (350) Bourbigot, S.; Duquesne, S. *J. Mater. Chem.* **2007**, *17*, 2283.
- (351) Lu, S. Y.; Hamerton, I. *Prog. Polym. Sci.* **2002**, *27*, 1661.
- (352) Birnbaum, L. S.; Staskal, D. F. *Environ. Health Perspect.* **2004**, *112*, 9.
- (353) Guidance on Feasible Flame-Retardant Alternatives to Commercial Pentabromodiphenyl Ether. UNEP/POPS/COP.4/INF/24. Conference of the Parties of the Stockholm Convention on Persistent Organic Pollutants Fourth Meeting, Geneva, 4-8 May 2009.
- (354) Commission Decision 2010/571/EU. *Official Journal of the European Union*, 2010, **L 251**, 28.

- (355) Polybrominated Diphenyl Ethers Regulations. *Canada Gazette Part II*, 2008, **142**, 1663.
- (356) Polybrominated Diphenyl Ethers (PBDEs) Action Plan. EPA-HQ-OPPT-2010-0146-0002; U.S. EPA, 2009.
http://www.epa.gov/opptintr/existingchemicals/pubs/pbdes_ap_2009_1230_final.pdf
(accessed Apr 9, 2012).
- (357) Chen, L.; Wang, Y. Z. *Polym. Adv. Technol.* **2010**, *21*, 1.
- (358) Laoutid, F.; Bonnaud, L.; Alexandre, M.; Lopez-Cuesta, J. M.; Dubois, P. *Mater. Sci. Eng., R* **2009**, *63*, 100.
- (359) Levchik, S. V.; Weil, E. D. *J. Fire Sci.* **2006**, *24*, 345.
- (360) Zhang, S.; Horrocks, A. R. *Prog. Polym. Sci.* **2003**, *28*, 1517.
- (361) Weil, E. D. In *Kirk-Othmer Encyclopedia of Chemical Technology*; John Wiley & Sons, Inc.: New York, 2000; Vol. 11, p 484.
- (362) Granzow, A. *Acc. Chem. Res.* **1978**, *11*, 177.
- (363) Lewin, M. *Polym. Degrad. Stab.* **2005**, *88*, 13.
- (364) White, R. H.; Sweet, M. S. In *Recent Advances in Flame Retardancy of Polymeric Materials: Proceedings of 3rd Annual BCC Conference*; Lewin, M., Ed.; Business Communications Company, Inc.: Stamford, CT, 1992, p 250.
- (365) Chattopadhyay, D. K.; Raju, K. *Prog. Polym. Sci.* **2007**, *32*, 352.
- (366) Allcock, H. R. *Chemistry and Applications of Polyphosphazenes*; Wiley-Interscience: Hoboken, 2003.
- (367) De Jaeger, R.; Gleria, M. *Prog. Polym. Sci.* **1998**, *23*, 179.
- (368) Fei, S. T.; Allcock, H. R. *J. Power Sources* **2010**, *195*, 2082.
- (369) Ranganathan, T.; Zilberman, J.; Farris, R. J.; Coughlin, E. B.; Emrick, T. *Macromolecules* **2006**, *39*, 5974.

- (370) Chang, Y. L.; Wang, Y. Z.; Ban, D. M.; Yang, B.; Zhao, G. M. *Macromol. Mater. Eng.* **2004**, 289, 703.
- (371) Huang, Z. G.; Shi, W. F. *Polym. Degrad. Stab.* **2006**, 91, 1674.
- (372) Huang, Z. G.; Shi, W. F. *Eur. Polym. J.* **2006**, 42, 1506.
- (373) Liu, Y.; Li, J.; Wang, Q. *J. Appl. Polym. Sci.* **2009**, 113, 2046.
- (374) Hoffmann, T.; Pospiech, D.; Haussler, L.; Komber, H.; Voigt, D.; Harnisch, C.; Kollann, C.; Ciesielski, M.; Doring, M.; Perez-Graterol, R.; Sandler, J.; Altstadr, V. *Macromol. Chem. Phys.* **2005**, 206, 423.
- (375) Becker, G.; Uhl, W.; Wessely, H. J. *Z. Anorg. Allg. Chem.* **1981**, 479, 41.
- (376) Yam, M.; Chong, J. H.; Tsang, C. W.; Patrick, B. O.; Lam, A. E.; Gates, D. P. *Inorg. Chem.* **2006**, 45, 5225.
- (377) Noonan, K. J. T.; Gates, D. P. *Macromolecules* **2008**, 41, 1961.
- (378) Noonan, K. J. T.; Feldscher, B.; Bates, J. I.; Kingsley, J. J.; Yam, M.; Gates, D. P. *Dalton Trans.* **2008**, 4451.
- (379) Gillon, B. H.; Patrick, B. O.; Gates, D. P. *Chem. Commun.* **2008**, 2161.
- (380) Gillon, B. H.; Gates, D. P. *Chem. Commun.* **2004**, 1868.
- (381) Tienvieri, T.; Huusari, E.; Sundholm, J.; Vuorio, P.; Kortelainen, J.; Nystedt, H.; Artamo, A. In *Mechanical Pulping*; Sundholm, J., Ed.; Fapet Oy: Helsinki, 1999; Vol. 5, p 157.
- (382) Hu, T. Q.; Zhao, M.; Bicho, P.; Losier, P. In *Proceedings to 2010 PAPTAC Annual Meeting – Mechanical Pulping I* Montreal, QC, 2010.
- (383) Sundholm, J. In *Mechanical Pulping*; Sundholm, J., Ed.; Fapet Oy: Helsinki, 1999; Vol. 5, p 16.
- (384) TAPPI Test Method T 461 cm-00 (2000).
- (385) Green, J. J. *Fire Sci.* **1992**, 10, 470.

- (386) Green, J. J. *Fire Sci.* **1996**, *14*, 353.
- (387) Lomakin, S. M.; Zaikov, G. E. *Ecological Aspects of Polymer Flame Retardancy*; VSP Books: Zeist, 1999.
- (388) Green, J. J. *Fire Sci.* **1996**, *14*, 426.
- (389) Ravey, M.; Pearce, E. M. *J. Appl. Polym. Sci.* **1999**, *74*, 1317.
- (390) Benbow, A. W.; Cullis, C. F. *Combust. Flame* **1975**, *24*, 217.
- (391) Yeh, K.; Birky, M. M.; Huggett, C. *J. Appl. Polym. Sci.* **1973**, *17*, 255.
- (392) Pitts, J. J. In *Flame Retardancy of Polymeric Materials*; Kuryla, W. C., Papa, A. J., Eds.; Marcel Dekker, Inc.: New York, 1973; Vol. 1, p 133.
- (393) Fu, Q. R.; Argyropoulos, D. S.; Tilotta, D. C.; Lucia, L. A. *J. Anal. Appl. Pyrolysis* **2008**, *82*, 140.
- (394) PAPTAC Standard Method C.5 (2003).
- (395) Gates, D. P. *Top. Curr. Chem.* **2005**, *250*, 107.
- (396) Gillon, B. H.; Noonan, K. J. T.; Feldscher, B.; Wissensz, J. M.; Kam, Z. M.; Hsieh, T.; Kingsley, J. J.; Bates, J. I.; Gates, D. P. *Can. J. Chem.* **2007**, *85*, 1045.
- (397) Gates, D. P. The University of British Columbia, Vancouver, BC. Personal communication, 2012.
- (398) Krummenacher, I. The University of British Columbia, Vancouver, BC. Personal communication, 2012.
- (399) Matyjaszewski, K.; Woodworth, B. E.; Zhang, X.; Gaynor, S. G.; Metzner, Z. *Macromolecules* **1998**, *31*, 5955.
- (400) Braunecker, W. A.; Matyjaszewski, K. *Prog. Polym. Sci.* **2007**, *32*, 93.
- (401) Wetter, C.; Gierlich, J.; Knoop, C. A.; Muller, C.; Schulte, T.; Studer, A. *Chem.-Eur. J.* **2004**, *10*, 1156.

- (402) Stalmach, U.; de Boer, B.; Videlot, C.; van Hutten, P. F.; Hadziioannou, G. *J. Am. Chem. Soc.* **2000**, *122*, 5464.
- (403) Benoit, D.; Chaplinski, V.; Braslau, R.; Hawker, C. J. *J. Am. Chem. Soc.* **1999**, *121*, 3904.
- (404) Klebach, T. C.; Lourens, R.; Bickelhaupt, F. *J. Am. Chem. Soc.* **1978**, *100*, 4886.
- (405) van der Knaap, T. A.; Klebach, T. C.; Visser, F.; Bickelhaupt, F.; Ros, P.; Baerends, E. J.; Stam, C. H.; Konijn, M. *Tetrahedron* **1984**, *40*, 765.